U.PORTO
FEUP FACULDADE DE ENGENHARIA
UNIVERSIDADE DO PORTO

Hydrolysis of sodium borohydride for hydrogen generation: Study of the by-product and its recycling

Diogo Luís Almeida Silva

Dissertation presented to obtain the degree of

Doctor in Chemical and Biological Engineering

Supervisor: Professor Alexandra Rodrigues Pinto

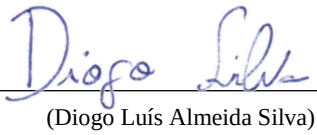
ALiCE

ceft
TRANSPORT PHENOMENA RESEARCH CENTER

January 2023

Statement of originality

I certify that this work does not contain any material that has been used, or will be used, for the award of any other degree or diploma in my name or anyone, in any university or institution. Moreover, I certify that, to the best of my knowledge, this work does not contain any material previously published or written by another person, except where due reference has been made in the text.



(Diogo Luís Almeida Silva)

Statement

In order to fulfil the Rules of Ethics of the Doctoral Program of Chemical and Biological Engineering (PDEQB), we hereby declare that all the contents of the thesis presented by Diogo Luís Almeida Silva, entitled "Hydrolysis of sodium borohydride for hydrogen generation: Study of the by-product and its recycling", are exclusively from the author. The contents of chapter 2 – subchapter 2.3 and chapter 3 - subchapter 3.2 present an exception since they were obtained in collaboration with Helder Xavier Teixeira Nunes for the writing of thesis "On-demand hydrogen generation through sodium borohydride for fuel cell applications". Accordingly, all the results here shown, excluding the exceptions described which resulted in the provisional patent application and approval number 118331 T, were obtained by the author of the thesis and resulted in the original publications presented further ahead.

(Alexandra Maria Pinheiro da Silva Ferreira Rodrigues Pinto)

(Diogo Luís Almeida Silva)

Abstract

Hydrogen production using water splitting via electrolysis powered by renewable energy sources has been identified worldwide as one of the main components of the pathway to hydrogen energy development. However, off-grid energy systems are becoming increasingly popular as a means of providing energy in areas/sectors where traditional grid connections are not feasible or cost-effective.

Hydrogen can be generated from the hydrolysis of sodium borohydride ($NaBH_4$) - a chemical hydride with high H_2 content – at moderate temperature and the H_2 obtained is pure and can be directly converted to electric energy in off-grid applications. Nevertheless, its regeneration from the by-product is critical to the success of this solution. The main goal of this work was to understand which by-product is formed in the hydrolysis reaction, how operating conditions can influence its formation, optimize operation in order to produce the borate(s) with more interest for the recycling process as well as the development of recycling to $NaBH_4$ processes.

The objective was to understand the main by-product of the $NaBH_4$ hydrolysis and if the rearrangement of $NaBO_2 \bullet 2H_2O$ into $NaB(OH)_4$ was dependent of the presence of additive carboxymethyl cellulose (CMC) or any other additive. Standard post-treatment of the by-product after extraction from the reactor was applied, where it is dried and stored open-to-air at room temperature. It was observed that the formation of $NaB(OH)_4$ was not exclusive of the presence of CMC but other borates and non-borates are also formed. The formation of these by-products was explained by the presence of air - in particular CO_2 and H_2O - which slowly reacted with the borate and generate Na_2CO_3 and dehydrated tincalconite ($Na_2B_4O_7$). To confirm this possibility, an innovative handling process of the by-product was developed and implemented, that avoids at maximum its exposure to air while drying and storage, since the by-product was dried in a vacuum desiccator and stored inside it. This innovative post-treatment of by-product has demonstrated that $NaB(OH)_4$ is obtained and maintained pure or very close to pure, which is crucial to assure its recycling back to $NaBH_4$, since not only it reduces the energy demand due to the absence of molecular water while the literature on the recycling practically only considers the study of commercial $NaBO_2$ and $NaBO_2 \bullet 2H_2O$. Several experiments were performed to confirm this finding and also to widen the hydrolysis conditions that validate it. Therefore, $NaB(OH)_4$ was observed to be formed for

hydrolysis with excess of water between 6 and 15, as well as catalyst loadings between 0.2 and 0.4 g/g. The innovative level and the important results of this process justified the elaboration of a patent request and registration (provisional patent number 118331 T) at UP IN, which will be converted to regular, non-provisional patent in Portugal and extended internationally.

This patented post-treatment process of the by-product of $NaBH_4$ hydrolysis was further developed and adapted in order to optimize the formation of other borates, such as tincalconite and $NaB(OH)_4 \cdot 2H_2O$. Therefore, new post-treatments were studied, which considered a drying chamber (low humidity environment), low air exposure and different drying temperatures. Moreover, the combination of different post-treatments was considered, such as vacuum drying and storage without vacuum. The most interesting results revealed that exposing the dried under vacuum by-product up to 48 h and 96 h in the drying chamber (low humidity conditions) did not alter the purity of $NaB(OH)_4$. When, drying the same by-product under a low temperature and high humidity environment tends to form pure $NaB(OH)_4 \cdot 2H_2O$, with consistent results observed. Nevertheless, it has a less practical interest than $NaB(OH)_4$.

Moreover, the regeneration of the sodium borohydride from its by-product was studied to close the $NaBH_4$-H_2 cycle. First, the mechano-chemical recycling of $NaB(OH)_4$ with MgH_2 was studied. Experiments were performed in a mixer mill with a grinding jar specifically designed to prevent H_2 leaks. Although the formation of $NaBH_4$ was not observed, $Mg(OH)_2$ was detected – an intermediate of the process, widely reported in literature –indicating that some reactant was converted. The electrochemical regeneration of $NaBH_4$ from boric acid ($B(OH)_3$) – a by-product of the $NaBH_4$ acidic hydrolysis was considered as an alternative route. CV experiments of the $B(OH)_3$ reduction to BH_4^- were performed for the first time, as far as the author is aware. A reduction peak associated to the borohydride formation was observed at the expected potential range; however, its formation was not confirmed when a physical RE was implemented in the cell. The experiments also showed that $B(OH)_3$ had a positive effect on the boron-doped diamond working electrode, by mitigating the hydrogen evolution reaction and widening its electrochemical window. This result opens the way to further continue this type of recycling alternative.

The work ended with an economic analysis of the hydrolysis of sodium borohydride to generate green H_2 and the by-product regeneration to the borohydride salt considering the up-to-date cost of reactants and the $NaBH_4$ recycling methods reported in literature. It was demonstrated that the electrochemical $NaBH_4$ regeneration is the most cost-effective promising type of process since the thermo- and mechano-chemical processes require the extraction of the borohydride, which tends to use a highly cost solvent. A cost comparison with other green H_2 production technologies indicates that the H_2 production from the hydrolysis of sodium borohydride can become competitive in the European/American market, however it is essential to further develop the cost analysis considering the energy and equipment costs in the future, as well as the valorization (recycling or commercial) of by-products such as MgO, which has a very high commercial interest. A last and very important conclusion that opens new paths for further increase in the TRL of this off-grid hydrogen generation system (with high potential for niche applications and maritime), is the strong possibility of considering the valorization of the $NaB(OH)_4$ - the hydrolysis by-product obtained in an extremely high purity level by using the patent protected by-product handling process, coming out of present work. This product has a very high commercial value and targets numerous applications which can contribute to make the process economically viable.

Keywords: Hydrogen; sodium borohydride; by-product of hydrolysis; $NaB(OH)_4$; regeneration; boric acid.

Resumo

O hidrogénio (H_2) é considerado um vetor energético com grande potencial sobretudo se for produzido a partir de eletricidade renovável (H_2 verde), podendo ser armazenado e transportado ou reconvertido para a rede quando necessário. No entanto, os sistemas de energia fora-da-rede são considerados como possível solução para fornecimento de energia em áreas/sectores onde as ligações tradicionais à rede não são viáveis ou não são rentáveis. O hidrogénio pode ser gerado a partir da hidrólise do borohidreto de sódio ($NaBH_4$) - um hidreto químico com elevado teor de H_2 - a temperatura moderada, com um grau de pureza muito elevado e pode ser diretamente convertido em energia elétrica. No entanto, a sua regeneração a partir do subproduto da reação de hidrólise é fundamental para o sucesso desta solução. O objetivo principal deste trabalho foi compreender que subproduto se forma na reação de hidrólise, como é que as condições de funcionamento podem influenciar a sua formação, otimizar o funcionamento de modo a produzir o(s) borato(s) com mais interesse, bem como o estudo de algumas alternativas para o processo de regeneração.

Pretendeu-se identificar o principal produto formado na reação de hidrólise e se o rearranjo do $NaBO_2 \bullet 2H_2O$ para $NaB(OH)_4$ estava dependente da presença ou não do aditivo carboximetilcelulose (CMC) ou de qualquer outro aditivo. O pós-tratamento padrão do subproduto após a extração do reator aplicado consistiu na secagem e armazenamento ao ar livre e à temperatura ambiente. Verificou-se com este tratamento que a formação de $NaB(OH)_4$ não foi exclusiva de experiências com aditivo CMC, mas é o principal subproduto de hidrólise. No entanto, foram também identificados boratos estruturalmente diferentes e outros compostos. A formação destes subprodutos pode ser explicada pela presença de ar – em particular CO_2 e H_2O – que reage lentamente com o borato, produzindo Na_2CO_3 e borax desidratado ($Na_2B_4O_7$). Para confirmar esta possibilidade, foi desenvolvido e implementado um novo processo inovador de manuseamento do subproduto, que evita ao máximo a sua exposição ao ar durante a secagem e armazenamento. Assim, após a extração do reator onde é realizada a hidrólise do $NaBH_4$, o subproduto foi seco num exsicador a vácuo e armazenado no seu interior, obtendo-se hidróxido de sódio bórico ($NaB(OH)_4$) puro ou quase puro – considerado o melhor borato para regenerar $NaBH_4$. Realizou-se um conjunto de experiências para confirmar este resultado e validar o método. Verificou-se a obtenção do $NaB(OH)_4$

aplicando o tratamento após a hidrólise realizada com excesso de água entre 6 e 15 e uma carga de catalisador de 0.2 a 0.4 g/g. O grau de inovação e os importantes resultados deste processo justificaram a elaboração de um pedido e registo de patente (patente provisória número 118331 T) na UP IN que se tornará em breve definitiva em Portugal e alargada internacionalmente.

O processo patenteado de pós-tratamento do subproduto da hidrólise foi desenvolvido e adaptado de forma a otimizar a formação de outros boratos, tais como a tincalconite e o $NaB(OH)_4 \bullet 2H_2O$. Assim, foram estudados outros pós-tratamentos, que consideraram o efeito da secagem numa estufa (baixa humidade), exposição limitada ao ar e secagem a alta e baixa temperaturas. Processaram-se ainda os subprodutos através de uma combinação entre vários tratamentos, tais como secagem a vácuo e armazenamento sem vácuo. Os resultados mais interessantes revelaram que a exposição do subproduto seco sob vácuo até 48 h e 96 h na câmara de secagem (condições de baixa humidade) não alterou a pureza do $NaB(OH)_4$. A secagem do mesmo subproduto a baixa temperatura e alta humidade tende a formar $NaB(OH)_4 \bullet 2H_2O$ com resultados consistentes. Contudo este composto tem menor interesse prático do que o $NaB(OH)_4$.

Numa segunda fase do trabalho, estudaram-se alguns processos de regeneração. O processo de "ball milling" de $NaB(OH)_4$ com MgH_2 foi efetuado num moinho com um vaso de moagem especificamente desenhado para evitar fugas de H_2. Apesar de não se ter verificado a formação do borohidreto, identificou-se o composto $Mg(OH)_2$ – intermediário do processo de regeneração largamente reportado na literatura - resultado que indica que algum reagente foi convertido.

Estudou-se igualmente a regeneração eletroquímica a partir do ácido bórico ($B(OH)_3$), um subproduto da hidrólise ácida do $NaBH_4$. As experiências de voltametria cíclica de redução do $B(OH)_3$ para BH_4^- foram realizadas pela primeira vez tanto quanto o autor tem conhecimento. Foi observado um pico de redução na gama de potencial esperado para a formação do borohidreto. Contudo, a presença deste pico não se confirmou quando um elétrodo de referência foi implementado na célula. Foi igualmente constatado que a presença de $B(OH)_3$ teve um efeito positivo no elétrodo de boro dopado de diamante, já que mitigou a reação de evolução do hidrogénio e alargou a sua janela eletroquímica.

Estes resultados abrem um caminho para continuar a desenvolver este tipo de processo de reciclabilidade.

O trabalho terminou com uma análise económica ao processo de produção de H_2 a partir da hidrólise do borohidreto de sódio e à regeneração dos subprodutos de novo até ao sal, considerando os custos atualizados dos reagentes envolvidos nos processos. Foi demonstrado que a regeneração eletroquímica (em que produção de H_2 e regeneração do borohidreto ocorrem em simultâneo) é o tipo de processo mais rentável e promissor, uma vez que os processos termo- e mecano-químicos requerem a extração do borohidreto, que tende a utilizar um solvente de alto custo. Foi também apresentada uma comparação de custos com outras tecnologias de produção H_2 verde. Esta comparação indicou que a produção de H_2 a partir da hidrólise do borohidreto de sódio pode tornar-se competitiva no mercado europeu/americano, contudo é essencial incorporar na análise de custos, os custos energéticos, de equipamento, bem como a valorização (por reciclagem ou venda) dos subprodutos como o MgO. Uma última e muito importante conclusão que abre novos caminhos para um maior aumento do nível de maturação tecnológica (TRL) deste sistema de geração de hidrogénio fora-da-rede (com elevado potencial para aplicações no setor marítimo), é a forte possibilidade de se considerar a valorização do subproduto da reação de hidrólise, $NaB(OH)_4$, obtido com um grau de pureza extremamente elevado através, da utilização do processo de pós-tratamento do subproduto, protegido pela patente. Este produto tem um valor comercial muito elevado e visa numerosas aplicações que podem contribuir para tornar o processo economicamente viável.

Palavras-chave: Hidrogénio; borohidreto de sódio; subproduto da hidrólise; $NaB(OH)_4$; regeneração; ácido bórico.

List of publications/contributions in the scope of this thesis

- Nunes, H.X.*; Silva, D.L.*; Rangel, C.M.; Pinto, A.M.F.R. Rehydrogenation of Sodium Borates to Close the NaBH4-H2 Cycle: A Review. Energies 2021, 14, 3567. https://doi.org/10.3390/en14123567
  (equal contribution)

Contribution: Conceptualization, H.X. Nunes and D.L. Silva; writing - original draft preparation, H.X. Nunes and D.L. Silva; writing – review and editing, C.M. Rangel and A.M.F.R. Pinto; supervision - C.M. Rangel and A.M.F.R. Pinto; Fund acquisition, C.M. Rangel and A.M.F.R. Pinto

- Method to process borate by-products from sodium borohydride hydrolysis (2022, Dec 22). Patent no. 118331 T
  Inventors: Alexandra Rodrigues Pinto, Diogo Silva, Hélder Nunes, Lucas Marcon and Cármen Rangel

Contribution: experimental data acquisition: Diogo Silva and Hélder Nunes; writting - original draft preparation: Diogo Silva and Hélder Nunes; writting – review and editing: Lucas Marcon, Cármen Rangel and Alexandra Pinto; supervision: Alexandra Pinto; Fund acquisition: Cármen Rangel and Alexandra Pinto.

- Gómez-Coma, L.; Silva, D.L.; Ortiz, A.; Rangel, C.M.; Ortiz-Martínez, V.M.; Pinto, A.M.F.R.; Ortiz, I. Sustainable Additives for the Production of Hydrogen via Sodium Borohydride Hydrolysis. Appl. Sci. 2023, 13, 6995. https://doi.org/10.3390/app13126995

Contribution: experimental data acquisition: L. Gómez-Coma and D.L. Silva; writting - original draft preparation: L. Gómez-Coma; writting – review and editing: D.L. Silva, A. Ortiz, V.M. Ortiz-Martínez, A.M.F.R. Pinto and I. Ortiz; supervision: A.M.F.R. Pinto; Fund acquisition: I. Ortiz, C.M. Rangel, A. Ortiz and A.M.F.R. Pinto.

Supervisor: Alexandra Rodrigues Pinto

Professora Doutora Alexandra Maria Pinheiro da Silva Ferreira Rodrigues Pinto

PhD student: Diogo Silva

Diogo Luís Almeida Silva

Acknowledgments

First, I want to thank my supervisor, professor Alexandra Pinto, for giving me the opportunity to be here writing this thesis and for all the support along the last years.

Then, Hélder Nunes and Lucas Marcon, for the support during my experiments, and particularly, for always staying positive and optimist.

For the CEFT and particularly the E206, for making my work more fun and enjoyable and for all the general support when I needed it.

For the LEPABE, that allow me to use their centrifuge and LSRE-LCM that allowed me to use their ball miller.

For my friends and family, since these years, it was essential to have moments outside work to relax and recharge.

Also, I want to thank the most important person for me, my wife Catarina Moreira, because this journey has not been made alone and for all the support and joy that you bring to my world.

At last, I would like to thank all the financial support that contributed to developed of this thesis. This work was financially supported by LA/P/0045/2020 (ALiCE), UIDB/00532/2020 and UIDP/00532/2020 (CEFT), funded by national funds through FCT/MCTES (PIDDAC). Also, this work is supported by the Fundo Europeu de Desenvolvimento Regional (FEDER)" through the Programa Operacional Regional do Norte (NORTE2020) "HyGreen&LowEmissions - Tackling Climate Change Impacts: the role of Green Hydrogen production, storage and use, together with low emissions energy systems" (NORTE-01-0145-FEDER-000077) and by Interreg Atlantic Area under the HYLANTIC Project – Atlantic Network for Renewable Generation and Supply of Hydrogen to promote High Efficiency (EAPA_204/2016). FEDER also supported this work via CEFT.





Contents

1. Introduction 1
1.1. Current status on energy sources and demand 1
1.2. Hydrogen as an energy vector with strong potential 3
1.3. Hydrogen generation and storage 5
1.4. Sodium borohydride as a hydrogen carrier 8
2. State of the art 13
2.1. Hydrolysis of sodium borohydride for hydrogen – energy applications 13
2.1.1. Catalyst 13
2.1.2. Alkaline hydrolysis 14
2.1.3. Reactor geometry and excess of water 16
2.1.4. Additives 18
2.1.5. Fuel cell applications 18
2.2. Hydrolysis of sodium borohydride by-product 19
2.2.1. By-products reported in literature 20
2.2.2. Quantitative analysis of the by-product composition 22
2.3. Rehydrogenation of sodium borates to close the $NaBH_4$-H_2 cycle 25
2.3.1. Thermo-chemical processes 29
2.3.2. Mechano-chemical processes 34
2.3.3. Electrochemical processes 44
2.4. Motivation and thesis layout 51
3. Experimental study of the by-product of sodium borohydride hydrolysis 55
3.1. Influence of additives on the by-product 55
3.1.1. Experimental procedure 56
3.1.2. Results and Discussion 62
3.2. Innovative handling process of the by-product of sodium borohydride hydrolysis 67

3.2.1. Experimental procedure 68
3.2.2. Results and discussion 71
3.3. Implementation of other by-product handling processes to optimize the by-product composition 80
3.3.1. Experimental procedure 81
3.3.2. Results and Discussion 83
3.4. Conclusions 94
4. Experimental study of the regeneration process of the borates to sodium borohydride 97
4.1. Ball milling of the $NaB(OH)_4$ back to sodium borohydride 97
4.1.1. Experimental procedure 98
4.1.2. Results and discussion 103
4.2. Electrochemical synthesis of $NaBH_4$ from boric acid 112
4.2.1. Experimental procedure 113
4.2.2. Results and discussion 117
4.3. Conclusions 128
5. $NaBH_4$-H_2 Economic analysis 129
5.1. Analysis procedure and general considerations 129
5.2. Results and discussion 133
5.3. Conclusions 143
6. Main conclusions and future work 145
7. Follow-up work 149
References 151
Appendix A – Patent no. 118331 T 167

Index of Figures

Figure 1.1. Supply risk of raw materials in EU (a) and corresponding key technologies (b) [9]. 3

Figure 1.2. Density of main energy fuels [12]. 4

Figure 1.2. Global H_2 production source distribution [14]. 6

Figure 1.3. H_2 production per source in 2021 and projections for 2030 and 2050 [14]. . 7

Figure 1.4. Share of access to electricity in 2020 (adapted from [17]). 7

Figure 2.1. Effect of excess of water *x* on the gravimetric Hydrogen storage capacity, adapted from [29]. 16

Figure 2.2. Simplification of the reactions occurring inside a Proton Exchange Membrane fuel cell [45]..... 19

Figure 2.3. Demonstration of the XRD characterization technique [57]..... 23

Figure 2.4. X-ray diffractometer and its main components [58]. 23

Figure 2.5. Michelson's interferometer of a FT-IR spectroscopy characterization technique[62]. 24

Figure 2.6. Example of an interferogram based on FT-IR characterization technique [65]. 25

Figure 2.8. The Brown and Schlesinger process for the $NaBH_4$ production. 26

Figure 2.9. Topics of research articles and their impact on the regeneration of $NaBH_4$, from 2014 to 2021 [71]..... 27

Figure 2.10. Timeline of published articles dedicated to $NaBH_4$ regeneration [71]. 28

Figure 2.11. Infographic view of the type of process reported in the research articles, published since 2000, dedicated to $NaBH_4$ regeneration [71]..... 28

Figure 2.12. Reported yields for $NaBH_4$ regeneration through thermochemical processes (legend: open circles - temperature; closed circles – pressure. Closed and open circles in the same horizontal level correspond to the same paper (same yield)) [71]. 31

Figure 2.13. $NaBH_4$ yield vs a) Temperature T and b) Pressure P for 1 h reaction [86]. 32

Figure 2.14. Values of $NaBH_4$ yield vs $NaBO_2/Na_2O$ molar ratio [74]. 33

Figure 2.15. Example of ball mill [96]. 34

Figure 2.16. Representation of mechanochemical process [97]. 35

Figure 2.17. Reported yields for $NaBH_4$ regeneration through mechano-chemical processes (legend: closed circles - time of milling; open circles - year of publication. Closed and open circles in the same horizontal level correspond to the same paper (same yield)) [71]. 37

Figure 2.18. $NaBH_4$ yield vs. t without (left) and with (right) CH_3OH. Adapted from [53]. 38

Figure 2.19. Influence of t of milling (left) and MgH_2 excess (right) in the $NaBH_4$ yield, adapted from [111]. 43

Figure 2.20. Additive influence on the $NaBH_4$ yield, adapted from [69]. 43

Figure 2.21. Scheme of an Electrochemical cell (adapted from [115]). 45

Figure 2.22. Polarization curve and types of losses [120]. 46

Figure 2.23. Example of a CV analysis [121]. 47

Figure 2.24. Desulfurization efficiency for the electrode combinations studied (adapted from [126]). 49

Figure 2.25. Constant vs pulse voltage impact on the desulfurization efficiency (adapted from [127]). 50

Figure 3.1. Cylindrical reactor and conical and planar shape bases used in hydrolysis experiments. 56

Figure 3.2. Egg shaped reactor used in hydrolysis experiments. 57

Figure 3.3. Experimental P-T curves of a typical hydrolysis reaction. 58

Figure 3.4. XRD patterns of the by-products of hydrolysis experiments #30 to #34 after post-treatment 2. 75

Figure 3.5. XRD patterns of the by-product of hydrolysis experiments #34 after post-treatments 1 (a) and 2 (b) [131]. 76

Figure 3.6. Influence of additive SDS on the by-product composition from FTIR patterns of the by-products of hydrolysis experiments #36/37 (no additive) and #42 (0.25 % SDS). 78

Figure 3.7. XRD patterns of the by-product #49 composition considering post-treatment 2 (a), vacuum drying and open-to-air storage (b) and vacuum drying, open-to-air exposure and desiccator storage in vacuum (c). 85

Figure 3.8. XRD patterns of the by-product #50 composition considering post-treatment 1, samples 1 (a) and 2 (b) and post-treatment 2, samples 1 (c) and 2 (d). 86

Figure 3.9. XRD patterns of the by-product #52 considering post-treatment 1 (a), open-to-air drying, storage in vacuum and exposure in the drying chamber for 24 h (b), 48 h (c), 72 h (d) and 96 h (e), post-treatment 3 (f) and by-product drying in the drying chamber and storage in vacuum (g). 89

Figure 3.10. XRD patterns of by-products #30 to #34 and #57, considering their low temperature drying (post-treatment 6). 92

Figure 3.11. XRD patterns of the by-product #34 considering post-treatment 1 (a) and 6 (b). 93

Figure 3.12. Effect of the exposure conditions of the by-product of $NaBH_4$ hydrolysis on its composition (legend: a. drying, b. post-drying, c. storage). 94

Figure 4.1. Photograph of the original grinding jar (white) and jar built in this work (stainless-steel) for the ball milling experiments to recycle $NaB(OH)_4$ back to $NaBH_4$.99

Figure 4.2. Grinding jar (a) and 2D design (left small part in b and right bigger part of the jar in c) used in the ball milling experiments to recycle $NaB(OH)_4$ back to $NaBH_4$. 100

Figure 4.3. Visual representation of the experimental procedure performed for the study of the recycling of the $NaBH_4$ hydrolysis by-product (from post-treatment 2 for this example). 102

Figure 4.4. XRD pattern of by-product composition before and after ball milling 1.0 g of borate (x = 16, post-treatment 1) with 0.8 g of MgH_2 (experiment #4). 105

Figure 4.5. XRD pattern of by-product composition in each step of ball milling 1.0 g of borate (x = 11, post-treatment 1) with 0.8 g of MgH_2 (experiment #5). 107

Figure 4.6. XRD pattern of by-product composition in each step of ball milling 1.0 g of borate (x = 15, post-treatment 2) with 0.8 g of MgH_2 (experiment #6). 109

Figure 4.7. Electrochemical installation considered for the electrochemical experiments performed (the difference between the figure is on the atmosphere inside the cell: left - air exposure; right – N_2 bubbling). 114

Figure 4.8. Boron electrochemical window and its dependence on pH and potential applied [135]. 115

Figure 4.9. $NaBH_4/H_2$ cycle considering the electrochemical recycling of boric acid. 116

Figure 4.10. CV tests performed for 0.2 M and 1 M boric acid under 4 M acetic acid based on electrochemical experiment #1. 118

Figure 4.11. CV tests performed for 1 M boric acid under 4 M acetic acid based on electrochemical experiment #2. 118

Figure 4.12. CV tests performed for 0.16 M (tests 1 – 7) and 0.32 M (tests 8 – 11) boric acid under 5 M acetic acid based on electrochemical experiment #3. 120

Figure 4.13. CV tests 0 – 2 performed for 0.2 M boric acid under 5 M acetic acid based on electrochemical experiment #4. 121

Figure 4.14. CV tests performed for 0.2 M (1 – 8) and 0.4 M (9 – 14) boric acid under 5 M acetic acid based on electrochemical experiment #4. 122

Figure 4.15. CV tests performed for 0.2 M (1 – 8) and 0.4 M boric acid (9 – 14) under 5 M acetic acid based on electrochemical experiment #4. 123

Figure 4.16. CV tests performed for 0.16 M (2 and 3), 0.32 M (4 and 5) and 0.48 M boric acid (7 and 8) under 5 M acetic acid based on electrochemical experiment #5. 124

Figure 4.17. CV tests performed for 0.03 M (3 and 4) and 0.06 M boric acid (5 and 6) under 5 M sulfuric acid based on electrochemical experiment #6, considering a Ti CE. 126

Figure 4.18. CV tests performed for 0.03 M (8 and 9) and 0.06 M boric acid (10 and 11) under 5 M sulfuric acid based on electrochemical experiment #6, considering a Ni CE. 126

Figure 4.19. CV tests performed for 0.03 M (13 - 15) and 0.06 M boric acid (16 and 17) under 5 M sulfuric acid based on electrochemical experiment #6, considering a RuO2 coated Ti CE. 126

Figure 4.20. CV tests performed for 0.03 M (20 and 21) and 0.06 M boric acid (22 and 23) under 5 M sulfuric acid based on electrochemical experiment #6, considering a IrO2 coated Ti CE. 127

Figure 5.1. Cost to regenerate $NaBH_4$ for the different thermo- (T), mechano- (M) and electrochemical (E) processes. 134

Figure 5.2. Cost to generate H_2 considering a 10 % $NaBH_4$ hydrolysis for the different thermo- (T), mechano- (M) and electrochemical (E) processes. 135

Figure 5.3. Cost to generate H_2, with and without (green bars) extraction of $NaBH_4$ considering a 10 % $NaBH_4$ hydrolysis for the different thermo- (T), mechano- (M) and electrochemical (E) processes. 136

Figure 5.4. Cost to generate H_2 for: 13 % (up) and 20 % (down) $NaBH_4$ hydrolysis for the different thermo- (T), mechano- (M) and electrochemical (E) processes. 137

Figure 5.5. Cost to generate H_2, with and without (green bars) extraction of $NaBH_4$ for 13 % (a) and 20 % (b) $NaBH_4$ hydrolysis for the different thermo- (T), mechano- (M) and electrochemical (E) processes. 138

Figure 5.6. Cost to regenerate $NaBH_4$ using M4 method with different extraction solvents. 140

Figure 5.7. Cost to generate H_2 using M4 method with different extraction solvents and influence of the $NaBH_4$ commercial cost (lower: CH; higher: EU). 141

Figure 5.8. Green H_2 production cost gap and variation with location (Europe (EU), America (AM) and Asia (AS)) as well as H_2 production cost from the $NaBH_4$ hydrolysis [141]. 142

Figure A.1: Schematic representation of an embodiment of a hydrogen synthesis method comprising the disclosed method to recover the borate by-product (1). 172

Figure A.2: Embodiment of the separation of the by-product by sedimentation of the catalyst. 173

Figure A.3: Embodiment of the by-product appearance after drying. 173

Figure A.4: Embodiment of results of by-product comparison (in mass %) between air exposure or vacuum drying. 173

Figure A.5: Embodiment of the hydrolysis' by-product composition (in mass %) under vacuum drying, for four different samples (numbered as 1,2,3 and 4). 173

Figure A.6: Embodiment of X-ray powder diffraction spectra for $NaB(OH)_4$ obtained by common drying process (“common drying”) or by the method described in the present disclosure (“present disclosure”). 173

Index of Tables

Table 1.1. Main properties of H_2 and common fuels [13]. 5

Table 1.2. DoE's H_2 targets evolution since 2010 for on-board vehicle storage and to small and medium power portable equipment [26]–[29][27], [28]. 10

Table 2.1. Some of catalysts with highest HGR reported for the hydrolysis of $NaBH_4$.14

Table 2.2. Studies performed on the NaOH concentration optimization. (MW-microwave environment). 15

Table 2.3. Influence of the reactor geometry and *x* on the H_2 generation from the $NaBH_4$ hydrolysis. 17

Table 2.4. By-product composition of $NaBH_4$ hydrolysis reported in literature. 20

Table 2.5. Higher-yield reports on the thermo-chemical regeneration of $NaBH_4$. 30

Table 2.6. Higher-yield reports on the mechanochemical regeneration of $NaBH_4$. 36

Table 3.1. Operating conditions of the hydrolysis experiments containing up to 0.15 % PAA and 1.0 % CMC additives and excess of water ($11 < x < 16$). 60

Table 3.2. Operating conditions varied in each hydrolysis experiment performed (#1 to 22), while maintain remaining parameters, for analysis of the influence of each parameter studied. 61

Table 3.3. Performance of each hydrolysis experiment performed, by analysis of the H_2 yield, generation rate (HGR), induction time and storage densities (GHSC and VHSC). 62

Table 3.4. Influence of the CMC additive on the by-product, through the XRD analysis of the by-products composition (in weight percentage) of hydrolysis experiments #1 and #2 (no additive), #3 and #4 (0.25 % CMC) and #5-8 (1.0 % CMC). 64

Table 3.5. Study of by-product of $NaBH_4$ hydrolysis with additive PAM, through the XRD analysis of the by-product's composition (in weight percentage) of hydrolysis experiments #12 to #14 (0.10 % PAA). 64

Table 3.6. Influence of the Ni-Ru catalyst on the by-product, through the XRD analysis of by-products composition (in weight percentage) of hydrolysis experiments #15 to #17 (Ni-Ru foam) and #18 (Ni-Ru powder) with a 0.01 Ni-Ru/NaBH4 mass ratio. 65

Table 3.7. Influence of excess of water *x* on the by-product, through the XRD analysis of by-products composition (in weight percentage) of hydrolysis experiments #19/20 (*x* = 11) and #21/22 (*x* = 16). 66

Table 3.8. Operating conditions of the hydrolysis experiments containing up to 1.0 % CMC, 1.0 % BCD and 0.25 % SDS additives and excess of water ($6 < x < 16$) and post-treatments performed on each by-product formed (*catalyst acidic treatment). 70

Table 3.9. Operating conditions varied in each hydrolysis experiment performed (#23 to 49), while maintain remaining parameters, for analysis of the influence of each parameter studied. 71

Table 3.10. Performance of each hydrolysis experiment performed, by analysis of the H2 yield, generation rate (HGR), induction time and storage densities (GHSC and VHSC) (*catalyst acidic treatment). 72

Table 3.11. By-product composition of hydrolysis experiments #23 to #29 from XRD analysis after post-treatment 1. 74

Table 3.12. By-product composition (in weight percentage) of hydrolysis experiments #30 to #34 from XRD analysis after post-treatment 2. 74

Table 3.13. By-product composition (in weight percentage) of hydrolysis experiment #34 from XRD analysis after post-treatments 1 and 2 [131]. 75

Table 3.14. By-product composition (in weight percentage) of hydrolysis experiments #30 to #33 from XRD reanalysis after post-treatments 1 and 2. 77

Table 3.15. Influence of additives CMC and BCD on the by-product, through the XRD analysis of the by-product composition (in weight percentage) of hydrolysis experiments #35 (no additive), #38 and #39 (0.25 % CMC), #40 (1.0 % CMC) and #41 (1.0 % BCD). 78

Table 3.16. Influence of additive SDS on the by-product, through the FTIR analysis of the by-product composition of hydrolysis experiments #36/37 (no additive) and #42 (0.25 % SDS). 78

Table 3.17. Influence of excess of water *x* on the by-product, through the XRD analysis of the by-product composition (in weight percentage) of hydrolysis experiments #43 and #44 (*x* = 11) and #45 (*x* = 6). 79

Table 3.18. Influence of catalyst loading on the by-product, through the XRD analysis of the by-product composition (in weight percentage) of hydrolysis experiments #46 and #47 (0.20 g/g) and #48 (0.05 g/g). 80

Table 3.19. Description of the conditions and equipment used in each post-treatment performed to the by-product. 82

Table 3.20. Operating conditions of the hydrolysis experiments containing up to 1.0 % additive CMC and excess of water (x = 6 or 15) and post-treatments performed on each by-product formed. 82

Table 3.21. Performance of each hydrolysis experiment performed, by analysis of the H_2 yield, generation rate (HGR), induction time and storage densities (GHSC and VHSC). 83

Table 3.22. By-product composition of hydrolysis experiment #49 (in weight percentage) from XRD analysis after post-treatment 2, after dried in vacuum (post-treatment 2) and exposed and stored open-to-air and after dried in vacuum (post-treatment 2) exposed to air and stored in vacuum. 84

Table 3.23. By-product composition of experiment #50 composition (in weight percentage) from XRD reanalysis after post-treatment 1 (samples 1 -1 and 1 – 2) and after post-treatment 3 (samples 3 -1 and 3 – 2). 85

Table 3.24. By-product #50 composition (in weight percentage) from XRD reanalysis after post-treatments 1 and 3. 87

Table 3.25. By-product composition of hydrolysis experiment #51 (in weight percentage) from XRD analysis after post-treatment 1 and after dried in the drying chamber (post-treatment 3) stored in vacuum and stored open-to-air. 87

Table 3.26. By-product composition of hydrolysis experiment #52 (in weight percentage) from XRD analysis after post-treatment 1, after dried open-to-air (post-treatment 1) with exposure after dry in the drying chamber for 24 h (b,1), 48 h (b,2), 72 h (b,3) and 96 h (b,4) all with storage in vacuum, after post-treatment 3 and after dried and exposed in the drying chamber (post-treatment 3) with vacuum storage. 88

Table 3.27. By-product composition of hydrolysis experiment #53 (in weight percentage) from XRD analysis after post-treatment 2 and after dried in vacuum (post-treatment 2)

with exposure after dry in the drying chamber for 24 h (b,1), 72 h (b,2), 96 h (b,3) all with storage in vacuum. 90

Table 3.28. By-product composition of hydrolysis experiment #54 (in weight percentage) from XRD analysis after post-treatments 2 and 4. 90

Table 3.29. By-product composition of hydrolysis experiments #55 and #56 (in weight percentage) from XRD analysis after post-treatments 1 (56 – 1), 4 (56 – 4) and 5 (55 – 5 and 56 – 5). 91

Table 3.30. By-product composition of hydrolysis experiment #30 to #34 and #57 (in weight percentage) from XRD analysis after post-treatment 6. 91

Table 3.31. By-product composition of hydrolysis experiment #34 (in weight percentage) from XRD reanalysis after post-treatments 1 and 6. 93

Table 4.1. Operating conditions of the hydrolysis experiments performed with excess of water ($11 < x < 16$) and post-treatments performed on each by-product formed. 98

Table 4.2. Operating conditions of the ball milling experiments performed: the mass of by-product, the mass of MgH_2, MgH_2/By-product molar ratio (* assuming 100 % borate), the ball to powder ratio (BPR), the mass of C_3H_9N and the type of filter used. 103

Table 4.3. Performance of each hydrolysis experiment performed given by analysis of the H_2 yield, generation rate (HGR), induction time and storage densities (GHSC and VHSC). 103

Table 4.4. Values obtained from XRD analysis of by-product composition before and after ball milling 1.0 g of borate ($x = 16$, post-treatment 1) with 0.8 g of MgH_2 (experiment #4). 104

Table 4.5. Values obtained from XRD analysis of by-product composition in each step of ball milling 1.0 g of borate ($x = 11$, post-treatment 1) with 0.8 g of MgH_2 (experiment #5). 106

Table 4.6. Values obtained from XRD analysis of by-product composition in each step of ball milling 1.0 g of borate ($x = 15$, post-treatment 2) with 0.8 g of MgH_2 (experiment #6). 108

Table 4.7. Operating conditions of ball milling applied to the borates formed through hydrolysis post-treatment 2 (experiments #6 and #7): mass of by-product, mass of MgH_2, ball to powder ratio (BPR), mass of C_3H_9N and type of sample storage. 110

Table 4.8. Values from XRD analysis of by-product composition in each step of ball milling 0.70 g of borate (x = 15, post-treatment 2) with 0.87 g of MgH_2 (experiment #7). 111

Table 4.9. Operating conditions of electrochemical experiments performed to study the $B(OH)_3$ recycling back to $NaBH_4$..... 117

Table 4.10. Operating conditions of electrochemical experiment #3 to study the $B(OH)_3$ recycling back to $NaBH_4$, under 5 M acetic acid electrolyte. 119

Table 4.11. Operating conditions of electrochemical experiment #4 to study the $B(OH)_3$ recycling back to $NaBH_4$ under 5 M acetic acid electrolyte. 121

Table 4.12. Operating conditions of electrochemical experiment #5 to study the $B(OH)_3$ recycling back to $NaBH_4$. 124

Table 4.13. Operating conditions of electrochemical experiment #6 to study the $B(OH)_3$ recycling back to $NaBH_4$. 125

Table 5.1. Methods considered for the $NaBH_4$-H_2 economic analysis (legend: T – thermochemical, M – mechanochemical, E – electrochemical). 130

Table 5.2. Lower market price of compounds considered in the hydrolysis/regeneration of $NaBH_4$. 132

Table 5.3. influence of the $NaBH_4$ concentration on the 1 kg H_2 generation cost through the hydrolysis of $NaBH_4$..... 133

Table A.1 – Literature review on the efficiency of borate re-hydrogenation. 168

Notation and glossary

a_i	Chemical activity of a compound	
d	Distance between crystal layers	m
E^0_{cell}	Standard cell potential	V
E_i	Potential	V
F	Faraday's constant	C mol^{-1}
GHSC	Gravimetric Hydrogen Storage Capacity	wt. %
HGR	Hydrogen generation rate	L min^{-1} g^{-1}_{cat}
HHV	Higher heating value	MJ/kg
n	Number of electrons	
P	Pressure	atm
R	Ideal gas constant	J $mol^{-1} K^{-1}$
T	Temperature	K
T0	Initial temperature	K
VHSC	Volumetric Hydrogen Storage Capacity	kg m^{-3}
$\Delta\hat{s}$	Variation of enthalpy	J K^{-1}
θ	Angle of ray incidence	
λ	Wavelength of a ray	m
v_i	Stoichiometric coefficient	

List of acronyms

BCD	Beta-cyclodextrin
BDD	Boron doped-diamond
CCUS	Carbon capture, utilization and storage

CE	Counter-electrode
CMC	Carboxymethyl cellulose
CN	Cellulose nitrate
CV	Cyclic voltammetry
Egg	Small reactor with shape of an egg
FT-IR	Fourier-transform Infrared spectrometry
HER	Hydrogen evolution reaction
IL	Ionic liquid
LR	Large reactor
NMR	Nuclear magnetic resonance
PAA	Polyacrylamide
PTFE	Polytetrafluoroethylene
PEMFC	Proton exchange membrane fuel cell
RE	Reference electrode
SDS	Sodium dodecyl sulfate
SHE	Standard Hydrogen Electrode
SRc	Small conical bottom reactor
TRL	Technology Readiness Level
TSR	Total sulfur removal
WE	Working electrode
x	Excess of water
XPS	X-ray photo-electron spectroscopy
XRD	X-ray diffraction

1. Introduction

This chapter gives an overview of the world's current energy status and introduces the importance of replacing the fossil fuels for clean energy sources. The hydrogen vector as a potential green alternative is here presented and a resume of its characteristics, production and storage is made. At the final section, the chemical hydrides, and more specifically, the sodium borohydride and its hydrolysis at room to moderate temperature, is described as a green off-grid and on-demand safe source of energy, to combat for example the lack of access to electricity in sub-Saharan Africa.

1.1. Current status on energy sources and demand

The recent years have introduced a new status on the energy sources and demand. If in one hand the covid-19 pandemic lockdown in early 2020 decreased the electricity demand, it quickly recovered and surpassed pre-covid levels close to the end of the same year and then, in 2022, the Russian-Ukraine war aggravated the world's energetic instability, negatively affecting the progress made till then to stabilize [1], [2].

Russia is the world's largest exporter of fossil fuels and the Europe's ban due to the war has ruptured the Russia-Europe flows, believed to be permanent. With this, inflation has increased, particularly in the energy sector, exposing consumers to higher bills and supply shortages. Extra gas storage, alternative imports and lower demand measures were introduced to overcome the 2022-2023 winter. Nevertheless, outside the EU, the effects of this energy crisis are even higher: it is expected that at least 70 million people who recently gained access to electricity will likely lose the ability to afford that access. In fact, this increase is the first to be reported since 2000, stopping the progress that was made, mainly in the sub-Saharan Africa and developing countries in Asia. Moreover, around 100 million people will lose access to clean fuels for cooking, exposing them to health risks. And the winter of 2023-24 is expected to be even tougher [1].

In the middle of a crisis, drivers for new solutions must be urgently adopted. In this energy crisis, the reduced access to Russia's fossil fuels supply, must be counter-balanced by investments in other energy sources. And since the world has been exposed to an overall increase of the planet's average temperature due to increased CO_2 emissions, clean

electricity production and distribution must increase in the near future. Moreover, they are considered to be enough to surpass the global electricity demand [1].

In the today's private market and investors, for every dollar spent globally on fossil fuels, 1.5 dollars are spent on clean energy technologies (supply, efficiency and end-use), with this clean energy focus visible since only 2021. By 2030, this ratio is expected to increase to 5 dollars on clean energy supply and 4 dollars on efficiency and end-uses. However, this is not enough. A rise of around 2.5 °C in the global average temperatures is expected by 2100. Almost 650 billion dollars are spent each year on upstream oil and natural gas and the highest annual rise in CO_2 emissions has been reported in 2021, reaching 36.6 Gt CO_2 that year [1].

A 1.5 °C stabilization in the rise in global average temperatures, alongside universal access to modern energy by 2030 was agreed [3] and the countries have in general implemented measures to achieve this objective. The Japan's Green Transformation program [4] provides a major funding boost for technologies including nuclear, hydrogen and ammonia. South Korea is looking to increase the share of nuclear and renewables in its energy mix [5]. The European Union has banned fossil fuel car selling after 2035 [6] and India has established a target of 500 GW in 2030 for its domestic renewable capacity and that two-thirds of the country's electricity demand must be obtained from renewable sources.

Still, the share of fossil fuels in the global energy mix is 80% (with a higher dependence in Africa, Asia and Oceania [7]) and it is predicted to decrease only to 75% by 2030 and to 60% by 2050. Moreover, China is the only developed country significantly investing in clean energy each year in emerging and developing economies since the Paris Agreement in 2015 [1].

Moreover, demand for critical minerals for clean energy technologies is set to more than double in 2030, for example, Si and Ag for solar photovoltaic panels and Li for batteries [1], although almost half of the raw materials available (30) are in critical supply risk, including Li and Si [8]. The list of raw materials and their supply risk and key technologies is presented in Figure 1.1.

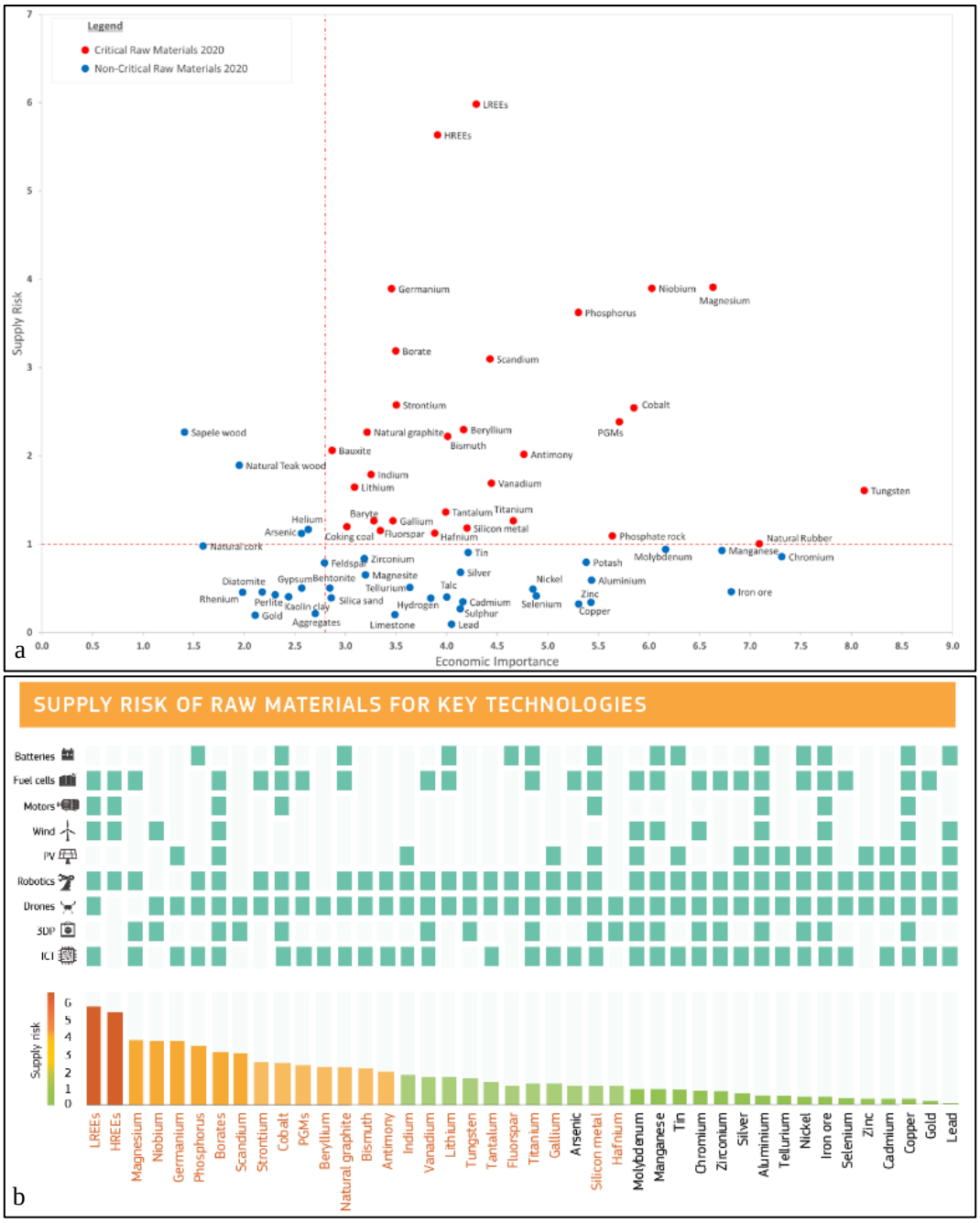


Figure 1.1. Supply risk of raw materials in EU (a) and corresponding key technologies (b) [9].

For all these matters, it is essential to find clean energy sources that allow clean electricity supply without compromising the planet's available sources. This is where Hydrogen can enter the scene.

1.2. Hydrogen as an energy vector with strong potential

Hydrogen (H_2) has been considered an energy vector with strong potential. It is the most abundant element in the universe, with around 75 % of all matter, while also being by far the lightest element in the universe [10]. Moreover, it is colorless, odorless and found

everywhere [11]. Figure 1.2 provides the volumetric and gravimetric densities of the main fuels. As observed, H_2 has the highest gravimetric density (120 MJ/kg), almost three times higher than diesel and gasoline.

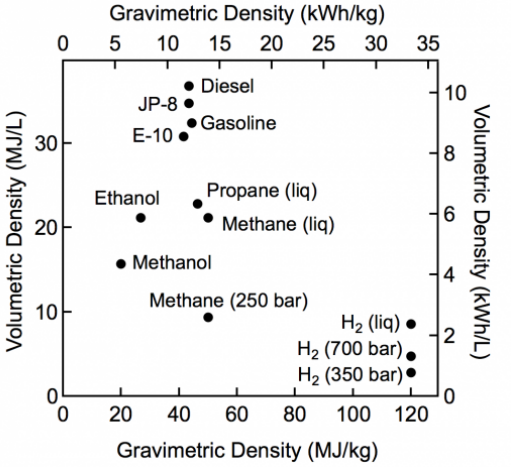


Figure 1.2. Density of main energy fuels [12].

Despite its clear advantages compared to other fuels, Hydrogen presents important drawbacks that has limited its influence: it has one of the lowest volumetric densities, it is not found in its molecular form and it is lighter than air and flammable, which hardens its storage and handle in safe conditions [2]. Table 1.1 presents, in detail, the main properties of hydrogen, as well as common fuels. From the properties described, we note the low vapor specific gravity and density as well as flash and boiling points. On the other hand, the specific heat and flame velocity of H_2 are higher than the other fuels. These properties presented indicate that despite its higher calorific power, careful handling and safety of hydrogen is necessary.

Table 1.1. Main properties of H_2 and common fuels [13].

Property (unit)	Hydrogen	Methane	Propane	Methanol	Ethanol	Gasoline
Molecular mass (g/mol)	2.02	16.04	44.1	32.04	46.07	100 - 105
Vapor specific gravity (air = 1)	0.0696	0.555	1.55	-	-	3.66
Density (kg/m^3)	0.0838	0.668	1.87	791	789	751
Viscosity (g/cm-s)	$8.8x10^{-5}$	$1.1x10^{-4}$	$8.0x10^{-5}$	$9.2x10^{-3}$	$1.2x10^{-2}$	$3.7x10^{-3}$-$4.4x10^{-3}$
Specific heat, Cp (kJ/(kg·K)	14.29	2.23	2.40	2.63	2.72	2.22
Boiling point (K)	20.15	111.15	231.05	337.65	351.65	300.15 - 498.15
Flash point (K)	20.15	85.15	169.15	284.15	286.15	230.15
Max flame velocity in air (m/s)	2.83	0.45	0.46	-	-	-

1.3. Hydrogen generation and storage

EU's H_2 demand has been predicted to achieve 30 Mt in 2030 and increase even further to 100 Mt in 2050. From those 100 Mt, 50 Mt are dedicated to the transportation and 45 Mt to industrial applications. Remaining 5 Mt will be used on combined, buildings and power generation. This H_2 is expected to be produced from renewable sources, which include biomass combustion and electrolysis, and from fossil fuels technologies with carbon capture and storage or pyrolysis. From these methods, electrolysis is considered the main one, corresponding to more than 70 Mt of H_2 predicted production in 2050 (1.600 GW of electrolyzers installed). However, electrolysis can only be considered green if the electric energy is obtained from renewable sources. For that, 1.800 GW of solar and wind capacities are expected to be installed until 2050.

Today, H_2 is considered as one of the main energy vectors with higher potential to replace fossil fuels. It is a fuel already established in the industry, however, with the need to reduce the carbon emissions to the atmosphere, its investments have been increasing each year in its green production (mainly USA, China and EU). Figure 1.2 presents the main methods used to produce hydrogen. As observed, H_2 is mainly produced from natural gas without carbon capture, utilization and storage (CCUS), followed by coal gasification and as by-product of other processes such as naphtha reforming and less than 1 % is generated

with low-emission methods (0.70 % fossil fuels with CCUS and 0.04 % water electrolysis). Nevertheless, although only 35 kt of H_2 were produced from water electrolysis, there has been an increase of 20 % compared to 2020. And this value percentage is related to electric energy coming exclusive from renewable source (compared to the tradition 4 % associated with all sources of electric energy).

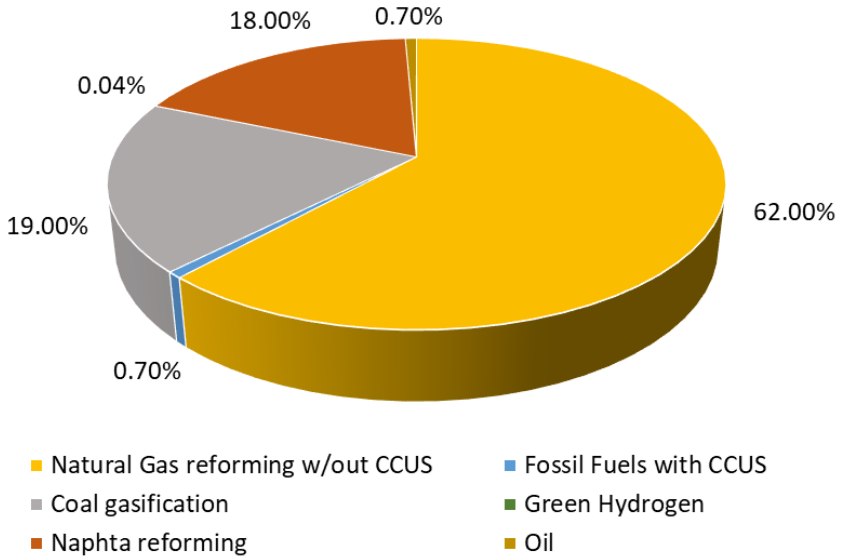


Figure 1.2. Global H_2 production source distribution [14].

To increase the H_2 production from low-carbon or green technologies it is essential to achieve comparative costs compared to the fossil fuels. 2021 H_2 production range costs as well as projections for 2030 and 2050 are presented in Figure 1.3. We observe that for natural gas, the current costs are higher with CCUS, as well as projections for 2030 and 2050. On the other hand, H_2 production from coal is and is expected to always be cheaper with CCUS. Regarding green H_2, its production costs predicted for 2030 and 2050 varies significantly with the source of electricity. Onshore and offshore wind electricity is similar, however solar photovoltaic (PV) is the cheapest of the three. At last, nuclear costs are the highest of all the sources analyzed. Nevertheless, these costs were determined before the Russian-Ukrainian war and their effects on the fossil fuel global market [14].

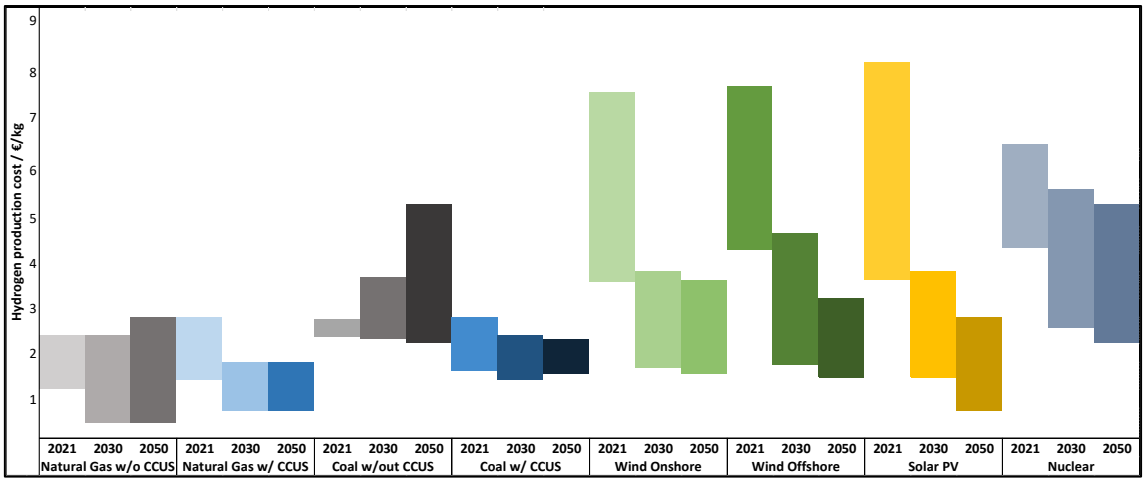


Figure 1.3. H_2 production per source in 2021 and projections for 2030 and 2050 [14].

As for the hydrogen storage, it is normally stored in high-pressure tanks, under pressures of up to 700 bar [15] or in liquid state at temperatures below -253 ºC. Although there have been significant improvements, this type of storage is still a challenge. Moreover, this is not the solution for decentralized energy generation – for example, in the maritime sector - or in places where there is a lack of access to electricity. Figure 1.4 presents the rate of access to electricity estimated in 2020 [16]. In the figure, limited access to electricity is observed almost only in Africa. In fact, it is clear that in the central region of Africa (Niger, Chad, Central African Republic, Zaire and South Sudan) less than 20 % had access. For this matter, new methods to generate and store H_2 are needed, while reducing its cost and increasing its safety [4], [5].

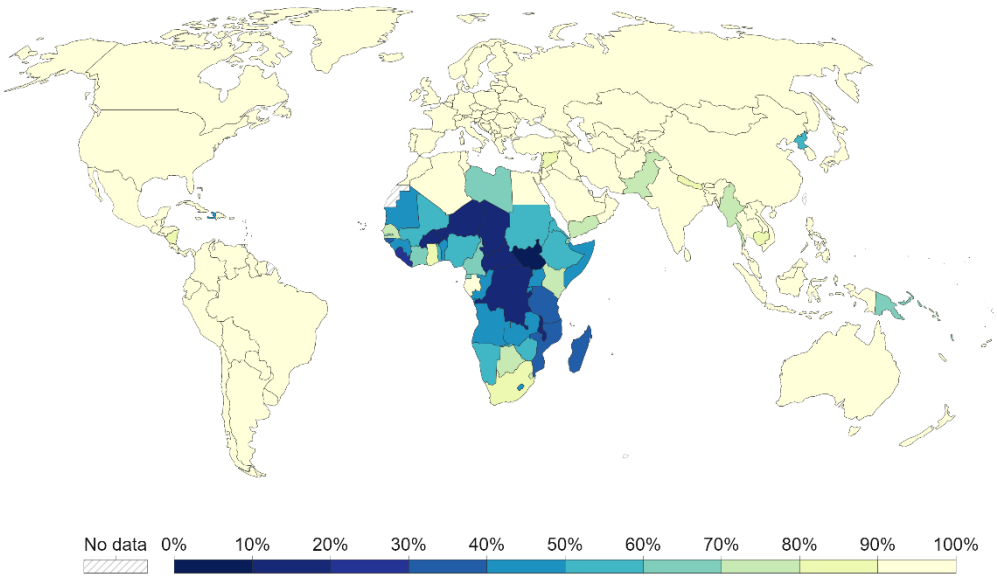


Figure 1.4. Share of access to electricity in 2020 (adapted from [17]).

1.4. Sodium borohydride as a hydrogen carrier

Chemical hydrides can be an interesting alternative to physical storage. They contain hydrogen in their composition, which can release it when necessary, making them easier to handle and transport. The chemical hydrides with higher hydrogen content and more widely reported in literature are ammonia borane (19.6 wt. % H content) and sodium borohydride ($NaBH_4$, 10.7 wt. % H content [18]–[23]). From these, $NaBH_4$ has particular potential, given that, although it has lower hydrogen content, it can easily release it through the hydrolysis at room to moderate temperature, as presented in Equation 1.1 (as opposed to ammonia borane where its hydrolysis takes considerably longer times [24]). This way, it can be a safe and clean method to simultaneously generate and store H_2.

$$NaBH_4 + 2\ H_2O \rightarrow NaBO_2 + 4\ H_2 + \text{heat} \quad (1.1)$$

The hydrogen generated is obtained pure and can be directly fed to a Proton Exchange Membrane fuel cell (PEMFC) to produce electric energy. Moreover, it is possible to control the pressure of the hydrogen since it is dependent on the mass of reactants that is added to the reactor.

As observed in Equation 1.1, a by-product is formed in the hydrolysis of sodium borohydride. This by-product, sodium metaborate ($NaBO_2$) retains typically 2 or 4 water molecules [22]. For this matter, the hydrolysis of sodium borohydride must be performed with excess of water, *x*, as observed in Equation 1.2.

$$NaBH_4 + (2+x)\ H_2O \rightarrow NaBO_2 \bullet x\ H_2O + 4\ H_2 + \text{heat} \quad (1.2)$$

Although increasing *x* increases the H_2 generation rate (HGR) and yield, the density of the hydrogen stored decreases significatively. This has a considerable impact on the use of sodium borohydride as source of hydrogen, since it does not meet the USA Department of Energy (DoE) H_2 targets for light-duty vehicles [25]. In fact, in 2007, a no-go recommendation [25] was reported for the use of this H_2 storage technology in on-board vehicles. This report based their decision on the incapacity to achieve the 2010 H_2 targets and the concerns over the overall system cost, including the difficulty to regenerate sodium borohydride from its by-product. Yet, it can meet the DoE's technical performance targets for use in small and medium power portable equipment if the weight of the system is significantly reduced [26]. Table 1.2 presents the evolution of the H_2 targets defined by the DoE with for on-board vehicle H_2 storage, while also including the

current H_2 targets for small to medium power portable equipment. It can be observed a tendency to increase the demand for the H_2 storage capacities from 2020 to ultimate for on-board vehicles and from 2015 to 2020 for power portable equipment, as opposed to the storage system cost, which is expected to be lower with time.

Table 1.2. DoE's H_2 targets evolution since 2010 for on-board vehicle storage and to small and medium power portable equipment [26]–[29][27], [28].

Storage parameter	**Units**	**On-board vehicles**						**Small power portable equipment**		**Medium power portable equipment**	
		2010	2015	2017	2020	2025	Ultimate	2015	2020	2015	2020
Gravimetric capacity	kWh/kg	1.5	1.8	1.8	1.5	1.8	2.2	0.7	1.3	0.7	1.3
	kg H_2/kg	0.045	0.055	0.055	0.045	0.055	0.065	0.020	0.040	0.020	0.040
Volumetric capacity	kWh/L	0.9	1.3	1.3	1.0	1.3	1.7	1.0	0.7	1.0	1.7
	kg H_2/L	0.028	0.040	0.040	0.030	0.040	0.050	0.030	0.020	0.030	0.050
Storage system cost	\$/kg H_2	-	-	400	333	300	266	3000	1000	6700	3300
	\$/kwh	-	-	12	10	9	8	90	30	200	100

Overall, if its disadvantages are overcome, sodium borohydride as source of H_2 can have a positive impact on on-demand production, at room to moderate temperature, green and off-grid, i.e., without need of electricity demand.

2. State of the art

This chapter gives an extensive overview of the sodium borohydride as a hydrogen-energy source, from its hydrolysis to its regeneration. Initially, the optimization of the hydrogen generation will be detailed with the reference of works considering the optimization of the main parameters that affect the hydrogen generation reaction. Next, a more detailed study will be focused on the by-product of the hydrolysis reaction. Finally, a review of the rehydrogenation of borate compounds gives the current status on the regeneration of sodium borohydride to close the $NaBH_4$-H_2 cycle. The chapter closes with the motivation of this thesis and its layout.

2.1. Hydrolysis of sodium borohydride for hydrogen – energy applications

As referred in chapter one, the hydrogen storage density is significantly affected by the stoichiometric self-hydrolysis of sodium borohydride. Therefore, a deep understanding on the way the different parameters involved affect this reaction is needed to optimize the hydrogen generated, i.e., its yield, generation rate and storage density. The most important factors are the use of a catalyst and/or an inhibitor, the reactor size and geometry, the excess of water used and additives that can be used to promote the reaction. The following sections describe the literature review on the influence of each of these aspects on the reaction characteristics and in particular on the optimization of the hydrogen generation from sodium borohydride.

2.1.1. Catalyst

Although the hydrolysis of sodium borohydride is an exothermic reaction, a catalyst is required to increase the HGR to acceptable values, which is required for portable applications. In the literature, there have been reports on the use of different classes of catalysts - metallic salts, reduced transition, supported metals, and others. Demirci et al. [29] and Abdelhamid [30] reviewed the catalytic performance of the hydrolysis of sodium borohydride. Table 2.1 presents some of the catalysts with higher performance and their HGR reported.

Table 2.1. Some of catalysts with highest HGR reported for the hydrolysis of $NaBH_4$.

Catalyst	Temperature / ºC	HGR / (L/(min·g_{cat}))	Ref
Co-B	30	26.0	[31]
$Ru_{60}Co_{20}Fe_{20}$	20	41.7	[32]
10 wt. % PtRu-$LiCoO_2$	25	560	[33]
Pt-C	20	23.1	[34]
Ni-Ru	25	33.0	[18]
Ru	25	96.8	[35]
Ru/Co-TiO_2	30	172.0	[36]

As observed in Table 2.1, the catalysts with the best performance require the use of rare metals, such as Pt and Ru. However, some of them can be reused considerable times without significant loss of activity. This is the example of the Ni-Ru catalyst referred on the table, which can be used more than one hundred times [18].

Acids can also be used in the hydrolysis of $NaBH_4$ since they act as a catalyst of the reaction. Although the HGRs are lower when compared to metallic catalysts, they do not have any metal in their composition, which can be environmentally better, depending on the acid considered. Common acids used are acetic acid and hydrochloric acid, with HGRs up to 4.0 and 4.9 L/min, respectively [37]. Schlesinger et al. [38] reported a complete study on the acidic hydrolysis of sodium borohydride using 30 solid acidic compounds in alkaline-free experiments (variable $NaBH_4$-acid weight mixture). Higher H_2 yields after 10 minutes-reaction were achieved with succinic acid, boric oxide, oxalic acid and malic acid. Among these, oxalic acid had the highest HGR and lower induction time.

Murugesan et al. [39] also studied different mineral and benign acids as catalyst of the $NaBH_4$ hydrolysis reaction and observed that benign acids (formic acid and acetic acid) require higher concentrations (12 N vs 3 N) to achieve H_2 yields close to those obtained with mineral acids (hydrochloric acid and sulfuric acid). Moreover, the HGR is higher for those mineral acids.

2.1.2. Alkaline hydrolysis

Hydrolysis of sodium borohydride can be performed following two procedures. The first is to mix the sodium borohydride and the catalyst in powder form in the reactor and the

reaction is initiated by injecting the established amount of water (alkaline-free hydrolysis). The second method is the use of an inhibitor of the reaction – for example sodium hydroxide, NaOH (alkaline hydrolysis). This way, a solution containing the reactants and NaOH is prepared and the hydrogen formation begins when the solution is injected to the reactor containing the catalyst previously placed inside. This happens since the spontaneous release of H_2 through the hydrolysis of sodium borohydride is slower under high pH, which is obtained with the addition of the strong base, which correlates with the need for a catalyst, instead of the hydrolysis in acidic pH which does not.

Comparing the two methods, the first can produce results close to the ones using the inhibitor. However, the second method allows for a better contact between the reactants and it is easier to use in consecutive reactions, since the solution prepared can be stored with increased shelf-life. Moreover, optimal concentration of NaOH in solution is important to avoid spontaneous hydrolysis of the borohydride. Table 2.2 summarizes the studies performed on the NaOH concentration used.

Table 2.2. Studies performed on the NaOH concentration optimization. (MW- microwave environment).

$NaBH_4$ conc. / wt %	**Catalyst**	**NaOH conc. range / wt %**	**NaOH optimal / wt. %**	**HGR / $mL.min^{-1}.g_{cat}^{-1}$**	**Ref**
10	Ni-based	1, 7, 10	7	2500	[40]
1.5	Ni-B	0, 3, 5, 7	5	380	[41]
	No-B (MW)	0, 3, 5, 7	3	1300	
1 to 25	Ru	1, 5, 10	1	480	[42]
1.5	Ni-B	0, 10, 20	20	330	[43]
1.5	Ru	0, 10, 20	0	600	

Observing the data in the table above, an optimal concentration of NaOH cannot be found, since it depends on the $NaBH_4$ concentration and the catalyst considered. However, some conclusions can be drawn: Ferreira et al. [40] and Ekinci et al. [41] observed that HGR increases initially with the NaOH concentration and then decreases. Moreover, these authors concluded that the NaOH addition to the reaction had a positive effect on the H_2 generation rate. Amendola et al. [42] also added that the decrease of HGR occurs when the OH^- ions in excess block the available water molecules for the reaction, while Ekinci et al. [41] justified by the decrease of the by-product solubility followed by its precipitation and clinging to the catalyst surface. Moreover, it is worth mentioning that

the induction time of the reaction presents a contrary behavior to the HGR dependence on the NaOH concentration, i.e., it decreases with the HGR increase [40] and increases for NaOH concentrations higher than the optimal [43].

At last, Hua et al. [43] presented contradictory results that can only be explained by the interaction between the reactants and the catalyst: for a Ni-B catalyst, the HGR benefited from the increase of NaOH (similar to Ekinci et al.'s [41] Ni-B catalyst experiment, although at lower concentration); and for a Ru catalyst, the presence of NaOH had a negative impact on the HGR (although Amendola et al. [42] concluded NaOH presence had a positive effect on the reaction, the optimal concentration found was only 1 wt. % and the lower concentration of NaOH considered in the Hua report was 10 wt. %).

2.1.3. Reactor geometry and excess of water

One of the crucial factors that affects the hydrolysis of sodium borohydride is the reactor geometry as well as its material properties. It is essential to assure good isolation to avoid hydrogen leak. Moreover, the system must consider materials that can handle high pressures. On the interior geometry, the hydrogen generation benefits from a higher contact between the reactants and the catalyst.

The excess of water *x* is another important parameter that impacts the hydrolysis of sodium borohydride. The by-product formed retains part of water which reduces the H_2 yield and HGR. For that matter, optimization of *x* is essential to increase the hydrogen generated, but it should also be lower enough to avoid the decrease of the hydrogen storage capacity. Figure 2.1 presents the influence of *x* in the gravimetric hydrogen storage capacity (GHSC). The data presented above the curve represent the GHSC values for integral numbers of *x* up to *x* = 5.

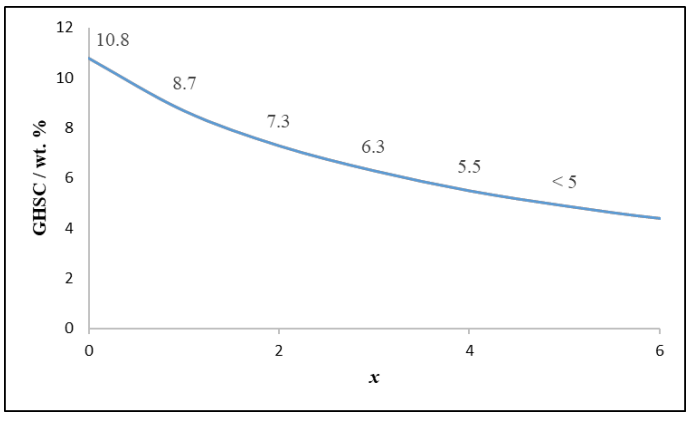


Figure 2.1. Effect of excess of water *x* on the gravimetric Hydrogen storage capacity, adapted from [29].

It is also important to take in account the precipitation of the by-product (the solubility limit is 28.2 g/100 mL @ 25 ºC).

Few reports are observed in the literature regarding the study of the reactor geometry and the effect *x* on the hydrogen generated. Typically, the authors perform the hydrolysis in unique systems, for example, a reaction vessel (e.g., a conical flash sealed) and an inverted burette (to measure the hydrogen generated). Table 2.3 displays data from the hydrolysis occurring in different reactor shapes and *x* values. As far as found in literature, only these studies have considered the reactor geometry and their relation with the *x* factor and were performed by Pinto et al. [18], Ferreira et al. [22], and Nunes et al. [23], all authors working at the research hosting the present work. Therefore, based on these reports, these reactors were considered for the experiments performed in this thesis.

Table 2.3. Influence of the reactor geometry and *x* on the H_2 generation from the $NaBH_4$ hydrolysis.

Reactor	**Volume / cm^3**	***x***	**H_2 yield / %**	**GHSC / wt. %**	**VHSC / kg/m^3**	**Ref**
Cylinder (flat bottom)	229	0	37	3.8	42	
		1	57	5.0	56	[22]
		2	76	6.1	68	
	646	16	100	5.0	55	[18]
Cylinder (conical bottom)	229	0	79	8.1	92	
		1	89	7.7	86	[22]
		2	96	6.9	77	
		16	100	6.1	66	[18]
	369	16	100	5.3	58	[18]
Ovoid	9	16	100	-	-	[23]

The results allow to conclude that the stainless-steel conical bottom used by Ferreira et al. [22] presents considerably higher hydrogen yields and storage capacities and lower induction times for x = 0, 1 and 2 compared to the results obtained in the same reactor with flat bottom, due to the closer contact between the reactants and the catalyst. The authors also observed that the HGR was higher for smaller reactor volumes and conical bottom [18].

The same observations can be made for x = 16 by Pinto et al. [18]. However, the hydrogen yield variation was not as significant. A small stainless-steel ovoid reactor was also

considered by Nunes et al. [23], and a higher HGR was obtained, nevertheless, at very low hydrogen storage capacities.

2.1.4. Additives

The addition of a compound to a reaction can have a positive effect on its characteristics, particularly in the yield and reaction rate. However, regarding the hydrolysis of sodium borohydride, few studies on this aspect have been reported in the literature.

One study was performed by Ferreira et al. [19] which considered as additive the organic polymer sodium carboxymethyl cellulose (CMC). The authors observed that the HGR increased with the addition of 0.25 % CMC; however, although the induction time was considerably higher, a significant improvement of the HGR was noticed when 1.0 % CMC was used. This was explained by the increase of the H_2 bubble velocity formation.

Another important observation was the increase of the H_2 solubility in the liquid phase (0.182 for 0.25 % CMC, compared to 0.068 for 1.0 % CMC and 0.009 without additive). Considering this increase, the by-product of reaction was analyzed by x-ray diffraction (XRD). A rearrangement of the sodium metaborate dehydrated ($NaBO_2 \bullet 2H_2O$) into sodium boron hydroxide ($NaB(OH)_4$), with 0.25% CMC was detected. The authors reported this as a step forward on the regeneration of sodium borohydride from the by-product of its hydrolysis, since its regeneration requires the evaporation of the water molecules and, this way, a high-energy consuming step is eliminated ($\Delta H^{o}_{H_2O,\ 100\ ^{o}C} = 40.66$ kJ/mol).

The surfactant sodium dodecyl sulfate (SDS) was also studied as a potential additive in the hydrogen generation [44]. The HGR and gravimetric storage density increased significatively. These results were explained by the higher H_2 dissolution in the liquid phase and the difference of polarity between the solution before and after the reaction. Moreover, the influence of 0.25 % SDS on the by-product formed was identified and an anhydrous structure composed of $NaBO_3$ and $NaBO_4$ molecules was found.

2.1.5. Fuel cell applications

One of the advantages of the hydrogen production from the hydrolysis of sodium borohydride is that it can be directly fed to a PEMFC to generate energy. Figure 2.2

presents a PEMFC, demonstrating the conversion of hydrogen in water and electric energy [45].

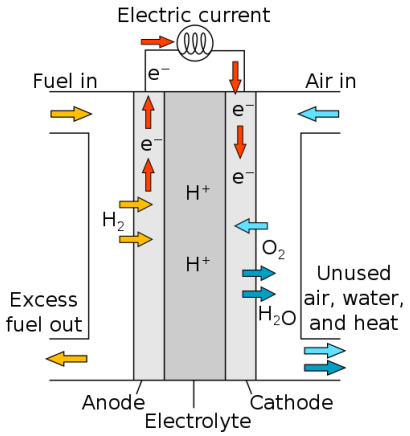


Figure 2.2. Simplification of the reactions occurring inside a Proton Exchange Membrane fuel cell [45].

The reactions that fundament a PEM fuel cell are the oxidation of H_2 and the reduction of oxygen (O_2) into water, Equations (2.1) and (2.2), respectively.

$$H_2 \rightarrow 2\,H^+ + 2\,e^- \tag{2.1}$$

$$\frac{1}{2}\,O_2 + 2\,H^+ + 2\,e^- \rightarrow H_2O \tag{2.2}$$

The main advantage of this fuel cell is its low-temperature operation, its high-power density and quick start-up times being the most studied type of fuel cell. However, it requires pure H_2 to work, is sensitive to the presence of CO and uses noble-metal catalysts [46]. The hydrogen coming out of the sodium borohydride hydrolysis has a very high purity level, adequate to be directly used in a PEMFC.

2.2. Hydrolysis of sodium borohydride by-product

The DOE no-go recommendation for the sodium borohydride as hydrogen carrier introduced the need to regenerate the sodium borohydride from its by-product as a crucial limitation of this technology that must be overcome to close the $NaBH_4$-H_2 cycle. Moreover, the study of the by-product of the hydrolysis with additive CMC performed by Ferreira et al. [19] presented a new variable to the issue: the optimization of the by-product composition to decrease the energy demand of its recycling. This subsection presents the borates reported in the literature. Then, a brief description of each compound

is presented and, finally, the main techniques used to identify these by-products are described.

2.2.1. By-products reported in literature

Many borates have been observed to be formed during the hydrolysis of sodium borohydride. Although sodium metaborate ($NaBO_2$) was the by-product expected for stoichiometric reaction, its di-hydrated form ($NaBO_2 \cdot 2H_2O$) has been the main borate observed. Sodium metaborate tetra-hydrate ($NaBO_2 \cdot 4H_2O$) has also been observed and the hydrolysis performed in acidic medium has yield boric acid ($B(OH)_3$) [47]. Table 2.4 summarizes most of the by-products observed in the hydrolysis of sodium borohydride, reported in literature.

Table 2.4. By-product composition of $NaBH_4$ hydrolysis reported in literature.

$NaBH_4$ conc. %	Solvent	Additive	T / K	Compound	Ref
10	H_2O (l)	-	Room	$NaBO_2 \cdot 2H_2O$	[19]
40	H_2O (g)	-	383	$NaBO_2 \cdot 2H_2O$	[48]
10	H_2O (l)	0.25 % CMC	Room	$NaB(OH)_4$	[19]
42-81	Propylamine	Various	Room	$Na_2B_4O_5(OH)_4 \cdot (H_2O)_3$	[49]
34	H_2O (l)	-	Room	$Na_2B_2O_4 \cdot (H_2O)_8$	[50]
10	H_2O (l)	HCl	Room	$B(OH)_3$	[51]

As observed by the table, most by-products were obtained by hydrolysis at room temperature. Moreover, the main borate obtained is $NaBO_2 \cdot 2H_2O$ or $NaB(OH)_4$, for reactions with different concentrations of $NaBH_4$ and temperature. $B(OH)_3$ is the by-product for acidic hydrolysis (pH < 9) and $Na_2B_2O_4 \cdot (H_2O)_8$ has the same structure of $NaBO_2 \cdot 4H_2O$, which is another expected borate by-product.

Yet, these observations are inconsistent with the review of Andrieux et al. [52] who reported the variations on the borate formed and its dependence on the excess of water *x*, temperature of reaction and $NaBO_2$ molar fraction. This way, the authors have presented other hydrated forms of sodium metaborate and the conditions for their formation. The formation of these low hydrated borates is important to increase the hydrogen storage capacity, however no other report validated their presence.

A brief characterization of each borate by-product is now presented:

Sodium metaborate ($NaBO_2$)

It has a molar weight of 65.80 g/mol, a fusion point and boiling point of 966 ºC and 1434 ºC, respectively, a water density of 0.2 g/cm^3 and a density of 2.46 g/cm^3 [53]. It is formed by decomposition of $NaBO_2$ •1/3 H_2O at temperatures between 190 and 280 ºC. Based on Andrieux et al. [52], it is formed as by-product in hydrolysis with $x < 1/3$.

Sodium metaborate one-third-hydrate ($NaBO_2$ •1/3 H_2O)

It is the less hydrated form of $NaBO_2$, formed by decomposition of $NaBO_2$•2/3 H_2O at temperatures between 110 and 150 ºC. Based on Andrieux et al. [52], it is formed as by-product in hydrolysis with $1/3 < x < 2/3$.

Sodium metaborate two-thirds-hydrate ($NaBO_2$ • 2/3 H_2O)

Coexists with $NaBO_2$ •1/3 H_2O for temperatures between 150 ºC and 230 ºC. Based on Andrieux et al. [52], it is formed as by-product in hydrolysis with $1/3 < x < 4$.

Sodium metaborate di-hydrate ($NaBO_2$ • $2H_2O$)

It is formed by decomposition of $NaBO_2$ •4 H_2O at 65 ºC and starts to decompose at 100 ºC. Based on Andrieux et al. [52], it is formed as by-product in hydrolysis with $2/3 < x < 6$.

Sodium boron hydroxide ($NaB(OH)_4$)

It is the same compound as $NaBO_2$•$2H_2O$, however with a chemical structure where OH^- ions are present instead of structural water H_2O. From the recycling point of view, the energy demand is lower since the dehydration of the borate is not necessary.

Sodium metaborate tetra-hydrate ($NaBO_2$•$4H_2O$)

It is the sodium metaborate more hydrated observed and its typically the only commercial sodium metaborate, i.e., to use other sodium metaborate, its dehydration is required. Precipitates at 60 ºC. Based on Andrieux et al. [52], it is formed as by-product in hydrolysis with $x > 4$.

Sodium boron hydroxide hydrate ($NaB(OH)_4$•$2H_2O$)

It is the same compound as $NaBO_2 \bullet 4H_2O$, however two water molecules are present in the compound as structural water, i.e., in the form of OH^- ions. From the recycling point of view, the energy demand is lower since less dehydration of the borate is necessary; however it is a more complex borate to recycle than $NaB(OH)_4$.

Tincalconite ($Na_2B_4O_5(OH)_4 \bullet (H_2O)_3$)

It is a less hydrated form of borax, the main borate that is used to produce $NaBH_4$. Its formation is associated to the post-hydrolysis reaction of $NaBO_2$ with $B(OH)_3$, as explained by Uysal et al. [54], Equation (2.3):

$$NaBO_2 + 2\ B(OH)_3 \rightarrow Na_2B_4O_7 + 3\ H_2O \quad (2.3)$$

Boric acid ($B(OH)_3$)

As previously referred, its formation occurs for acid hydrolysis (pH < 9) of sodium borohydride, Equation (2.4):

$$B(OH)_4^- + H^+ \leftrightarrow B(OH)_3 + H_2O \quad (2.4)$$

It has a fusion point of 171 ºC and a boiling point of 300 ºC. It is partly soluble in water but its solubility increases with the temperature. It has a density of 1.5 g/cm^3 and decomposes at 100 ºC in B_2O_3 and water.

2.2.2. Quantitative analysis of the by-product composition

The techniques used to characterize the by-product of sodium borohydride hydrolysis must consider the identification of the chemical composition of the by-product. Moreover, the by-product is typically analyzed in solid state: it is obtained liquid (due to the excess of water used) and then dried at room temperature after the H_2 generation and release/ transfer to another reservoir. The most used characterization technique in literature is the x-ray diffraction (XRD) while Fourier Transform Infra-red spectroscopy (FT-IR) is also considered. These techniques are now briefly explained.

X-ray diffraction (XRD)

X-ray diffraction is a technique used to identify the composition of a sample, based on its crystalline structure. Figure 2.3 presents schematically how this method works. Each

crystal has a specific structure that can be identified. To classify the crystal's structure, the Bragg's law must be respected, Equation 2.5 [55],

$$n\lambda = 2d\sin\theta \tag{2.5}$$

where n is an integer, λ is the wavelength of the x-ray, *d* is the distance between the crystal layers and θ is the angle of incidence [56]. This technique is performed by directing an x-ray beam on the crystal. When that happens, an x-ray detector detects the intensity peak and the angle of diffraction of the ray. After enough intensity peaks are registered for the same crystal, a pattern is created. Next, angles of diffraction are converted to d-spacings (i.e., the coordinates of the crystal) and their analysis gives the crystal structure of the sample [55].

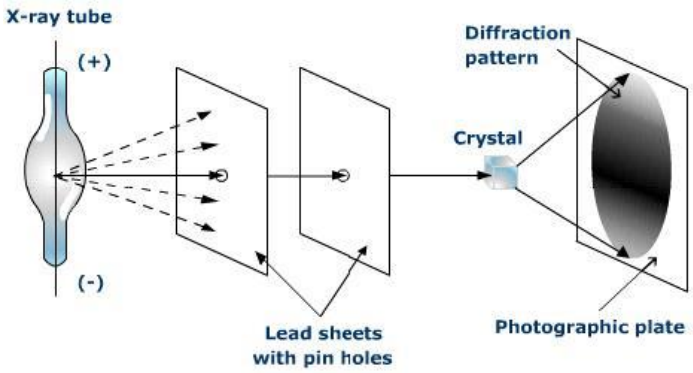


Figure 2.3. Demonstration of the XRD characterization technique [57].

An x-ray diffractometer is visible in Figure 2.4 and its main components are identified. The goniometer observed is responsible for the rotation of the sample to obtain a more concise analysis and the detector, in the direction of the x-ray beam [55].

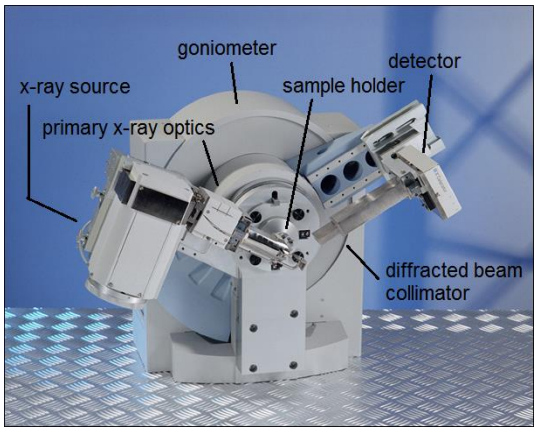


Figure 2.4. X-ray diffractometer and its main components [58].

This non-destructive technique can identify, easily and efficiently, the structure of samples, which are in turn easy to prepare. Moreover, if all the information regarding the

compounds observed is discerned by the analysis program, it can quantify the weight of each compound in the composition of a sample. However, the sample must be homogeneous, it must be in the form of powder and overlay of intensity peaks can occur, hardening its analysis [55].

Fourier Transform Infrared spectroscopy (FT-IR)

Fourier Transform Infrared spectroscopy is one of the most important characterization techniques and it is based on the incidence of infrared (IR) light through a sample. Molecules who suffer a change in their dipole moment under incident IR radiation (IR active), vibrate or rotate with the radiation incidence [59]. If this occurs at the right wavelength, these molecules are IR active and some of the radiation is absorbed, while the remaining is transmitted [60].

FT-IR characterization of a sample is based on the Michelson's interferometer (Figure 2.5), created by Albert Michelson in 1893 [61]. It uses a detector to register the absorbed radiation, which is treated, in a computer, using Fourier transformation, resulting in a pattern that relates the percentage of transmittance with the wavelength of the radiation. This pattern is compared to standard ones, to identify the composition of the sample.

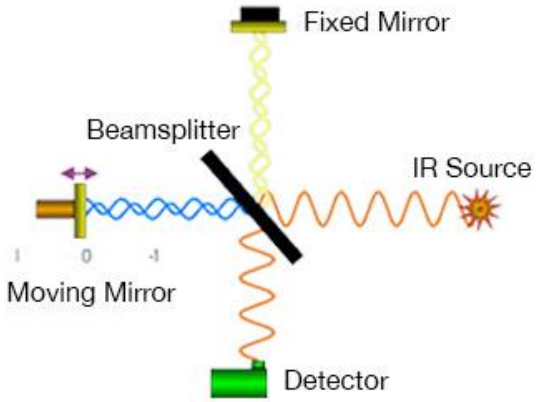


Figure 2.5. Michelson's interferometer of a FT-IR spectroscopy characterization technique[62].

As observed in Figure 2.6, a beam splitter is used as well as two mirrors, one moving and one fixed. These mirrors reflect only 50 % of the striking light [61]. The signal detected varies depending on the position of the moving mirror. When the wave signal of the moving mirrors is the direct opposite of the fixed mirror, in such a way that they cancel each other, a zero signal is obtained by the detector [63], [64]. This is referred to as an

interferogram and it is treated to give the final spectrum of the sample. An example of an interferogram is observed in Figure 2.8.

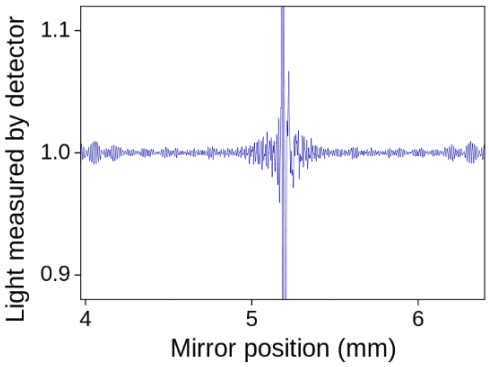


Figure 2.6. Example of an interferogram based on FT-IR characterization technique [65].

This is a high-resolution method of characterization, whose components do not require slits to achieve it and have short wavelength limit. Compared to dispersive spectroscopy, it is a faster method; however, it is not as accurate [66].

2.3. Rehydrogenation of sodium borates to close the $NaBH_4$-H_2 cycle

$NaBH_4$ is mainly produced using the Brown–Schlesinger process. This process was developed in the early 1950s [15,22] and is composed of seven steps, as presented in Figure 2.8. Its main reaction is presented in Equation (2.6), where sodium hydride (NaH) and trimethylborate ($B(OCH_3)_3$) react at a temperature between 225 ºC and 275 °C [15,42].

$$B(OCH_3)_3 + NaH \rightarrow NaBH_4 + NaOCH_3 \quad (2.6)$$

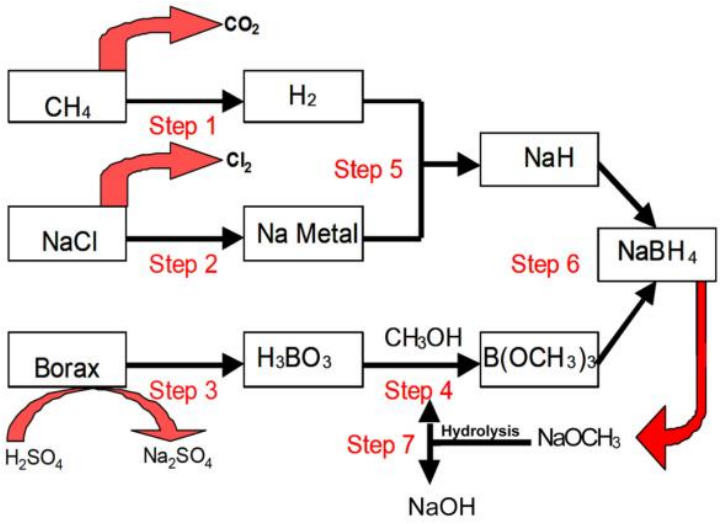


Figure 2.8. The Brown and Schlesinger process for the $NaBH_4$ production.

The disadvantage of this process is its inefficiency, mainly associated to the synthesis of Na, and the need of high-energy consumption reactions due to high pressures and temperatures. To solve these problems, an adaptation of this process has been presented by Liu et al. [67]. In this upgrade, the by-products are reused in a closed system where $NaBO_2$ and ammonia borane (NH_3BH_3) are, simultaneously, produced and recycled from $NaBH_4$. Also, the metallic Na is obtained by electrolysis of sodium chloride (NaCl) in a seawater treatment using electricity from renewable sources. Hydrogen produced from the seawater would be integrated in the formation of NaH, eliminating step 1 of the Brown and Schlesinger process and reducing its emissions impact. The introduction of NH_3BH_3 in the process is another source of H_2, in replacement of step 3. Nevertheless, it is still a complex process where many reactions are involved, in fact, there is an increase in the number of steps compared to the Brown and Schlesinger process, due to the by-product reuse and recycling.

An alternative process to produce $NaBH_4$ at industrial scale is the Bayer process, which is represented in Equation (2.7) [68]–[70]. The compound $Na_2B_4O_7 \cdot 7SiO_2$ reacts with Na at 700 °C under a H_2 atmosphere. This process has a high-risk potential since the reaction occurs at a temperature higher than the temperature at which the $NaBH_4$ decomposes (400-500 ºC). Moreover, it produces Na_2SiO_3 as a by-product, which is a residue with low commercial value that is difficult to discard [33,58].

$$Na_2B_4O_7 \cdot 7SiO_2 + 16Na + 8H_2 \rightarrow 4NaBH_4 + 7Na_2SiO_3 \quad (2.7)$$

For this matter, it is essential to find an alternative process to regenerate sodium borohydride from its hydrolysis by-product, which is cost-effective and green. However, despite this need to close the hydrogen cycle from $NaBH_4$ hydrolysis, only 5.5 % of the published articles highlight the topic "regeneration" [71] as well seen on Figure 2.9. As reviewed by Demirci et al. [72], from the 260 research articles published in the 2000's up to 2013 dedicated to "the hydrogen cycle with hydrolysis of sodium borohydride", only 8.9 % of the papers were dedicated to the $NaBH_4$ regeneration and more than half of them reported progresses in the catalytic activity of the hydrolysis reaction.

This lack of research in recycling, was again referred in 2021 by Nunes et al. [71]. A number of 217 research papers published from 2014 to 2021, were considered by the research of "hydrogen from $NaBH_4$ hydrolysis". The research articles were categorized in four topics: "catalysis", "fundamentals", "regeneration" and "others". "Catalysis" highlighted the performance and characterization of catalysts; "fundamentals" fixated on the reaction mechanisms, kinetics, and thermodynamics; "regeneration" was dedicated to the synthesis of $NaBH_4$ from borates obtained as by-product in its hydrolysis; and "other" focused on the experimental and computational study of reactors, prototypes, and developed systems. The reports on "catalysis" have now accounted for more than 80 % of all studies reported, Figure 2.9.

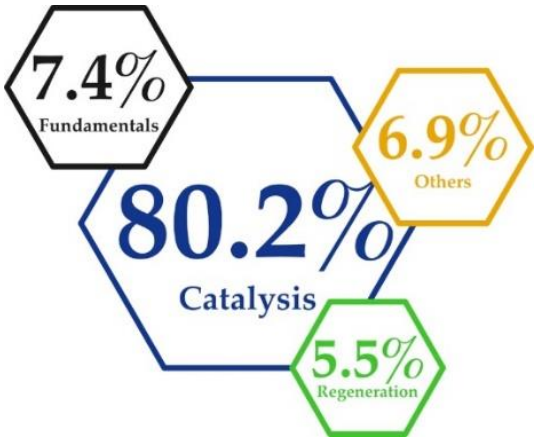


Figure 2.9. Topics of research articles and their impact on the regeneration of $NaBH_4$, from 2014 to 2021 [71].

Nevertheless, important advances have been made through the years [71]. As reviewed by the authors, from all the research articles published regarding the $NaBH_4$ hydrolysis by-product recycling since the early 2000s, only three studies were dedicated to this topic before the DOE's no-go recommendation [69], [73], [74]. On the other hand, the remaining 96% of the papers on this topic were published after the DOE's 2007 report

[25], as observed in Figure 2.10. That indicates that the low interest in the $NaBH_4$ regeneration was more evident prior to the DOE's no-go report, and that a shy progress has been made to invert that decision, although only in the number of papers published compared to before 2007.

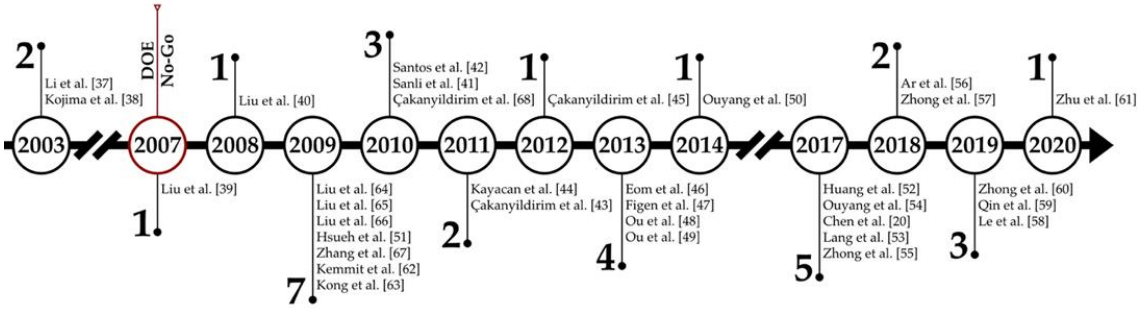


Figure 2.10. Timeline of published articles dedicated to $NaBH_4$ regeneration [71].

The authors also noted that 12 reviews were published regarding the hydrogen generation through boron-based hydrides [30], [72], [75]–[80]. From those (twelve), almost all (ten) focused on the $NaBH_4$ hydrolysis and less than half (five) highlight the importance of recycling the by-product to close the $NaBH_4$-H_2 cycle [72], [75], [76], [81]–[84].

From the literature reports on the regeneration of sodium borohydride, three types of chemical processes can be organized based on the energy source: thermo, mechano, and electro. Until 2015, the regeneration of sodium borohydride was mainly achieved through thermochemical processes [41,42], as observed in Figure 2.11. However, since 2016, there has been a transition to cleaner processes to regenerate this compound, with mechano-chemical processes being the most used ones [20,43,45,50,52–61,68]. Although in theory, the electrosynthesis of $NaBH_4$ can be the best type of process, the difficulty to overcome the challenges of efficient $NaBH_4$ electrosynthesis has contributed to the development of the mechano-chemical regeneration.

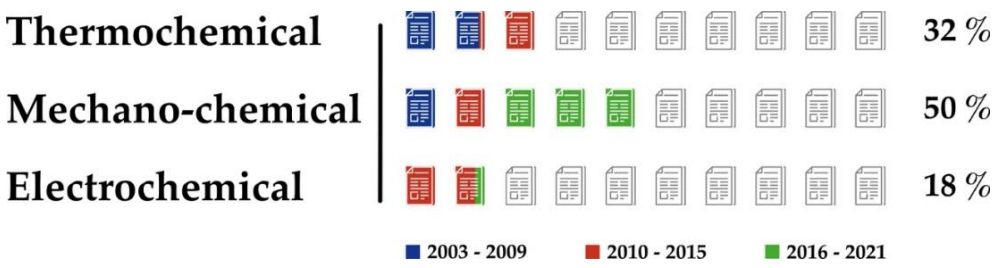


Figure 2.11. Infographic view of the type of process reported in the research articles, published since 2000, dedicated to $NaBH_4$ regeneration [71].

These three types of processes and their main references are reported in the following sub-sections.

2.3.1. Thermo-chemical processes

Thermo-chemical processes involve chemical reactions with heat as source of energy, i.e., occurring at high pressure and temperature. Many thermo-chemical processes have been studied with higher or lower success, as reviewed by Muir et al. [79] and Cloutier et al. [85]. Twelve papers have been reported in the literature and summarized in Table 2.5.

Table 2.5. Higher-yield reports on the thermo-chemical regeneration of $NaBH_4$.

Boron compound	Other reactants	Yield / %	Ref
$NaBO_2$	Mg	69.0	[86]
	Mg	63.5	[87]
	Mg + 23.5 % Ni	80.0	[88]
	MgH_2	90.4	[89]
	MgH_2	90.0	[90]
	MgH_2	93.0	[91]
	MgH_2	97.0	[73]
	Mg, Si	98.0	[73]
	Al	69.0	[92]
	CH_3OH, $NaAlH_4$	80.0	[93]
$NaBO_2 \cdot 0.5\ H_2O$	Mg	28.8	[87]
$NaBO_2 \cdot H_2O$	Mg	12.3	[87]
$Na_2B_4O_7$	Mg, H_2	93.0	[94]
$Na_4B_2O_5$	Al, H_2, Na_2O	65.8	[74]
Na_3BO_3	Si	47.0	[95]

The data reported on Table 2.5 show that it is possible to recycle different borates to sodium borohydride. However, the higher the complexity of the borate, the lower the yield of the process. Accordingly, $NaBO_2$ is the most studied borate and presents the best recycling yield. Nevertheless, it is essential to consider the need for drying this by-product as observed by the lower yield of hydrated sodium metaborate recycling. Moreover, the optimal $NaBH_4$ is obtained by the reaction of $NaBO_2$ with magnesium hydride (MgH_2), Equation 2.8. However, the commercialization of this hydride has decreased, which has in general increased significantly its value.

$$NaBO_2 + 2MgH_2 \rightarrow NaBH_4 + 2MgO \quad (2.8)$$

As alternative, Mg under H_2 atmosphere has been considered, however, with a negative impact in the $NaBH_4$ yield. Other alternative to consider is the use of Mg with Si, as considered by Kojima et al. [73]. Eom et al. [86] also considered replacing Mg with Ca. Although thermodynamically Ca is more suitable than Mg as a reducing agent, the authors concluded that Ca does not act as an effective catalyst in the H_2-H^- conversion, since only a small amount of $NaBH_4$ was formed.

This type of processes requiring the use of high temperature and pressure show a high impact on the $NaBH_4$ yield as elucidated in Figure 2.12. Same color circles correspond to the same author and open and closed circles relate to temperature and pressure values, respectively. Also, closed and open circles in the same horizontal level correspond to the same paper (same yield).

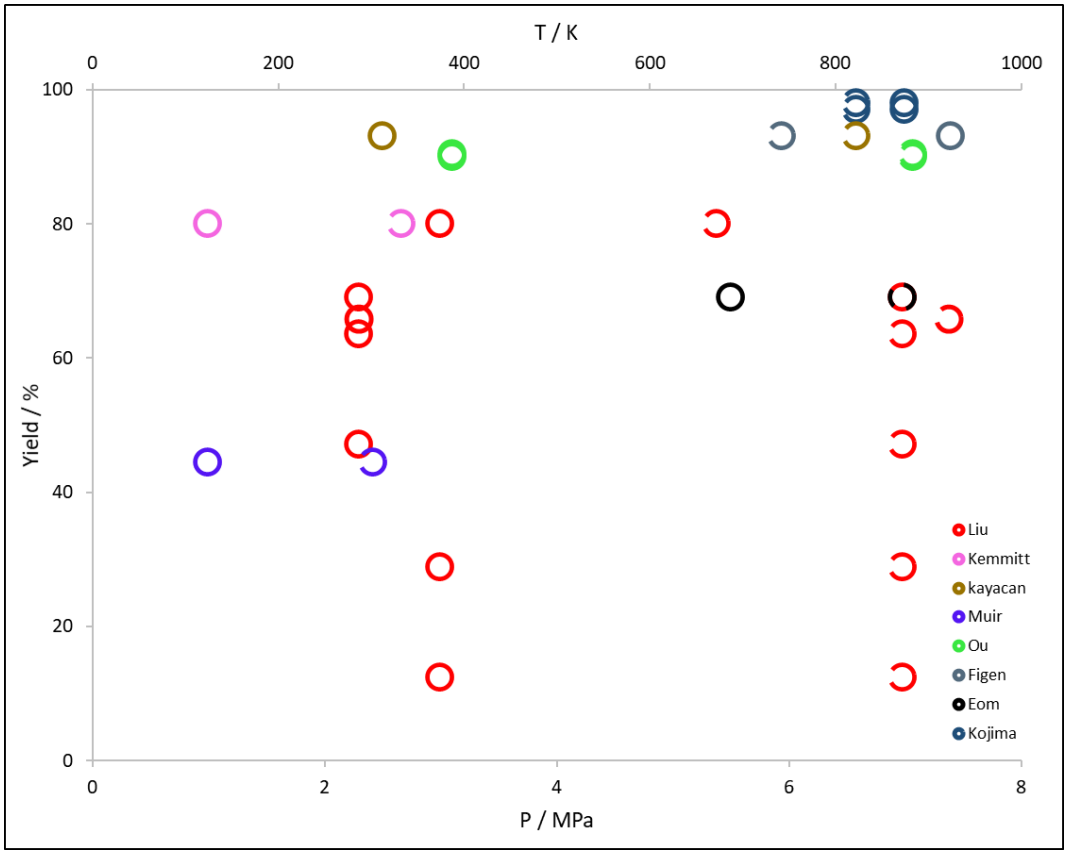


Figure 2.12. Reported yields for $NaBH_4$ regeneration through thermochemical processes (legend: open circles - temperature; closed circles – pressure. Closed and open circles in the same horizontal level correspond to the same paper (same yield)) [71].

From the figure, it is possible to observe that the $NaBH_4$ yield can range from 10 % to almost 100 %. Kojima et al. works reported the highest yield reported for the combination of high pressure and temperature. Moreover, the authors have in general considered a temperature range of 800-900 K and a pressure range of 2-4 MPa.

More in detail, the study of the temperature of the reaction presented in Equation 2.8 was performed by Ou et al. [89] at 3.1 MPa H_2. The authors performed the reaction at constant increments of temperature from 293 to 884 K followed by a constant decrease to 293 K and the $NaBH_4$ yield was determined based on the H_2 pressure variation. A $NaBH_4$ regeneration of 90.4% was achieved, while most of the $NaBH_4$ was formed between T =

873 K and T = 884 K. Therefore, Ou et al. [90] added the pressure and time of reaction as optimization parameters in a following study. In order to promote the hydrogen adsorption for $NaBH_4$ formation, the authors set the H_2 pressure between 2.1 and 3.1 MPa and observed that after 1.5 h, at 907 K, maximum borate conversion to $NaBH_4$ was achieved. When the reaction was performed at 857 K, the authors observed that 8 h were required to obtain the same $NaBH_4$ yield.

Eom et al. [86] also studied the temperature and pressure of reaction to optimize the $NaBH_4$ yield for the reaction of $NaBO_2$ with Mg under H_2 atmosphere, Equation 2.9. The temperature was first studied for a 6 MPa H_2 pressure and the $NaBH_4$ yield increased up to T = 873 K, the maximum temperature applied. Then, a H_2 pressure variation was applied for the optimal temperature (873 K). When the reaction reached 1 h, an optimal 69 % $NaBH_4$ yield was obtained for 873 K and 5.5 MPa. These variations can be observed in Figure 2.13.

$$NaBO_2 + 2Mg + 2H_2 \rightarrow NaBH_4 + 2MgO \quad (2.9)$$

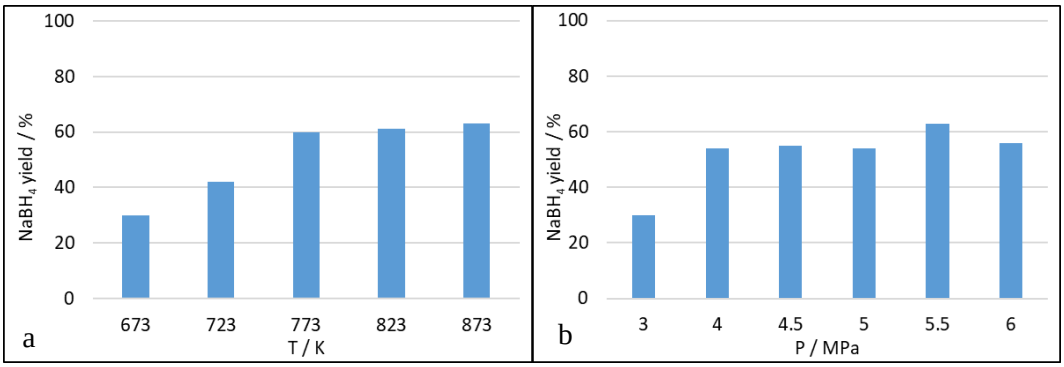


Figure 2.13. $NaBH_4$ yield vs a) Temperature T and b) Pressure P for 1 h reaction [86].

The addition of Si to the reaction represented by Equation 2.9 was also considered to promote the $NaBH_4$ formation, Equations 2.10 and 2.11. After 2 h of reaction, an optimal 98 % yield was obtained for 823 K and 7 MPa H_2.

$$2Mg + Si \rightarrow Mg_2Si \quad (2.10)$$

$$NaBO_2 + Mg_2Si + 2H_2 \rightarrow NaBH_4 + 2MgO + 2Si \quad (2.11)$$

A eutectic alloy of Mg with 23.5 % Ni in the recycling of $NaBO_2$ was also reported [88]. The studies were performed at 673 K and 3.0 MPa H_2, and it was observed an increase of 3 wt. % of H_2 absorbed on the Mg surface, corresponding to an increase of 8 % in the

$NaBH_4$ yield. The authors concluded that the Mg alloy induced the hydrogen dissociation and diffusion during the reaction.

The influence of Al as a reducing agent in the $NaBO_2$ recycling was considered by Liu et al. [74] but no $NaBH_4$ was formed. The authors then reported a mix of Al with tetrasodium diborate ($Na_4B_2O_5$) and sodium oxide (Na_2O), as represented by Equation 2.12.

$$4Al + 6H_2 + Na_4B_2O_5 + NaBO_2 + Na_2O \rightarrow 3NaBH_4 + 4NaAlO_2 \quad (2.12)$$

An optimal $NaBH_4$ yield of 65.8 % was achieved. The studies were carried out at 873 K with a $NaBO_2/Na_2O$ molar ratio between 1.5 and 4. Figure 2.14 presents the influence of this ratio on the $NaBH_4$ yield. As observed in the figure, without varying the $NaBO_2$ concentration, the increase of Na_2O has a positive effect on the regeneration of $NaBH_4$ [74].

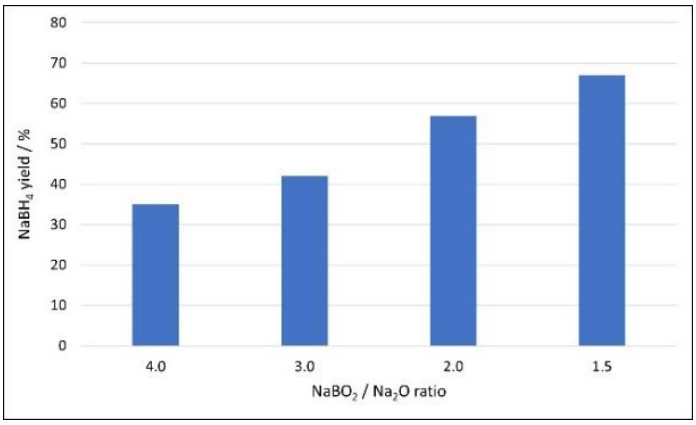


Figure 2.14. Values of $NaBH_4$ yield vs $NaBO_2/Na_2O$ molar ratio [74].

The same authors also studied the influence of several additives in the reaction represented by Equation 2.9. The authors reported that Fe and Ni have the same effect on the $NaBH_4$ formation. The addition of 5 wt. % of these metals not only increased the $NaBH_4$ yield (Fe: 88 %; Ni: 82 %) but also decreased the reaction temperature (Fe: 283 K; Ni: 313 K). Moreover, increasing the Fe concentration up to 20 wt. % promoted the $NaBH_4$ generation rate for identical yields. The authors also observed that the addition of 5 wt. % of Co allowed the formation of $NaBH_4$ with 85 % yield, and the addition of the same amount of Cu did not show any significant effect on the reaction yield.

Overall, although no reports have been published in literature since 2015, significant progress was made in the thermochemical regeneration of $NaBH_4$. Close to 100 % $NaBH_4$

yield was achieved for the $NaBO_2$ recycling and various alternatives to MgH_2 (Mg, Al, Mg2Si) as well as additives of the reaction were studied. However, a lack of study of alternative borates is noticed, including the absence of $NaBO_2 \cdot 2H_2O$ and/or $NaB(OH)_4$ recycling, the main by-product of the $NaBH_4$ hydrolysis. Moreover, the high pressures and temperatures required are limitations of this type of process.

2.3.2. Mechano-chemical processes

The mechanochemical type of processes use mechanical movement, instead of heat, to generate the required energy to form the products of reaction. These processes occur inside a ball mill, as the one presented in Figure 2.15.



Figure 2.15. Example of ball mill [96].

The process is explained as simplified in the Figure 2.16. Reactants in powder form are placed inside a cylinder attached to a ball mill. Alongside them, a high-density sphere is used. At high rotation speed of the cylinder, the sphere will impact on the reactants, crushing and mixing them, promoting the reaction. After milling, the mixture is removed from the cylinder and the products of reaction extracted. This cylinder must be isolated from the exterior, due to normal use of H_2 atmosphere in high pressure and the sphere must not react with the reactants, to avoid unnecessary by-products [97].

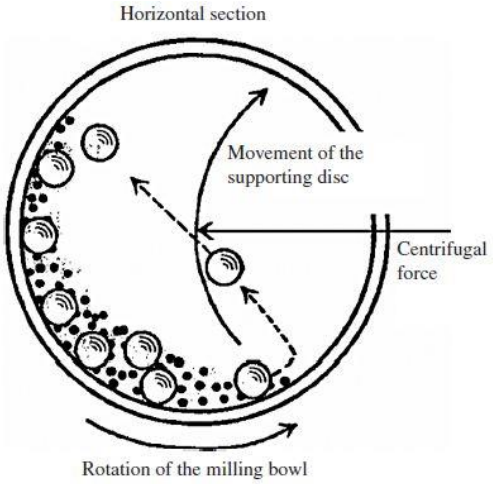


Figure 2.16. Representation of mechanochemical process [97].

The main advantages of this process compared to the thermochemical ones is that it does not require a heat source, since the energy is obtained from the movement of the mill, which makes it a greener process, if the electric energy used is provided by a clean source. These processes consider identical reactions as the ones of the thermochemical path, although with different efficiencies. This fact can be better observed in the Table 2.6. The reports on the regeneration of sodium borohydride through mechanochemical processes are here described.

Table 2.6. Higher-yield reports on the mechanochemical regeneration of $NaBH_4$.

Boron compound	Other reactants	Additive	Yield / %	Ref
$NaBO_2$	Mg, Al	-	99.7	[98]
	MgH_2	-	71.0	[99]
	MgH_2	-	76.0	[100]
	MgH_2	CH_3OH	89.0	[101]
	NaH, SiO_2	-	32.0	[102]
$NaBO_2 \cdot 2\ H_2O$	Mg	-	68.6	[103]
	MgH_2	-	89.8	[104]
	Mg_2Si	-	78.0	[105]
	Mg, Mg_2Si	-	86.0	[106]
	$Mg_{17}Al_{12}$	NaH	57.0	[107]
$NaBO_2 \cdot 4\ H_2O$	Mg	-	64.1	[103]
	Mg-Al	-	99.5	[98]
	MgH_2	-	88.3	[104]
	Mg_2Si	-	74.0	[108]
B_2O_3	MgH_2	Na	25.0	[109]
	MgH_2, $NaNH_2$	-	53.0	[110]
$Na_2B_4O_7$	MgH_2	-	38.0	[111]
	MgH_2	-	78.0	[69]
$Na_2B_4O_7 \cdot 10H_2O$	Mg, Na_2CO_3	-	78.9	[112]

While there have been reports on the ball milling borates with other compounds (e.g., Mg_2Si and $Mg_{17}Al_{12}$), MgH_2 and Mg have produced the highest $NaBH_4$ yields, particularly in reaction with sodium metaborate and its hydrated states. However, as referred before, the commercial availability of this compound has been limited, which requires the use of those alternatives.

Since the time of milling (t), i.e., the time of reaction is an essential factor in this type of process, an overview of the effect of this parameter in the $NaBH_4$ regeneration yield is essential. Moreover, since it is a type of process being developed more recently, the year of the report can also be interesting to analyze. These two factors are highlighted in Figure 2.17. The regeneration yields are presented along with the time of milling (closed circles) and the year of publication of the articles (open circles). Also, closed and open circles in the same horizontal level correspond to the same paper (same yield). As observed, higher yields are achieved when using higher milling times; nevertheless, regenerating $NaBH_4$ for more than 35 h is a considerable energy-consuming process. These higher yield values have been obtained since 2017, which may reflect a gradual improvement of these processes. Similar to Figure 2.12, same color points correspond to the same first author.

A wide variety of groups has progressively been focusing on mechano-chemical sodium borohydride regeneration, as opposed to the thermochemical processes, which have been more studied by a more restricted collection of authors.

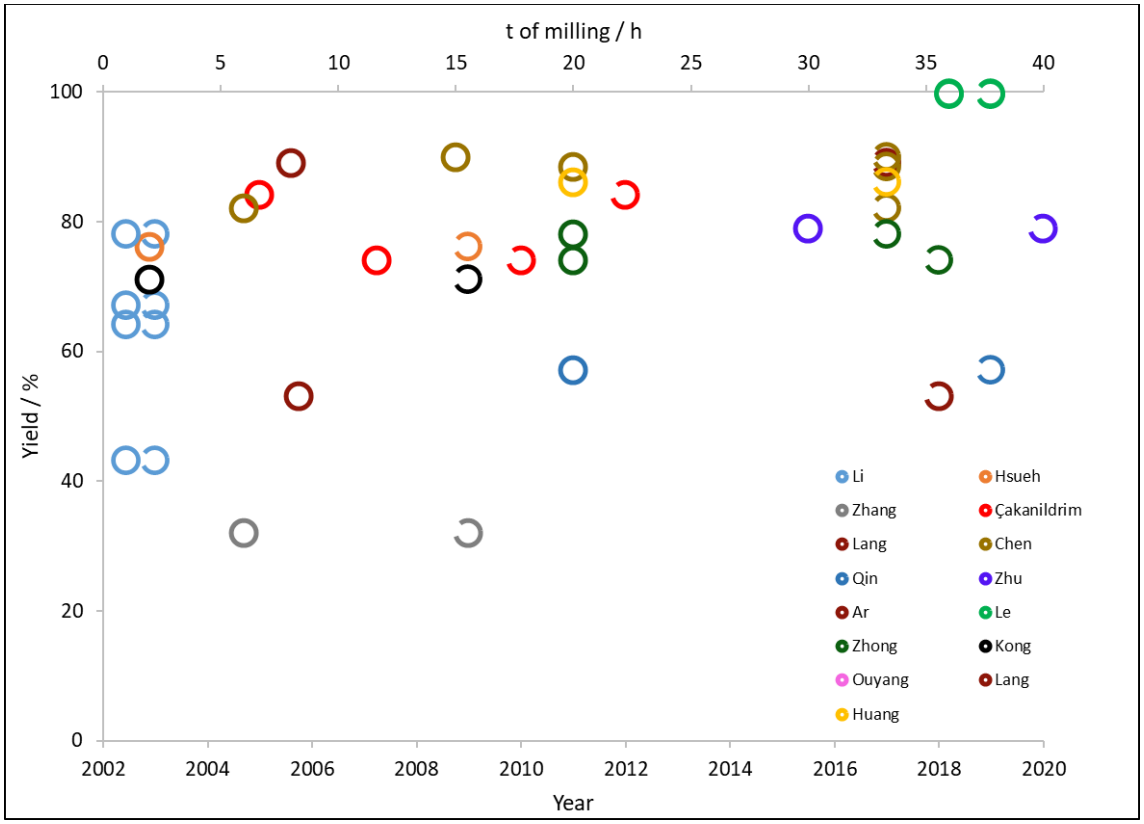


Figure 2.17. Reported yields for $NaBH_4$ regeneration through mechano-chemical processes (legend: closed circles - time of milling; open circles - year of publication. Closed and open circles in the same horizontal level correspond to the same paper (same yield)) [71].

Another disadvantage of this type of processes is the need to extract the sodium borohydride produced after reaction, which will be described later.

Le et al. [98] ball milled $NaBO_2$ with a Mg-Al based alloy with a ball to powder mass ratio (BPR) of 20, as described in Equation 2.9. The authors analyzed the $NaBH_4$ formation during 36 h. Although a maximum $NaBH_4$ yield of 99.7 % was reported for the 36 h experiment, there was not a significant increase of the yield after 12 hours of milling (97.2 % at 12 h and 98.2 % at 24 h).

One of the first reports on the mechano-chemical $NaBH_4$ regeneration was the one of Kong et al. [99] where $NaBO_2$ and MgH_2 were mixed as represented by Equation 2.8. Several parameters and their impact on the $NaBH_4$ yield were studied and optimized, namely: time of milling, $MgH_2/NaBO_2$ molar ratio, and BPR. Regarding the time of

milling, the $NaBH_4$ formation was observed after 0.5, 1 and 2 hours; $NaBH_4$ was observed after 1 hour of reaction while 71.0 % yield was achieved after 2 h. The molar ratio and the BPR also had a positive effect on the $NaBH_4$ yield. Three molar rations were considered: 1.54 (below stoichiometric), 2.00 (stoichiometric) and 2.07 (above stoichiometric). As expected, when MgH_2 is used in excess, the $NaBH_4$ formation increases (71 %) compared to stoichiometric reaction (61.0 %) and a MgH_2 in deficit (34.0 %). Three BPR were also considered: 10, 30 and 50. As the authors observed, there was a significantly positive impact of the BPR increase in the $NaBH_4$ formation.

Similar to the thermochemical processes, additives can be added to the mechanochemical regeneration of $NaBH_4$. In that matter, Lang et al. [53] studied the influence of methanol (CH_3OH) as an additive to the $NaBO_2$-MgH_2 mixture, as represented by Equation 2.8 and reported a slight increase of the $NaBH_4$ yield with the increase of the time of milling from 8 to 10 h. On the other hand, in the absence of methanol, times of milling higher than 4 h had no impact on the $NaBH_4$ formation. Nevertheless, the best yield reported with and without additive methanol were similar, but without additive this yield was obtained with a lower time of milling. These results can be observed in Figure 2.18.

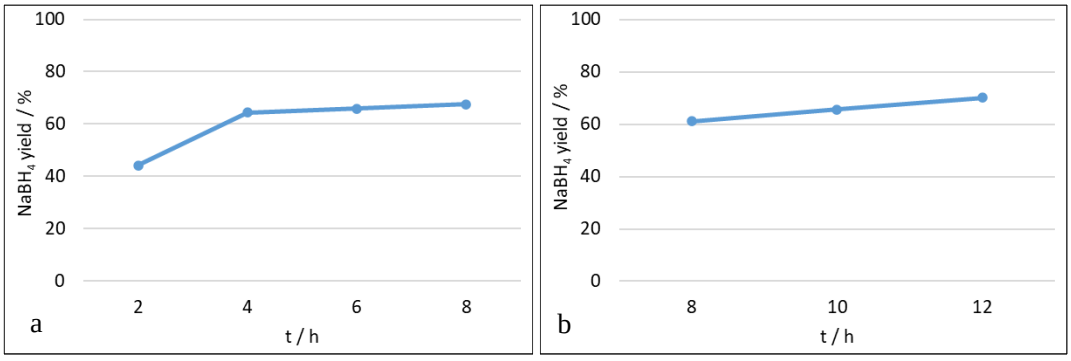


Figure 2.18. $NaBH_4$ yield vs. t without (left) and with (right) CH_3OH. Adapted from [53].

As alternative to ball milling with Mg, Zhang et al. [102] considered the recycling of $NaBO_2$ with NaH and silicon oxide (SiO_2), as observed in Equation 2.13.

$$NaBO_2 + 4NaH + 2SiO_2 \rightarrow NaBH_4 + 2Na_2SiO_3 \quad (2.13)$$

NaH and $NaBO_2$ was initially milled for 4 h and SiO_2 was then added to the mix for additional 2 h. To avoid the decomposition of NaH, the mixture was then pressured into pellets and then calcinated at 480 ºC. When this pressure was increased from 10 to 30 MPa, the $NaBH_4$ yield had a significant increase from 8.0 to 32.0 %. Nevertheless, this

is a very low efficient process, compared to the ones where Mg is used in the reaction. Similar consideration (replacing Mg) had been studied in the thermochemical literature and similar conclusions had been observed.

Given that $NaBO_2$ is not a direct by-product of the $NaBH_4$ hydrolysis, and it is obtained by dehydration, it is important to consider the di- and tetrahydrate forms of this borate. $NaBO_2 \cdot 2H_2O$ is considered as the main by-product of the hydrolysis while $NaBO_2 \cdot 4H_2O$ is the main hydrated metaborate that is commercially available. The mechanochemical recycling of these compounds is described in Equations 2.14 and 2.15 below. Similar to $NaBO_2$ recycling, $Mg + H_2$ and other alternatives are reported.

$$NaBO_2 \cdot 2H_2O + 4MgH_2 \rightarrow NaBH_4 + 4MgO + 4H_2 \quad (2.14)$$

$$NaBO_2 \cdot 4H_2O + 6MgH_2 \rightarrow NaBH_4 + 6MgO + 8H_2 \quad (2.15)$$

Ouyang et al. [103] studied the influence of the time of milling, excess of Mg and BPR on the $NaBH_4$ regeneration, in the mechano-chemical recycling of $NaBO_2 \cdot 2H_2O$ with Mg. The obtained conversion was below the expectations where a yield of 68.6 % was obtained after 15 h of milling, with 37.5 % excess of Mg and a BPR of 50.

In the work of Chen et al. [104], the borates were mixed with MgH_2, as observed in Equation 2.14. The experiments with $NaBO_2 \cdot 2H_2O$ were performed with 25 % MgH_2 excess and an 84.5 % $NaBH_4$ yield was obtained when the reaction reached 5 h. After that, 10 more hours were necessary to observe a significant increase in the yield (90.0 %).

As alternative to MgH_2 and Mg, Zhong et al. [105] studied the recycling of $NaBO_2 \cdot 2H_2O$ at room temperature in an Ar atmosphere by ball milling the borate with Mg_2Si, as represented by Equation 2.16. $NaBH_4$ was regenerated with a 78.0 % yield, in 20 h of ball milling. An optimal value of 3 for the Mg_2Si /$NaBO_2 \cdot 2H_2O$ molar ratio was obtained.

$$NaBO_2 \cdot 2H_2O + 2Mg_2Si \rightarrow NaBH_4 + 4MgO + 2Si \quad (2.16)$$

Huang et al. [106] also studied the ball milling of $NaBO_2 \cdot 2H_2O$ with Mg_2Si and add Mg in excess, as observed by Equation 2.17.

$$NaBO_2 \cdot 2H_2O + 2Mg + Mg_2Si \rightarrow NaBH_4 + 4MgO + Si \quad (2.17)$$

The reaction was performed in a vibrational ball mill under Ar atmosphere. The results presented a $NaBH_4$ yield of 86.0 %, in similar conditions to the report of Zhong et al. [105], i.e., 20 h of ball milling and a Mg: Mg_2Si: $NaBO_2$ molar ratio of 2.5:1:1.

Qin et al. [107] also studied the recycling of $NaBO_2 \cdot 2H_2O$, by milling it with $Mg_{17}Al_{12}$ in the presence of additive sodium hydride (NaH). The experiments showed that 5 wt. % NaH had a considerable impact, since the reaction yield doubled. However, the $NaBH_4$ formation was limited to a 57.0 % yield, which is considerably lower compared with the reports here presented and in the literature.

The $NaBH_4$ formation from the $NaBO_2 \cdot 2H_2O$ recycling with Mg was reported by various authors [101], [102], [104], [105]. $B(OH)_4^-$ was detected in the first minutes of the ball milling. Also, the presence of intermediate magnesium hydroxide ($Mg(OH)_2$), after 10 min of milling was detected, which was fully converted to MgO when the reaction reached 1 h, as Equation 2.18. The presence of this compound is important since its consumption during the process is responsible for the appearance of molecular hydrogen in the reaction medium.

$$NaBO_2 \cdot 2H_2O + 2MgH_2 \rightarrow NaBH_4 + 2Mg(OH)_2 \quad (2.18)$$

Moreover, the intermediate borate $BH_3(OH)^-$ was detected through NMR analysis during the ball milling of this dehydrated borate, which indicates the formation of intermediates $BH(OH)_3^-$ and $BH_2(OH)_2^-$, although with a short lifetime to be detected in the NMR analysis [103]. Based on this, the intermediate reactions that lead to the formation of $NaBH_4$ are represented in Equations 2.19 to 2.25 (where the overall reaction for Equations 2.19 to 2.23 is represented by Equation 2.18), and the overall reaction of the ball milling is represented by Equation 2.14 above.

$$NaBO_2 \cdot 2H_2O \rightarrow NaB(OH)_4 \quad (2.19)$$

$$NaB(OH)_4 + MgH_2 \rightarrow NaBH(OH)_3 + MgH(OH) \quad (2.20)$$

$$NaBH(OH)_3 + MgH(OH) \rightarrow NaBH_2(OH)_2 + Mg(OH)_2 \quad (2.21)$$

$$NaBH_2(OH)_2 + MgH_2 \rightarrow NaBH_3(OH) + MgH(OH) \quad (2.22)$$

$$NaBH_3(OH) + MgH(OH) \rightarrow NaBH_4 + Mg(OH)_2 \quad (2.23)$$

$$2MgH_2 \rightarrow 2Mg + 2H_2 \quad (2.24)$$

$$2Mg(OH)_2 + 2Mg \rightarrow 4MgO + 2H_2 \quad (2.25)$$

Regarding the reports on the recycling of $NaBO_2 \cdot 4H_2O$, Ouyang et al. [103] studied the $NaBH_4$ regeneration in a mechano-chemical recycling of $NaBO_2 \cdot 4H_2O$ with Mg, similar to the one for $NaBO_2 \cdot 2H_2O$ [103]. The obtained conversion was lower than the experiment with $NaBO_2 \cdot 4H_2O$ since a yield of 64.1 % in the same conditions (15 h reaction, 37.5% excess of Mg and a BPR of 50) was reached.

Le et al. [98] also ball milled this borate with a Mg-Al based alloy waste from the first $NaBO_2$ experiment (described above [98]) with a BPR of 20. The authors analyzed the $NaBH_4$ formation during 36 h and a maximum $NaBH_4$ yield of 99.5 % was reported for the 36-h experiment.

Similar experiment with $NaBO_2 \cdot 4H_2O$ was performed by Chen et al. [104]. An optimal $NaBH_4$ yield of 88.3 % was achieved after 20 h milling with 37.5 % excess of MgH_2.

Zhong et al. [108] studied the recycling of $NaBO_2 \cdot 4H_2O$ in the same conditions and tried to optimize the reaction parameters. A 74.0 % $NaBH_4$ yield was obtained after 20 h milling, with a $Mg_2Si/NaBO_2 \cdot 4H_2O$ molar ratio of 4.

The $NaBH_4$ formation from $NaBO_2 \cdot 4H_2O$ with Mg_2Si was also studied and $NaBO_2 \cdot 2H_2O$ was found to be an intermediate borate in the process, as reported in Equation 2.26. This way, the remaining reaction mechanism for the $NaBH_4$ synthesis can be described as above reported, where intermediate $Mg(OH)_2$ was detected.

$$NaBO_2 \cdot 4H_2O + Mg_2Si \rightarrow NaBO_2 \cdot 2H_2O + 2MgO + Si + H_2 \quad (2.26)$$

Another borate that has been considered to regenerate $NaBH_4$ is boron oxide (B_2O_3). This borate is present as main structure of the borates previously presented, this way being a less complex compound, which can increase the $NaBH_4$ production.

Çakanyildirim et al. [109] considered the mixture of this borate with Na and MgH_2 (30 % excess), as demonstrated by Equation 2.27. The time of milling was studied (from 1.7

to 18.3 h), as well as the B_2O_3/Na ratio (0.6 to 1.4). Although the increase of the time of milling has a positive effect on the $NaBH_4$ yield, the highest value (25.0 %) was obtained with a 1.2 B_2O_3/Na ratio after 13.3 h. Nevertheless, it is a low yield compared to other borates for the same time of milling.

$$Na + 3MgH_2 + B_2O_3 \rightarrow 2NaBH_4 + 3MgO + Mg \quad (2.27)$$

Ar et al. [110] also reported the mechano-chemical regeneration of $NaBH_4$ from B_2O_3, by mixing the borate with $NaNH_2$ and MgH_2 as observed by Equation 2.28.

$$NaNH_2 + 3MgH_2 + B_2O_3 \rightarrow NaBH_4 + 3MgO + NH_4BH_4 \quad (2.28)$$

Several experiments were carried out with a milling time varying from 6.7 to 13 h. The value of 8.3 h milling has been found as the optimal time, since further reaction increases the formation of MgO instead of the desirable $NaBH_4$. Following this observation, the authors confirmed that excess of MgH_2 is necessary since, at the end of the reaction, it was observed that a part of this hydride was fixed to the mill's wall and did not react. However, if the amount of MgH_2 is too high, it may decrease the contact between the reactants and decrease the $NaBH_4$ yields. Thus, the authors concluded that the optimal value for the MgH_2 excess is 35 %.

Given that, as observed in Figure 2.8, $NaBH_4$ is obtained originally from borax ($Na_2B_4O_7$) minerals, this borate recycling has been reported by Çakanyildirim et al. [111]. An excess of MgH_2 up to 70 % was studied and also a time of milling from 3.3 to 10 h. Figure 2.19 presents the variation of $NaBH_4$ with these parameters. As observed, the optimal values found were 10 % and 6.7 h. Regarding the time of milling, no significant $NaBH_4$ formation was observed with higher values. On higher MgH_2 excess than 10 %, a decrease of the $NaBH_4$ production was observed, since it possibly difficults the mixture between the reactants.

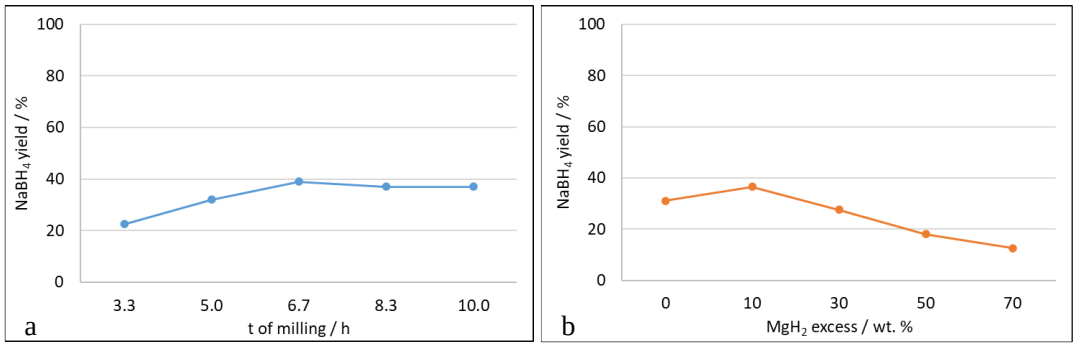


Figure 2.19. Influence of t of milling (left) and MgH_2 excess (right) in the $NaBH_4$ yield, adapted from [111].

This study has given a 38.0 % $NaBH_4$ yield, which is considerably lower than the $NaBO_2$ recycling. Some additives (Na, NaH and Na_2CO_3) have also been considered for this process, however no positive effect on the $NaBH_4$ formation was observed.

On the same hand, same experiments were carried out by Li et al. [69] for 1 h, and the influence of three additives was studied: Na_2O_2, NaOH, and Na_2CO_3. Figure 2.20 presents the influence of the additives on the $NaBH_4$ yield. The best additive was Na_2CO_3 with a 78.0 % $NaBH_4$ yield achieved. The authors justified this result by the low reactivity of Na_2CO_3 with $NaBH_4$, as opposed to Na_2O_2 that oxidated it and NaOH, who reacted with $Na_2B_4O_7$ to form $NaBO_2$ and water.

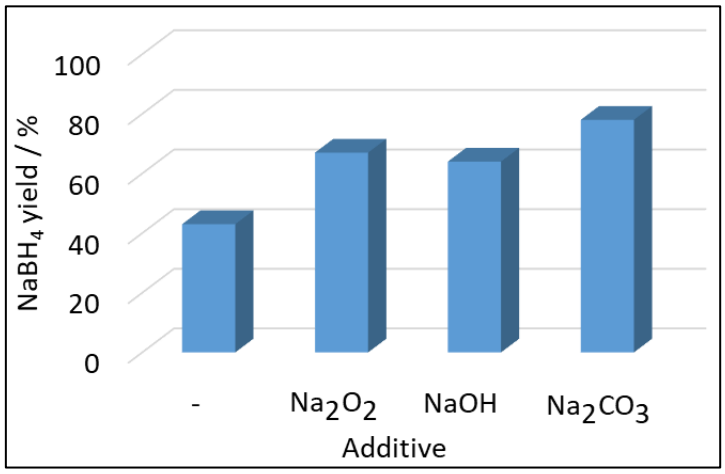


Figure 2.20. Additive influence on the $NaBH_4$ yield, adapted from [69].

Borax decahydrate ($Na_2B_4O_7 \cdot 10H_2O$) has also been studied to regenerate $NaBH_4$. Zhu et al. [112] developed a low-cost system to close the $NaBH_4$-H_2 cycle based on the recycling of this borate by ball milling it with Na_2CO_3 and Mg, as represented by Equation 2.29.

$$Na_2B_4O_7•10H_2O + Na_2CO_3 + 20Mg \rightarrow 4NaBH_4 + 20MgO + CH_4 \quad (2.29)$$

As previously referred and reaffirmed by the authors, borax presents more similarities with $NaBH_4$ and a higher reactivity than $NaBO_2$, which makes the regeneration of $NaBH_4$ easier. An optimal yield of 78.9 % was obtained for 30 h of ball milling and an excess of Mg of 23.75 %.

At last, as referred before, one of the disadvantages of the mechano-chemical processes is the need to extract the $NaBH_4$ after reaction. In literature, there are few reports on this study. The main method to extract the borohydride is by dissolving the products of reaction in isopropylamine, then filter and dry it to evaporate the solvent [99], [100], [102], [113]. As alternative, ethylenediamine has been used instead of isopropylamine [69], [101], [106], [114].

These reports demonstrate the progress that has been made on the mechanochemical regeneration of $NaBH_4$. Close to 100 % yields have been reported, however with considerably high times of milling. Moreover, in general, increasing the hydration of the borate has a negative impact on the $NaBH_4$ yield, however it reduces the need to introduce another source of hydrogen to the reaction since it is present in the water, e.g., Mg can be used instead of MgH_2. At last, the recycling of synthesized $NaB(OH)_4$ was not considered in literature and given it can be obtained through the $NaBH_4$ hydrolysis with additive CMC (please recall section 2.1.4), its recycling is essential and can have a positive impact on the $NaBH_4$ yield compared to the recycling of $NaBO_2•2H_2O$.

2.3.3. Electrochemical processes

Electrochemical regeneration of $NaBH_4$ can be considered as an alternative to the types of processes presented above. Electrochemical synthesis is a process that involves the transfer of electrons between compounds for the reaction to happen as is schematized in Figure 2.21. This type of reactions occurs in an electrochemical cell whose main components are two electrodes (anode and cathode) each containing a solution (the electrolyte) and connected to an external circuit.

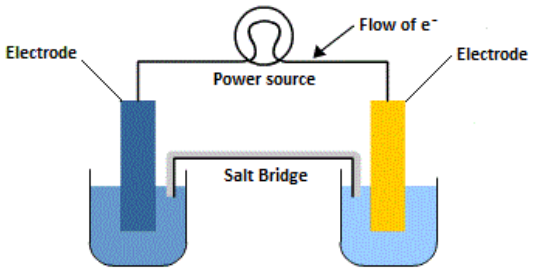


Figure 2.21. Scheme of an Electrochemical cell (adapted from [115]).

The electrodes must be electrically conductive materials and must adsorb the reactants at their surface, to allow for their oxidation or reduction. The electrolyte is essential to warrant the correct means to promote the reduction and/or oxidation of any intended compound. The electrode where oxidation occurs (the anode) generates electrons and ions. These electrons are removed through the external circuit and are transferred to the other electrode (the cathode) and from it to the reactants (and ions that crossed) to be reduced. The oxidized and reduced compounds are the products of reaction. The electrodes can also participate in the reaction by being oxidized or reduced and forming other compounds. These are called active electrodes [116].

In Figure 2.24, the electrochemical cell presents the electrodes separated by a salt bridge. Nevertheless, both compartments can be mixed in the same electrolyte.

There are two types of electrochemical cells, based on the cell's potential: galvanic and electrolytic [117]. In a galvanic cell, the redox reaction, i.e., the oxidation and reduction reactions, occurs spontaneously and the products of reaction are obtained without the need to introduce electric energy to the cell. This way, in these reactions, electric energy is obtained, by the extraction of the electrons produced at the anode. On the other hand, in an electrolytic cell, the reactions do not initiate spontaneously, so the use of electric energy is required.

From the two types of existing electrochemical cells, this thesis focuses on the electrolytic cell, where electric energy enters the cell to promote a chemical reaction. This serves as an alternative to the regeneration of the sodium borohydride from the by-product. These processes are desired due to its low energy consumption, cleanliness, and reduced cost compared to the thermo- and mechanochemical processes.

Additionally, there are two modes of operation of a cell: galvanostatic and potentiostatic. In the first, a current is implied to the cell and its potential is read since electric energy is

generated. The cell's potential can be determined based on the Nernst equation, Equation 2.30, in function of the standard potential of the reactions and the cell conditions [118],

$$E_{cell} = (E_{cathode} - E_{anode}) + \frac{\Delta\hat{s}}{nF}(T\text{-}T_0) - \frac{RT}{nF}\ln\left(\frac{\pi a_{products}^{\upsilon i}}{\pi a_{reactants}^{\upsilon i}}\right) \quad (2.30)$$

where $(E_{cathode} - E_{anode})$ is the standard cell potential, E_{cell}^0; $\Delta\hat{s}$ is the variation of entropy of the system; n is the number of electrons transferred; F is the constant of Faraday (F = 96 485 A/mol); T and T_0 are the temperatures of operation and standard, respectively; and $a_i^{\upsilon i}$ is the chemical activity of the products and reactants raised to its stoichiometric coefficient.

The cell potential is not constant during the process, and it decreases with the current applied. In the potentiostatic mode, the Nernst equation is used in the same way; however, a potential is applied to the cell and a current is obtained if a reaction is developing. In this mode, electric energy is consumed. Figure 2.22 demonstrates a typical polarization curve in electrolysis mode, where the main resistances to the cell's performance are demonstrated and the range where they are more significant [119]. Several resistances are highlighted: the activation and mass transport losses, occurring mainly at the low and high current densities, respectively; and the ohmic losses increasing linearly with the current.

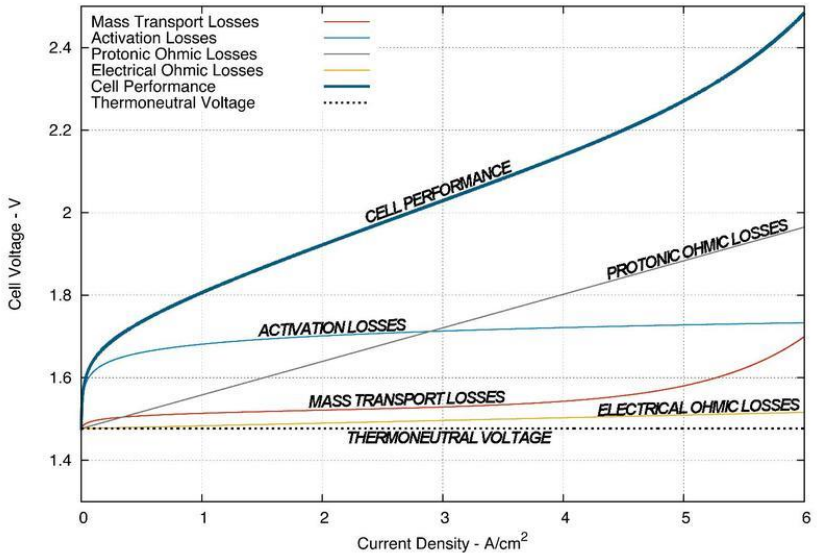


Figure 2.22. Polarization curve and types of losses [120].

To detect what reactions (oxidation or reduction) can occur in a determined system (composed of two electrodes, an electrolyte and a reference electrode) cyclic voltammetry

(CV) analysis is usually performed. These tests are denoted by the variation of the current at specific potentials, as observed by the peaks in Figure 2.23. In these tests, the electrode where the main reactions are being studied is defined as the working electrode (WE), while the counter-electrode (CE) is the auxiliar electrode of the electrochemical cell.

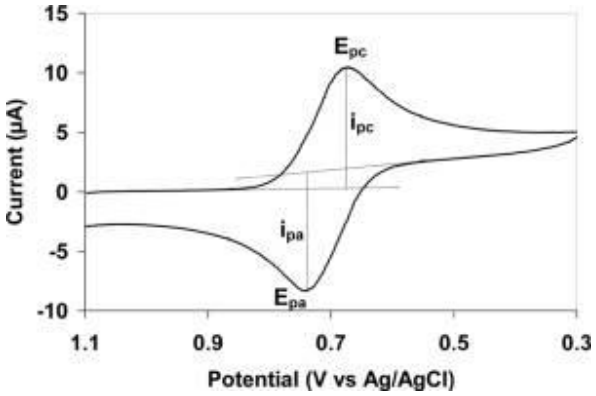


Figure 2.23. Example of a CV analysis [121].

The regeneration of sodium borohydride from sodium metaborate can theoretically be obtained mainly through its direct electroreduction, as shown in Equations 2.31 and 2.32. In the anode, an aqueous solution containing NaOH is dissociated in Na^+ and hydroxide (OH^-) ions. The OH^- are then oxidized to release 8 e^-, which cross to the cathode side, where a $NaBO_2$ aqueous solution is present. There, dissolution of $NaBO_2$ molecules release the BO_2^- ions which in the presence of the free electrons and water are reduced to BH_4^-, generating OH^- as by-product. Therefore, in the cell's balance the OH^- ions are equally consumed and produced. Excess of Na^+ can then assure the formation of $NaBH_4$; nevertheless, further H_2 generation is assured by hydrolysis of generated BH_4^-.

$$\text{Cathode: } BO_2^- + 6H_2O + 8e^- \rightarrow BH_4^- + 8OH^- \quad (2.31)$$

$$\text{Anode: } 8OH^- \rightarrow 4H_2O + 2O_2 + 8e^- \quad (2.32)$$

Although there have been claims of sodium borohydride synthesis, those results have not been replicated [122]. This fact is justified by parallel reactions that compete with this process at the applied potentials in the cathode, for example, the hydrogen evolution reaction (HER), where water decomposes into H_2 and OH^-. These reactions are favored instead of the BO_2^- reduction, due to the need for the cell to operate in alkaline (concentrated NaOH) electrolytes.

Other electrochemical processes have been referred in the literature; however, the results obtained were similar to the direct electroreduction process. From what the author could

find, the first references that confirm the $NaBH_4$ electrosynthesis (as reported in the literature) were Zhu et al. [67], [123], [124]. A 15.1 % current efficiency $NaBH_4$ electrosynthesis was reported at atmospheric pressure and room temperature. The electrochemical cell was composed of a copper WE and a lead CE. Then, 1 M aqueous sulfuric acid (H_2SO_4) solution was added to the anode and 1 M NaOH and 0.2 M $NaBO_2$ solution was added to the cathode. A cathodic peak was observed at -1.17 V, which is indicative of the BO_2^- reduction. Moreover, the increase of NaOH favored the electrosynthesis; however, excessive NaOH hardens the products' adsorption and conduction. Similar observation was made for the $NaBO_2$ concentration. Nevertheless, the process' efficiency is low.

Efficient electrosynthesis of $NaBH_4$ was achieved by Shen et al. [125]. Given the high cost of $NaBH_4$ and its use as an effective reducing agent, the authors considered its electrosynthesis as an intermediate step in a desulfurization experiment of a coal water slurry at ambient pressure and room temperature. The electrochemical cell consisted of cathode and anode reservoirs separated by a potassium chloride (KCl) bridge. On the cathode side, a solution containing 0.1 to 0.45 M $NaBO_2$ and 0.025 M NaOH was initially added. Then, the coal was added, and the mix was maintained under stirring. The anode side was composed of an iron sulfide (FeS_2) and NaOH solution. The cathode was Pb and the anode was graphite (C). After the synthesis of BH_4^- at the cathode, its hydrolysis promoted the formation of hydrogen that reduced the FeS_2 to hydrogen sulfide (H_2S). Then, at the anode, the reaction with NaOH allowed the separation and removal of the sulfur.

Equations 2.33–2.35 represent the primary reactions of the experiment. BH_4^- electrosynthesis was achieved as represented by Equation 2.31 above.

$$2H_2O + BH_4^- + FeS_2 \rightarrow Fe + H_2S + S + BO_2^- + 3H_2 \quad (2.33)$$

$$H_2S + 2NaOH \rightarrow Na_2S + 2H_2O \quad (2.34)$$

$$2H_2O + 2Na_2S + O_2 \rightarrow 2S + 4NaOH \quad (2.35)$$

The BO_2^- concentration, electrolytic time, and voltage were studied between 0.09 and 0.46 M, 1 and 5 h, and 2.5 and 3.3 V, respectively. An optimal total sulfur removal (TSR) of 36.6 % was achieved with 0.18 M, 4 h, and 3.0 V, respectively. Considering the BO_2^- as

an intermediate essential step of the process, these parameters also benefited the BH_4^- formation.

The group continued these experiments and the electrochemical cell was also optimized, to increase the TSR and the BH_4^- formation. Considering similar electrochemical cells—however, with a combined anode and cathode reservoir [126] - the group studied again the BO_2^- concentration, electrolytic time, and voltage. However, the optimal values did not suffer a considerable change (0.20 M, 4 h and 3.5 V). Moreover, the NaOH concentration and electrodes were analyzed. The NaOH concentration was studied up to 0.38 M. It was observed that 0.05 M NaOH was the optimal value to promote the TSR, since further increase favored the pH and reduced the hydrogen generation from the BH_4^- hydrolysis. Regarding the electrodes, the anode/cathode considered were: Pb/Pb, C/Pb, Ti/Pb, C/Cu, and C/Zn. The results were slightly in favor of the last, as observed in Figure 2.24. In this way, graphite not only better promotes the TSR but also presents significant advantages to consider, such as easy to process, reduced waste and price, and good thermostability and conductivity.

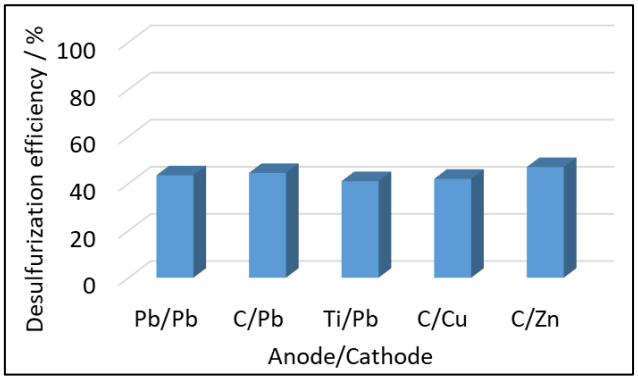


Figure 2.24. Desulfurization efficiency for the electrode combinations studied (adapted from [126]).

The same group also studied the desulfurization of gasoline [127] in an electrochemical cell composed of a Boron-doped diamond (BDD) electrode in the cathode (WE) and a C electrode in the anode (CE), separated by a cation exchange membrane. After BH_4^- formation, a model of gasoline was added to the cathode, and after the reaction, nickel chloride hexahydrate ($NiCl_2 \bullet 6H_2O$) was also added. Cyclic voltammetry tests were performed using 0.15 M $NaBO_2$; a reduction peak was observed between -1.2 and -1.8 V, while the hydrogen and oxygen evolution reactions were initiated at voltage below -1.8 V and above 0.6 V, respectively. Moreover, pulse voltage was applied during the reaction. Forward and reverse pulse voltages were optimized considering these limits.

Overall, the best TSR achieved was with a forward and reverse pulse of -1.5 V (applied after 1.5 s) and 0.3 V (applied after 0.5 s), respectively. This result was explained by avoiding at maximum the HER (happening simultaneously with the BH_4^- electrosynthesis), and the reverse pulse voltage was enough to attract the BO_2^- ions to the BDD electrode while avoiding the oxygen evolution reaction. Figure 2.25 presents this impact on the desulfurization process. We observe that for all potentials applied pulse voltage always has a positive impact on the process and the difference between both is the highest at -1.5 V. Moreover, we notice the efficiency of the process increases with the potential for up to -1.8 V in constant voltage and only up to -1.5 V in pulse voltage, explained since the reduction peak was observe between -1.2 V and -1.8 V and the pulse voltage limits the hydrogen evolution reaction occurring for potentials starting at -1.8 V.

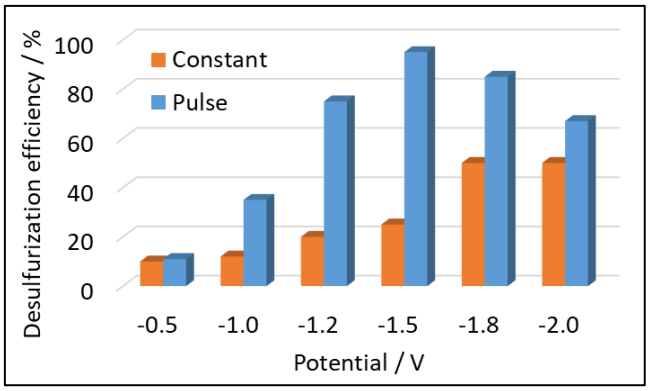


Figure 2.25. Constant vs pulse voltage impact on the desulfurization efficiency (adapted from [127]).

Regarding the BH_4^- electrosynthesis step, other cell parameters were also studied: $NaBO_2$ and NaOH concentrations, electrolytic time, and stirring rate. First, 0.15 M of $NaBO_2$ was maintained as an optimized value from previous experiments, since higher concentrations did not contribute to further increase of the TSR. The optimal NaOH concentration was 0.1 M, since although it is important to maintain the cell as alkaline to avoid too fast BH_4^- hydrolysis, its excess reduces the oxygen evolution voltage, promoting it and complicating the BO_2^- transfer to the BDD electrode. Excess stirring rate was also observed to affect the BO_2^- transfer, so 400 rpm was the best value defined. The higher efficiency of the desulfurization process was 97.0 %.

More recently, the group studied the addition of ionic liquids (IL) to the desulfurization process of gasoline [128]. The use of ILs as electrolyte has been increasingly reported in the literature due to their characteristics, which make them more suitable than water and other electrolytes. In the BH_4^- electrosynthesis, they avoid the need to control the

hydrogen and oxygen evolution reactions and present a wider electrochemical window. Moreover, they can be recovered at the end of the experiment. Similar electrochemical cells to previous study were considered by the group. In this experiment, the WE was a glassy carbon electrode, and the CE was a Pt wire. The IL was added to both the electrodes reservoirs in the cell, while water was only present due to the $NaBO_2$ solution and the need of hydrogen for the BH_4^- electrosynthesis. The cyclic voltammetry tests performed indicated a reduction peak between -2.2 and -3.0 V associated to the BH_4^-. Moreover, the hydrogen and oxygen evolution reactions were observed at -3.0 and 2.0 V, respectively. As expected, the electrochemical window using IL is wider than that of water. Forward and reverse pulse voltage was equally applied, and their parameters were optimized. The optimal values to promote the BH_4^- electrosynthesis and the TSR (97.0 %) were a forward pulse voltage of -2.6 V (0.6 s forward pulse time) and reverse pulse voltage of 0.5 V (0.5 s reverse pulse time). If these pulse times were too long, the reactions did not benefit; if they were too short, the reactions did not occur.

Based on these results and assuming that an efficient electrosynthesis of BH_4^- is essential for the desulfurization of the coal water slurry, it is possible to affirm that $NaBH_4$ can be obtained through an electrochemical process and that it is an alternative to the thermo- and mechano-chemical processes. Nevertheless, it is essential to promote the $NaBH_4$ regeneration as the main aim instead of an intermediate step in another process. In that order, both the use of ILs and the pulse voltage are possible improvements of the direct electroreduction of $NaBO_2$, as observed in the studies regarding the desulfurization electrochemical processes here presented. In addition, as noted in the thermo- and mechano-chemical regeneration processes section, the study of hydrated $NaBO_2$ is crucial, since it is the main by-product of the $NaBH_4$ hydrolysis and it is demonstrated that its recycling is not as easy. Considering the practicability and possibly low cost of these processes, the electrochemical regeneration of $NaBH_4$ must be considered with the envision of different routes.

2.4. Motivation and thesis layout

As described in this chapter, following the 2007 DoE's no-go recommendation on the hydrolysis of sodium borohydride as source of H_2 in power applications, there is a need to clarify, find new ways and optimize the rehydrogenation of the borate hydrolysis by-product to obtain sodium borohydride and close the cycle. There is still a clear lack of

references covering this essential topic. Moreover, different authors have presented unclear discussions on what borate is formed as by-product of hydrolysis.

For that matter, the main goal of this thesis is to understand the composition of the by-product of the $NaBH_4$ hydrolysis: what is the main borate formed, how operating conditions can influence its formation and how to optimize its purity, in order to facilitate its recycling process. With that, it is aimed by this thesis to find a clean and cost-effective method to regenerate sodium borohydride from the reaction by-product. Also, no economic analysis on this technology has been published before. So, as a third goal of this thesis, is to perform an economic analysis based on the current status of the hydrolysis of sodium borohydride and its regeneration technology.

This PhD thesis results from the work carried out at CEFT (Centro de Estudos de Fenómenos de Transporte) in the Chemical Engineering Department of Faculty of Engineering in Oporto University (FEUP), throughout the period between July 2018 and January 2023. The thesis is organized in 6 chapters.

Chapter 1, **Introduction**, presents a general introduction concerning the current state on energy sources and its demand as well as the strong potential of the energy vector Hydrogen. Afterward, it presents the chemical hydrides and its hydrogen storage capabilities, and among them more specifically, sodium borohydride as an advantageous hydrogen carrier.

Chapter 2, **State of the Art**, is devoted to the detailed description of the sodium borohydride as a hydrogen carrier with three subchapters: firstly, it introduces the hydrolysis of sodium borohydride and its advantages and limitations compared to other sources of hydrogen; secondly, it summarizes the different routes for the formation of the by-product of sodium borohydride hydrolysis; and it finishes with the review on the known pathways of the rehydrogenation of sodium borohydride to close the $NaBH_4$-H_2 cycle.

Chapter 3, **Experimental study of the sodium borohydride hydrolysis by-product**, describes the work that was developed on the optimization of the hydrolysis reaction towards the obtention of the optimal reaction by-product to decrease the energy gap required for its rehydrogenation.

Chapter 4, **Experimental study of the sodium borohydride regeneration**, describes the methods studied to regenerate sodium borohydride and close the $NaBH_4$-H_2 cycle, and the obtained results. The mechano-chemical regeneration of sodium borohydride from by-product $NaB(OH)_4$ as well as the electrosynthesis of the borohydride from boric acid were studied.

Chapter 5, **$NaBH_4$-H_2 Economic analysis**, gives a sensitive analysis on the economic viability of $NaBH_4$ as source of hydrogen on moderate power applications.

Chapter 6, **Conclusions and future work**, where the main conclusions of the present work are summarized and lines of possible future work are suggested.

Chapter 7, **Follow-up,** resumes all the main results achieved in this thesis (Chapter 3), from the first observations regarding the innovative by-product post-treatment developed, to its optimization and the provisional patent application and approval to a start-up creation and a possible commercial valorization.

3. Experimental study of the by-product of sodium borohydride hydrolysis

This chapter reports the results obtained in this thesis related to the study of the by-product of sodium borohydride hydrolysis. Before the regeneration of $NaBH_4$ is defined, it is essential to understand in what conditions the by-product of its hydrolysis is formed, its structure and how it can be optimized. It is divided into three subchapters, excluding the conclusions. The first one follows the Ferreira et al. [19] report, which observed a rearrangement of the by-product in the presence of additive CMC. This way, $NaB(OH)_4$ was formed, a borate which does not contain water molecules in its structure, therefore easier to recycle to $NaBH_4$. Then, a new innovative process to treat the by-product is implemented, that assures pure or close to pure $NaB(OH)_4$, is described in subchapter 3.2. This promising low-cost, easy to implement post-process is essential to optimize the by-product recycling back to $NaBH_4$. Subchapter 3.3 describes variations to the process introduced in 3.2, to understand different effects on the by-product formed, such as, temperature of drying and humidity. The structure of each subchapter is based on the description of the adopted experimental procedure and on the corresponding results and discussion. The chapter ends with the outline of the main conclusions.

3.1. Influence of additives on the by-product

The report of Ferreira et al. [19] demonstrated the importance of the study of the sodium borohydride hydrolysis by-product including possible effect of additives on its formation. A deep understanding of the impact of additives in the structure of the hydrolysis byproduct is essential and therefore the study of the influence of additive CMC was performed. The authors experiments were replicated, and the CMC's concentration was varied. Moreover, other additive - polyacrylamide (PAA) - was considered in the research activities to realize if the impact on the by-product composition was due to the CMC or it could have another explication. This additive was selected mainly due to the combination of three factors: similar properties when compared to CMC; low synthesis cost and availability in the laboratory. Similar to CMC, PAA is a white powder, water-soluble, non-toxic, that can be used in a broad range of applications [129].

3.1.1. Experimental procedure

Catalytic hydrolysis of $NaBH_4$ was performed in two stainless-steel reactors with different geometries: a cylindrical reactor and an egg-shaped reactor with a volume of 9 cm^3 represented in the photographs shown in Figures 3.1 and 3.2. As observed in Figure 3.1, there are stainless bottoms that can be placed inside the reactor to reduce the internal volume of the reactor where the H_2 is produced. Two reactors were used for the reported hydrolysis experiments: the reactor without any reducing bottom (LR, internal volume of 646 cm^3) and the reactor with both reducing pieces (SRc, internal volume of 229 cm^3). The correct sealing of the reactor is assured by an axial installation of an O-ring. Moreover, the temperature inside the reactor was measured by two thermocouples – one close to the bottom of the reactor and one close to the top of the interior - and the pressure inside the reactor was controlled using a pressure gauge [40]. Both temperatures and pressure are recorded with a data acquisition system using Lab View software.

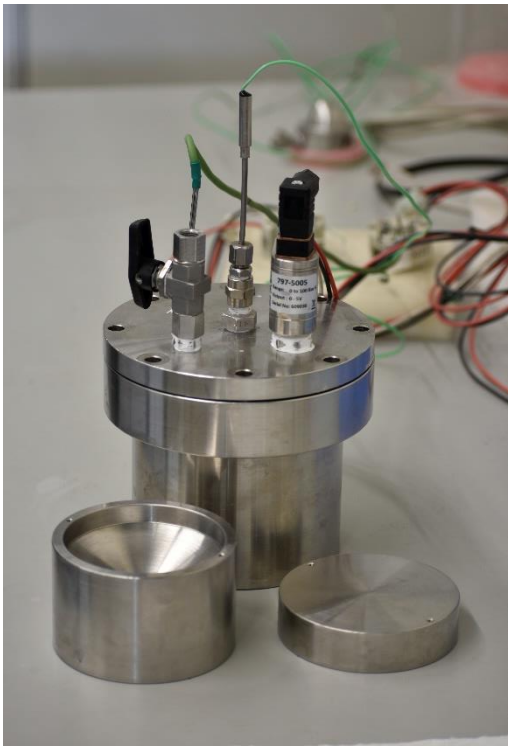


Figure 3.1. Cylindrical reactor and conical and planar shape bases used in hydrolysis experiments.

The egg-shaped geometry was considered by Nunes et al. [23] based on the results obtained with the SRc, i.e., the promotion of the mixture of the solution with the catalyst with a conical base. Moreover, the authors had previously observed the accumulation of water in the top of the SRc after the reaction, which could be responsible for a decrease

in the H_2 generated. Similar to the LR and SRc, the temperature and pressure inside the reactor are measured with a k-thermocouple and pressure gauge, respectively, and recorded using Lab View.

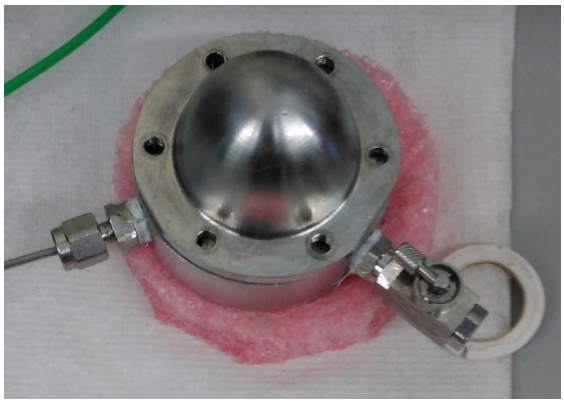


Figure 3.2. Egg shaped reactor used in hydrolysis experiments.

Solutions of the reactants sodium borohydride (Panreac Química SA – 123314,1608, 96 % purity) and water along with sodium hydroxide (EKA UN1823, 98 % purity) were prepared as described: i) water is initially added to a glass flask; ii) sodium hydroxide is then dissolved in distilled water; iii) after that, sodium borohydride is dissolved in the previous solution. the sodium hydroxide acts as an inhibitor of the reaction, to avoid spontaneous formation of hydrogen outside the reactor. Finally, additives in small concentration are added to the solution. All dissolutions are prepared under magnetic stirring at room temperature. Then, if the SRc is considered for the hydrolysis experiment, it is prepared by placing the interior bases inside the LR. After that, the Ni-Ru catalyst powder is place in the interior bottom of the reactor and the reactor is sealed to avoid any H_2 release during the experiment. The $NaBH_4$ solution prepared is then injected in the reactor. All hydrolysis experiments were performed at room temperature and without stirring. The reaction is considered complete when the pressure inside the reactor is constant and stable, indicating no more H_2 is expected to be generated. Figure 3.3 presents the variation of temperature and pressure inside the reactor during a typical hydrolysis reaction. An increase of the temperature inside the reactor (higher for the bottom - close to the reaction - than on the top of the interior is expected) indicates the H_2 generation and heat release, which decreases throughout the experiment and stabilizes again at the initial temperature of the reaction. Therefore, for the performance of this reaction, the initial or final temperature inside the reactor was considered instead of the momentary peak.

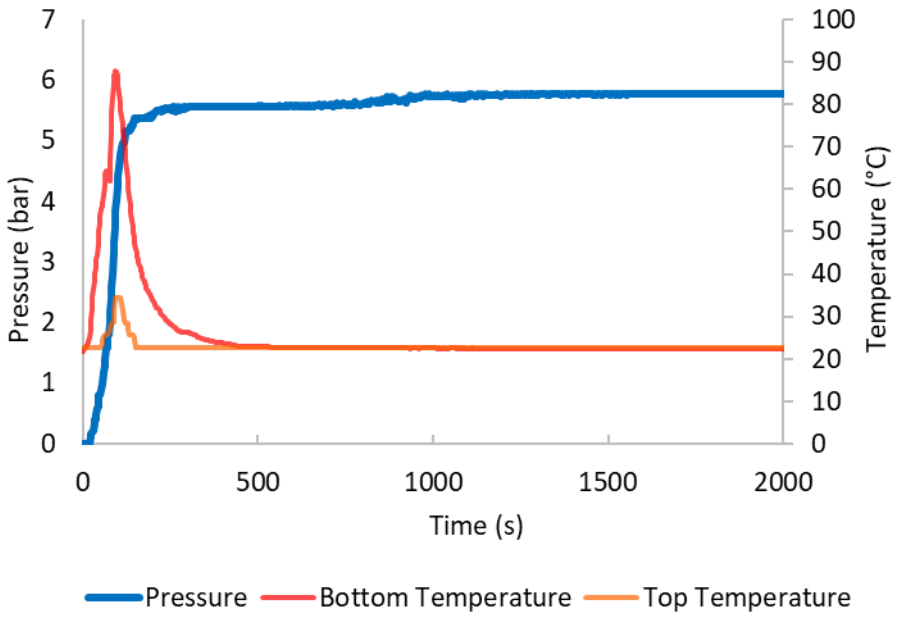


Figure 3.3. Experimental P-T curves of a typical hydrolysis reaction.

After reaction completion, the hydrogen produced is carefully released to the atmosphere and the by-product is extracted to a centrifuge tube. There, sedimentation of the catalyst allows its separation from the by-product, which is then placed in a petri dish to be dried open-to-air and at room temperature. Samples of dried by-product are at last prepared by milling to powder size and analyzed by XRD.

The catalyst used is a Ni-Ru powder, with a density of 1.7 g/cm^3. It was prepared, as described by Nunes et al. [23], from a mixture of precursors in deionized water - impregnating small quantities of ruthenium in the nickel salts (Riedel-de Haën) - by chemical reaction with 10 wt. % stabilized $NaBH_4$ solution (Rohm and Haas), as the reducing environment. When the reduction was complete the catalyst was appropriately decanted, washed, filtered, dried and heat-treated at 383 K, and kept in a desiccator until use. Furthermore, an X-Ray Photo-electron Spectroscopy (XPS) analysis was performed to a fresh sample of the synthetized catalyst, and atomic concentrations of Ni and Ru of 21.96 at. % and 2.53 at. %, respectively, were obtained. After reaction, it can be reused without losing its activity. For that, after the reaction and separation from the by-product, it is washed in distilled water and decanted at least three times to remove all impurities and then dried for 1 h at 80 ºC.

Hydrogen yield and generation rates as well as induction time, GHSC and VHSC are calculated as represented in Equations 3.1 to 3.5.

$$\eta = \frac{P_{H_2,\,obtained}}{P_{H_2,\,theorical}} \times 100 \quad (3.1)$$

$$HGR\ /\ L.min^{-1}g^{-1}_{catalyst} = \frac{RT}{V_{gas}} \times 60 \times \frac{V_{molar,\,STP}}{m_{catalyst}} \quad (3.2)$$

$$\text{induction time} = t\,(P_{relative} = 0.5\ \text{bar}) \quad (3.3)$$

$$GHSC\ /\ wt.\% = \frac{m_{H_2}}{V_{system}} \times 100 \quad (3.4)$$

$$VHSC\ /\ kg \cdot m^{-3} = \frac{m_{H_2}}{V_{system}} \times 1000 \quad (3.5)$$

The operation conditions of each hydrolysis experiment performed with up to 0.15 % PAA and 1.0 % CMC additives and excess of water ranging from x = 11 to x = 16 are displayed in Table 3.1. x = 16 (or x = 15, since the presence of more than 0.25 % additive reduces the excess of water while maintaining the mass of $NaBH_4$) was chosen in the majority of the experiments given it was previously optimized by the group (please recall Chapter 2). As alternative, x = 11 was also studied, given it is the minimum excess of water that avoids the $NaBO_2$ precipitation. As observed in Table 3.1, while experiments #3 and #4 considered the use of 0.25 % CMC – as performed by Ferreira et al. [19]-, experiments #5 to #8 were performed with a higher concentration (1.0 % CMC). Moreover, all experiments using additive PAA (#9 to #14) were performed in the egg reactor. The particular interest of this was to analyze the impact of this additive on the hydrolysis reaction and then, if it had a positive impact on the H_2 production, its by-product was extracted and analyzed. Due to the size of the egg, 1 cm^3 reaction was adequate. On the SRc experiments, 5 cm^3 solution was ideal to extract enough by-product for analysis. At last, the experiments in the LR reactor considered a volume of 50 cm^3 since in experiments #15 to #17, a Ni-Ru foam with identical characteristic to the Ni-Ru powder was used which required its full immersion in the solution, thus 50 cm^3 was the ideal volume. Experiment #18 was performed to compare the results with these experiments.

Table 3.1. Operating conditions of the hydrolysis experiments containing up to 0.15 % PAA and 1.0 % CMC additives and excess of water ($11 < x < 16$).

#	Reactor	Volume	x	Ni-Ru/$NaBH_4$ mass ratio	Additive
1	SRc	5	16	0.40	-
2	SRc	5	16	0.40	-
3	SRc	5	15	0.40	0.25 % CMC
4	SRc	5	15	0.40	0.25 % CMC
5	SRc	5	15	0.40	1.0 % CMC
6	SRc	5	15	0.40	1.0 % CMC
7	SRc	5	15	0.40	1.0 % CMC
8	SRc	5	15	0.40	1.0 % CMC
9	Egg	1	16	0.40	0.01 % PAA
10	Egg	1	16	0.40	0.10 % PAA
11	Egg	1	16	0.40	0.15 % PAA
12	Egg	1	16	0.40	0.10 % PAA
13	Egg	1	16	0.40	0.10 % PAA
14	Egg	1	16	0.40	0.10 % PAA
15	LR	50	16	0.01	-
16	LR	50	16	0.01	-
17	LR	50	16	0.01	-
18	LR	50	16	0.01	-
19	SRc	5	11	0.40	-
20	SRc	5	11	0.40	-
21	SRc	5	16	0.40	-
22	SRc	5	16	0.40	-

All these experiments were performed to understand the impact of the $NaBH_4$ hydrolysis and the influence of its parameters on the by-product composition. Table 3.2 summarizes the studies that were performed by each experiment.

Table 3.2. Operating conditions varied in each hydrolysis experiment performed (#1 to 22), while maintain remaining parameters, for analysis of the influence of each parameter studied.

Experiment #	Parameter analysis
1 – 8	Additive CMC
9 - 14	Additive PAA
15 – 18	Ni-Ru: powder and foam
19 - 22	Excess of water, *x*

Experiments #1 and #2 were performed without additive to compare with experiments #3 and #4 with 0.25 % CMC and #5 to #8 with 1.0 % CMC. With this, the optimal concentration of CMC is expected to be found.

Then, to understand if the results obtained with additive CMC could be replicated with other additives, PAA was chosen (experiments #9 to #14) based on the high viscosity of the compound; also, the influence of its concentration was optimized. This way, as observed in the Table 3.1, experiments performed had increased concentration and the optimal value was observed to be 0.10 %. For that matter, only the by-products of experiments # 12 to #14 were analyzed.

At last, by-products of experiments #19 to #22 differ on the excess of water. Although $x = 16$ has been the value optimized by the group, $x = 11$ is the minimal value to allow the maximum $NaBO_2$ solubility in the solution's mean.

Additionally, some of these by-products were reanalyzed to understand the effect of time on its composition during storage without use. The XRD analysis was performed in the Laboratório Central de Análises of the Aveiro University. The XRD patterns were recorded in an Empyrean diffractometer of Malvern Panalytical at room temperature using monochromatic Cu K-α radiation (λ = 1.5406 Å). The range of the XRD patterns were $4\ º < 2\theta < 70\ º$. The identification of the compounds in the patterns was performed by comparison with XRD databases, identifying the main chemical elements and compounds expected to be observed and comparing their patterns with the by-product one, as previously described in Chapter 2 Section 2.2.2. This analysis took at least one week to one month, considering the shipping of the by-products samples, the XRD analysis execution and the delivery of its results. It was chosen in detriment of FTIR and NMR since it is the main method reported in literature and has been used by the group in previous experiments and this way there is a term of comparison (analysis using the same equipment and conditions).

3.1.2. Results and Discussion

Table 3.3 presents the results of the hydrolysis experiments, namely, the H_2 yield, HGR, induction time and GHSC and VHSC.

Table 3.3. Performance of each hydrolysis experiment performed, by analysis of the H_2 yield, generation rate (HGR), induction time and storage densities (GHSC and VHSC).

#	Yield / %	HGR / $L.min^{-1}.g_{cat}^{-1}$	Induction time / s	GHSC / wt. %	VHSC / $kg.m^{-3}$
1	100	1.4	62	2.1	23.5
2	81	1.2	10	1.6	17.1
3	100	18.8	17	2.1	22.8
4	100	19.9	20	2.2	24.6
5	100	3.0	23	2.2	24.5
6	100	2.4	34	2.2	24.0
7	100	2.4	46	2.2	24.2
8	39	4.3	25	0.5	6.0
9	97	1.1	28	2.0	21.7
10	90	4.3	37	1.8	20.2
11	89	1.2	39	1.8	20.0
12	87	1.5	35	1.8	19.6
13	89	1.0	48	1.8	19.9
14	89	1.2	40	1.8	20.1
15	100	3.6	155	2.3	23.6
16	96	3.0	166	2.0	20.7
17	98	2.9	167	2.1	21.7
18	100	0.3	591	2.2	23.6
19	98	24.4	60	2.5	27.8
20	100	33.3	11	2.7	30.2
21	100	17.0	23	2.1	23.3
22	57	19.2	27	1.0	10.9

From Table 3.3, we observe almost all CMC experiments (#3-8) were completed reactions (100 % H_2 yield), allowing to achieve the highest storage capacities (GHSC and CHSC) possible for conditions performed, except for experiment #8, which had a problem with the solution injection into the reactor. Comparing with simple hydrolysis experiments without additive (#1 and #2), we observe similar results in experiment #1

and a slight worse in experiment #2 (H_2 yield of 80 %). It is also notable the variation of the HGRs in these experiments. Maximum HGR was achieve with 0.25 % CMC (exps #3 and 4, more than 10 times the HGR without additive), followed by 1.0 % CMC (exps. #5-8, 2-4 times the HGR without additive). Regarding the induction times, they were similar in all experiments, except for experiment #1, which was higher.

Considering now the composition of the by-products formed in these experiments, Table 3.4 presents the mass percentage of each compound that was observed in the XRD analysis performed. The first note that is extrapolated from the results with and without additive CMC is the formation of $NaB(OH)_4$ and the absence of $NaBO_2 \bullet 2H_2O$. Therefore, not only were the results of Ferreira et al. confirmed but the rearrangement of the by-product is not exclusive of the presence of CMC. In fact, comparing the by-products of experiments #2 (no additive) and #8 (1.0 % CMC), no difference is visible between them. The second note to be highlighted from the table is the formation of a non-borate, thermonatrite ($Na_2CO_3 \bullet 2H_2O$) in all by-products except of #1. This is a major drawback on the recyclability of the byproduct back to $NaBH_4$, since this compound cannot be recycled and also reduces the efficiency of the recycling process, by reducing the amount of borate formed. Since it is not formed during the $NaBH_4$ hydrolysis since no carbon compound is involved in that step, this compound can only be formed in the post-reaction, i.e., in the by-product drying or after drying. A third note can also be registered from the results of the Table 3.4: in experiments #5/6 and #7, another borate ($Na_2B_4O_5(OH)_4 \bullet 3H_2O$, also named tincalconite) was formed. This is a less hydrated form of borax, therefore a compound well known to be recycled back to $NaBH_4$. However, it can be observed that, its formation is associated to the highest percentage of $Na_2CO_3 \bullet 2H_2O$ of the experiments performed and its mass percentage is not similar in both experiments. In fact, by-product of experiment #8 was performed in similar conditions (1.0 % CMC) and $Na_2B_4O_5(OH)_4 \bullet 3H_2O$ was not observed in the XRD analysis.

Table 3.4. Influence of the CMC additive on the by-product, through the XRD analysis of the by-products composition (in weight percentage) of hydrolysis experiments #1 and #2 (no additive), #3 and #4 (0.25 % CMC) and #5-8 (1.0 % CMC).

Compound	Experiment #						
	1	2	3	4	5/6	7	8
$NaB(OH)_4$	100 %	90 %	72 %	62 %	29 %	21 %	91 %
$Na_2CO_3•H_2O$	-	10 %	28 %	38 %	53 %	42 %	9 %
$Na_2B_4O_5(OH)_4•3H_2O$	-	-	-	-	18 %	37 %	-

To understand if these results are valid using other additives and in other conditions, we can now observe again Table 3.3, particularly the study of the by-product composition of the hydrolysis with additive PAA (experiments #9 – 14). Besides experiment #9 which had an H_2 yield close to 100 % and the HGR in experiment #10 four times higher than the remaining experiments, we can define a concordance with these results: an average 89 % yield, HGR of 1 $L.min^{-1}.g_{cat}^{-1}$, and induction time between 35 – 48 s and GHSC and VHSC of 1.8 wt. % and 20 kg/m^3, respectively. Given that experiments #12 to #14 had the same PAA concentration and consistency, their by-products were extracted for analysis. Table 3.5 presents the XRD analysis of the by-products of these experiments.

Table 3.5. Study of by-product of $NaBH_4$ hydrolysis with additive PAM, through the XRD analysis of the by-product's composition (in weight percentage) of hydrolysis experiments #12 to #14 (0.10 % PAA).

Compound	Experiment #		
	12	13	14
$NaB(OH)_4$	12 %	-	32 %
$NaB(OH)_4•2H_2O$	32 %	47 %	30 %
$Na_2CO_3•H_2O$	36 %	41 %	32 %
$Na_2B_4O_5(OH)_4•3H_2O$	20 %	12 %	6 %

With this analysis, it can be observed that formation of $NaB(OH)_4$ is also possible in a smaller reactor as the egg and in the presence of other additives, such as PAA. Also, the same non-borate ($Na_2CO_3•2H_2O$) was formed and in higher mass percentage, and this time the presence of $Na_2B_4O_5(OH)_4•3H_2O$ was observed in all experiments and in smaller difference in mass percentage (14 % from 12 to 14, compared to 19 % from experiment 5/6 to 7). Moreover, although $NaB(OH)_4$ was formed, it was not the main borate by-product. This is attributed to sodium boron hydroxide hydrate ($NaB(OH)_4•2H_2O$). This borate, as referred in chapter 2 (State of the art) is expected, since similarly to $NaB(OH)_4$,

$NaBO_2$ can also retain four water molecules during the $NaBH_4$ hydrolysis. However, in this case, the presence of PAA could have helped retain more water due to its high viscosity, which increased its retention in the borate formed. This compound presents four water molecules attached to the metaborate, however due to the rearrangement of the borate's structure, it only has two structural molecules. Nevertheless, due to its hydration, although it is today the main borate commercially available, it is less interesting to regenerate $NaBH_4$ from.

The third study that was performed based on the experiments considered in Table 3.3 was the effect of the Ni-Ru catalyst support (experiments #15 to #18). Ni-Ru foam was used in experiments #15 to #17 while a Ni-Ru powder was considered in experiment #18. As expected, the hydrolysis with the powder had a worse performance regarding the HGR and induction time since to compare the same amount of catalyst used, the ratio of the mass of $NaBH_4$ per mass of catalyst was lower in the powder experiment, so less catalyst was available in each moment of the reaction. Nevertheless, the H_2 yield and GHSC and VHSC were the same in all experiments. The by-products of these experiments were also analyzed and the results are present in Table 3.6.

Table 3.6. Influence of the Ni-Ru catalyst on the by-product, through the XRD analysis of by-products composition (in weight percentage) of hydrolysis experiments #15 to #17 (Ni-Ru foam) and #18 (Ni-Ru powder) with a 0.01 Ni-Ru/$NaBH_4$ mass ratio.

Compound	**Experiment #**			
	15	16	17	18
$NaB(OH)_4 \bullet 2H_2O$	71 %	55 %	64 %	100 %
$Na_2B_4O_5(OH)_4 \bullet 3H_2O$	-	16 %	8 %	-
$Na_2CO_3 \bullet H_2O$	29 %	29 %	28 %	-

Given that in general the catalyst does not interfere with the products of reaction but only with the reaction's rate, major breaking results were not expected. However, the formation of the low or higher hydrated borates could be influence by the time the reaction can take to be complete. Looking again to Table 3.3, we note the HGR was higher than other experiments previously performed, even with PAA and 0.25 % CMC; however, the induction times of this study in particular were the highest of all experiments described in the table and from the analysis of Table 3.6, we observe, in fact, developments regarding the by-products formed. The absence of $NaB(OH)_4$ and main presence of $NaB(OH)_4 \bullet 2H_2O$ is notorious in all four by-products. Particularly, pure $NaB(OH)_4 \bullet 2H_2O$

was formed when the induction time was the highest of all (experiment #18). Thus, it can be assumed that the hydrolysis of higher volumes of solution combined with lower catalyst loadings can increase the hydration of the by-products obtained.

At last, Table 3.3 also presents the performance for the experiments with x = 11 (#19/20) and x = 16 (#21/22). Although a lack of consistency is observed in the similar experiments, no significant variations can be observed when comparing the different x values (H_2 yield close or equal to 100 %, low induction times, GHSC higher than 2.0 wt. % and VHSC from 23.0 to 30.0 kg/m^3) except for the HGRs, which are higher for lower $NaBH_4$ concentration.

In this case, the by-products of equal excess of water were dried together and were stored for 2 years and their XRD analyzed was performed after storing without outside interference. Table 3.7 presents the composition of these by-products.

Table 3.7. Influence of excess of water x on the by-product, through the XRD analysis of by-products composition (in weight percentage) of hydrolysis experiments #19/20 (x = 11) and #21/22 (x = 16).

Compound	Experiment #	
	19/20	21/22
$Na_2B_4O_5(OH)_4 \cdot 3H_2O$	54 %	54 %
$Na_2CO_3 \cdot H_2O$	30 %	37 %
$Na_3H(CO_3)_2 \cdot 2H_2O$	16 %	9 %

From the analysis, interesting notes can be written: no $NaB(OH)_4$ or $NaB(OH)_4 \cdot 2H_2O$ is present, $Na_2B_4O_5(OH)_4 \cdot 3H_2O$ is the only borate and the main compound and a new non-borate is observed –hydrated sodium bicarbonate ($Na_3H(CO_3)_2 \cdot 2H_2O$), also named trona. This mineral is a compound that is normally dissociated to originate various compounds, for example, thermonatrite. Equation 3.1 presents the formation of $NaHCO_3$, which occurs at a temperature between 57 ºC and 100 ºC [130].

$$Na_2CO_3 + CO_2 + H_2O \rightarrow 2NaHCO_3 \quad (3.1)$$

The formation of these compounds had already been reported by Uysal et al. [54], however under a CO_2 atmosphere. The authors reported that the prolonged exposure of sodium metaborate to CO_2 could lead to the formation of Na_2CO_3 and dehydrated borax, as described by Equations 3.2 and 3.3.

$$2NaBO_2 + CO_2 + 3H_2O \rightarrow Na_2CO_3 + 2H_3BO_3 \quad (3.2)$$

$$2NaBO_2 + 2H_3BO_3 \rightarrow Na_2B_4O_7 + 3H_2O \quad (3.3)$$

It can be assumed that the by-product of $NaBH_4$ hydrolysis suffers variations in its composition with considerable time without use. Moreover, we observe from Equation 3.3 that three water molecules are produced and tincalconite is also composed of three water molecules. Although the high presence of tincalconite can be interesting due to its similarity with borax – the main borate used to synthesize $NaBH_4$ – its composition is only high after long periods stored, it is not consistent nor close to pure and the remaining by-product is of no use to recycling back to $NaBH_4$.

To summarize this subchapter, the formation of $NaB(OH)_4$ is not exclusive of the presence of additive CMC but it is the main by-product of $NaBH_4$ hydrolysis. However, other borates and non-borates have been observed, which not only decrease the $NaB(OH)_4$ purity but also are less interesting to recycle back to $NaBH_4$. The analysis of the by-product after a long period of storage and the report of Uysal et al. [54] have introduced a possible explication of the formation of these compounds. From that itcan be extrapolated that a major factor is determinant for the optimization of the $NaB(OH)_4$ formation: air exposure (CO_2 and H_2O) after the by-product is extracted from the reactor and under storage. To confirm this, a new handling process of the by-product has been performed, that avoids at maximum its exposure to air. The results of this study of the by-product are a crucial step forward on its recycling back to $NaBH_4$ and have never been published in literature before, which have led to a provisional patent application (number 118331 T) [131] which was written along the results described in the following section 3.2, in order to optimize the post-treatment process.

3.2. Innovative handling process of the by-product of sodium borohydride hydrolysis

The study of the influence of additives CMC and PAA, as well as the excess of water used and catalyst support on the by-product of $NaBH_4$ hydrolysis allowed to observe that the rearrangement of the by-product into $NaB(OH)_4$ was not exclusive of the additive CMC. In fact, Demirci et al. [72] had already referred to this borate as the main by-product; however, it missed the experimental confirmation of this observation. However, the influence of exposure time on the extraction and treatment of the by-product has been observed to be critical on the $NaB(OH)_4$ optimization, since other borates and non-borates

are formed which interfere with the recycling back to $NaBH_4$. Therefore, a new procedure was studied to limit the air exposure to the minimum, in order to clarify its effect on the formation of other compounds besides $NaB(OH)_4$. The study of this handling process of the by-product is a critical step forward on its recycling back to $NaBH_4$.The results have been subject of a provisional patent application (number 118331 T) [131] written and developed alongside the study of this process and explained in detail in this section.

3.2.1. Experimental procedure

Having in mind that the by-product's composition has presented a significant number of different borates and non-borates, it is of highly importance to find a method that not only presents the borate by-product with the higher purity possible (pure if possible) but that method allows consistent results throughout the experiments performed in various conditions. As resumed in the subchapter 3.1 and picking from the results on the analysis of the by-products #1 to #22 - in particular the reanalysis of by-products #19 to #22-, we denote a parameter that affects all of them: air exposure time. Since the by-product of the $NaBH_4$ hydrolysis is performed in similar conditions, the formation of different borates can only be explained by the reactions' by-product post-treatment, which is performed under uncontrolled conditions.

With this in mind, a new post-reaction treatment described in the provisional patent application number 118331 T [131] was adopted: after the hydrolysis reaction is finished and the by-product is extracted and separated from the catalyst - which will have the same treatment as reported in the subchapter 3.1 - it is transferred to a petri dish and placed open in a desiccator. There, the desiccator is closed, and vacuum is applied. After drying, the by-product is removed from the desiccator, milled and stored under vacuum. This is important to assure minimal air exposure throughout all the process from its formation to its analysis.

Hydrolysis experiments were performed as explained in the subchapter 3.1. Table 3.8 presents the list of experiments that were performed to test this innovative process. Again, the majority of the experiments considered $x = 16$ and $x = 15$, considering the use of 96 % and 98 % pure $NaBH_4$, respectively. $x = 11$ and $x = 6$ were also studied: $x = 6$ is the minimum excess of water that allows the separation of the catalyst from the by-product and posterior drying and analysis (based on previous tests performed). And regarding the catalyst, for experiments #44, #47 and #48 it had an acidic treatment before the

experiment, where it was washed under 1 M HCl instead of distilled water, in order to improve its activity in a parallel study to the by-product analysis. Various experiments were considered to confirm the replicability of the results. Also, experiments with additives CMC, sodium dodecyl sulfate (SDS) and beta-cyclodextrin (BCD) were considered. These new additives were added to the reaction due to their expected positive effect on the HGR and possible interference in the by-product formation. Moreover, some of these experiments considered the drying of the by-product of each experiment in two separate methods: half using the air exposure drying, as explained in subchapter 3.1, and half using a vacuum desiccator. To simplify, these methods will be defined as post-treatment 1 and post-treatment 2, respectively. However, to have minimal control of the conditions, the by-product exposed to air in post-treatment 1 was placed in a drying box, turned off and with the doors opened. This was done to avoid natural and forced convection occurring from interferences due to other experiments in the laboratory, while maintaining low air flow.

Table 3.8. Operating conditions of the hydrolysis experiments containing up to 1.0 % CMC, 1.0 % BCD and 0.25 % SDS additives and excess of water ($6 < x < 16$) and post-treatments performed on each by-product formed (*catalyst acidic treatment).

#	Reactor	Volume	*x*	Ni-Ru/$NaBH_4$ mass ratio	Additive	Post-treatment
23	SRc	5	16	0.4	-	1
24	SRc	5	16	0.4	-	1
25	SRc	5	16	0.4	-	1
26	LR	15	16	0.2	-	1
27	SRc	5	16	0.4	-	1
28	SRc	10	16	0.4	-	1
29	SRc	5	16	0.4	-	1
30	SRc	10	15	0.4	-	1,2
31	SRc	10	15	0.4	-	1,2
32	SRc	50	15	0.4	-	1,2
33	LR	10	15	0.4	-	1,2
34	LR	5	15	0.4	-	1,2
35	SRc	5	15	0.4	-	2
36	SRc	5	15	0.4	-	2
37	SRc	5	15	0.4	-	2
38	SRc	10	15	0.4	0.25 % CMC	2
39	SRc	5	15	0.6	0.25 % CMC	2
40	SRc	5	15	0.4	1.0 % CMC	2
41	SRc	5	15	0.4	1.0 % BCD	2
42	SRc	5	15	0.4	0.25 % SDS	2
43	SRc	5	11	0.4	-	2
44	SRc	10	11	0.4*	-	2
45	SRc	5	6	0.4	-	2
46	SRc	2	15	0.2	-	2
47	SRc	5	15	0.2*	-	2
48	SRc	5	15	0.05*	-	2

The information displayed in Table 3.8 concerns the set of experiments representing the core section of this thesis. The majority of the by-products were treated with the new process, i.e., post-treatment 2 [131]. Table 3.9 presents how these by-products were analyzed and their conclusions were obtained.

Table 3.9. Operating conditions varied in each hydrolysis experiment performed (#23 to 49), while maintain remaining parameters, for analysis of the influence of each parameter studied.

Experiment #	Parameter analysis
23 – 29	Post-treatment 1 compared to #1 and #2 of subchapter 3.1
30 – 34	Post-treatment 1 vs 2, Volume and Reactor
35 - 42	Additives
43 – 45	Excess of water, *x*
46 - 48	Catalyst loading

By-products #23 - #29 were dried using the post-treatment 1 and their composition analyzed and compared with the by-products #1 and #2 from subchapter 3.1. Moreover, they serve as a standard base to confirm the instability of the by-product composition. Then the by-product of experiments #30 to #34 allow a direct comparison between post-treatments 1 and 2. Additionally, in these experiments, the volume of reaction as well as the reactor used vary to understand their effect on the by-product formed using the post-treatment 2. In these experiments, the additive hydrolysis of $NaBH_4$ was followed. Three additives were used: CMC (experiments #38 to #40), BCD (experiment #41) and SDS (experiment #42) and their by-products were dried in the desiccator and analyzed. The excess of water *x* was also studied: by-products of experiments #43 and #44 were obtained from the hydrolysis of $NaBH_4$ with an $x = 11$ and by-product of experiment #45 with excess of water of $x = 6$. Finally, three experiments considered the study of the ratio of mass of catalyst per mass of $NaBH_4$: 0.2 g/g (experiment #46 and #47) and 0.05 g/g (experiments #48). Given that in section 3.1 lower catalyst loadings had an impact on the by-products formed, the values of 0.2 and 0.05 g/g were chosen since they present a significant reduction from the standard 0.4 ratio considered in the majority of the experiments. Moreover, these ratios were considered based on the short availability of the catalyst.

3.2.2. Results and discussion

Table 3.10 presents the summary of some performance parameters concerning the hydrolysis experiments #25 to #49 that were considered in Table 3.9. it is worth mentioning that the performance of experiments #23 and #24 was not analyzed, due to a mechanical problem associated to the thermocouple and pressure gauge; nevertheless, the

reaction occurred as expected, i.e., the time of reaction was similar to the standard one within the same conditions as well as the by-product extraction.

Table 3.10. Performance of each hydrolysis experiment performed, by analysis of the H_2 yield, generation rate (HGR), induction time and storage densities (GHSC and VHSC) (*catalyst acidic treatment).

#	Yield / %	HGR / $L.min^{-1}.g_{cat}^{-1}$	Induction time / s	GHSC / wt. %	VHSC / $kg.m^{-3}$
25	68	11.6	140	1.3	14.8
26	84	1.7	81	1.6	18.0
27	82	1.5	234	1.6	17.3
28	94	11.9	142	2.0	21.4
29	97	1.7	214	1.9	21.2
30	90	1.0	81	1.8	20.2
31	92	1.0	74	1.9	20.6
32	76	1.0	109	1.4	16.2
33	97	0.9	139	1.9	21.5
34	94	1.7	362	1.8	20.3
35	92	8.3	50	1.8	20.6
36	82	1.2	66	1.6	17.9
37	98	1.4	66	2.0	22.1
38	94	2.1	86	1.9	21.1
39	85	10.0	36	1.6	18.1
40	91	1.3	66	1.8	20.2
41	55	0.9	70	1.0	10.7
42	100	0.4	129	2.1	23.0
43	92	0.6	126	2.4	26.5
44	82	50.5*	23	2.1	23.2
45	97	1.4	50	3.8	41.3
46	100	1.1	172	2.1	22.9
47	58	36.7*	9	1.1	11.5
48	95	50.5*	39	2.0	21.5

The data displayed in Table 3.10 show a significant variation of the performance of these experiments. Concerning the H_2 yield, most of the experiments achieved a 90 % yield as expected and almost all achieved at least 80 %. We can observe that the majority of experiments had a HGR around 1 to 2 $L.min^{-1}.g_{cat}^{-1}$. The remaining ones present a

significantly higher HGR: on one side the HGR of experiments #38 and #39 (0.25 % CMC) is higher than the HGR of experiment #40 (1.0 % CMC), in a similar trend to the performance of experiments with CMC in subchapter 3.1 (experiments with 0.25 % CMC (#3 and #4) had higher HGR than the ones using 1.0 % CMC (#5 to #8)). Also, experiment #39 used a Ni-Ru/$NaBH_4$ mass ratio of 0.6, which justifies its higher HGR compared to experiment #38; then, for experiments #44, #47 and #48, we can observe the acidic treatment of the NiRu powder had a very positive effect on the HGR, since it reached values at least 30 times higher than normal non-additive $NaBH_4$ hydrolysis. At last, similar GHSC and VHSC values to the ones of experiments #1 to #22 were obtained in subchapter 3.1, as expected since it varies with the H_2 yield which was also similar.

Table 3.11 presents the XRD analysis of the by-products with post-treatment 1, i.e., by-products #23 to #29. In this analysis (and in some further analysis XRD in this chapter to be presented in this chapter) the mass percentage of each compound was not possible to determine. Accordingly, the discussion is based on the compounds present in each by-product. Observing their composition, it is possible to conclude that, as expected, there is no difference between the air exposure drying open-to-air described in subchapter 3.1 and the post-treatment 1 (glove box air-exposure drying). No link can be found between the same parameters (reactor, volume, *x*) and the by-product composition, as well as same hydrolysis performances. However, from this analysis, we can extract four important results: first, $Na_2CO_3 \cdot H_2O$ and $NaB(OH)_4$ and/or $NaB(OH)_4 \cdot 2H_2O$ are again observed in most of the by-products, similar to experiments of subchapter 3.1; second, $NaBO_2 \cdot 4H_2O$ is detected in two by-products (#24 and #27), which, although its mass percentage was not determined, can indicate that in fact a rearrangement of the by-product exists but requires time and the right conditions; and the third is the presence of $NaBO_2$ in the composition of by-products #26, #27 and #29. This is an unexpected result, which can be formed due to eventual accidental water evaporation while prolonged exposure to time and heat. However, although the formation of $NaBO_2$ would be of major relevance, the formation of this compound cannot be reliable, since the conditions for its formation cannot be replicated/optimized.

Table 3.11. By-product composition of hydrolysis experiments #23 to #29 from XRD analysis after post-treatment 1.

Compound	Experiment #						
	23	24	25	26	27	28	29
$NaBO_2$	-	-	-	✓	✓	-	✓
$NaB(OH)_4$	✓	✓	-	-	-	-	-
$NaB(OH)_4 \bullet 2H_2O$	-	✓	✓	-	-	✓	✓
$NaBO_2 \bullet 4H_2O$	-	✓	-	-	✓	-	-
$Na_2CO_3 \bullet H_2O$	✓	-	✓	✓	✓	-	✓
$Na_2B_4O_5(OH)_4 \bullet 3H_2O$	-	-	✓	-	✓	-	-

The following tables describe a comparison between the by-products post-treatments 1 and the innovative post-treatment 2. By-products from experiments #30 to #34 were extracted and dried as described in the provisional patent application number 118331 T [131] and described in this thesis as post-treatment 2. The same volume dried was considered for both. After the post-treatments were complete, they were sent for XRD analysis after 1.5 months. Table 3.12 describe the composition of the by-products using the post-treatment 2. Observing the table, there is obvious the importance of the vacuum drying. Pure or close to pure $NaB(OH)_4$ was obtained in all by-products. Moreover, this is the desired by-product to regenerate $NaBH_4$, also not being affected by the parameters considered (reactor and volume of reaction).

Table 3.12. By-product composition (in weight percentage) of hydrolysis experiments #30 to #34 from XRD analysis after post-treatment 2.

Compound	Experiment #				
	30	31	32	33	34
$NaB(OH)_4$	100 %	97 %	92 %	97 %	99 %
Na_2CO_3	-	3 %	8 %	3 %	1 %

Figure 3.4 presents the peak analysis of the by-products #30 to #34. As observed, there is a predominant peak in all by-products at around 17 º, corresponding to $NaB(OH)_4$. The absence of an intensity increase in the 0 – 5 º range in all by-products indicate that no amorphous (no crystalline) compound is present.

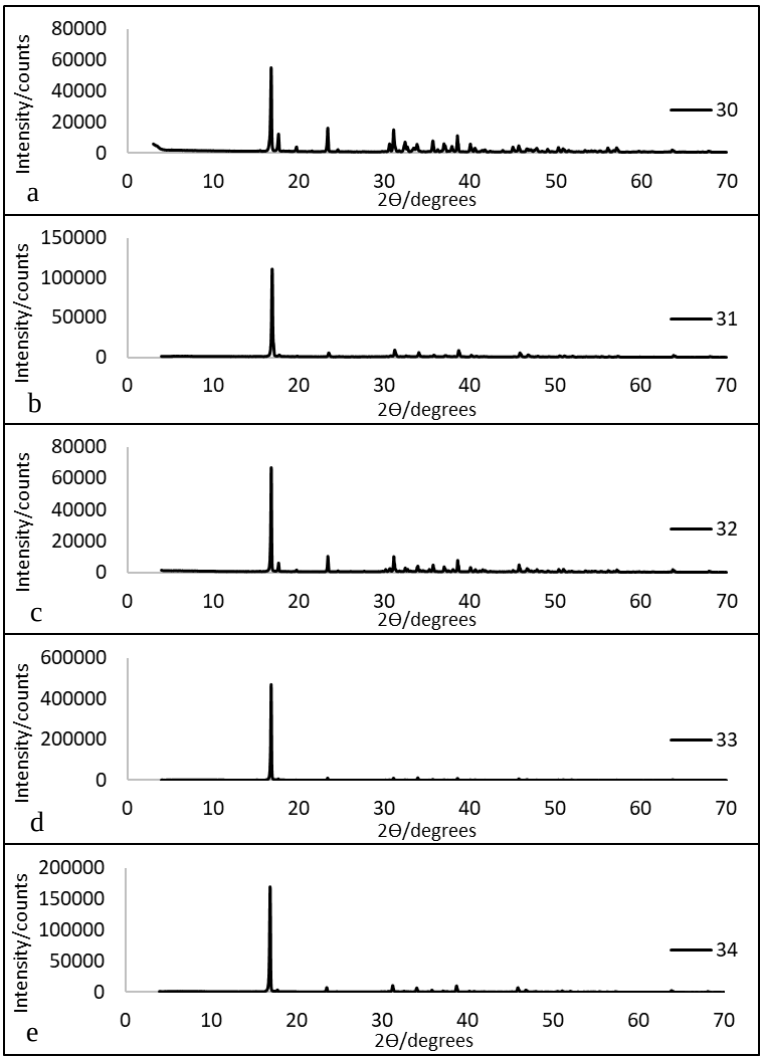


Figure 3.4. XRD patterns of the by-products of hydrolysis experiments #30 to #34 after post-treatment 2.

As comparison, Table 3.13 shows the composition of the by-product #34 with the two post-treatments. The difference between them is notable. Even on the non-borate by-product formed, the absence of water is noteworthy, as opposed to the by-product exposed to air. This observation [131] is a step forward on the by-product recycling back to $NaBH_4$, since all contaminants are removed prior to the recycling process.

Table 3.13. By-product composition (in weight percentage) of hydrolysis experiment #34 from XRD analysis after post-treatments 1 and 2 [131].

Compound	Post-treatment	
	1	2
$NaB(OH)_4$	69 %	99 %
Na_2CO_3	-	1 %
$Na_2CO_3 \cdot H_2O$	31 %	-

Figure 3.5 presents the XRD peaks of this by-product comparing both post-treatments [131]. As observed, the $NaB(OH)_4$ peak at 17 º is less intense and other peaks are formed in the post-treatment 1, indicating a $NaB(OH)_4$ less concentrated. Once again, similar to by-products in runs #30 to #34, no amorphous compound was detected in the analysis.

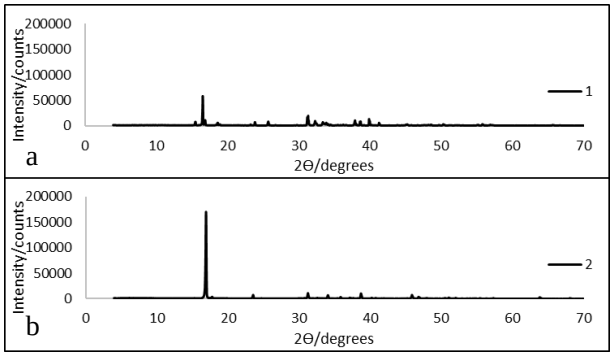


Figure 3.5. XRD patterns of the by-product of hydrolysis experiments #34 after post-treatments 1 (a) and 2 (b) [131].

These by-products were then reanalyzed after 3.5 months, to understand the influence of storage time. Nevertheless, all by-products were stored without use from the moment when they were treated. This reanalysis can be observed in Table 3.14. The designation X-1 and X-2 is the designation for post-treatment 1 and 2, respectively. X represents the experimental number. Again, the vacuum drying has maintained the pure or close to pure $NaB(OH)_4$ formation, while time has further decrease its purity in the air exposure drying, even replacing this borate with others ($NaBO_2$, $Na_2B_4O_5(OH)_4 \bullet 3H_2O$, $HNa_2BO_3 \bullet H_2O$). This way, these results confirm the negative impact of the air exposure on the by-product, after it is extracted and stored. An innovative method to treat the by-product of $NaBH_4$ hydrolysis for its optimal recycling has been found, which has a crucial impact on the future of this technology, since the recycling of the by-product back to $NaBH_4$ is essential and almost all reports on literature have considered the study of commercial borate, as referred in the state of the art (chapter 2). Therefore, these results gave birth to a provisional patent application request approved [131].

Table 3.14. By-product composition (in weight percentage) of hydrolysis experiments #30 to #33 from XRD reanalysis after post-treatments 1 and 2.

Compound	Experiment # - Post-treatment								
	30 – 1	30 - 2	31 - 1	31 - 2	32 - 1	32 – 2.1	32 – 2.2	33 - 1	33 - 2
$NaBO_2$	✓	-	-	-	✓	-	-	✓	-
$NaBO_2 \bullet 2H_2O$	-	-	-	100 %	-	-	-	-	-
$NaB(OH)_4$	✓	88 %	-	-	-	89 %	100 %	-	✓
$Na_2CO_3 \bullet H_2O$	✓	12 %	-	-	✓	11 %	-	✓	✓
$Na_2B_4O_5(OH)_4 \bullet 3H_2O$	-	-	34 %	-	✓	-	-	-	-
$HNa_2BO_3 \bullet H_2O$	-	-	66 %	-	-	-	-	-	-

With the innovative post-treatment process described in this thesis as post-treatment 2 confirmed and replicated, the study of additives for the $NaBH_4$ hydrolysis was considered using this post-treatment. CMC (by-product #38 to #40), BCD (by-product #41) and SDS (by-product #42) additives were used. Their by-product composition can be seen in Table 3.15, for the XRD analysis. For these experiments, FT-IR analysis was also performed, and the results can be observed in Table 3.16. By-product #36/37 was performed without additive, to act as a direct comparison with the additive hydrolysis. Although the formation of $NaBO_2$ was again observed in the by-product of experiment #38, the remaining analysis are indicative of the positive effect of the vacuum drying on the by-product optimization. Only the additive SDS can have a less positive effect on the by-product, since $NaB(OH)_4 \bullet 2H_2O$ was formed and its mass percentage could not be confirmed. Although, the same can be said regarding the formation of $NaB(OH)_4 \bullet 2H_2O$ in experiment #35 with no additive, the efficiency of the post-treatment 2 has already been proven in experiments #30 to #34 and is again confirmed in experiment #36/37 through another analytical method (FT-IR). Figure 3.6 complements the FTIR analysis of these by-products.

Table 3.15. Influence of additives CMC and BCD on the by-product, through the XRD analysis of the by-product composition (in weight percentage) of hydrolysis experiments #35 (no additive), #38 and #39 (0.25 % CMC), #40 (1.0 % CMC) and #41 (1.0 % BCD).

Compound	Experiment #				
	35	38	39	40	41
$NaBO_2$	-	✓	-	-	-
$NaB(OH)_4$	✓	-	100 %	100 %	100 %
$NaB(OH)_4 \bullet 2H_2O$	✓	-	-	-	-
$Na_2CO_3 \bullet H_2O$	-	✓	-	-	-

Table 3.16. Influence of additive SDS on the by-product, through the FTIR analysis of the by-product composition of hydrolysis experiments #36/37 (no additive) and #42 (0.25 % SDS).

Compound	Experiment #	
	36/37	42
$NaB(OH)_4$	100 %	✓
$NaB(OH)_4 \bullet 2H_2O$	-	✓

Peaks corresponding to the B-O-H bond indicate the formation of $NaB(OH)_4$ on the by-product #36/37, while the absence of peaks on the C-O bonds (1725 – 1750 cm^{-1}) indicate absence of Na_2CO_3 and $Na_2CO_3 \bullet H_2O$. Moreover, the presence of a peak on the H-O-H bond range on the by-product #42 indicates the formation of $NaB(OH)_4 \bullet 2H_2O$, while on by-product #36/37 it is absent.

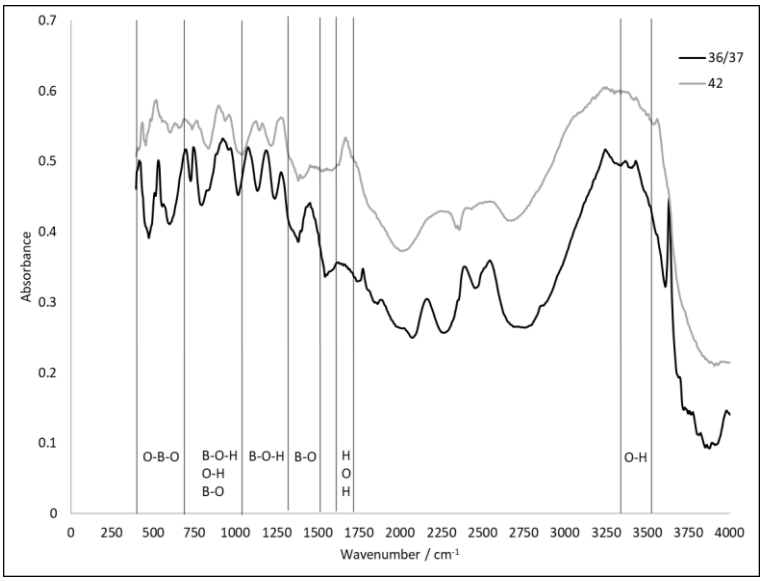


Figure 3.6. Influence of additive SDS on the by-product composition from FTIR patterns of the by-products of hydrolysis experiments #36/37 (no additive) and #42 (0.25 % SDS).

All these by-products were obtained for x = 15; however, it is essential to understand if this post-treatment 2 can be applied to less excess of water. With this in mind, the hydrolysis of $NaBH_4$ under lower excess of water was studied, namely with x = 11 (experiments #43 and #44) and x = 6 (experiment #45). The XRD analysis of these by-products is presented in the table below, Table 3.17. As observed, the $NaBH_4$ hydrolysis with an x = 6 has given close to pure $NaB(OH)_4$, similar to the results for x = 15. On the other hand, the results for x = 11 have not been consistent, since different compounds have been formed and only one contained $NaB(OH)_4$ (by-product of experiment #43, in low purity). Interesting is the composition of by-product #44: although no $NaB(OH)_4$ was formed, it is only composed of borate compounds, which is a positive note. Nevertheless, since the by-product for x = 6 is similar to x = 15, the same composition should be applied to x = 11. Therefore, experiments #43 and #44 should be replicated.

Table 3.17. Influence of excess of water x on the by-product, through the XRD analysis of the by-product composition (in weight percentage) of hydrolysis experiments #43 and #44 (x = 11) and #45 (x = 6).

Compound	Experiment #		
	43	44	45
$NaB(OH)_4$	44 %	-	94 %
$NaBO_2 \bullet 2H_2O$	-	✓	-
$NaB(OH)_4 \bullet 2H_2O$	-	✓	-
Na_2CO_3	26 %	-	6 %
$Na_2CO_3 \bullet H_2O$	16 %	-	-
$Na_2B_4O_5(OH)_4 \bullet 3H_2O$	14 %	-	-
$Na_3B_3O_5(OH)_2$	-	-	-
$Na_2B_5O_7(OH)_3 \bullet 2H_2O$	-	✓	-

Finally, the effect of the catalyst loading on the by-product of $NaBH_4$ hydrolysis was studied and the XRD analysis is present in Table 3.18. Although the mass percentage of each compound was not obtained, we can note the presence of $NaB(OH)_4$ when a ratio of 0.2 g_{cat}/g_{NaBH_4} was used (experiments #46 and #47), and although Na_2CO_3 is formed in experiment #46 we observe similar trend to the first studies of the post-treatment 2 in Table 3.12, i.e., the absence of molecular water, which allowed to widen the catalyst loading range of the patent application [131]. On the other hand, when a ratio of 0.05 g/g

was used, only $Na_2B_4O_5(OH)_4•3H_2O$ was observed as a borate compound. It can indicate that a slower reaction can favor the formation of complex borates instead of $NaB(OH)_4$.

Table 3.18. Influence of catalyst loading on the by-product, through the XRD analysis of the by-product composition (in weight percentage) of hydrolysis experiments #46 and #47 (0.20 g/g) and #48 (0.05 g/g).

Compound	Experiment #		
	46	47	48
$NaB(OH)_4$	✓	100 %	-
Na_2CO_3	✓	-	-
$Na_2CO_3•H_2O$	-	-	✓
$Na_2B_4O_5(OH)_4•3H_2O$	-	-	✓
$Na_3H(CO_3)_2•2H_2O$	-	-	✓

In conclusion, an innovative post-treatment of the by-product was studied to limit its exposure to air while drying and stored. Thus, after extraction from the reactor where the hydrolysis of $NaBH_4$ is performed, the by-product was dried in a vacuum desiccator and stored under vacuum, instead of in air. This process has demonstrated that $NaB(OH)_4$ is obtained and maintained pure or close to pure, which is crucial to assure its efficient recycling back to $NaBH_4$. Therefore, this post-treatment of the by-product has been subject of a provisional patent application approved [131]. Based on these observations, experiments with additives (CMC and BCD) were performed confirming the formation of this borate and hydrolysis experiments with lower excess of water (x = 6) and catalyst loading (mass ratios of 0.2) allowed to widen the range at which $NaB(OH)_4$ is formed pure or close to pure and were included in the patent application approved [131].

3.3. Implementation of other by-product handling processes to optimize the by-product composition

Having presented an innovative process to extract and dry the by-product of $NaBH_4$ hydrolysis (patent number 118331 T [131]) and studied the effect of different parameters on its composition (additives, excess of water, volume of reaction, reactor and catalyst loading), it is important to make adaptations of this process in order to optimize the formation of other borates such as tincalconite and $NaB(OH)_4•2H_2O$.

In that regard, different conditions were introduced to the post-treatment process: the temperature of drying; the consideration of the drying chamber as equipment for the by-

product drying; and the storage conditions of the by-products after drying were studied. This subchapter reports these detailed procedures as well as the results obtained. This study has allowed to understand where the effect of air exposure has a higher impact on the formation of $NaB(OH)_4$ and the conditions for the optimization of $NaB(OH)_4 \cdot 2H_2O$.

3.3.1. Experimental procedure

Hydrolysis experiments were performed similarly to the ones described in subchapter 3.1 and four new by-product post-treatments (#3 to #6) of the by-products formed were considered. To understand the stability of the by-product, the effect of the temperature drying was introduced to the post-treatment. First, considering the effect of a low-humidity/forced convection atmosphere on the by-product composition, a drying chamber was considered – post-treatment 3. The by-product was dried close to room temperature to compare with other post-treatments.

In post-treatment 4, air exposure drying was again considered, however instead of transferring the by-product to a petri dish, it was dried directly on the centrifuge tube (after separation from the catalyst) used to extract the by-product and the catalyst from the hydrolysis reactor. This experiment was considered to understand the impact of very limited space available for the by-product to dry.

Moreover, high and low temperature drying were studied, denominated post-treatments 5 and 6, respectively. For the higher temperature experiments, the glove box was used for the effect and the by-product was maintained at 45 ºC, closer to the temperature at which $NaB(OH)_4 \cdot 2H_2O$ is not expected to be formed, based on Andrieux et al. [52]. On the other hand, low temperature drying was performed in a refrigerator at 2 ºC.

In the different alternative, a mixture of post-treatments was considered, i.e., the by-product was dried using one method, and is stored using another, while further treatments can also be applied. Table 3.19 summarizes the post-treatments studied. Mixed post-treatments are represented by an "$i^a + i^b + i^c$" where i identifies the post-treatment considered and the letters a, b and c mean the post-treatment is applied while drying, after it is dried and while stored, respectively. For example, $1^a + 2^b + 3^c$ means drying the by-product in the glove box, expose the by-product dried in the desiccator and after that store it without use in the drying chamber. As another example, $1^{a,b} + 3^c$ means drying the by-product in the glove box and store it in the drying chamber. Experiments with post-treatments 1 and/or 2 were performed for direct comparison.

Table 3.19. Description of the conditions and equipment used in each post-treatment performed to the by-product.

Post-treatment	Equipment used for drying (condition)
1	Glove box (normal air exposure)
2	Desiccator (vacuum)
3	Drying chamber (low humidity, forced convection)
4	Centrifuge tube (low air exposure)
5	Glove box (high temperature, air exposure)
6	Refrigerator (low temperature, air exposure)
$i^a + i^b + i^c$	Combination of processes, i-post-treatment type, a–drying, b-after drying, c-storage

Table 3.20 presents the hydrolysis experiments performed. Given the better performance obtained, SRc with excess of water x = 15 was mainly used, while experiment #58 was the only to consider the use of additive (1.0 % CMC), given it has already been confirmed in subchapters 3.1 and 3.2 that it does not have an impact on the type of by-product formed. Also, the Ni-Ru/$NaBH_4$ mass ratio was mainly 0.4 or close to, except for experiment #51.

Table 3.20. Operating conditions of the hydrolysis experiments containing up to 1.0 % additive CMC and excess of water (x = 6 or 15) and post-treatments performed on each by-product formed.

#	Reactor	Volume	x	Ni-Ru/$NaBH_4$ mass ratio	Additive	Post-treatment
49	SRc	10	15	0.4	-	$2, 2^{a,c} + 1^b$
50	SRc	10	15	0.4	-	1, 3
51	SRc	10	15	0.2	-	$1, 3^{a,b} + 2^c, 3^{a,b} + 1^c$
52	SRc	5	15	0.4	-	$1, 1^{a,c} + 3^b, 3, 3^{a,b} + 1^c$
53	SRc	5	15	0.4	-	$2, 2^{a,c} + 3^b$
54	SRc	10	15	0.4	-	2, 4
55	SRc	5	15	0.4	-	5
56	LR	25	15	0.5	-	1, 4, 5
57	SRc	5	15	0.4	1.0 % CMC	6

Post-treatments that were performed for each by-product formed are also described in Table 3.20. As opposed to the previous experiments, where a comparation between the by-products of experiments was made, the objective of this subchapter is to compare post-treatments, so to assure that all hydrolysis conditions and performance are the same, each

by-product is processed through different post-treatments, and is analyzed individually. The only exception is the by-product of experiment #58 which was compared with the by-products of experiments #30, #31 and #34, performed as described in Table 3.20, to whom post-treatment 7 was also applied.

3.3.2. Results and Discussion

The hydrolysis performance of the experiments #49 to #58 is presented in Table 3.21 below (performance of experiment #54 was not recorded due to installation limitations, however the time of experiment was within regular values). Similar to previous experiments, high H_2 yield production with low induction time has been possible in most of the reactions. Moreover, additive CMC (experiment #58) did not show a positive impact on the H_2 production (lower H_2 yield and average HGR and induction time). As observed in previous experiments (#3 to #8 of subchapter 3.1 and #38 to #40 of subchapter 3.2), its positive effect on the HGR and the induction time is most associated to the use of 0.25 % CMC instead of the value 1.0 % CMC used in this experiment.

Table 3.21. Performance of each hydrolysis experiment performed, by analysis of the H_2 yield, generation rate (HGR), induction time and storage densities (GHSC and VHSC).

#	Yield / %	HGR / $L.min^{-1}.g_{cat}^{-1}$	Induction time / s	GHSC / wt. %	VHSC / $kg.m^{-3}$
49	99	2.3	48	2.0	22.4
50	64	0.8	68	2.8	28.3
51	93	2.1	51	1.9	21.0
52	94	1.4	61	1.9	21.4
53	85	1.4	63	1.7	18.4
55	76	2.5	56	1.5	16.6
56	96	0.7	77	1.9	21.5
57	90	6.2	90	1.8	20.0
58	79	1.4	71	1.5	16.9

Tables 3.22 to 3.31 present the XRD analysis of the by-products' composition for experiments #49 to #58. As explained above, since each by-product is subjected to different post-treatments to assure the absence of other factors in the study, each by-product is discussed individually.

The by-product formed in experiment #49 was extracted and dried in a desiccator as described previously in subchapter 3.2 and designated as post-treatment 2. Its composition was analyzed by XRD and $NaB(OH)_4$ and $NaB(OH)_4•2H_2O$ were formed. Although $NaB(OH)_4•2H_2O$ is formed besides $NaB(OH)_4$ and its concentration was not possible to determine, it is expected to be low since experiments performed previously indicated pure or close to pure $NaB(OH)_4$. Then, part of this by-product was exposed to air for 24 h. After this, half of it was stored in vacuum (post-treatment $2^{a,c} + 1^{b}$) while the other half was maintained stored under no vacuum (post-treatment $2^{a} + 1^{b,c}$). The objective of this separation was to study the effect of a 24-h air exposure on the by-product. The composition of these by-products indicates that the main impact on the borate formation occurs while it is being dried in vacuum, since pure borate was observed in both air exposure treatments after all water was removed ($NaB(OH)_4$ or $NaBO_2•2H_2O$), as seen in Table 3.22. Moreover, the absence of $NaB(OH)_4•2H_2O$ in the post-treatments $2^{a} + 1^{b,c}$ and $2^{a,c} + 1^{b}$, confirms the low mass percentage of this compound in the analysis of this by-product prior to the air exposure study (post-treatment 2). Figure 3.7 validates this analysis, as a main peak at 17 º corresponding to $NaB(OH)_4$ is observed in all three analysis. Nevertheless, in the post-treatment $2^{a,c} + 1^{b}$, the low intensity of the peak and the concave curve in the 0 – 20 º range indicates this by-product cannot be considered as pure, due to the presence of amorphous species that cannot be identified in this analysis, possibly contributing to the $NaBO_2•2H_2O$ detection. Therefore, it indicates the need to assure vacuum storage of the by-product after dry and to replicate this experiment with another technique (for example, FT-IR).

Table 3.22. By-product composition of hydrolysis experiment #49 (in weight percentage) from XRD analysis after post-treatment 2, after dried in vacuum (post-treatment 2) and exposed and stored open-to-air and after dried in vacuum (post-treatment 2) exposed to air and stored in vacuum.

Compound	Post-treatment		
	2	$2^{a} + 1^{b,c}$	$2^{a,c} + 1^{b}$
$NaB(OH)_4$	✓	100 %	-
$NaBO_2•2H_2O$	-	-	100 %
$NaB(OH)_4•2H_2O$	✓	-	-

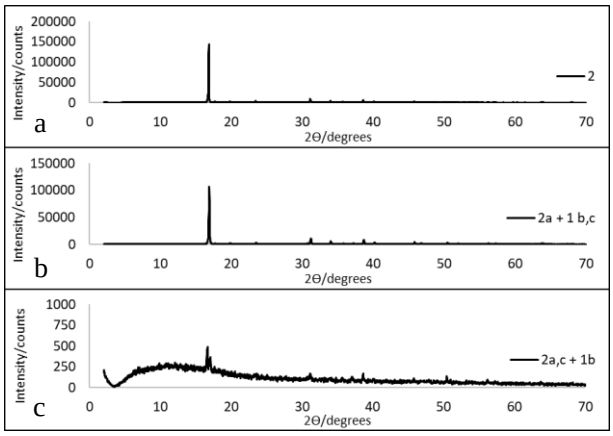


Figure 3.7. XRD patterns of the by-product #49 composition considering post-treatment 2 (a), vacuum drying and open-to-air storage (b) and vacuum drying, open-to-air exposure and desiccator storage in vacuum (c).

Table 3.24 presents the results of the analysis of the by-product #50, considering now the study of post-treatment 3 (drying chamber). Two separate parts of the by-product were dried using the post-treatment 1 and two parts using the post-treatment 3. The aim of this separation was to understand the homogeneity of the by-product. As observed, although the by-product is composed of only borate compounds, the post-treatment has a clear impact on the borate formed. The by-product obtained through glove box drying (described as post-treatment 1) is pure $NaB(OH)_4 \bullet 2H_2O$; nevertheless, as observed in previous experiments (subchapters 3.1 and 3.2) using this method, it is inconsistent and difficult to replicate in the same conditions. On the other hand, drying under low humidity and forced convection exposure (post-treatment 3) led to the formation of pure $NaB(OH)_4$, which can be an indication that low water vapor exposure can also prevent the formation of other by-products. Moreover, the samples analyzed through each post-treatment have equal composition, which indicates the homogeneity of the by-product.

Table 3.23. By-product composition of experiment #50 composition (in weight percentage) from XRD reanalysis after post-treatment 1 (samples 1 -1 and 1 – 2) and after post-treatment 3 (samples 3 -1 and 3 – 2).

Compound	Post-treatment # - sample			
	1 - 1	1 – 2	3 - 1	3 – 2
$NaB(OH)_4$	-	-	100 %	100 %
$NaB(OH)_4 \bullet 2H_2O$	100 %	100 %	-	-

Figure 3.8 below presents in detail the XRD pattern of the by-product of experiment #50. As observed there is no main peak at 17 º in the post-treatment 1 (analysis 1-1 and 1-2), indicative of the absence of $NaB(OH)_4$, as opposed to the post-treatment 3 (analysis 2-1

and 2-2), where it was formed pure. The resemblance between the same post-treatment by-products confirms the homogeneity of the process.

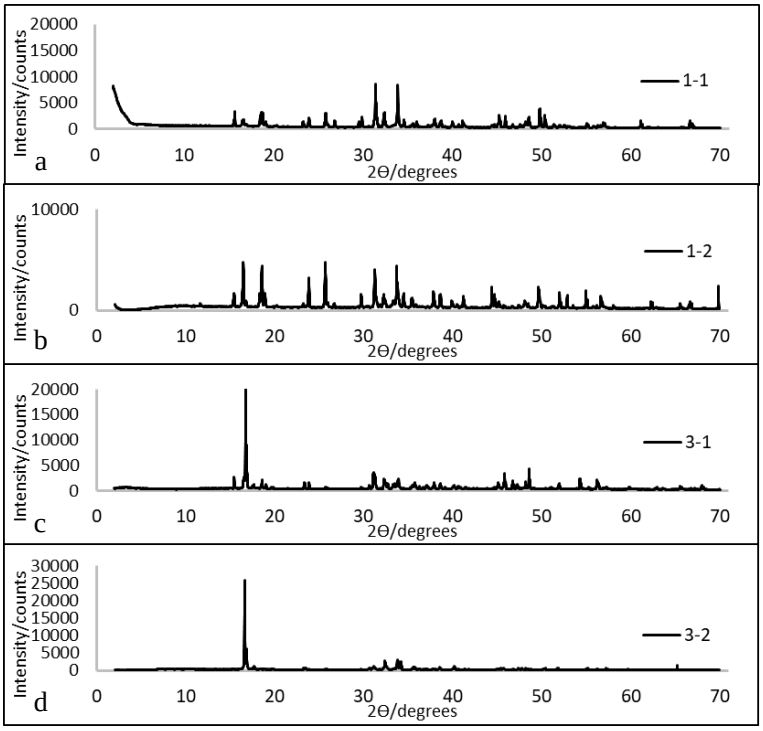


Figure 3.8. XRD patterns of the by-product #50 composition considering post-treatment 1, samples 1 (a) and 2 (b) and post-treatment 2, samples 1 (c) and 2 (d).

Table 3.24 presents the reanalysis of by-product of experiment #50, ten months later. As expected, the prolonged exposure of the by-products to air has provoked alterations in its composition on both post-treatments, with particular emphasis on the consumption of pure $NaB(OH)_4$ to form 55 % $Na_2B_4O_5(OH)_4 \bullet 3H_2O$, 31 % $HNa_2BO_3 \bullet H_2O$ and 14 % $Na_3H(CO_3)_2 \bullet 2H_2O$ when it was processed based on post-treatment 3.

Table 3.24. By-product #50 composition (in weight percentage) from XRD reanalysis after post-treatments 1 and 3.

Compound	Post-treatment	
	1	3
$NaB(OH)_4 \bullet 2H_2O$	✓	-
$Na_2B_4O_5(OH)_4 \bullet 3H_2O$	✓	55 %
$HNa_2BO_3 \bullet H_2O$	✓	31 %
$Na_2B_{12}H_{12} \bullet 4H_2O$	✓	-
$Na_3B_3O_5(OH)_2$	✓	-
$Na_2B_5O_7(OH)_3 \bullet 2H_2O$	✓	-
$Na_3H(CO_3)_2 \bullet 2H_2O$	-	14 %

Experiment #51 also considered the study of post-treatment 3. Table 3.25 presents the XRD pattern of the composition of its by-product. Again, for comparison, post-treatment 1 was performed. Moreover, by-product dried in the drying chamber (post-treatment 3) was stored in vacuum (post-treatment $3^{a,b} + 2^{c}$) and open-to-air (post treatment $3^{a,b} + 1^{c}$). From the table, we can observe that, as opposed to by-product #50 analysis, there is no significant variation in the $NaB(OH)_4$ purity (63 – 68 %) with both drying methods. Moreover, the composition of the by-product stored in the drying chamber is similar to the by-product stored open-to-air, indicating that air exposure after the by-product is dry has no effect on its composition.

Table 3.25. By-product composition of hydrolysis experiment #51 (in weight percentage) from XRD analysis after post-treatment 1 and after dried in the drying chamber (post-treatment 3) stored in vacuum and stored open-to-air.

Compound	Post-treatment		
	1	$3^{a,b} + 2^{c}$	$3^{a,b} + 1^{c}$
$NaB(OH)_4$	63 %	65 %	68 %
$HNa_2BO_3 \bullet H_2O$	-	35 %	32 %
$Na_2CO_3 \bullet H_2O$	37 %	-	-

Then, by-product #52 was dried in the globe box as described by post-treatment 1 and after drying it was exposed in the drying chamber for 24 h (sample b,1), 48 h (sample b,2), 72 h (sample b,3) and 96 h (sample b,4). The composition of the samples analyzed can be observed in Table 3.27. As expected, when post-treatment 1 was applied only, the mass percentage of $NaB(OH)_4$ was low and $Na_2CO_3 \bullet H_2O$ high. When exposed in the

drying chamber, however, an increase of the $NaB(OH)_4$ was observed to 100 % purity at 48 h and 96 h. This way, the exposure to a low humidity environment had a positive effect on the by-product, possibly since all compounds with molecular water dried during exposure and reacted with the low humidity environment. The exception was the by-product analyzed at 72 h (post-treatment $1^a + 3^{b,3} + 2^c$), which nevertheless had a reduction on the mass percentage of the non-borate $Na_2CO_3•H_2O$ and the formation of tincalconite. Alternatively, part of the by-product was dried only using the post-treatment 3. When this by-product was stored in vacuum (post-treatment $3^{a,b} + 2^c$) $NaB(OH)_4$ and $NaB(OH)_4•2H_2O$ were formed. However, when stored considering only the by-product drying and storage in the drying chamber (post-treatment 3), 40 % $NaB(OH)_4$ and 60 % $Na_2B_4O_5(OH)_4•3H_2O$ was formed. This indicates that prolonged exposure allowed the formation of $Na_2B_4O_5(OH)_4•3H_2O$ in detriment of $NaB(OH)_4•2H_2O$, again indicating that the $NaB(OH)_4•2H_2O$ lost its hydration and reacted with the low humidity environment to form $Na_2B_4O_5(OH)_4•3H_2O$.

Table 3.26. By-product composition of hydrolysis experiment #52 (in weight percentage) from XRD analysis after post-treatment 1, after dried open-to-air (post-treatment 1) with exposure after dry in the drying chamber for 24 h (b,1), 48 h (b,2), 72 h (b,3) and 96 h (b,4) all with storage in vacuum, after post-treatment 3 and after dried and exposed in the drying chamber (post-treatment 3) with vacuum storage.

Compound	**Post-treatment**						
	1	$1^a + 3^{b,1} + 2^c$	$1^a + 3^{b,2} + 2^c$	$1^a + 3^{b,3} + 2^c$	$1^a + 3^{b,4} + 2^c$	3	$3^{a,b} + 2^c$
$NaB(OH)_4$	49 %	63 %	100 %	-	100 %	40 %	✓
$NaB(OH)_4•2H_2O$	-	-	-	-	-	-	✓
$Na_2CO_3•H_2O$	51 %	37 %	-	36 %	-	-	-
$Na_2B_4O_5(OH)_4•3H_2O$	-	-	-	64 %	-	60 %	-

In the analysis of the main peaks observed in the XRD pattern in Figure 3.9, a main peak at around 17 º is observed in all post-treatments except for $1^a + 3^{b,3} + 2^c$, in accordance with Table 3.26. In this case, a main peak was detected at around 37 º, corresponding to $Na_2CO_3•H_2O$. Smaller intensity peaks are observed throughout the 2θ range (at 10 º, 19 º 30 º) which correspond to tincalconite. These smaller peaks are also observed in post-treatment $3^{a,b} + 2^c$, since the same concentration of tincalconite was determined in both analysis. In the analysis of the by-product with post-treatment $1^a + 3^{b,4} + 2^c$, a concave curve below the peaks in the 3 – 30 º range is observed, indicating the presence of amorphous species. Therefore, in can be concluded that the optimal exposure time in the

drying chamber (post-treatment 3) after drying exposure to air (post-treatment 1) is 48 h, since other compounds (not amorphous after 48 h and amorphous after 72 h) are formed after that exposure time, decreasing the purity of $NaB(OH)_4$.

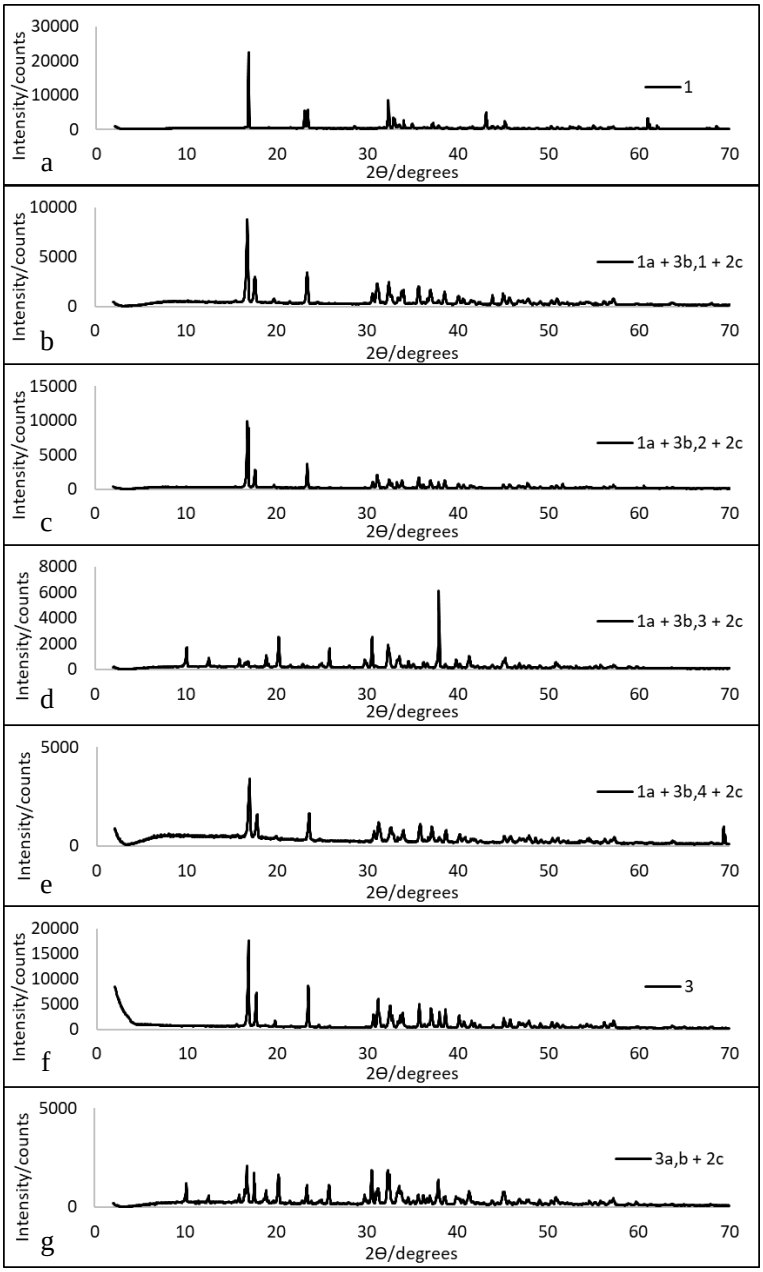


Figure 3.9. XRD patterns of the by-product #52 considering post-treatment 1 (a), open-to-air drying, storage in vacuum and exposure in the drying chamber for 24 h (b), 48 h (c), 72 h (d) and 96 h (e), post-treatment 3 (f) and by-product drying in the drying chamber and storage in vacuum (g).

In a similar trend, by-product #53 was extracted and processed based on the post-treatment 2. As expected, pure $NaB(OH)_4$ was formed as confirmed in the values displayed in Table 3.27. After drying, the by-product was placed in the drying chamber (post-treatment 3) and by-product samples were extracted after 24 h (post-treatment $2^{a,c}$

+ $3^{b,1}$), 72 h (post-treatment $2^{a,c}$ + $3^{b,2}$) and 96 h (post-treatment $2^{a,c}$ + $3^{b,3}$). Their analysis can be observed in Table 3.27. As opposed to by-product #52 (post-treatment 1), it was observed that after 96 h of exposure to a low humidity and forced convection environment the by-product maintained unaltered, except at 72 h of exposure $Na_2CO_3•H_2O$ was formed and $NaBO_2•2H_2O$ replaced $NaB(OH)_4$. In accordance with by-product #52, it indicates that $NaB(OH)_4$ is not affected by the low humidity environment after dried. Nevertheless, this and experiment #52 must be replicated to confirm these observations.

Table 3.27. By-product composition of hydrolysis experiment #53 (in weight percentage) from XRD analysis after post-treatment 2 and after dried in vacuum (post-treatment 2) with exposure after dry in the drying chamber for 24 h (b,1), 72 h (b,2), 96 h (b,3) all with storage in vacuum.

Compound	Post-treatment			
	2	$2^{a,c}$ + $3^{b,1}$	$2^{a,c}$ + $3^{b,2}$	$2^{a,c}$ + $3^{b,3}$
$NaB(OH)_4$	100 %	100 %	-	100 %
$NaBO_2•2H_2O$	-	-	✓	-
$Na_2CO_3•H_2O$	-	-	✓	-

Then, by-product #54 was processed based on post-treatment 4 and post-treatment 2 for comparison. The analysis indicate the formation of $NaBO_2$ and also impurity dolomite ($CaMg(CO_3)_2$) was unexpectedly observed, explained as a possible sample contamination, as observed in Table 3.28. As explained in the analysis of the by-products of experiments #26, #27 and #29 of subchapter 3.2, although it would be of greater interest, $NaBO_2$ is not possible to be formed since the sodium metaborate always retains 2 or 4 water molecules during the hydrolysis of $NaBH_4$. A possible explication for its presence can be the accidental prolonged exposure to a source of heat while stored which contributed to the water evaporation.

Table 3.28. By-product composition of hydrolysis experiment #54 (in weight percentage) from XRD analysis after post-treatments 2 and 4.

Compound	Post-treatment	
	2	4
$NaBO_2$	-	✓
$NaB(OH)_4$	✓	-
$NaB(OH)_4•2H_2O$	✓	-
$CaMg(CO_3)_2$	-	✓

At last, high (post-treatment 5) and low temperature (post-treatment 6) drying methods were studied. Post-treatment 5 performed on the by-products #55 and #56 considered its high temperature drying, and its XRD analysis is present in Table 3.29. For comparison, the post-treatments 1 and 4 were also applied to the by-product of experiment #56. As observed, regarding the post-treatment 5, the increase of the $NaB(OH)_4$ purity on by-product #55 could not be replicated in experiment #56. Moreover, although not in compliance with the composition of the by-product of experiment #54 (where pure $NaBO_2$ was formed), comparing the three post-treatments for experiment #56, post-treatment 4 (58 – 4) presents the most interesting result, due to its higher $NaB(OH)_4$ purity.

Table 3.29. By-product composition of hydrolysis experiments #55 and #56 (in weight percentage) from XRD analysis after post-treatments 1 (56 – 1), 4 (56 – 4) and 5 (55 – 5 and 56 – 5).

Compound	Experiment # - Post treatment			
	55 - 5	56 - 1	56 - 4	56 - 5
$NaB(OH)_4$	100 %	58 %	78 %	49 %
$Na_2CO_3•7H_2O$	-	42 %	22 %	51 %

Finally, the cold temperature effect was applied to the by-product of experiment #57 drying, as previously described as post-treatment 6. Additionally, this process was also applied to part of the by-products #30, #31, #33 and #34 after extraction from the hydrolysis reactor. Table 3.30 presents their composition. The XRD pattern in Figure 3.9 shows that $NaB(OH)_4•2H_2O$ is formed pure or close to pure (80 %) (by-products #30, #31, #33 and #34) and the exception is by-product #57. On the other hand, the $NaB(OH)_4•2H_2O$ formation, even though of lower interest compared to $NaB(OH)_4$ has indicated that the combination of low temperature and higher humidity can contribute to the optimization and stability of this borate.

Table 3.30. By-product composition of hydrolysis experiment #30 to #34 and #57 (in weight percentage) from XRD analysis after post-treatment 6.

Compound	Experiment #				
	30	31	33	34	57
$NaB(OH)_4•2H_2O$	100 %	80 %	100 %	100 %	-
$NaBO_2$	-	-	-	-	✓
$Na_2CO_3•H_2O$	-	20 %	-	-	✓

In Figure 3.10 we can confirm the presence of a main peak at 31 º corresponding to $NaB(OH)_4 \bullet 2H_2O$ in the analysis of the by-products #30, #31, #33 and #34 and absent in the by-product #57, where a main peak at around 24 º is present that corresponds to $NaBO_2$.

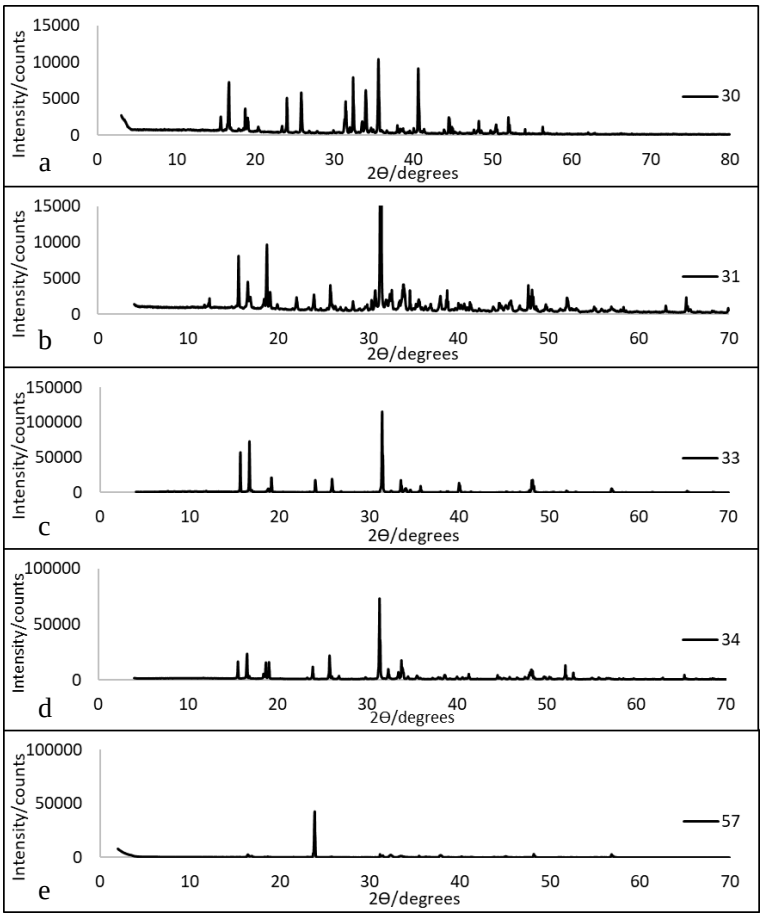


Figure 3.10. XRD patterns of by-products #30 to #34 and #57, considering their low temperature drying (post-treatment 6).

Additionally, by-product #34 was reanalyzed after 2 months of the first analysis, Table 3.31. The two samples of by-product #34 suffered different impacts: #34 – 1 observed the presence of a non-borate, which may indicate the heterogeneity of this by-product while #34 – 2 did not suffered any change to its composition. Although not consistent, this results can indicate a possible optimization of the $NaB(OH)_4 \bullet 2H_2O$ formation in the right conditions.

Table 3.31. By-product composition of hydrolysis experiment #34 (in weight percentage) from XRD reanalysis after post-treatments 1 and 6.

Compound	Post-treatment	
	1	6
$NaB(OH)_4 \bullet 2H_2O$	-	100 %
$NaBO_2 \bullet 4H_2O$	✓	-
$Na_2CO_3 \bullet 7H_2O$	✓	-

Figure 3.11 shows the main peaks present in the XRD analysis of by-product #34. The presence of a peak at around 31 º in both analysis suggest the similarities between $NaB(OH)_4 \bullet 2H_2O$ and $NaBO_2 \bullet 4H_2O$; however, similarly to by-products #49 $2^{a,c}$ + 1^{b} analysis, this hydrated form of sodium metaborate is detected with less intensity than its correspondent borate. Nevertheless, this is the only peak in common between both.

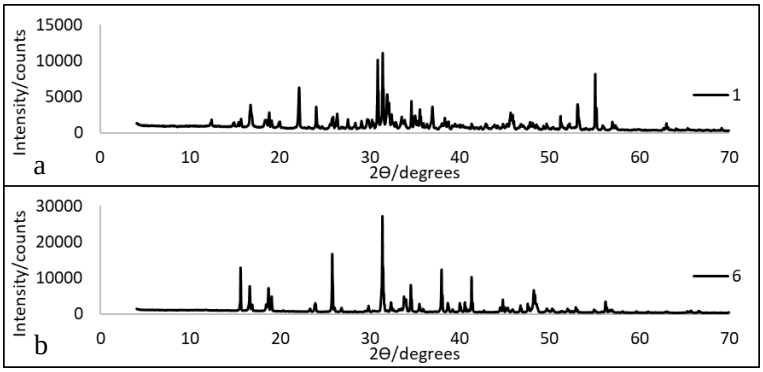


Figure 3.11. XRD patterns of the by-product #34 considering post-treatment 1 (a) and 6 (b).

In conclusion, the innovative process to treat the by-product of $NaBH_4$ hydrolysis developed in subchapter 3.2 was adapted in order to optimize the formation of other borates, such as tincalconite and $NaB(OH)_4 \bullet 2H_2O$. Therefore, four new post-treatments were studied and each by-product formed was processed by at least two different post-treatments for direct comparison. The first important observation was that the vacuum drying is essential to assure pure or close to pure $NaB(OH)_4$. since the main influence of air exposure on the by-product occurs during its drying and not after storage and the presence of air inside the desiccator, although closed, has a negative impact on the $NaB(OH)_4$. Although drying the by-product in a drying chamber seems to indicate only the formation of borates, its composition is not consistent, with a tendency to form tincalconite. Another result was that exposing the by-product dry up to 48 h and 96 h in the drying chamber had a positive effect on the purity of $NaB(OH)_4$ when first dried exposed to air and no effect when the by-product is first dried under vacuum, since no

reaction with the $NaB(OH)_4$ occured. Finally, drying under low air exposure or at high temperature did not show the consistency in the by-products composition; however, drying under a low temperature and high humidity environment (refrigerator, 2 ºC) tends to form pure $NaB(OH)_4 \bullet 2H_2O$, with consistent observed results. Although of less interest than $NaB(OH)_4$, it is important to understand the limits of the innovative process developed in subchapter 3.2 and subject of the provisional patent application approved [131] and it is the main hydrated $NaBO_2$ commercially available. Figure 3.12 resumes these observations.

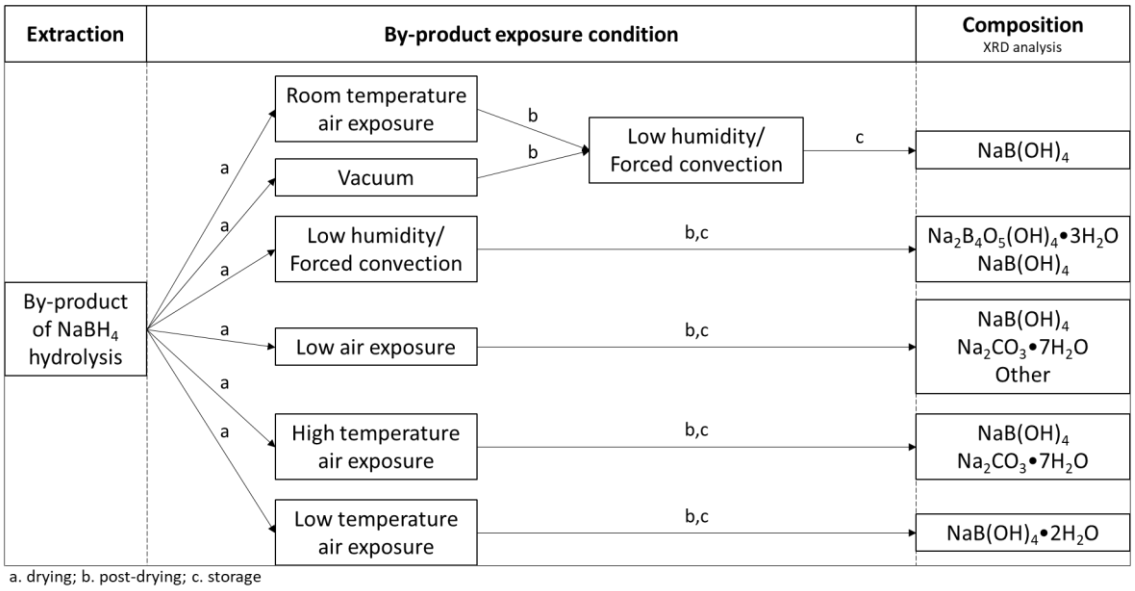


Figure 3.12. Effect of the exposure conditions of the by-product of $NaBH_4$ hydrolysis on its composition (legend: a. drying, b. post-drying, c. storage).

3.4. Conclusions

The identification of the by-product from the sodium borohydride hydrolysis is essential to optimize the recyclability process back to sodium borohydride, one of the most important drawbacks of this technology. Several experiments were planned and performed to understand the impact of different parameters on the type of by-product formed. One of the main goals was to validate the rearrangement of $NaBO_2 \bullet 2H_2O$ into $NaB(OH)_4$ in the presence of additive CMC. However, the results demonstrated the formation of this borate in the presence of another additive – PAA and without any additives contrarily to what was reported by Ferreira et al. [19]. Additionally, the composition of the solution of borates was not consistent throughout the experiments. An intensive experimental study with the goal of explaining these inconsistencies gave birth

to an innovative post-treatment of the by-product extracted from the reactor was developed. In the presence of vacuum drying and storage, pure or close to pure $NaB(OH)_4$ was formed and several experiments performed confirmed this result. For sake of comparison, other by-product post-treatments were considered. Interesting results were obtained when the by-product was dehydrated in a drying chamber and exposed to a low humidity environment, where high concentrations of tincalconite were formed. However, some inconsistencies were found since the prolonged exposure to air has demonstrated reaction with the borate, forming non-borates species such as $Na_2CO_3.H_2O$ and decreasing the purity of the desired borate. It was also verified that the low humidity environment had a positive impact on the by-product dried open-to-air and no effect when dried under vacuum, given that no reaction with dried $NaB(OH)_4$ occurred, but hydrated compounds were consumed, increasing the purity of $NaB(OH)_4$. Moreover, low temperature drying seemed to indicate a tendency to form pure $NaB(OH)_4 \bullet 2H_2O$; nevertheless, although consistency was found, this borate is less appropriate for the $NaBH_4$ regeneration process. The main output of this study, an innovative post-treatment developed and optimized in this thesis is a landmark on the future of the $NaBH_4$ as source of hydrogen in energy applications, since the pure or close to pure $NaB(OH)_4$ was formed in at least 15 experiments. The novel handling process subjected to a provisional patent application approved [131] – is not only essential to effectively regenerate the borohydride but also the absence of molecular water makes it the best borate to recycle back to $NaBH_4$ due to lower energy demand (no dehydration of the by-product is required).

4. Experimental study of the regeneration process of the borates to sodium borohydride

This chapter presents the experimental study of the regeneration of sodium borohydride from the borates obtained through the hydrolysis reaction. The results from the previous chapter enabled the control of the byproduct handing process towards the optimization of the $NaBH_4$ regeneration from the by-product formed that allows to close the $NaBH_4$-H_2 cycle [131]. Among the different possibilities for the regenerating process (please recall Chapter 2), it was decided to consider two types of processes: mechano-chemical and electrochemical. As explained in Chapter 2, these two types of processes are cleaner than the thermochemical processes. Moreover, although the electrochemical processes are expected to be the best cost-effective to regenerate $NaBH_4$, they have not been yet sufficiently developed and currently are not as efficient as the mechano-chemical processes. Therefore, one mechano-chemical and one electrochemical process was studied.

Considering the mechano-chemical regeneration, preliminary studies were performed with $NaB(OH)_4$ – the most interesting borate formed through the innovative handling process developed and patented [131] and the easiest to recycle. Alternatively, the process of electrochemical regeneration of $NaBH_4$ was studied from boric acid $B(OH)_3$. This alternative by-product was considered due to difficulty demonstrated in literature to regenerate $NaBH_4$ from $NaBO_2$ (please recall Chapter 2) and the facility to integrate the $NaBH_4$ hydrolysis and regeneration in the same system. After a detailed discussion of the $NaBH_4$ regeneration results, the chapter ends with the outline of the main conclusions.

4.1. Ball milling of the $NaB(OH)_4$ back to sodium borohydride

The mechano-chemical regeneration of $NaBH_4$ has been considered as the main alternative to the thermo-chemical processes, including the Brown and Schlesinger and Bayer processes. This type of processes is tendentially green, does not use high pressures and/or temperatures and has high efficiency. However, it requires extended ball milling times to regenerate $NaBH_4$ efficiently being the main borate studied and reported in literature the $NaBO_2$. Considering the by-product optimized in Chapter 3 – $NaB(OH)_4$ – through the innovative handling process developed and patented [131], the following

goals was to study its recycling. The experimental procedure and results are presented in this section. The recycling of synthesized $NaB(OH)_4$ has never been reported in literature, as far as the author could find.

4.1.1. Experimental procedure

A set of $NaBH_4$ hydrolysis experiments was performed as reported in the provisional patent application number 118331 T [131] and described in section 3.1. The SRc reactor was considered for the experiments, as well as the same Ni-Ru catalyst in a mass of catalyst per mass of $NaBH_4$ ratio of 0.4 g/g. x = 15/16 (depending on the $NaBH_4$ purity) was considered for the majority of experiments since these values are the most used excess of water values used in the optimization of the handling conditions that led to the formation of pure $NaB(OH)_4$. Additionally, 5 to 15 mL reactant solutions were considered, in order to produce enough by-product for the ball milling experiments. The other operating conditions of each experiment are displayed in Table 4.1. The main objective of these experiments was to optimize the process of recycling pure or close to pure $NaB(OH)_4$ back to $NaBH_4$ and understand the influence of less pure $NaB(OH)_4$ and the presence of other borates and non-borates in their recycling process. Consequently, only post-treatments 1 (air exposure drying) and 2 (vacuum drying in a desiccator) were performed to the by-products obtained in the hydrolysis experiments. These post-treatments were conducted as described in chapter 3.1 and 3.2. As then explained, the main difference between them is that post-treatment 2 optimizes the formation of $NaB(OH)_4$ by drying and storing the by-product under vacuum [131].

Table 4.1. Operating conditions of the hydrolysis experiments performed with excess of water ($11 < x < 16$) and post-treatments performed on each by-product formed.

Experiment #	x	Volume (mL)	Post-treatment
1	16	5	1
2	15	10	1
3	15	10	2
4	16	5	1
5	11	5	1
6	15	15	2
7	15	5	2

After each by-product was dried, it was milled to powder size and stored until use in the ball milling experiment. The recycling process was initiated by mixing each dried by-product with magnesium hydride (MgH_2) in a cylindrical grinding jar designed and built for the purpose. This grinding jar, presented in Figure 4.1, was adapted from the original one in order to avoid H_2 leak during the reaction. In the figure, the original grinding jar of the mill are the white vessels and the grinding jar designed and built to assure no H_2 leak are the inox vessels.



Figure 4.1. Photograph of the original grinding jar (white) and jar built in this work (stainless-steel) for the ball milling experiments to recycle $NaB(OH)_4$ back to $NaBH_4$.

The designed grinding jar has a different closing method – thread NPT locking system, designed in this work using the software SolidWorks. It was built in zirconia oxide (ZrO_2) with a stainless-steel coating. It has a cylindrical geometry with an internal diameter of 0.9 cm (internal volume of 15 cm^3). The stainless-steel coating is responsible for the thread locking system. This grinding jar has a groove with a 0.7 mm depth for a 24 mm diameter Viton O-ring to allow the crushing between the external and internal screw threads, thus promoting the isolation of hydrogen during the milling. It is worth to mention that the original grinding jar is placed inside the one conceived and designed for this work, as observed in Figure 4.2. The figure also presents the 2D design of the grinding jar built (the left small part in the top figure is presented in the middle figure, and the right bigger part of the jar is presented in the bottom figure).

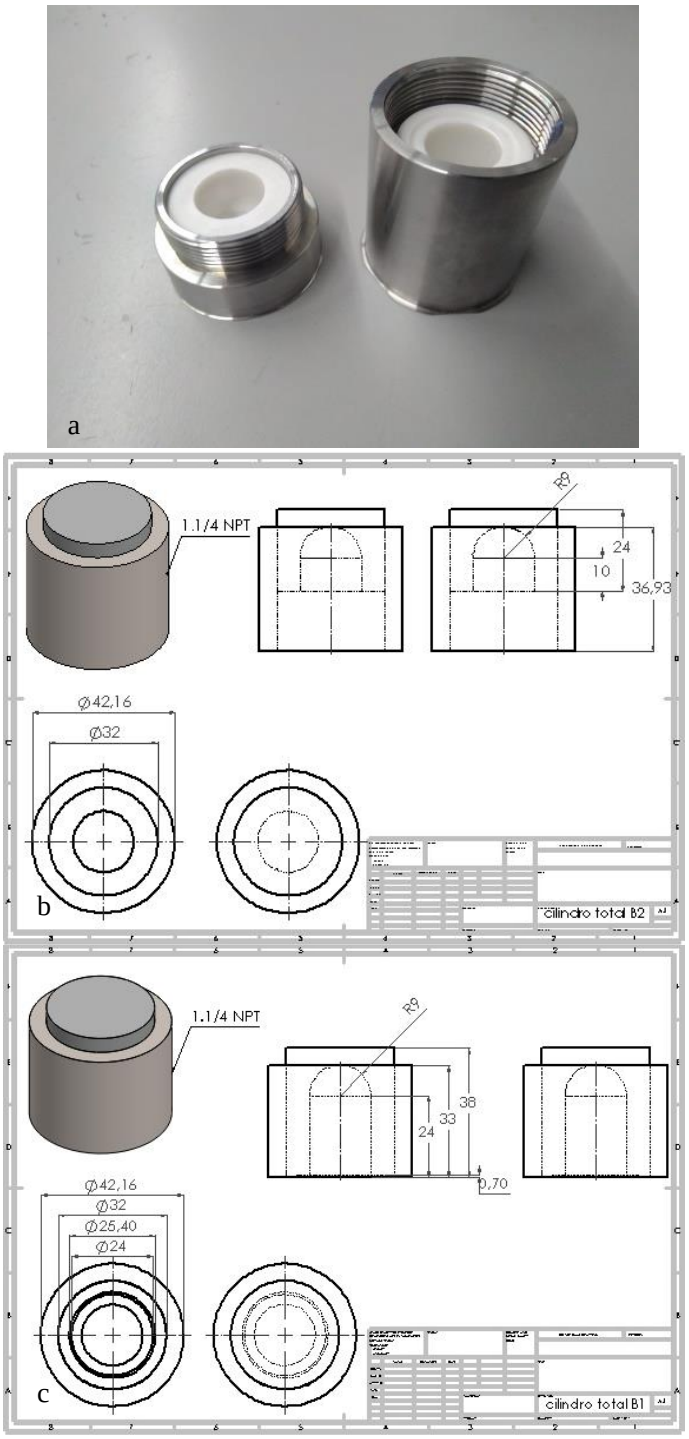


Figure 4.2. Grinding jar (a) and 2D design (left small part in b and right bigger part of the jar in c) used in the ball milling experiments to recycle $NaB(OH)_4$ back to $NaBH_4$.

The ball milling experiments were performed in a RETSCH mixer mill MM200 showed in Figure 2.3.2 in Chapter 2. The procedure was performed as follows: borate by-product and MgH_2 were mixed in the grinding jar and two zirconia balls with 10 mm diameter were added after. The mixer mill was chosen considering the only one available and the zirconia balls were used due to the need for a higher density material to better promote

the reaction, i.e., given their higher mass compared to other balls with the same size and lower mass, the zirconia can crush and mix the reactants more efficiently. Moreover, MgH_2 (Sigma-Aldrich, 683043, 96.5 % purity) was considered given that it is the main compound reported in literature to efficiently regenerate $NaBH_4$, as demonstrated in Chapter 2. Then, the jar was closed and parafilm was firmly placed around it to avoid any H_2 leak. After this step, the jar was correctly attached to the mixer mill and the reaction was performed for 2 hours at 1200 rpm (the maximum allowed by the available mixer mill and typically chosen in the literature, as also reported in Chapter 2). After the milling operation, the grinding jar was opened, and the mixture was extracted. The zirconia balls were rinsed with water and washed to be reused in the next experiment, while the extraction set (hopefully of $NaBH_4$ and MgO) was performed to the mixture. For that, isopropylamine (C_3H_9N) was used to dissolve the mixture and filtration in vacuum was applied to separate undissolved MgO and other compounds such as unreacted MgH_2 and non-borates present in the by-product formed. Vacuum was applied to ensure that the $NaBH_4$ would not react with water vapor. At a final step, the isopropylamine was evaporated in a glove box at 30 ºC (boiling point of isopropylamine) to obtain the filtrate dry. As described in Chapter 2.3.2, this solvent has a higher capacity to dissolve the $NaBH_4$ (6 g of $NaBH_4$ per 100 g of solvent) without reacting with it, therefore it is one of the solvents most reported in literature for this process. After drying the filtrate obtained, it was stored under vacuum and analyzed by XRD. Additionally, samples of the by-products before the ball milling and before extraction was performed were collected for posterior analysis. Similarly to the study of the by-product described in Chapter 3, the XRD analysis was performed in the Laboratório Central de Análises at the University of Aveiro, in an Empyrean diffractometer of the Malvern Panalytical. The XRD patterns were recorded at room temperature using monochromatic Cu K-α radiation (λ = 1.5406 Å) and the range of the XRD patterns were 4 º < 2θ < 70 º. In Figure 4.3, a visual representation of the experimental procedure is provided.

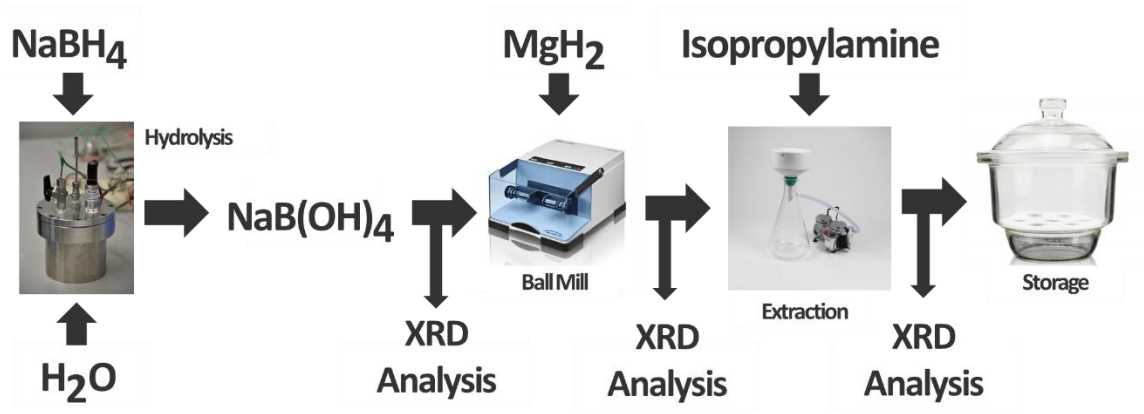


Figure 4.3. Visual representation of the experimental procedure performed for the study of the recycling of the $NaBH_4$ hydrolysis by-product (from post-treatment 2 for this example).

Table 4.2 displays the operating conditions used in the ball milling experiments, including the mass of by-product, the mass of MgH_2 and the ball to powder ratio (BPR). Regarding the $NaBH_4$ extraction, the mass of C_3H_9N and the filter used is also presented. In the table, the number after the mass of solvent used indicates the number of extractions that were done in each experiment. The type of filters used were cellulose (Filter-lab, PN1300150, pore size of 0.2 μm, filter A), cellulose nitrate (CN, Santorius stedim Biotech, 11407 – 47 – CAN, pore size of 0.2 μm, filter B), polytetrafluoroethylene (PTFE, GVS North America, 121587, pore size of 0.22 μm, filter C), nylon (Filter-lab, 180815006, pore size 0.22 μm, filter D) and polyester syringe-filter (PES, VWR, 514-0073, pore size 0.2 μm, filter E). The extraction with this syringe-filter (filter E) was performed differently than the described above. In this case, after the ball milling reaction, the mixture obtained and dissolved in the isopropylamine was transferred to a syringe. Then, the syringe-filter was attached to the syringe and the filtration occurred when the solution was injected and crossed the filter. Finally, the filtrate was evaporated to obtain hopefully pure $NaBH_4$ dry.

Table 4.2. Operating conditions of the ball milling experiments performed: the mass of by-product, the mass of MgH_2, MgH_2/By-product molar ratio (* assuming 100 % borate), the ball to powder ratio (BPR), the mass of C_3H_9N and the type of filter used.

Experiment #	Borate mass / g	MgH_2 mass / g	MgH_2/By-product molar ratio*	BPR	C_3H_9N mass / g	Filter
1	0.50	1.0	8.0	4.5	8.7 x 1	A
2	0.47	0.4	3.0	7.8	8.7 x 3	B
3	0.47	0.4	3.0	7.8	8.7 x 2	C
4	1.00	0.8	3.0	3.8	30 x 1	C
5	1.00	0.8	3.0	3.8	30 x 2	B, C
6	1.00	0.8	3.0	3.8	30 x 1	C
7	0.70	0.87	4.8	4.3	5.3 x 3	C, D, E

4.1.2. Results and discussion

The hydrolysis performance of the experiments is presented in Table 4.3. Almost all experiments had excellent performances, i.e., H_2 yields higher than 90 %, high HGRs, low induction times and high H_2 storage capacities. The exceptions were experiments #1 and #7, which had lower than expected H_2 yields - associated to injection problems - leading to low H_2 storage capacities.

Table 4.3. Performance of each hydrolysis experiment performed given by analysis of the H_2 yield, generation rate (HGR), induction time and storage densities (GHSC and VHSC).

#	Yield / %	HGR / $L.min^{-1}.g_{cat}^{-1}$	Induction time / s	GHSC / wt. %	VHSC / $kg.m^{-3}$
1	57	19.2	27	1.0	10.9
2	94	1.4	61	1.9	21.4
3	90	1.6	42	2.4	26.6
4	98	24.4	60	2.5	27.8
5	100	17.0	23	2.1	23.3
6	93	29.2	29	1.9	21.1
7	58	36.7	9	1.1	11.5

Considering now the recycling experiments, experiments #1 to #3 were performed as first experiments of this ball milling process to understand what would be the adequate minimum mass value of borate and MgH_2 to be used. Due to the limited borate mass used,

no significant products of reaction after extraction were obtained for analysis. That justified the repetition of experiments #1 and #3 using by-products produced in similar hydrolysis conditions but with higher mass values of reactants. Therefore, the results and discussion presented in this section is dedicated to experiments #4 to #7, considered to be performed in more adequate conditions.

Table 4.4 presents the XRD analysis of experiment #4 before and after ball milling and tentative extraction of $NaBH_4$. As observed, before the experiment $Na_2B_4O_5(OH)_4 \cdot 3H_2O$ accounted for more than half the composition of the by-product. After the recycling, although the concentration of this borate is lower due to the presence of other compounds, the formation of a less complex borate - $HNa_2BO_3 \cdot H_2O$ - is noted, which indicate that part of the $Na_2B_4O_5(OH)_4 \cdot 3H_2O$ reacted.

Table 4.4. Values obtained from XRD analysis of by-product composition before and after ball milling 1.0 g of borate (x = 16, post-treatment 1) with 0.8 g of MgH_2 (experiment #4).

Compound	**Ball milling + Extraction**	
	Before	After
$Na_2B_4O_5(OH)_4 \cdot 3H_2O$	56 %	34 %
$HNa_2BO_3 \cdot H_2O$	-	19 %
$Na_2CO_3 \cdot H_2O$	24 %	-
$Na_3H(CO_3)_2 \cdot 2H_2O$	20 %	11 %
MgH_2	-	32 %
$Mg(OH)_2$	-	5 %

Figure 4.4 present the main diffraction peaks observed in the XRD patterns of experiment #4. There we note the absence of the expected products of reaction $NaBH_4$ and MgO (diffraction peaks of $NaBH_4$ at 27.8 º, 31.9 º and 45.9 º [132] and diffraction peaks of MgO at 37.0 º, 43.0 º and 62.4 º [133]). Moreover, there is observed the reduction of the tincalconite diffraction peaks (20 º and 31 º) after the experiment and the appearance of three diffraction peaks (28 º, 36º and 55º) associated to unreacted MgH_2. Moreover, we note small intensity peaks at 19 º and 38 º associated to $Mg(OH)_2$.

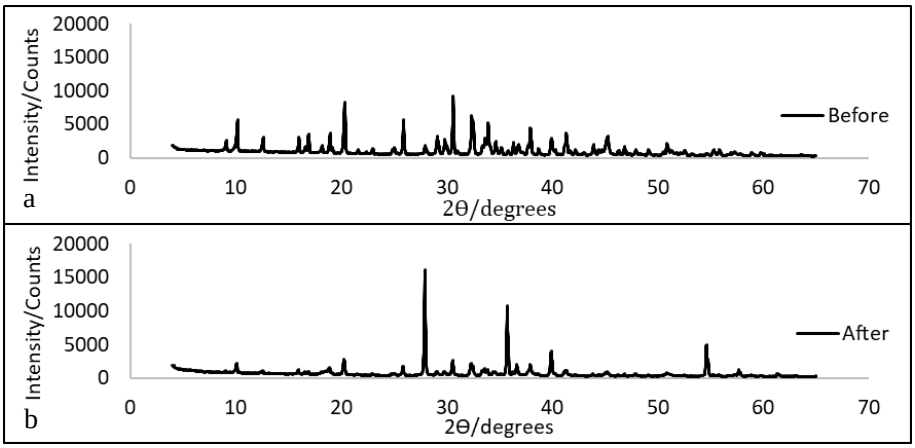


Figure 4.4. XRD pattern of by-product composition before and after ball milling 1.0 g of borate (x = 16, post-treatment 1) with 0.8 g of MgH_2 (experiment #4).

Additionally, the disappearance of carbon compounds is observed, which can be associated to the retention in the filter (filter C) or that they served as an additive of the ball milling. This finding was reported by Li et al. [111], who referred an increase of the $NaBH_4$ regenerated from $Na_2B_4O_5(OH)_4 \cdot 3H_2O$ in the presence of $Na_2CO_3 \cdot H_2O$. From this report and the one of Kayacan et al. [134], the ball milling of $Na_2B_4O_5(OH)_4 \cdot 3H_2O$ with MgH_2 can be represented by Equation 4.1.

$$Na_2B_4O_5(OH)_4 \cdot 3H_2O + 9MgH_2 \rightarrow 2NaBH_4 + 9MgO + B_2O_3 + 10H_2 \quad (4.1)$$

Then, formation of $Mg(OH)_2$ denotes that some MgH_2 was consumed and confirms it reacted with the by-product as expected, as this hydroxide compound is an intermediate of this ball milling process, as reported in literature by several authors ([104],[106],[103],[107]) and described in Chapter 2. These authors refer it is then consumed to form MgO, as recalled by Equations 4.2 and 4.3.

$$2Na_2B_4O_5(OH)_4 \cdot 3H_2O + 9MgH_2 \rightarrow 4NaBH_4 + 9Mg(OH)_2 + 2B_2O_3 + H_2 \quad (4.2)$$

$$9Mg(OH)_2 + 9MgH_2 \rightarrow 18MgO + 18H_2 \quad (4.3)$$

Experiment #5 was then performed and similar by-product composition was observed by the analysis of the XRD pattern (Table 4.5 and Figure 4.5) with $Na_2B_4O_5(OH)_4 \cdot 3H_2O$ as the only borate (49 %) and $Na_2CO_3 \cdot H_2O$ and $Na_3H(CO_3)_2 \cdot 2H_2O$ as the remaining compounds. After each step of the recycling process, samples were extracted and analyzed to understand the evolution of the process and its possible effect on the $NaBH_4$ formation before ball milling, after ball milling without extraction and after removal of

contaminants next to the extraction with isopropylamine. Therefore, it should present less magnesium compounds and more boron compounds. However, that has not been observed, based on the XRD analysis. The analysis of the sample obtained after ball milling indicate that no significant boron compound was formed in the reaction, except for the $Na_2B_4O_5(OH)_4 \bullet 3H_2O$ already formed in the by-product of the hydrolysis reaction. Moreover, similarly to experiment #4, no carbon compound was present in the XRD analysis of the filtrates (filter B in 1st extraction and filter C in 2nd extraction), confirming these compounds are oversized to the filters used. Finally, the presence of $Mg(OH)_2$ in the filtrates confirms again that some MgH_2 reacted with the by-product as expected. Then again, it was not detected on the sample coming out of the ball mill, which can be justified by the heterogeneity of the mixture, since during the reaction the MgH_2 distribution is not equal throughout the reaction medium. In Figure 4.5, the same intensity of the diffraction peaks at 28 º. 36 º and 55 º are observed in the sample collected after ball milling and both extracted samples in the XRD pattern, associated to unreacted MgH_2, as well as smaller diffraction peaks at 18 º and 38 º related to intermediate $Mg(OH)_2$. Moreover, the presence of amorphous species with the same intensity in all XRD analysis of this experiment, suggest that they have not interfered with the experiment.

Table 4.5. Values obtained from XRD analysis of by-product composition in each step of ball milling 1.0 g of borate (x = 11, post-treatment 1) with 0.8 g of MgH_2 (experiment #5).

Compound	By-product	Ball Milling	Filtrate of 1st Extraction – filter B	Filtrate of 2nd Extraction – filter C
$Na_2B_4O_5(OH)_4 \bullet 3H_2O$	49 %	31 %	44 %	54 %
$Na_2CO_3 \bullet H_2O$	33 %	22 %	-	-
$Na_3H(CO_3)_2 \bullet 2H_2O$	19 %	12 %	-	-
MgH_2	-	34 %	38 %	25 %
$Mg(OH)_2$	-	-	18 %	22 %

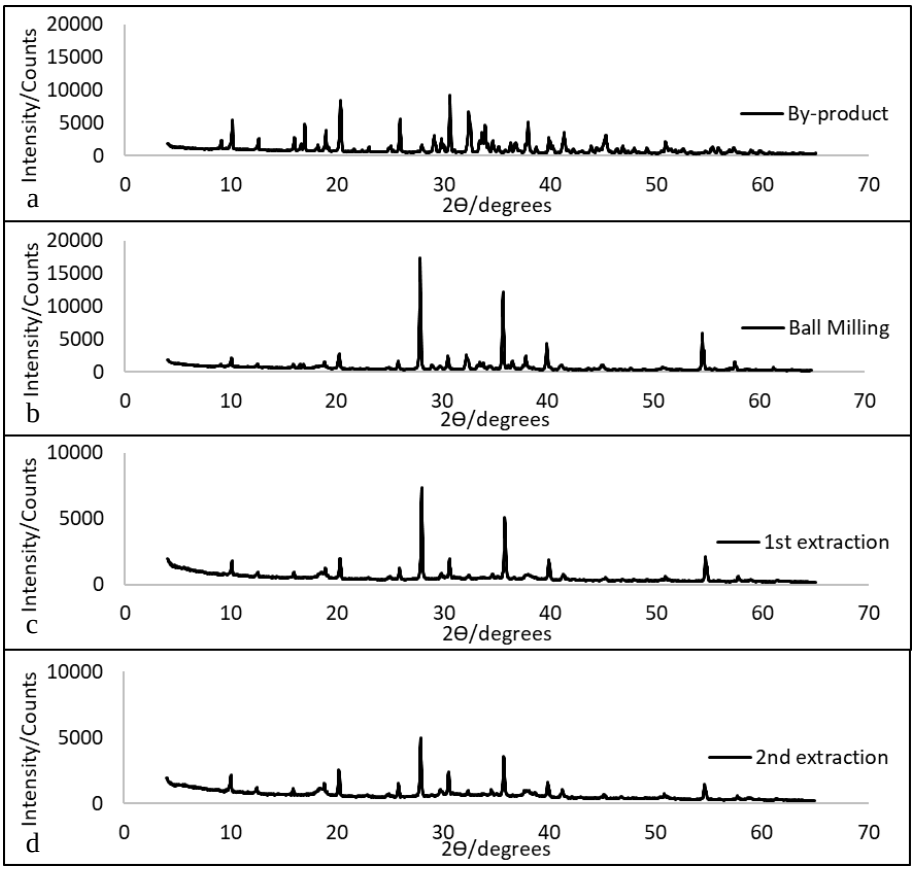


Figure 4.5. XRD pattern of by-product composition in each step of ball milling 1.0 g of borate (x = 11, post-treatment 1) with 0.8 g of MgH_2 (experiment #5).

All these experiments (#1 to #5) were performed for by-products obtained using post-treatment 1. Since post-treatment 2 has demonstrated optimal $NaB(OH)_4$ purity (100 % pure or close to it), the $NaBH_4$ regeneration should be studied for that by-product. It is important to recall that this has not been referred in literature due to the difficulty in obtain this borate with such a high level of purity (recall Chapter 2). Experiment #6 was then performed similarly to experiments #4 and #5. The results from the XRD analysis are displayed in Table 4.6. As expected, the $NaB(OH)_4$ was obtained pure from the $NaBH_4$ hydrolysis after post-treatment 2. The analysis of the XRD pattern did not detect any $NaBH_4$ or another borate in detectable amounts. Nevertheless, intermediate $Mg(OH)_2$ was formed at a much weight percentage than in previous reported results, which might indicate a more significant conversion of the borate into the borohydride in spite of not detectable. The reaction step describing the formation of this compound is recalled here in Equations 4.4 and 4.5. Also, a small pressure release when the milling jar was opened after the reaction was noted, which can only be associated to H_2 formed and as another indicative of the formation of $NaBH_4$. Other methods of characterization, for example

FT-IR, can be more efficient in identifying the formation of $NaBH_4$ from this recycling method.

$$NaB(OH)_4 + 2MgH_2 \rightarrow NaBH_4 + 2Mg(OH)_2 \quad (4.4)$$

$$2Mg(OH)_2 + 2MgH_2 \rightarrow 4MgO + 4H_2 \quad (4.5)$$

Moreover, analyzing the filtrate and retained, we observed that more than half of the magnesium compounds cross the filter (filter C), so it is essential to replace the filter for a more efficient one for this process. The presence of $Na_2CO_3 \cdot H_2O$ in the retained analysis was not expected since it was not observed in the by-product. This can be explained by inadequate isolation of the sample from air after the by-product was obtained and the ball milling was performed. Nevertheless, since the filtrate had no $Na_2CO_3 \cdot H_2O$, we notice its mass percentage is still low (13 %).

Table 4.6. Values obtained from XRD analysis of by-product composition in each step of ball milling 1.0 g of borate (x = 15, post-treatment 2) with 0.8 g of MgH_2 (experiment #6).

Compound	By-product	Ball Milling	Filtrate of extraction – filter C	Retained of extraction – filter C
$NaB(OH)_4$	100 %	64 %	15 %	29 %
$Na_2CO_3 \cdot H_2O$	-	-	-	13 %
MgH_2	-	22 %	36 %	26 %
$Mg(OH)_2$	-	14 %	49 %	32 %

Figure 4.6 complements graphically the results displayed in Table 4.6. As observed in the figures, the intensity of the $NaB(OH)_4$ diffraction peak at 17 º decreases with each step of the ball milling process, which is correlated to the lower weight percentage observed in Table 4.6. On the other hand, there is an increase of peaks at 28 º, 36 º and 55 º associated to MgH_2, as well as the appearance of diffraction peaks at 19 º and 38 º associated to $Mg(OH)_2$ in all XRD analysis performed after the ball milling reaction.

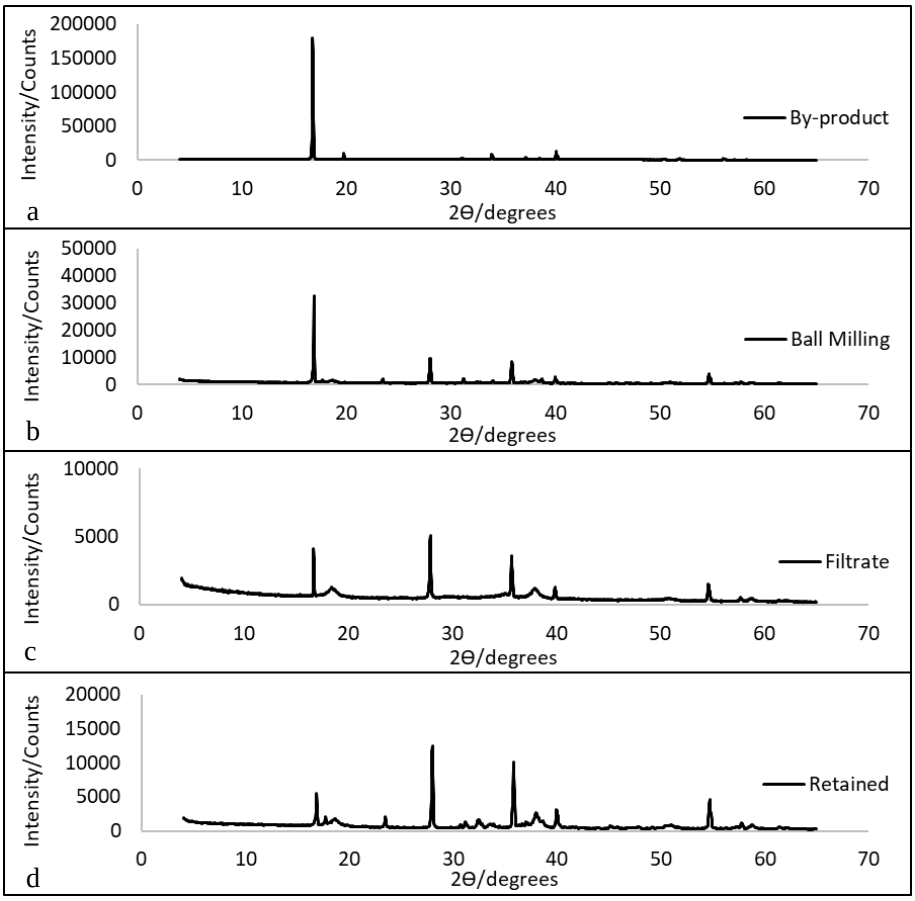


Figure 4.6. XRD pattern of by-product composition in each step of ball milling 1.0 g of borate (x = 15, post-treatment 2) with 0.8 g of MgH_2 (experiment #6).

Although the conditions for the ball milling experiments #4 and #5 allowed for an excess of MgH_2 to be used (due to the lower purity of the borates formed), the same conditions applied (to have a direct comparison between the use or not of the innovative handling post-treatment process patented and described in Chapter 3 as post-treatment 2, that assured optimal $NaB(OH)_4$ formation) were not enough for the ball mill of this borate, i.e., the MgH_2 used was below the reactions' stochiometric demand. Another experiment (#7) was performed to the same by-product used in experiment #6 in order to optimize the recycling of this borate back to $NaBH_4$. Table 4.7 presents for a better comparison the conditions of the performed ball milling experiments #6 and #7. The values displayed show that both the MgH_2 to $NaB(OH)_4$ molar ratio (over the stoichiometric value of 4, according to Equations 4.4 and 4.5) and BPR increased. Although the BPR was not high enough, given the limitations of the ball mill, it was the maximum considerable for the volume available (literature reports have considered a minimum BPR of 10 and an optimal one of 50, as described in Chapter 2). Nevertheless, the higher the BPR the better,

as demonstrated by the literature reports described in Chapter 2. To compensate for the low value of BPR, the time of milling was increased from 2 to 6 hours.

Table 4.7. Operating conditions of ball milling applied to the borates formed through hydrolysis post-treatment 2 (experiments #6 and #7): mass of by-product, mass of MgH_2, ball to powder ratio (BPR), mass of C_3H_9N and type of sample storage.

Experiment #	By-product mass / g	MgH_2 mass / g	MgH_2/By-product molar ratio	BPR	t / h	C_3H_9N mass / g	Sample storage
6	1.00	0.8	3.0	3.8	2	30.0 x 1	Air
7	0.70	0.87	4.8	4.3	6	5.4 x 3	Vacuum

Also, in experiment #7 three extractions were performed contrarily to only one in experiment #6 with the goal to compare the filters considered. The second and third extractions were performed to the retained from the first and second extraction, respectively. Nevertheless, the second extraction did not produce filtrate and consequently no retained has been analyzed. The absence of filtrate formation can be explained by the retention of all compounds in the filter used or the absence of dissolved compounds in the solvent used for the extraction crossed the filter and was fully evaporated, which indicated the need to promote a better dissolution of the compounds in the solvent.

Table 4.8 presents the XRD analysis of the by-product composition in each step of the ball milling experiment. Given that three extractions were performed in sequence to the products of the ball milling reaction, the retained of the third extraction is obtained from the three extractions that were performed. Therefore, a comparison between the filters used for the separation of the borohydride from the by-products and non-reactive reactants can be studied.

Table 4.8. Values from XRD analysis of by-product composition in each step of ball milling 0.70 g of borate (x = 15, post-treatment 2) with 0.87 g of MgH_2 (experiment #7).

Compound	Reaction		1st extraction – filter C		3rd extraction – filter E	
	By-product	Milled	Filtrate	Retained	Filtrate	Retained
$NaB(OH)_4$	100 %	23 %	35 %	35 %	48 %	48 %
Na_2CO_3	-	3 %	-	-	-	-
MgH_2	-	61 %	53 %	58 %	47 %	47 %
$Mg(OH)_2$	-	12 %	13 %	7 %	5 %	5 %

Although the conditions were adjusted to promote the by-product recycling back to $NaBH_4$ (by increasing the BPR, time of milling and the MgH_2 to $NaB(OH)_4$ molar ratio), the results of the XRD analysis of experiment #7 presented in Table 4.8 are similar to the ones obtained in experiment #6 and presented in Table 4.6, i.e., we observe a high percentage of unreacted $NaB(OH)_4$ and MgH_2 in the filtrate and retained, low presence of intermediate $Mg(OH)_2$ and absence of the expected products of the complete reaction - $NaBH_4$ and MgO. This can be explained by the low available internal volume of the grinding jar, which limits not only the mass of reactants that can be used but also the space available for the grinding balls to move inside the jar and crush and mix the reactants. It is therefore essential to repeat the experiments in a ball miller that can uses a grinding jar with higher internal volume. At last, comparing the filtrate with the retained of each extraction of experiment #7, we observe similar mass percentage of $NaB(OH)_4$, MgH_2 and $Mg(OH)_2$, which indicates that the filters used (C in 1st extraction and E in 3rd extraction) were not adequate for the process, as mentioned in the previous experiments in this section.

It is also worth mentioning the need to find alternative reductants for this recycling process, due to the currently low commercial availability of MgH_2. These alternatives can be Mg only and Mg_2Si, as described in Chapter 2, as well as Li compounds such as LiH, due to the abundance of Li in Portugal, with possible extraction and avoiding depending of external manufacturing as is the case of the Chinese Mg extraction. For that matter, a study of the environment impact of these compounds should also be considered in the future.

In summary, mechano-chemical experiments were performed in a Retsch MM200 ball miller to study the by-product of the $NaBH_4$ hydrolysis back to $NaBH_4$. For that,

considering the study performed in Chapter 3 of the post-treatment of the by-product - which lead to the development of a post-treatment that assures pure or close to pure $NaB(OH)_4$ – by-products formed and dried considering the traditional less pure air method and the innovative vacuum method optimized in this thesis (subchapter 3.2) were ball milled. $Mg(OH)_2$ was formed in all experiments performed and analyzed – an intermediate of the reaction previously reported in literature – which confirms that the by-product dried reacted with MgH_2 as expected. However, the XRD analysis of the experiments did not allow to observe any borohydride regenerated (neither the other product of the reaction, MgO), although the presence of a higher purity borate assure more $NaBH_4$ can be formed. This is mainly explained by the non-optimal operating conditions due to low availability of MgH_2 and the practical impossibility of working under sufficiently high ball to powder ratio (BPR). Further studies demand for an optimization of the conditions of this mechano-chemical processes by using grinding balls with a higher diameter or increase the number of balls used, and also to increase the internal volume of the grinding jar. A scale up of the ball miller is mandatory in future work. Additionally, the extraction of $NaBH_4$ should be performed with improved filters (such as PTFE with a lower pore size), given that the magnesium compounds involved in the recycling process cross the filter to the filtrate. At last, it is worth considering the study of alternatives to MgH_2 such as Mg, Mg_2Si and LiH, due to the current low commercial availability of MgH_2 and the study of the environmental impact of each of these compounds in the $NaBH_4$-H_2 cycle.

4.2. Electrochemical synthesis of $NaBH_4$ from boric acid

Electrochemical processes are, in theory, preferred to regenerate $NaBH_4$, since they present lower costs and lower energy demand compared to thermo- and mechano-chemical processes. However, as reported in Chapter 2, efficient electrosynthesis of $NaBH_4$ has not been obtained due to the difficulty to avoid parallel reactions associated to aqueous electrolytes, such as the hydrogen evolution reaction (HER) [122]. These happen due to the need to operate the electrochemical cell in an alkaline electrolyte (concentrated NaOH), favoring these reactions as opposed to the electrochemical reduction of BO_2^-. Therefore, although only $NaBO_2$ has been studied in this type of processes and an innovative post-treatment of the by-product has been developed and

patented in Chapter 3 forming pure or close to pure $NaB(OH)_4$, this borate is expected to suffer from the same (or higher) difficulties than $NaBO_2$. Thus, acidic by-products of the $NaBH_4$ hydrolysis should be considered. In this work, Boric acid ($B(OH)_3$) recycling was considered. This borate is formed in the acidic hydrolysis of $NaBH_4$, as described in Chapter 2. Moreover, the only by-product of the electrosynthesis is water, which could be integrated into the hydrolysis of regenerated $NaBH_4$, in a continuous $NaBH_4$ hydrolysis/regeneration cycle. This subchapter presents the experiments performed with this borate and the main conclusions obtained from it.

4.2.1. Experimental procedure

The electrochemical cell demonstrated in Figure 4.7 was built to perform the preliminary experiments of the $B(OH)_3$ recycling back to $NaBH_4$. The electrodes are inserted in the electrolyte through the opening of holes in the glass flask lid. Given that, besides the RE (the light blue head and black cable electrode in the figures) the electrodes are in rectangular and cylindrical shape and have no cable support, a copper wire was fixated to each to assure no release during the experiment. Although, copper was chosen due to its good electric conductivity, these wires were in minimal contact with the electrolyte to avoid the copper corrosion in the aqueous acid solutions. Then, the RE and these copper wires were connected to the electrochemical workstation. In some experiments, N_2 atmosphere was introduced in the cell to reduce the presence of oxygen from the air. Therefore, another hole in the lid was made to allow the N_2 addition through a tube connected to the N_2 source in the laboratory. In the Figure 4.7, the one on the right represents the experiment under N_2 bubbling and the figure on the left without it. $B(OH)_3$ was acquired for the experiments (Sigma-Aldrich, B0394, 99.5 % purity), although it could have been produced through the acidic hydrolysis of $NaBH_4$, as explained in Chapter 2.

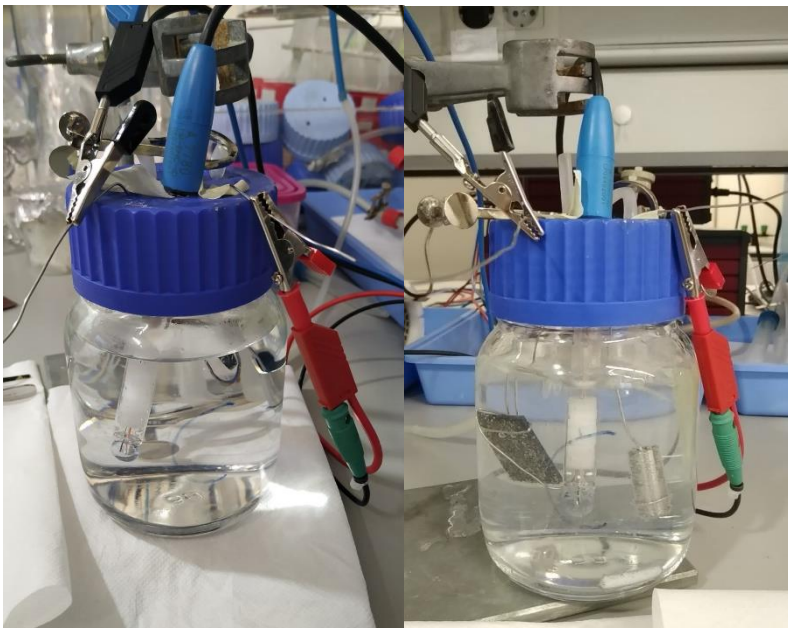


Figure 4.7. Electrochemical installation considered for the electrochemical experiments performed (the difference between the figure is on the atmosphere inside the cell: left - air exposure; right – N_2 bubbling).

A BDD electrode was used as cathode in the reduction of $B(OH)_3$, given it presented the most interesting results as WE in the $NaBO_2$ recycling literature (please recall Chapter 2). The reference electrode (RE) was an Ag/AgCl combined pH-reference electrode. As for the anode, various electrodes were chosen, namely, Ni and Ti uncoated and coated by ruthenium oxide (RuO_2) or iridium oxide (IrO_2) each. These were chosen based on their capacity to actively participate in the electrosynthesis as their oxidation can, in theory, assure enough electrons to allow the $B(OH)_3$ reduction. The Ti electrode was used initially to optimize the electrolyte conditions and avoid degradation on the coated electrodes. Equations 4.6 to 4.9 represent the main reactions with potential interest in this system, occurring at the anode for each electrode considered [135],[136] and the reaction representing the $B(OH)_3$ reduction to BH_4^- can be written as Equation 4.10. The reduction potential of this reaction is -0.48 V [135], as observed in the boron electrochemical window represented in Figure 4.8.

$$Ni \rightarrow Ni^{2+} + 2e^- \quad (4.6)$$

$$Ti + 2H_2O \rightarrow TiO_2 + 4H^+ + 4e^- \quad (4.7)$$

$$RuO_2 + 2H_2O \rightarrow RuO_4 + 4H^+ + 4e^- \quad (4.8)$$

$$2NH_4OH \leftrightarrow N_2 + 2H_2O + 6H^+ + 6e^- \quad (4.9)$$

$$B(OH)_3 + 7\,H^+ + 8\,e^- \rightarrow BH_4^- + 3\,H_2O \quad (4.10)$$

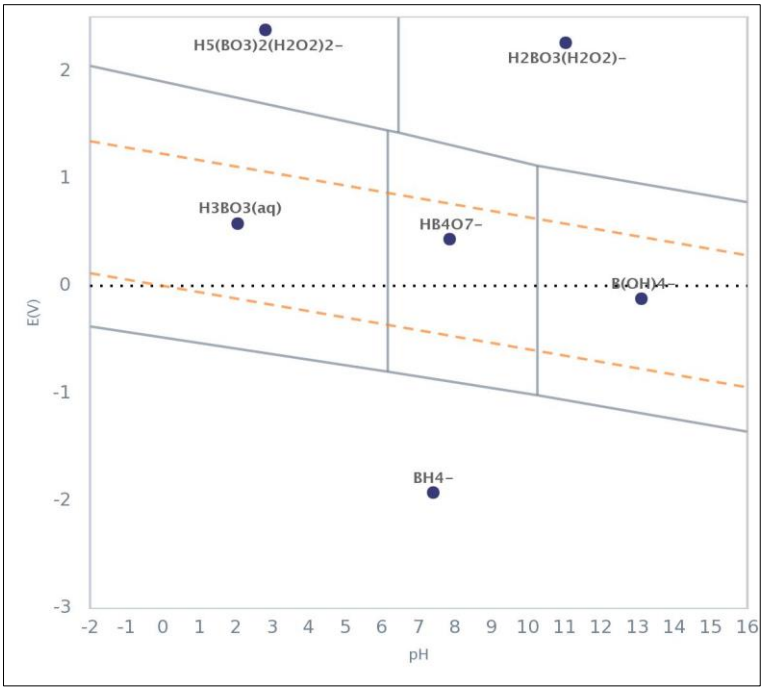


Figure 4.8. Boron electrochemical window and its dependence on pH and potential applied [135].

Given that low pH mean facilitates the $B(OH)_3$ reduction (lower potential), an acidic aqueous electrolyte was considered, and the best acids were studied. For that, their main characteristics should be a high dissociation constant in water and to not react with the electrodes, neither the reactants nor the reactor material itself (to avoid corrosion). Moreover, the main purpose of this study is to combine the generation of hydrogen with the regeneration of $NaBH_4$. Accordingly, it is important to consider the conditions that will allow for the future generation of hydrogen, i.e., the electrodes, the acidic solution and the electrochemical system must not compromise the generation of hydrogen in the reactor chosen for that purpose.

The electrodes do not represent a problem; however, the acidic solution must be well chosen: if the acid is strong (lower pH), the stainless-steel hydrolysis reactor cannot be used; if the acid is weak (pH closer to 7), it requires an amount of acid that can be higher than the volume supported by the reactor (to assure minimum H^+ concentration is available). This way, strong acid sulfuric acid (H_2SO_4) and weaker acid acetic acid (CH_3COOH) were selected to be used in the regeneration of $NaBH_4$ [137].

If optimal conditions can be found, based on the hydrolysis and regeneration of $NaBH_4$ and since all by-products can be integrated on both reactions and/or can be recycled, we can integrate both processes in a continuous H_2 generation system. Figure 4.9 describes this $NaBH_4/H_2$ cycle. The acidic hydrolysis of $NaBH_4$ (low pH) gives origin to H_2,

$B(OH)_3$ as the main by-product reported in literature and a salt due to the presence of an acid. This boron specie can, in theory, be recycled back to $NaBH_4$ through the electrochemical process studied in this thesis (Equation 4.10). At last, both salts formed in the hydrolysis and regeneration of $NaBH_4$ can be recycled (depending on the acid used) to close the cycle.

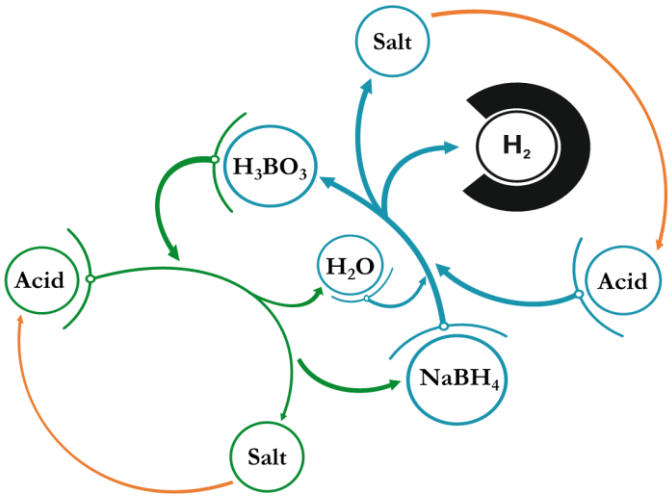


Figure 4.9. $NaBH_4/H_2$ cycle considering the electrochemical recycling of boric acid.

An acidic aqueous solution composed of one of the chosen acids and boric acid was prepared by adding those compounds to the glass beaker/reactor, in that order. After that, the electrodes were immersed in the solution. The electrodes were connected to a modular electrochemical workstation – the ZAHNER ZENNIUM – which allowed the study of the CVs of the electrodes considered, under specific electrolytes. Initially, CV tests were performed without the RE (In these tests, two-electrodes system was used, in which a theoretical RE is defined by the electrochemical workstation, and the standard E^0 of the RE defined is added to the potential imputed. In this case, the RE defined was Ag/AgCl with E^0 = 0.197 V, since it was the physical RE used in the remaining tests). When this was acquired, the attempts to observe the regeneration of sodium borohydride were performed open-to-air. After these tests, nitrogen bubbling was introduced to the electrochemical cell, to reduce the presence of oxygen in the electrolyte. In all experiments, CV analysis of the electrolyte (without boric acid) was performed in the same conditions, to obtain a blank test and discard parallel reactions associated to the electrolyte and not related to boric acid.

The operating conditions of the electrochemical experiments performed can be detailed in the table below, Table 4.9, displaying the CEs used (WE was BDD in all experiments),

as well as electrolyte and $B(OH)_3$ concentration are described. After each CV experiment, the main peaks observed were correlated with references in the literature to identify possible oxidation/reduction reactions involving $B(OH)_3$ and its recycling back to $NaBH_4$. From what is found in the literature, this study was never performed.

Table 4.9. Operating conditions of electrochemical experiments performed to study the $B(OH)_3$ recycling back to $NaBH_4$.

Experiment #	CE	Electrolyte	$B(OH)_3$ / M	N_2 bubbling
1	Ti	Acetic 4 M	0.20; 1.0	No
2	Ti	Acetic 4 M	1.0	No
3	Ti	Acetic 5 M	0.16; 0.32	No
4	Ti	Acetic 5 M	0.08; 0.20; 0.40	Yes
5	Ti	Acetic 5 M	0.16; 0.32; 0.48	No
6	Ti, Ni, IrO_2, RuO_2	Sulfuric 5 M	0.03;0.06	No

4.2.2. Results and discussion

Experiments #1 to #6 worked as the experiments of the study of $B(OH)_3$ recycling back to $NaBH_4$. Among these, trials #1 to #3 were initially performed without a RE. Accordingly, the CV experiments were performed first blank and without boric acid and the CVs replicated to verify identical curves. Figure 4.10 presents these CV tests, as well as a CV curves for acetic acid in water. As can be observed, when 0.20 M $B(OH)_3$ was used, no peaks were formed. However, with the increase of its concentration to 1.0 M, the appearance of a reduction peak at -1.7 V and an oxidation peak at 2.2 V, for a potential range between -3 and 3 V was observed. When repeating the CV at a wider potential range (]-4.0;4.0[V), these peaks now appeared at -2.2 V and 1.2 V, respectively. The variation of potential for these peaks can be explained by the presence of air exposure, which can have a prolonged effect on the cell (higher time of exposure of the electrodes) since the CVs at wider potential range were performed after the CVs at lower potential range, as well as the absence of RE. These peaks could not be correlated to any reaction reported in literature.

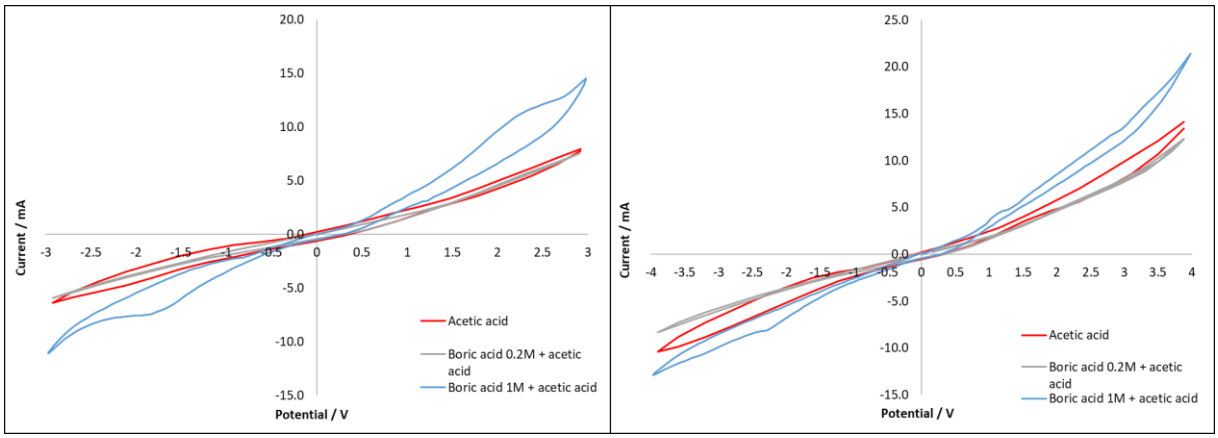


Figure 4.10. CV tests performed for 0.2 M and 1 M boric acid under 4 M acetic acid based on electrochemical experiment #1.

When the experiment #1 was replicated (experiment #2), the same peaks were not observed, Figure 4.11. In fact, the opposite was noted, since the acetic acid curve was flattened, indicating that the presence of the boric acid had a limiting effect on possible side reactions occurring in the electrolyte. Again, the absence of RE and air exposure had a negative effect on the replication of the experiments performed.

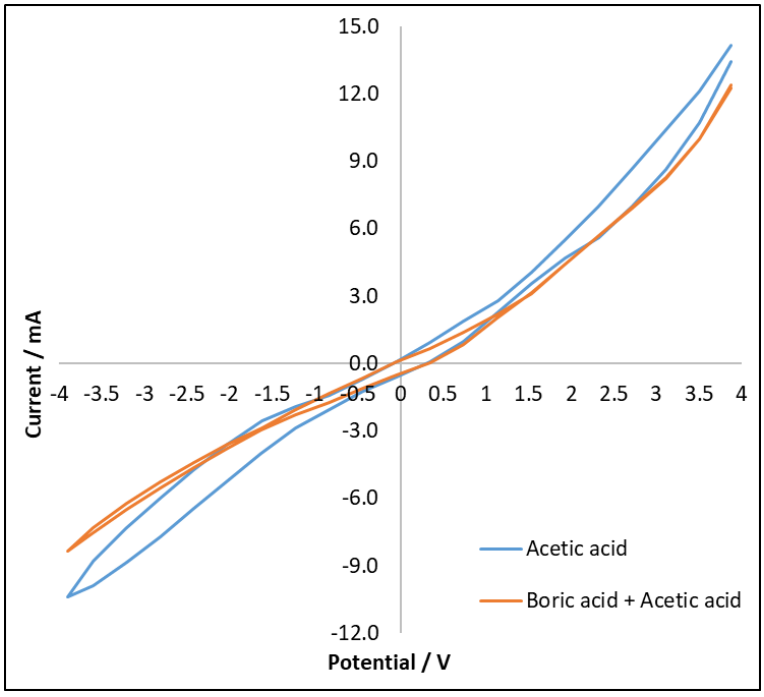


Figure 4.11. CV tests performed for 1 M boric acid under 4 M acetic acid based on electrochemical experiment #2.

Then, experiment #3 considered seven CV tests and the effect of the $B(OH)_3$ concentration and the scan rate at which the analysis is performed were studied as showed in Table 4.10. Tests 1 to 3 were performed in the Zahner ZENNIUM electrochemical workstation while tests 4 to 11 were performed in the XPOT module of the Zahner – a

module that is adequate for use with lower currents. The initial $B(OH)_3$ concentration was maintained closer to the used in the first two experiments, and was doubled (tests 8 – 11) to observe clearer effects on the CV. The scan rates used were considered to be not too high to avoid missing any peaks (100 mV/s) and not too low to avoid the appearance of interfere peaks, for example, with reaction with air (10 mV/s). The acetic acid concentration was increase from 4 to 5 M to decrease the pH of the electrolyte. Moreover, compared to the first two experiments, this CV tests were performed under a shorten potential range, in order to better define the pretended peaks.

Table 4.10. Operating conditions of electrochemical experiment #3 to study the $B(OH)_3$ recycling back to $NaBH_4$, under 5 M acetic acid electrolyte.

Test	$B(OH)_3$ / M	Scan rate / mV/s
1	0.16	100
2	0.16	50
3	0.16	10
4	0.16	100
5	0.16	50
6	0.16	25
7	0.16	10
8	0.32	100
9	0.32	50
10	0.32	25
11	0.32	10

Figure 4.12 presents the CV curves obtained from each test. The formation of a reduction peak was observed in the]-0.7;-0.5[V range (test 1), that decreased its intensity with the decrease of the scan rate (tests 2 and 3). Repeating these tests in the XPOT module (tests 4 – 7), showed the formation of this peak again; however, at lower scan rates, it was slightly pushed to higher potential ranges, indicating a more precise potential for this reaction (lower scan rate, higher number of potentials analyzed). Observing again the boron electrochemical window in Figure 4.8, this can be a first indication of the $B(OH)_3$ reduction to BH_4^-, since this peak fits in the presented range. Moreover, two other peaks appear at]0.5;0.8[V, which were again pushed to higher potentials at lower scan rates. When the $B(OH)_3$ concentration was doubled, the same peaks and variations with the scan rates were detected, however with an increase of the potential at which the peaks are

formed. This can be better observed for the scan rate of 100 mV/s (tests 4 and 8). These peaks, however, could not be correlated to the literature.

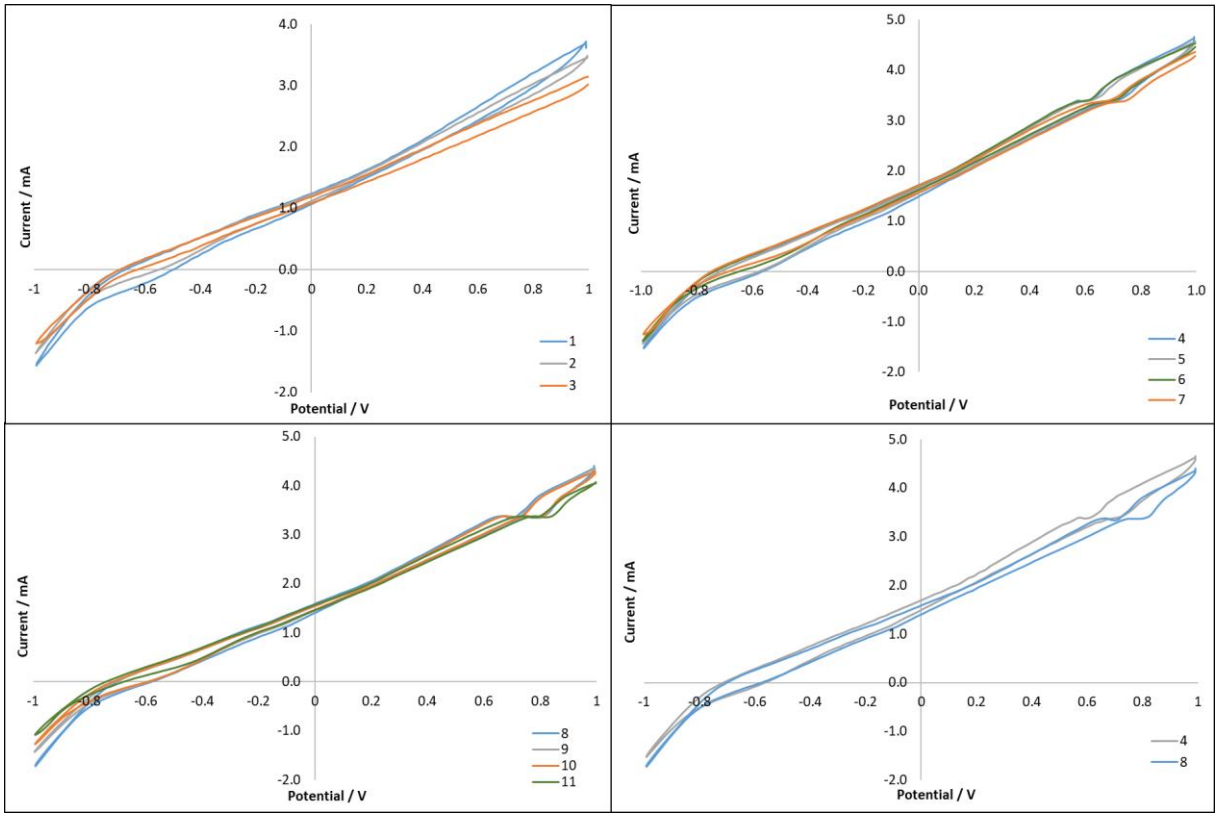


Figure 4.12. CV tests performed for 0.16 M (tests 1 – 7) and 0.32 M (tests 8 – 11) boric acid under 5 M acetic acid based on electrochemical experiment #3.

To replicate the potential $B(OH)_3$ reduction to BH_4^-, observed in experiment #3, the RE was introduced in experiment #4. Also, to avoid any air exposure interference in the electrolyte, tests were performed under N_2 bubbling for 8, 10 and 15 minutes. Table 4.11 gives the main features for the tests performed, where test 0 is the electrolyte CV test. While tests 1, 3 and 9 did not use N_2 bubbling, tests 7, 8, 13 and 14 were performed after the N_2 bubbling was turned off. Since most peaks were obtained for a scan rate of 100 mV/s, this was in general maintained in the experiment.

Table 4.11. Operating conditions of electrochemical experiment #4 to study the $B(OH)_3$ recycling back to $NaBH_4$ under 5 M acetic acid electrolyte.

Test	$B(OH)_3$ / M	Scan rate / mV/s	N_2 bubbling	Time / min
0	-	100	-	-
1	0.08	100	-	-
2	0.08	100	✓	10
3	0.20	100	-	-
4	0.20	100	✓	8
5	0.20	50	✓	15
6	0.20	100	✓	15
7	0.20	50	-	-
8	0.20	100	-	-
9	0.40	100	-	-
10	0.40	100	✓	8
11	0.40	50	✓	15
12	0.40	100	✓	15
13	0.40	50	-	-
14	0.40	100	-	-

Figures 4.13 to 4.15 present the results obtained for experiment #4. Test 0 is presented to discard any electrolyte parallel reactions. The effect of the N_2 bubbling was first introduced in test 2. Comparing with the results from test performed without it (Figure 4.14), a reduction was observed on the current throughout the curve, particularly on the potential ranges of]-0.5;-0.2[V and]0.3;0.6[V.

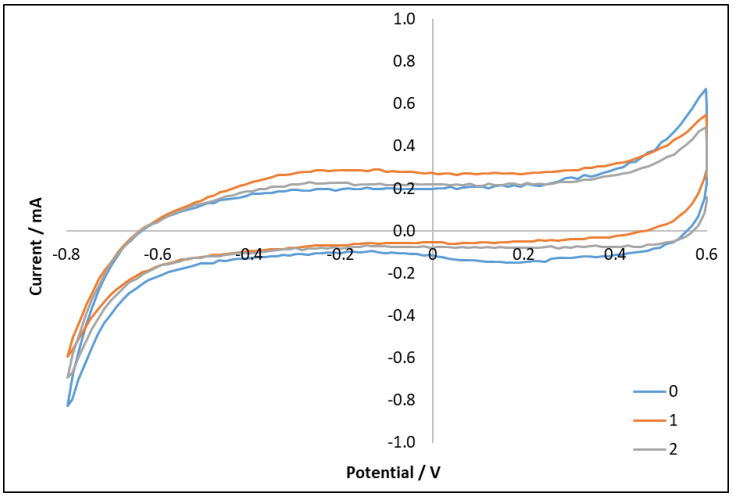


Figure 4.13. CV tests 0 – 2 performed for 0.2 M boric acid under 5 M acetic acid based on electrochemical experiment #4.

When the $B(OH)_3$ concentration was increased from 0.08 to 0.20 M (tests 3 – 8) (Figure 4.14), a similar trend was identified, with the possible formation of an oxidation peak at]-0.4;-0.2[V and maximum current at -0.3 V and the decrease of its intensity with the N_2 bubbling after 8 minutes. For the same concentration and a scan rate of 50 mV/s, no positive effect of the N_2 bubbling was observed, since the same peaks were formed with (test 7) and without it (test 5). With further increase of the $B(OH)_3$ concentration (tests 9 – 14), this peak is more defined with its maximum potential at -0.4 V as well as its disappearance with the N_2 bubbling after 8 minutes. Moreover, as opposed to 0.20 M $B(OH)_3$, when the N_2 bubbling was turned off after 15 minutes, the oxidation peak formed at -0.4 V decreased its intensity. Therefore, the effect of the N_2 bubbling in the experiment was not clearly identified as positive or negative and it can be affirmed that it introduced instability in the electrochemical cell. This can be explained since the intensive bubbling could have a opposite effect as the expected when considered, since it avoids air exposure but increases the interference between the electrodes and the electrolyte.

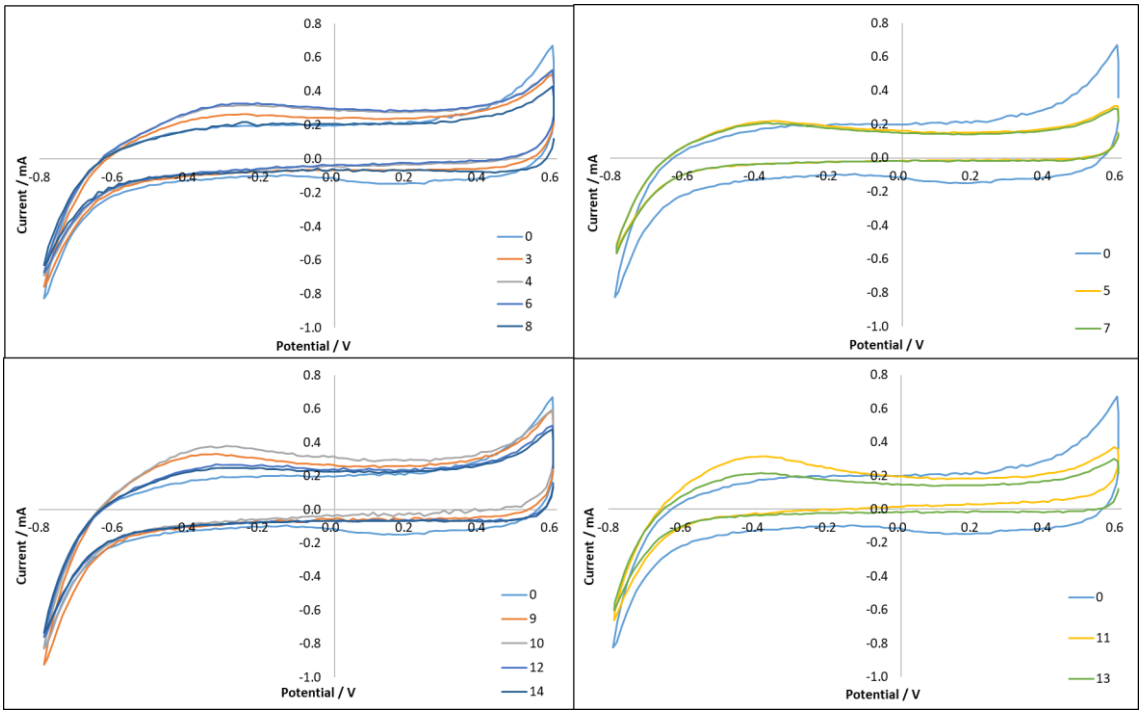


Figure 4.14. CV tests performed for 0.2 M (1 – 8) and 0.4 M (9 – 14) boric acid under 5 M acetic acid based on electrochemical experiment #4.

The influence of the $B(OH)_3$ concentration on its recycling back to $NaBH_4$ can be better observed in Figure 4.15, since it presents graphically a direct comparison between tests performed in the same conditions, while varying the $B(OH)_3$ concentration. Here, the formation of a peak is shown close to -0.4 V with the increase of the $B(OH)_3$

concentration from 0 (test 0) to 0.20 (test 3) to 0.40 (test 9), even when the N_2 bubbling is applied (tests 4, 5 and 6 vs tests 10, 11 and 12, respectively). This improvement almost disappears when the N_2 bubbling is stopped after 15 minutes (tests 7 and 8 vs tests 13 and 14, respectively). However, comparing these tests with the pre-N_2 bubbling, the peak at -0.4 V is less defined, particularly at a scan rate of 100 mV/s. Unfortunately, the reduction peak observed in experiment #3, at the range of the BH_4^- formation, could not be confirmed in the presence of the RE.

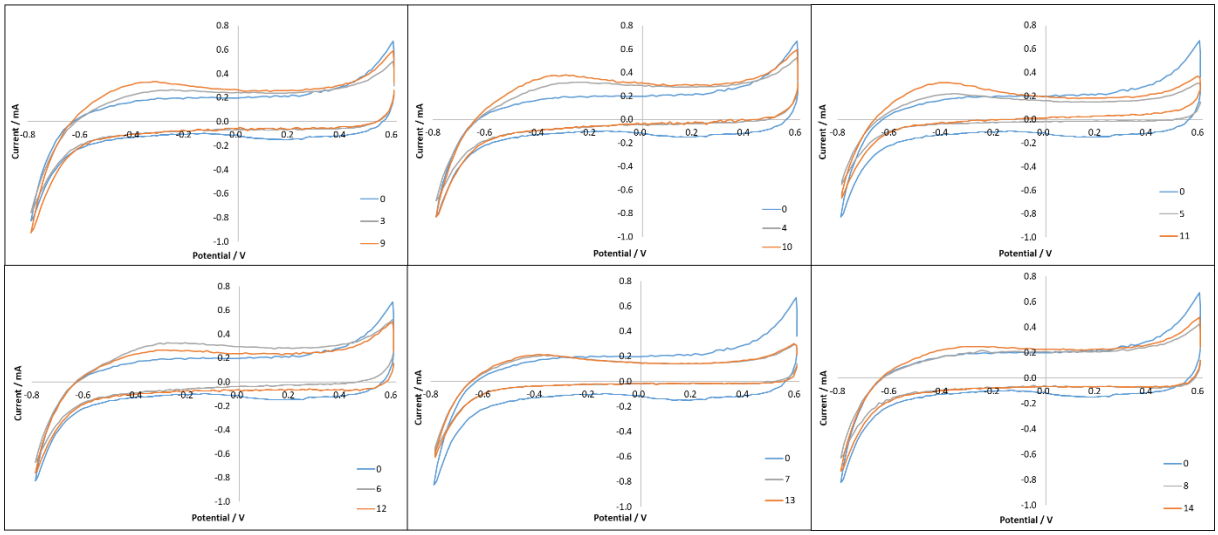


Figure 4.15. CV tests performed for 0.2 M (1 – 8) and 0.4 M boric acid (9 – 14) under 5 M acetic acid based on electrochemical experiment #4.

Similar tests were performed in experiment #5, however the N_2 bubbling was removed, since in experiment #4 it showed to not have a clear positive effect in the electrochemical cell. Moreover, a wider potential range was studied. Table 4.12 presents the main operating conditions for the tests performed. Assays 0/1 and 6 considered the blank and acetic acid 5 M electrolyte studied, respectively.

Table 4.12. Operating conditions of electrochemical experiment #5 to study the $B(OH)_3$ recycling back to $NaBH_4$.

Test	H_2O	Acetic Acid	$B(OH)_3$ / M
0	✓	-	-
1	✓	✓	-
2	✓	✓	0.16
3	✓	✓	0.16
4	✓	✓	0.32
5	✓	✓	0.32
6	✓	✓	-
7	✓	✓	0.48
8	✓	✓	0.48

Figure 4.16 present the curves obtained in the experiment. Although the N_2 bubbling was not used, considering its negative effect observed in experiment #4, the reduction peak that possibly indicated the BH_4^- formation was not observed in this experiment, neither any other oxidation nor reduction peak. It can indicate that the absence of a physical RE and the use of the theoretical one of the electrochemical workstation was misleading. Nevertheless, with 0.16 M $B(OH)_3$, we observe a significant increase of the current at -1.1 V, associated to the HER, i.e., in which at lower potentials the electrolyte starts to react. However, it decreases again with 0.32 M $B(OH)_3$. Moreover, when the potential range studied is reduced to -1.0 to 1.0 V, the use of 0.48 M $B(OH)_3$ has the same effect of the 0.16 M $B(OH)_3$ on -1.2 to 1.2 V. From these results, we can say that the $B(OH)_3$ has a positive effect on the BDD electrode, since it widens its electrochemical window, however optimal concentration must be found for each potential range considered.

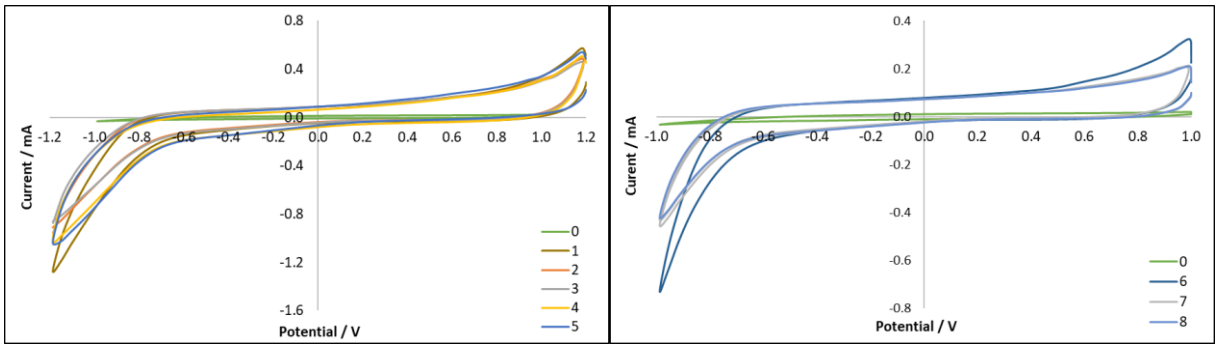


Figure 4.16. CV tests performed for 0.16 M (2 and 3), 0.32 M (4 and 5) and 0.48 M boric acid (7 and 8) under 5 M acetic acid based on electrochemical experiment #5.

Given the low expected results with acetic acid as electrolyte, experiment #6 considered at last the use of a stronger acid (sulfuric acid) and the CV analysis was performed with Ti, Ni, and their RuO_2 and IrO_2 coatings as CE. However, due the use of a low pH, the $B(OH)_3$ concentration was reduced. For each CE, tests were executed with 0.03 and 0.06 M $B(OH)_3$, to understand its effect on the BDD electrode with the different CEs used. Also, tests were performed for a potential range of]-1.0;1.0[V and]-0.8;0.8[V. Table 4.13 displays the operating conditions for the different tests.

Table 4.13. Operating conditions of electrochemical experiment #6 to study the $B(OH)_3$ recycling back to $NaBH_4$.

Test	CE	$B(OH)_3$ / M
1 - 2	Ti	-
3 - 4	Ti	0.03
5 - 6	Ti	0.06
7	Ni	-
8 - 9	Ni	0.03
10 - 11	Ni	0.06
12 – 13	RuO_2 coated Ti	-
13 – 15	RuO_2 coated Ti	0.03
16 - 17	RuO_2 coated Ti	0.06
18 - 19	IrO_2 coated Ti	-
20 - 21	IrO_2 coated Ti	0.03
22 - 23	IrO_2 coated Ti	0.06

The first tests were performed with the Ti CE, as used in the previous experiments. Figure 4.17 presents the curves obtained. Similar to experiment #5, the decrease in the current drop is lower with the increase of the $B(OH)_3$ concentration, indicating possible HER mitigation. However, this effect is only significant from 0.03 to 0.06 M $B(OH)_3$ added to the electrolyte.

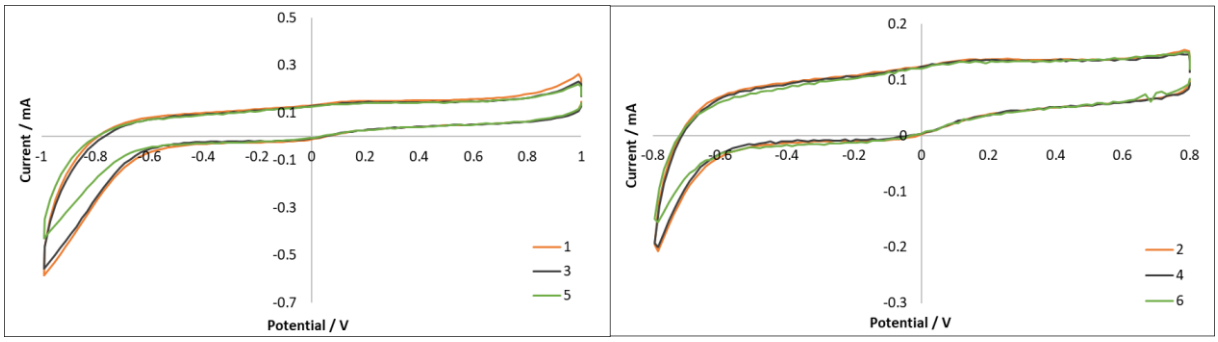


Figure 4.17. CV tests performed for 0.03 M (3 and 4) and 0.06 M boric acid (5 and 6) under 5 M sulfuric acid based on electrochemical experiment #6, considering a Ti CE.

Then, Ni CE was used in the CV and the results are presented in the plot of Figure 4.18. Now, contrary to the Ti CE, the addition of 0.03 M $B(OH)_3$ add the highest influence on the HER and its mitigation, while an increase on the current was visible throughout the curves in the presence of this borate.

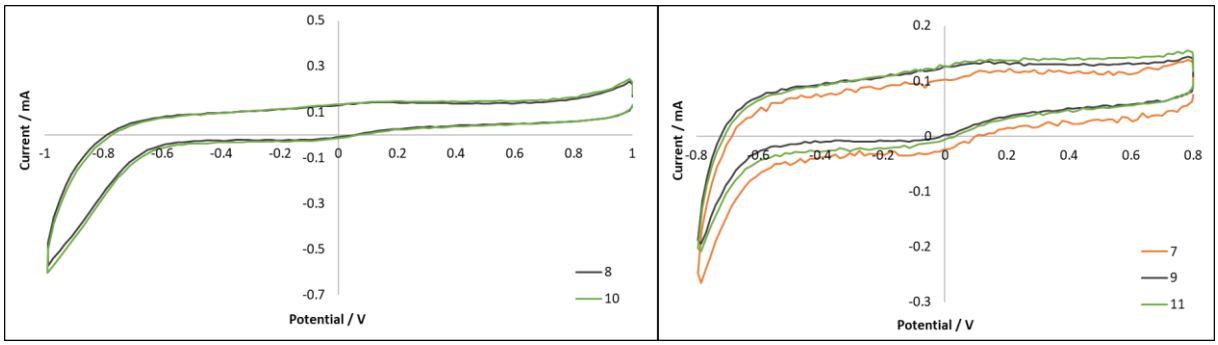


Figure 4.18. CV tests performed for 0.03 M (8 and 9) and 0.06 M boric acid (10 and 11) under 5 M sulfuric acid based on electrochemical experiment #6, considering a Ni CE.

Figure 4.19 presents the CV tests using the RuO_2 coated Ti CE. Similar to those involving Ti CE, the addition of 0.03 M $B(OH)_3$ did not have a significant impact on the curve (particularly on the]-0.8;0.8[V potential range.

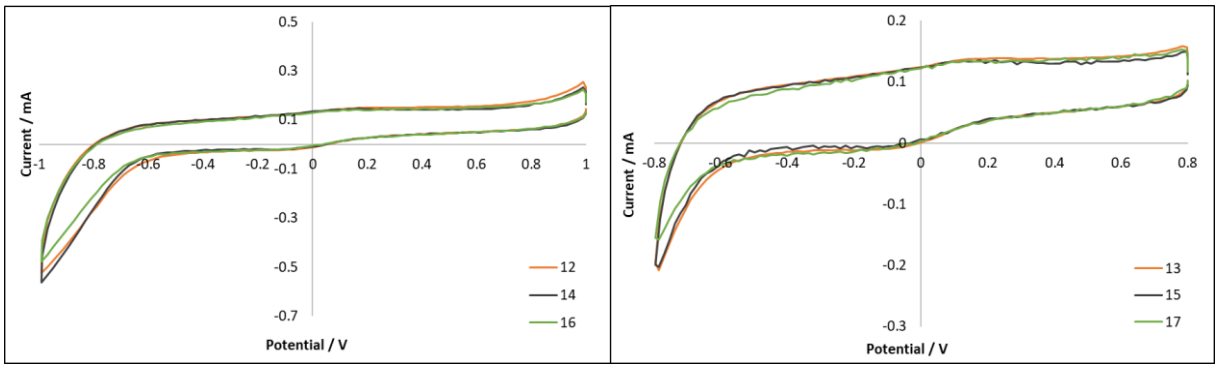


Figure 4.19. CV tests performed for 0.03 M (13 - 15) and 0.06 M boric acid (16 and 17) under 5 M sulfuric acid based on electrochemical experiment #6, considering a RuO_2 coated Ti CE.

Finally, the same can be said from the IrO_2 coated Ti CE, as evident by the curves in Figure 4.20. This confirms that the $B(OH)_3$ had a significant impact on the BDD electrochemical window for an acidic aqueous electrolyte. Yet, no peaks were observed in these experiments, which indicates no BH_4^- or other compounds are formed under these conditions.

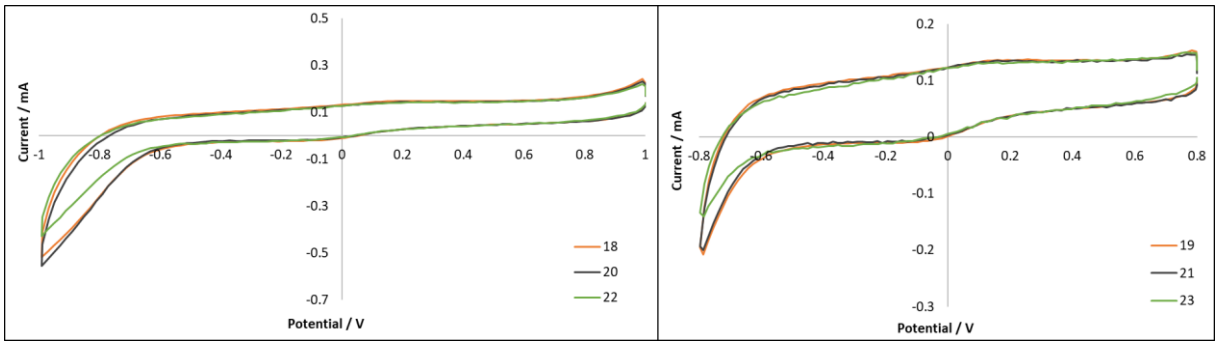


Figure 4.20. CV tests performed for 0.03 M (20 and 21) and 0.06 M boric acid (22 and 23) under 5 M sulfuric acid based on electrochemical experiment #6, considering a IrO_2 coated Ti CE.

To summarize, this subchapter describes an electrochemical method to recycle $B(OH)_3$ back to $NaBH_4$ was performed, as far as the author is aware, for the first time (no similar work was found in literature). This boron compound was considered since it can be obtained from the acidic hydrolysis of $NaBH_4$ and that the electrochemical processes are considered to be the best cost-efficient method to regenerate this borohydride and $NaBO_2$ still presents major obstacles to its efficient recycling due to the need to operate the electrochemical reduction of $NaBO_2$ in alkaline electrolytes, favoring parasite reactions such as the HER and oxygen related ones. No hydrated $NaBO_2$ was studied using this type of processes (neither $NaB(OH)_4$ - obtained pure through the innovative post-treatment process developed in Chapter 3), however, same difficulties or higher ones are expected since the electrolyte is the same. Moreover, with efficient $B(OH)_3$ recycling (which requires an acidic electrolyte), a system integrating the hydrolysis and regeneration of $NaBH_4$ in the same device could be of major relevance for this technology. Therefore, an electrochemical cell was mounted and CV experiments were performed to optimize the conditions of this process, particularly the acidic electrolyte and the electrodes used. Acetic and sulfuric aqueous solutions were used as electrolyte and a BDD was used as WE, with varying auxiliary electrodes. A reduction peak around the]-0.5;0.8[V range was observed, indicating possible formation of BH_4^-. However, it was observed with no physical RE (only a theoretical one used by the electrochemical

workstation) and, when a physical RE was implemented in the cell, the same peak was not detected. Moreover, N_2 bubbling was considered but it did not demonstrate to have a clear positive impact on the experiments. At last, it was found that the boric acid has a positive impact on the BDD electrochemical window for an acidic aqueous electrolyte, by mitigating the HER reaction.

4.3. Conclusions

The regeneration of the sodium borohydride from its by-product was studied to close the $NaBH_4$-H_2 cycle. Two methods were considered. The mechano-chemical recycling of $NaB(OH)_4$ – by-product obtained pure or close to pure in the innovative post-process studied in Chapter 3 – was performed. Experiments were performed with this borate pure and mixed with other compounds. No $NaBH_4$ was detected in the XRD analysis of the experiments; however the detected presence of $Mg(OH)_2$ – an intermediate in the process – indicates that part of the borates was converted as expected. Moreover, when the ball milling conditions (excess of MgH_2, time of milling and BPR) were changed in order to promote the reaction, no $NaBH_4$ was formed which indicates that it is essential to replicate the experiments in a ball miller with grinding jars with higher internal volume to promote the movement of the grinding balls inside the jar. Moreover, it is worthy to consider the study of other reducers such as Mg, Mg_2Si and LiH, to replace the low commercial availability of MgH_2. The electrochemical regeneration of $NaBH_4$ was also studied. An electrochemical cell was mounted for the study and CV experiments of the $B(OH)_3$ reduction were performed for the first time. A reduction peak was observed, indicating possible formation of BH_4^-. However, when a physical RE (with and without using N_2 bubbling to remove the presence of air) was implemented in the cell, the same peak was not again detected. At last, it was found that this borate has a positive effect on the BDD WE by mitigating the HER reaction and widening its electrochemical window. Nevertheless, these results are a first indication of the possible electrochemical regeneration of $NaBH_4$ and it is essential to optimization the electrolyte conditions as well as the electrodes used, including the built electrochemical cell, to reduce at minimum outside interferences as well as parasite reactions that difficults the $NaBH_4$ formation.

5. $NaBH_4$-H_2 Economic analysis

The 2007 DOE's no-go recommendation was based on the low H_2 storage targets for on-board vehicles; in part, this was due to the overall system weight and the cost of the $NaBH_4$. With that in mind, after major developments have been reported, including the innovative post-treatment of the by-product of $NaBH_4$'s hydrolysis developed during this work, described in Chapter 3, an economic analysis should be performed considering the up-to-date costs and the $NaBH_4$ recycling methods reported in the literature. This performed analysis is described in this chapter, has not yet been reported in literature and will be prepared as a publication in the near future.

5.1. Analysis procedure and general considerations

The aim of this analysis is to acquire knowledge of the most promising $NaBH_4$ regeneration type of process and what method is the best cost-effective for the recycling. Additionally, a cost comparison of H_2 generation by its hydrolysis with the current H_2 production technologies is also attempted.

With that in mind, it is important to note that this economic analysis was performed only considering the mass balance of the hydrolysis and each recycling method separately. It does not consider energy balances and equipment costs, therefore the costs presented in this analysis were calculated by default. However, regarding the equipment costs and considering the hydrolysis reactor as the most costly equipment of the integrated process, it is important to refer that the same equipment can be considered for all the considered methods, so it only affects the comparison with other H_2 technologies. Also, the end use (recycling or any commercial end use) of the by-products of each recycling method (for example, MgO, Si, Al and unreacted borate) was not considered in this analysis, except for $NaBH_4$ and H_2, which had a direct impact on the costs presented in this study.

Table 5.1 presents the methods considered for this sensitive analysis and the corresponding highest efficiency reported. These are the methods reported in chapter 2 – State of the art, for $NaBO_2$ and the main by-product borates ($NaB(OH)_4$ and $NaB(OH)_4 \cdot 2H_2O$) obtained in chapter 3. Other methods were not here considered due to their low efficiency (for example, B_2O_3), demonstrated difficulty for their production as by-product of the $NaBH_4$ hydrolysis ($Na_2B_4O_7$) and lack of information (for example,

the electrochemical regeneration of $NaBH_4$ from $B(OH)_3$, studied in Chapter 4). On the table, "Ti", "Mi" and "Ei" designations refer to thermochemical, mechanochemical and electrochemical methods, respectively, while "i" is the designation of each method in each type of process.

Table 5.1. Methods considered for the $NaBH_4$-H_2 economic analysis (legend: T – thermochemical, M – mechanochemical, E – electrochemical).

Method	Reaction	Efficiency / %	Ref
T1	$NaBO_2 + 2Mg + 2H_2 \rightarrow NaBH_4 + 2MgO$	69.0	[138]
T2	$NaBO_2 + 2MgH_2 \rightarrow NaBH_4 + 2MgO$	97.0	[73]
T3	$NaBO_2 + Mg_2Si + 2H_2 \rightarrow NaBH_4 + 2MgO + Si$	98.0	[73]
M1	$NaBO_2 + 2Mg + 2H_2 \rightarrow NaBH_4 + 2MgO$	67.7	[139]
M2	$NaB(OH)_4 + 2Mg_2Si \rightarrow NaBH_4 + 4MgO + 2Si$	78.0	[105]
M3	$NaBO_2 + 2MgH_2 \rightarrow NaBH_4 + 2MgO$	89.0	[101]
M4	$NaB(OH)_4 + 4MgH_2 \rightarrow NaBH_4 + 4MgO + 4H_2$	89.8	[104]
M5	$NaB(OH)_4 \bullet 2H_2O + 6MgH_2 \rightarrow NaBH_4 + 6MgO + 8H_2$	88.3	[104]
M6	$NaBO_2 + 4NaH + 2SiO_2 \rightarrow NaBH_4 + 2Na_2SiO_3$	32.0	[139]
M7	$NaB(OH)_4 + 1/5Mg_{17}Al_{12} \rightarrow NaBH_4 + 16/5MgO + 1/5MgAl_2O_4 + 2Al$	57.0	[107]
E1	$NaBO_2 + 2H_2O \rightarrow NaBH_4 + 2O_2$	97.0	[127]

Some considerations were assumed for this analysis. First, the prices considered for the products and reactants were the lower ones available in the market worldwide for any quantity available and its cost converted to 1 kg, for example, 20 kg of a compound costing 20 €, was assumed to be the same as 1 € for 1 kg of that compound. Therefore, shipping costs were not included. Also, for the $NaBO_2$ and its hydrated forms, the main commercial hydrated form is $NaB(OH)_4 \bullet 2H_2O$, however prices were found for $NaBO_2$ and $NaB(OH)_4$ outside Europe. Moreover, all prices in American dollars were converted to euro considering a conversion of 0.94 euro for each dollar. These prices are included in Table 5.2. The most recent update was in December 2022, therefore most prices are for that date. In some cases, the prices are from earlier dates, due to unaltered lower price. Moreover, it is important to note the difficulty to obtain commercial MgH_2

and $Mg_{17}Al_{12}$ due to the restricted offer available. In fact, these compounds are not commercially available in Europe, as far as the author could observe.

Table 5.2. Lower market price of compounds considered in the hydrolysis/regeneration of $NaBH_4$.

Compound	Price / €/kg	Supplier	Country	Date
NaBH4	9.40	ChemFine International Co.	China (CH)	Oct 2022
H_2O	0.20	Continente, 6116193	Portugal (PT)	Dez 2022
NaOH	11.50	Sigma-Aldrich, 1064679050	Europe (EU)	Dez 2022
$NaBO_2$	9.40	Zhuozhou Wenxi import and Export Co., Ltd	China (CH)	Oct 2022
$NaB(OH)_4$	502.50*	American Custom Chemicals Corporation, BOR0005516	USA	Dec 2021
$NaB(OH)_4 \bullet 2H_2O$	49.85	Alfa Aesar, 036736	United Kingdom (UK)	Dec 2022
Mg	36.80	Sigma-Aldrich, 8.45042	Europe (EU)	Dez 2022
MgH_2	0.94	Wuhan Wingroup Pharmaceutical Co., Ltd	China (CH)	Dez 2019
Mg_2Si	2,726.00	Strem Chemicals, Magnesium silicide (99.5% Mg), 93-1293	France (FR)	Dez 2021
NaH	269.78	Sigma-Aldrich, 452912	Europe (EU)	Dez 2022
SiO_2	24.19	Sigma-Aldrich, 84880	Europe (EU)	Dez 2022
$Mg_{17}Al_{12}$	0.94	Wuhan Wingroup Pharmaceutical Co., Ltd	China (CH)	Dez 2019
MgO	87.61	Sigma-Aldrich, 220361	Europe (EU)	Dez 2022
Si	148.52	Strem Chemicals, 93-1495	France (FR)	Dez 2022
Na_2SiO_3	30.91	Sigma-Aldrich, 1.05621	Europe (EU)	Dez 2022
$MgAl_2O_4$	313.96	Alfa Aesar, 022950	United Kingdom (UK)	Dez 2021
Al	41.36	Alfa Aesar, 010093	United Kingdom (UK)	Dez 2021
C_3H_9N	39.81	Alfa Aesar, A15044	United Kingdom (UK)	Dez 2022

*price for 5 mg

The second consideration is that all cost analysis were based on 1 kg H_2, based on three $NaBH_4$ aqueous solutions with concentrations of 10, 13 and 20 wt. % and each solution containing 1 wt. % NaOH. Moreover, the hydrolysis of $NaBH_4$ typically requires a catalyst but its cost has not been considered, since many catalysts are used in this reaction (please recall Chapter 2) with significant cost variation. An H_2 yield of 100 % was considered for the hydrolysis of sodium borohydride, since it was obtained in some experiments of this work (please recall Chapter 3) as well as for the borohydride extraction (which considered the solvent isopropylamine, most reported and used in this work) in the thermo- and mechanochemical processes, due to lack of information in literature. The economic analysis is presented for each value of $NaBH_4$ concentration and together with a cost comparison with other H_2 technologies.

5.2. Results and discussion

The first analysis was performed for the hydrolysis of sodium borohydride. Table 5.3 presents the main results for the H_2 generation through this reaction for each $NaBH_4$ concentration: total mass of solution required to obtain 1 kg H_2, the weight of the $NaBH_4$ cost on the total reactants ($NaBH_4$, H_2O and NaOH) cost required for the H_2 production and the H_2 generation cost, calculated dividing the cost of reactants by the higher heating value (HHV) of H_2 (HHV of H_2 = 141.88 MJ/kg [140]), in €/kWh, to allow direct comparison with other H_2 generation technologies costs (further in this chapter). The values displayed in the table show that the increase of $NaBH_4$ concentration, increases its weight on the total reactants cost but decreases the H_2 generation cost while also reducing the mass of solution required.

Table 5.3. influence of the $NaBH_4$ concentration on the 1 kg H_2 generation cost through the hydrolysis of $NaBH_4$.

$NaBH_4$ Wt. / %	**Mass of solution / kg**	**$NaBH_4$ cost / %**	**H_2 generation cost / €/kWh**
10	46.8	76.4	1.5
13	36.0	81.1	1.4
20	23.4	87.4	1.3

Considering now the analysis of the $NaBH_4$ regeneration, Figure 5.1 presents the cost to regenerate the borohydride in each studied method. It is calculated dividing the cost of the reactants (considering the mass of $NaB(OH)_4$ formed to generate 1 kg of H_2) by the mass of $NaBH_4$ regenerated. The cost of commercial $NaBH_4$ is also presented in the

figure. As predicted by the DOE and its no-go recommendation on this H_2 production source, the electrochemical is the best cost-effective regeneration type of process. It is also possible to observe an average cost of the thermochemical methods similar to the mechanochemical ones, except in what concerns T3 and M2 with much higher costs due to the abnormally high cost of Mg_2Si. Yet, the main conclusion from this figure, is that, considering the lower cost of commercial $NaBH_4$, it is more expensive to regenerate $NaBH_4$ from these methods, than to buy new $NaBH_4$.

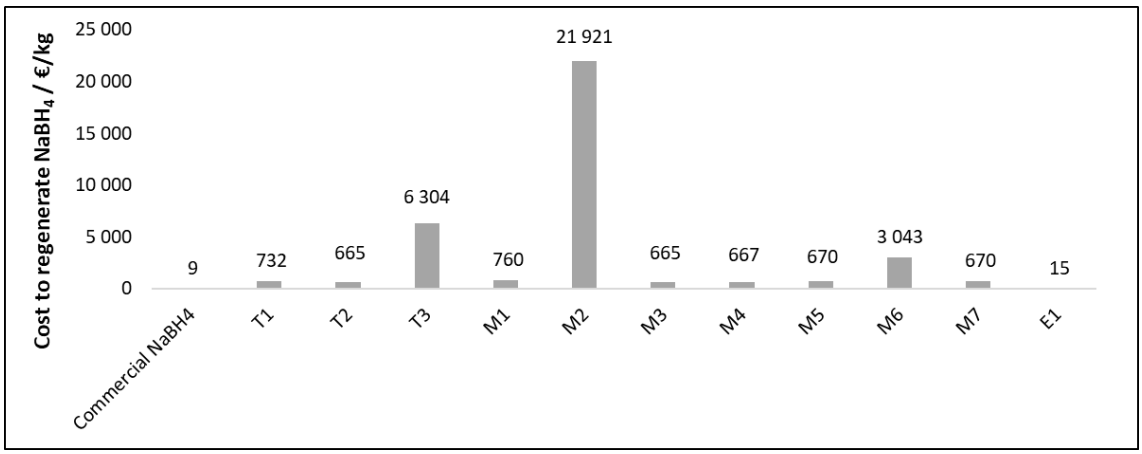


Figure 5.1. Cost to regenerate $NaBH_4$ for the different thermo- (T), mechano- (M) and electrochemical (E) processes.

To further explore the cost analysis, the maximum number of $NaBH_4/H_2$ cycles was considered using the same initial mass of $NaBH_4$, i.e., without adding new borohydride to the system and regenerating it through the same recycling process. It can be then expected that the cost to generate H_2 will significantly drop. The maximum number of cycles was reached when only 10 % of the initial mass $NaBH_4$ was available (after regenerating it in the last cycle) for a new hydrolysis step (although the hydrolysis was assumed to have an efficiency of 100 %, the higher efficiency reported in literature for each recycling method is lower than 100 %, therefore the mass of $NaBH_4$ regenerated is always lower than the mass used in the previous hydrolysis reaction). The result of this analysis was performed for all thermochemical and electrochemical methods while the best cost-effective mechanochemical methods for each by-product (M1, M4 and M5) were also considered. The positive impact of considering several cycles of using the regenerated $NaBH_4$ on the cost to generate H_2 is represented in Figure 5.2. As before, the cost values were calculated dividing the cost of reactants by the mass of H_2 produced in all cycles and converted to €/kWh (HHV = 141.88 MJ/kg).

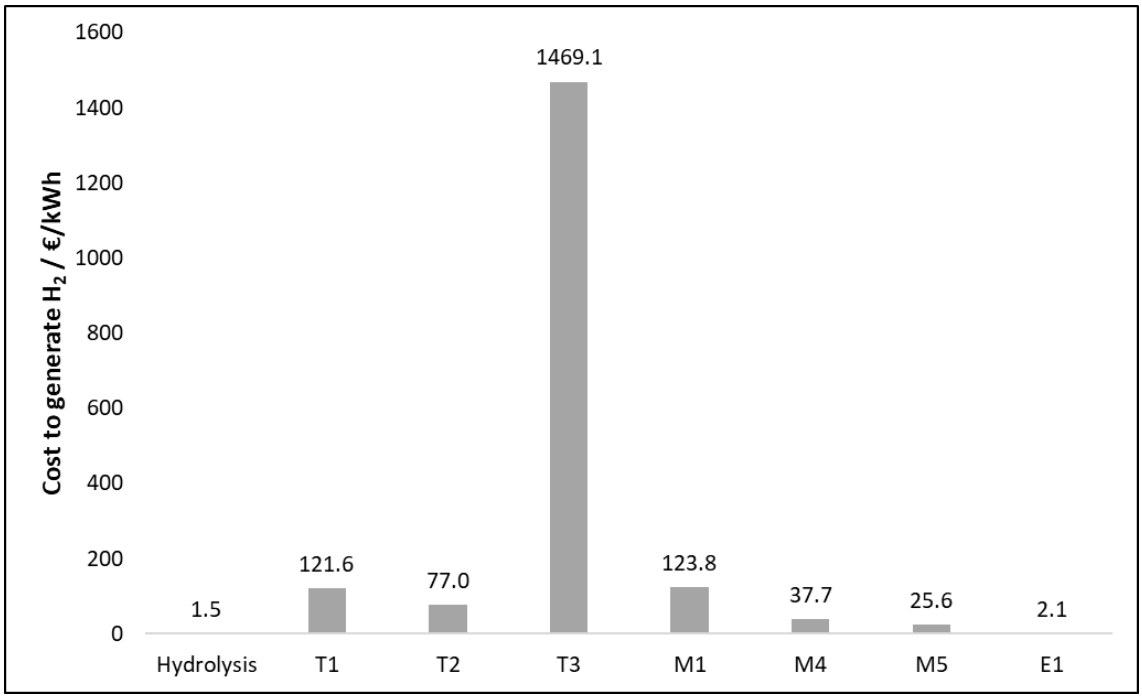


Figure 5.2. Cost to generate H_2 considering a 10 % $NaBH_4$ hydrolysis for the different thermo- (T), mechano- (M) and electrochemical (E) processes.

In spite of being significantly lower than in the previous analysis (Figure 5.1), all the regeneration methods back to borohydride are more expensive than the hydrolysis itself and only the electrochemical recycling of $NaBO_2$ (E1) is comparable to the hydrolysis H_2 generation costs. This can be, in fact, explained by the need to extract the borohydride in the thermo- and mechano-chemical methods. Figure 5.3 shows the impact of the extraction on the thermo- and mechanochemical methods. It is now evident, except for T3, that these regeneration methods become much more competitive, particularly T2, M4 and M5. In fact, their cost is lower than the electrochemical E1 and hydrolysis only. Also, these costs are lower than the cost to generate H_2 through a single hydrolysis (1.5 €/kWh), i.e., if no extraction was needed for these thermo- and mechano-chemical processes (T2, M4 and M5), it would be cheaper to perform a new hydrolysis with regenerated $NaBH_4$ than to use commercial $NaBH_4$.

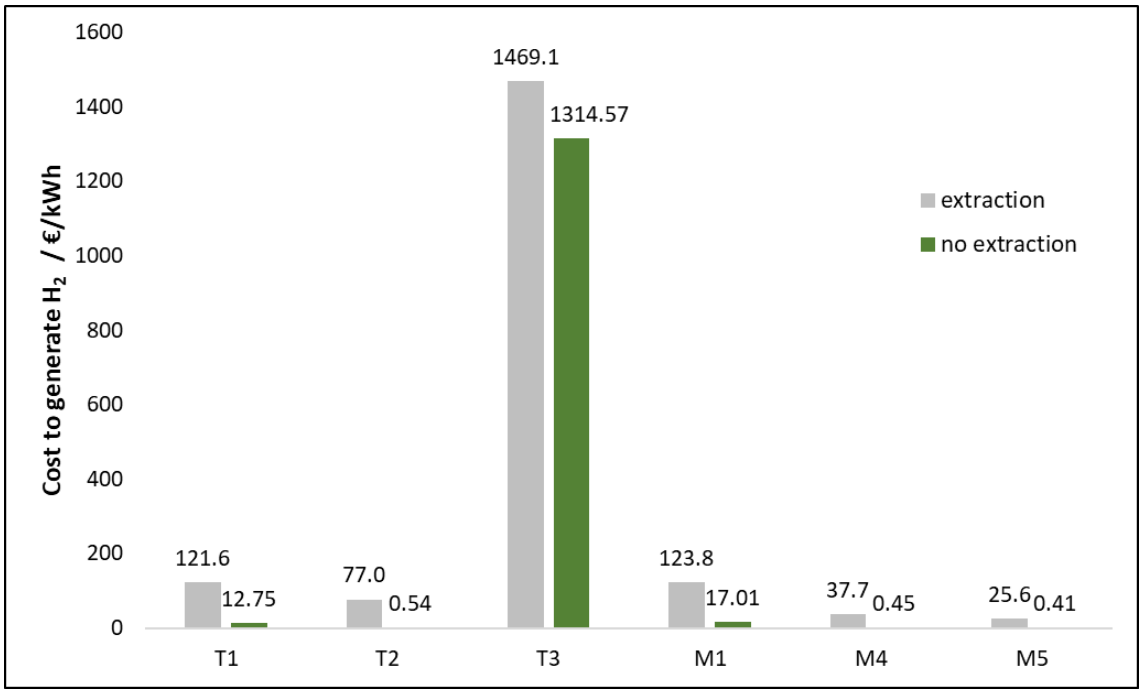


Figure 5.3. Cost to generate H_2, with and without (green bars) extraction of $NaBH_4$ considering a 10 % $NaBH_4$ hydrolysis for the different thermo- (T), mechano- (M) and electrochemical (E) processes.

Figure 5.4 presents the same approach for higher $NaBH_4$ concentrations (13 and 20 wt. % $NaBH_4$ hydrolysis). It is evident from the figure that no significant variations in the cost is observed with the increase of the $NaBH_4$ concentration (the highest difference between the same methods is 2 % - T2). This is explained by the low impact of the hydrolysis step on the $NaBH_4/H_2$ cycle costs.

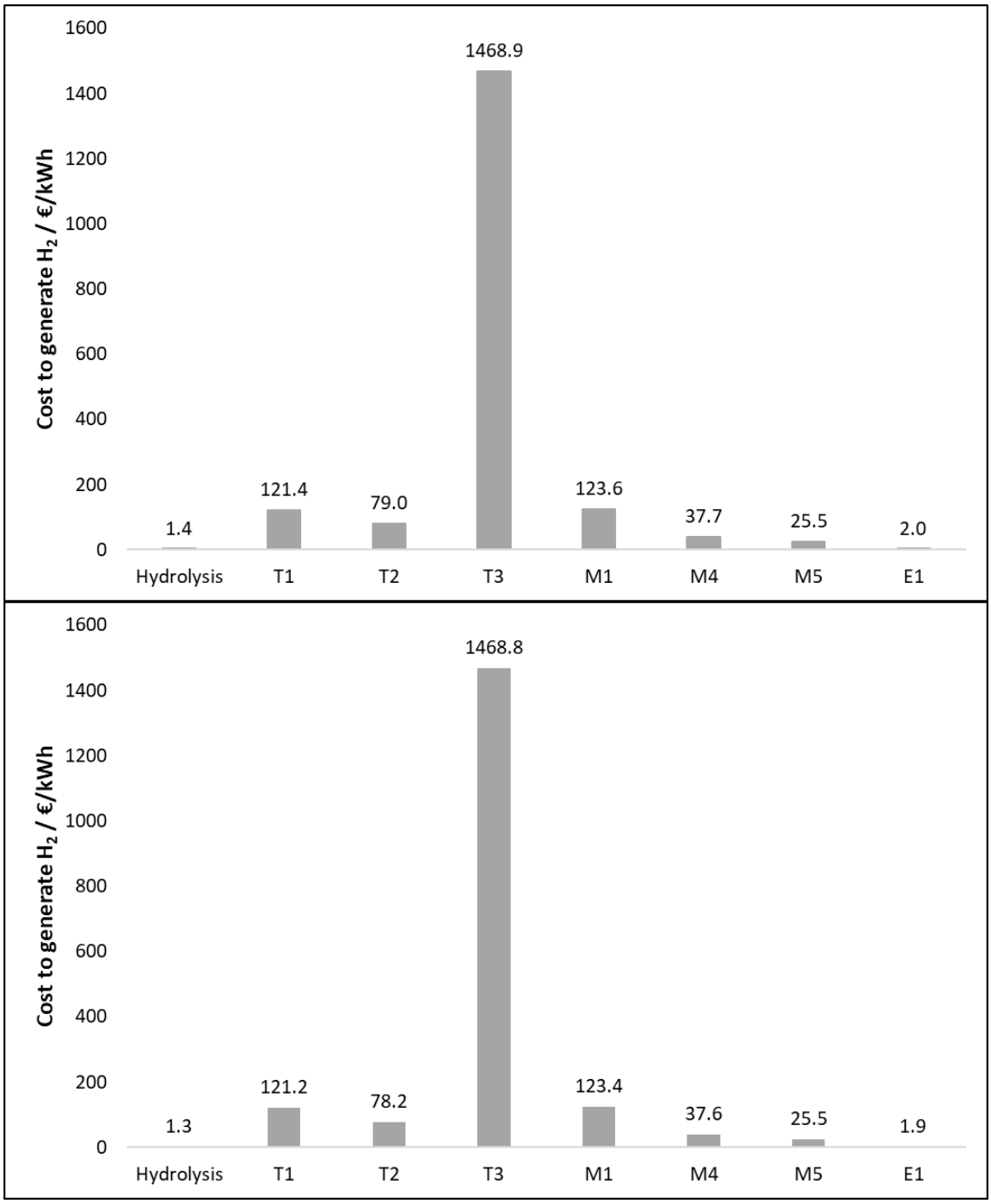


Figure 5.4. Cost to generate H_2 for: 13 % (up) and 20 % (down) $NaBH_4$ hydrolysis for the different thermo- (T), mechano- (M) and electrochemical (E) processes.

When the influence of the extraction of $NaBH_4$ is considered, as shown in Figure 5.5, significant impacts are once again found on costs. Moreover, although a decrease on the costs is observed for methods T2, M4 and M5 with the $NaBH_4$ concentration increase from 10 % to 20 %, this reduction is not significant. However, with the increase of the $NaBH_4$ concentration, it becomes even more visible the difference between the cost to

generate H_2 through regenerated and commercial $NaBH_4$ (although the differences are not significant, the increase of $NaBH_4$, decreases the cost to generate H_2).

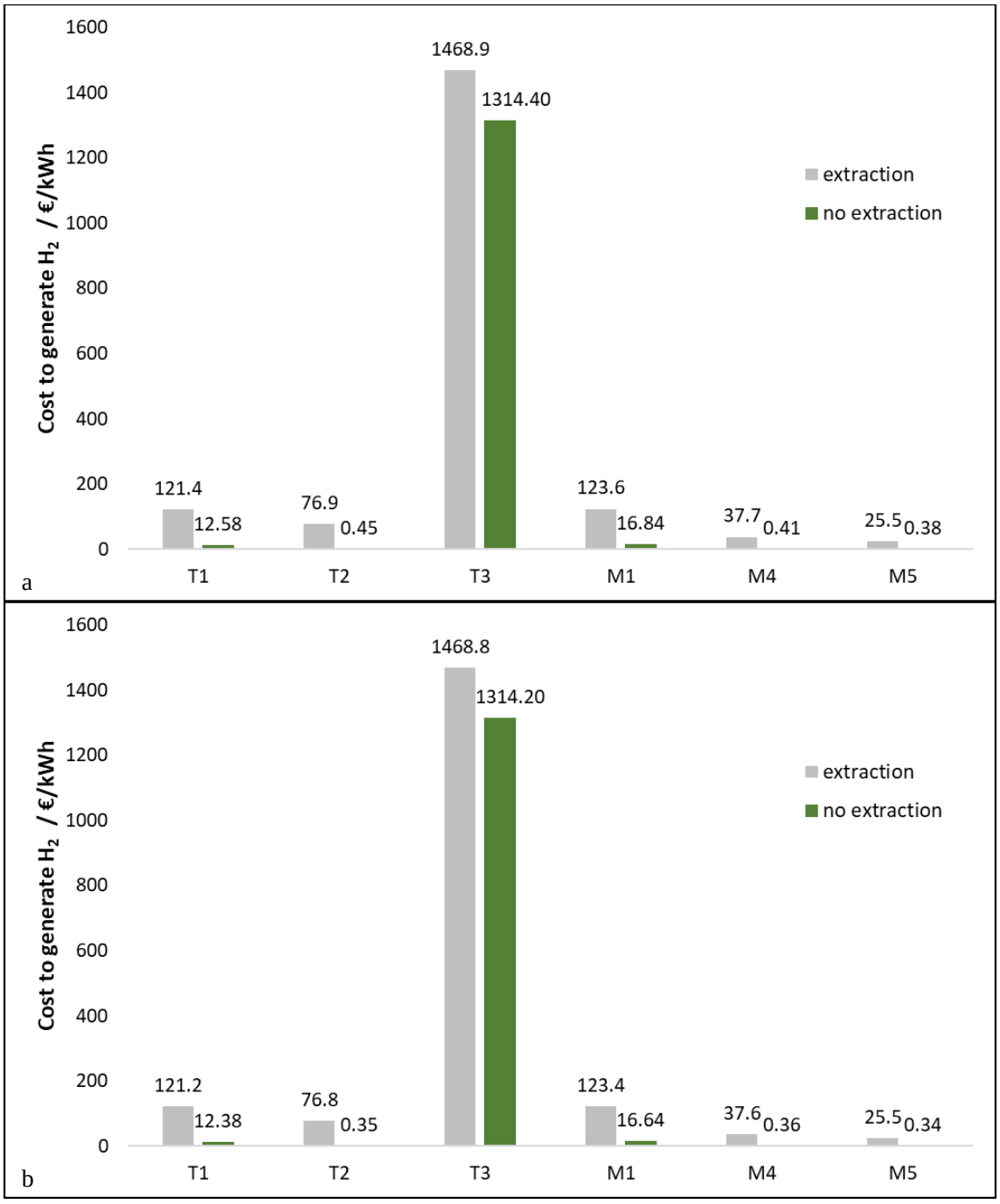


Figure 5.5. Cost to generate H_2, with and without (green bars) extraction of $NaBH_4$ for 13 % (a) and 20 % (b) $NaBH_4$ hydrolysis for the different thermo- (T), mechano- (M) and electrochemical (E) processes.

To better understand the impact of alternative solvents in the extraction costs, it was decided to choose the mechano-chemical process designed as M4 to further analysis. This process was chosen based on the by-product it recycles - $NaB(OH)_4$. However, given the short availability of MgH_2 worldwide, Mg was considered as an alternative. Since MgH_2

decomposes in Mg and H_2 as initial step of the ball milling, and H_2 is formed as by-product of the reaction, the efficiency of the process was considered the same as of the M4 process, as well as the same conditions that allowed the $NaBH_4$ regeneration. Nevertheless, the cost of Mg is significantly higher than MgH_2, as observed in Table 5.2.

To add to this analysis, a comparison between the lowest $NaBH_4$ cost (found in China CH, Table 5.2) and the lowest cost in the European Union EU (136.00 €/kg, Strem Chemicals, Sodium borohydride, 11-1121) was performed. Figure 5.6 presents the cost to regenerate $NaBH_4$ using this mechano-chemical process for different alternative solvents. The regeneration cost is presented considering the extraction with solvents isopropylamine, ethylamine (37.81 €/kg, Sigma-Aldrich, 471208, 66.0-72.0% in H_2O), ethylenediamine (29.28 €/kg, *ReagentPlus*®, E26266 ≥99%) and methylamine (20.21 €/kg, Sigma-Aldrich, 8.22091, 40 % solution in water for synthesis). These alternatives were considered, given the high capacity of amines to dissolve $NaBH_4$. It is noteworthy that, although they are less expensive, only ethylenediamine has been reported as a $NaBH_4$ extraction solvent. Therefore, for simplification and due to lack of information, this analysis considered 100 % efficiency for the $NaBH_4$ extraction with all solvents. EU and CH commercial $NaBH_4$ are presented for comparison.

It is evident from Figure 5.6, that the cost to regenerate $NaBH_4$ from its by-product using this method is always higher than commercial $NaBH_4$ except if no extraction is performed (when compared to EU commercial $NaBH_4$). It is more expensive to regenerate $NaBH_4$ with this method, than to buy new $NaBH_4$.

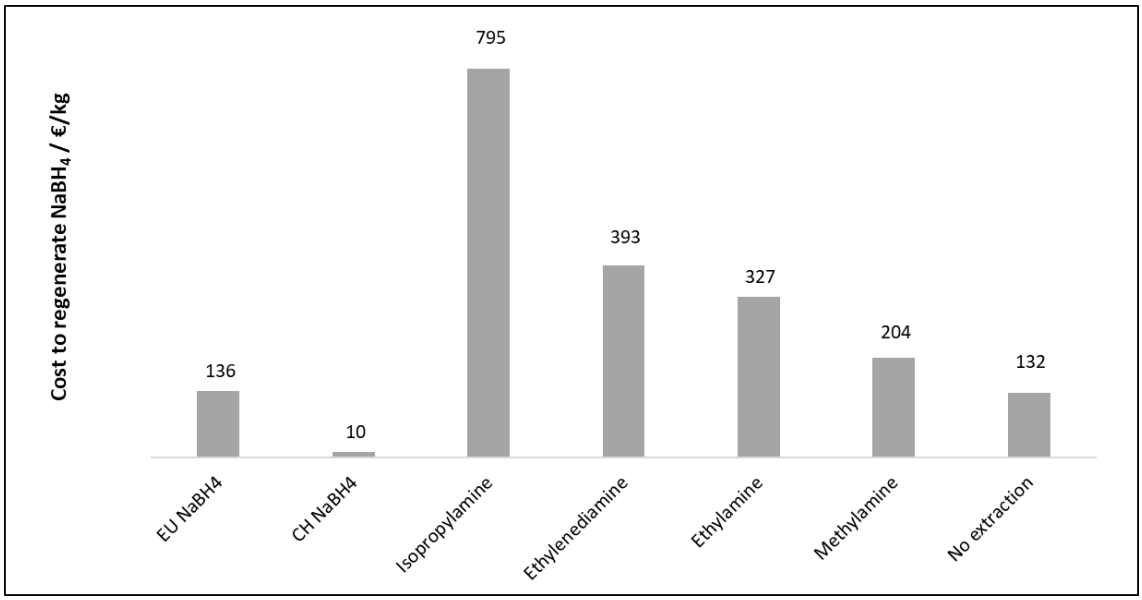


Figure 5.6. Cost to regenerate $NaBH_4$ using M4 method with different extraction solvents.

As before, the positive impact of considering several cycles of using the regenerated $NaBH_4$ on H_2 generation costs is presented in Figure 5.7. In spite of the cost decrease, the regeneration process is still significantly high for all the alternative solvents. However, considering the shipping costs of $NaBH_4$, the gap between the two commercial prices is expected to be shortened. Also, the higher $NaBH_4$ price (EU) has no significant impact on the generation of H_2 cost, compared to its regeneration cost (the difference between the two NaBH4 sources for each solvent used are negligible). This way, to make the recycling of the by-product economically viable, the main solution can be to regenerate the Mg from the by-product MgO or commercialize the MgO, which has a high commercial value. In fact, MgO has a commercial value (87.61 €/kg) higher than reactant Mg and the most expensive solvent (isopropylamine) combined (76.61 €/kg).

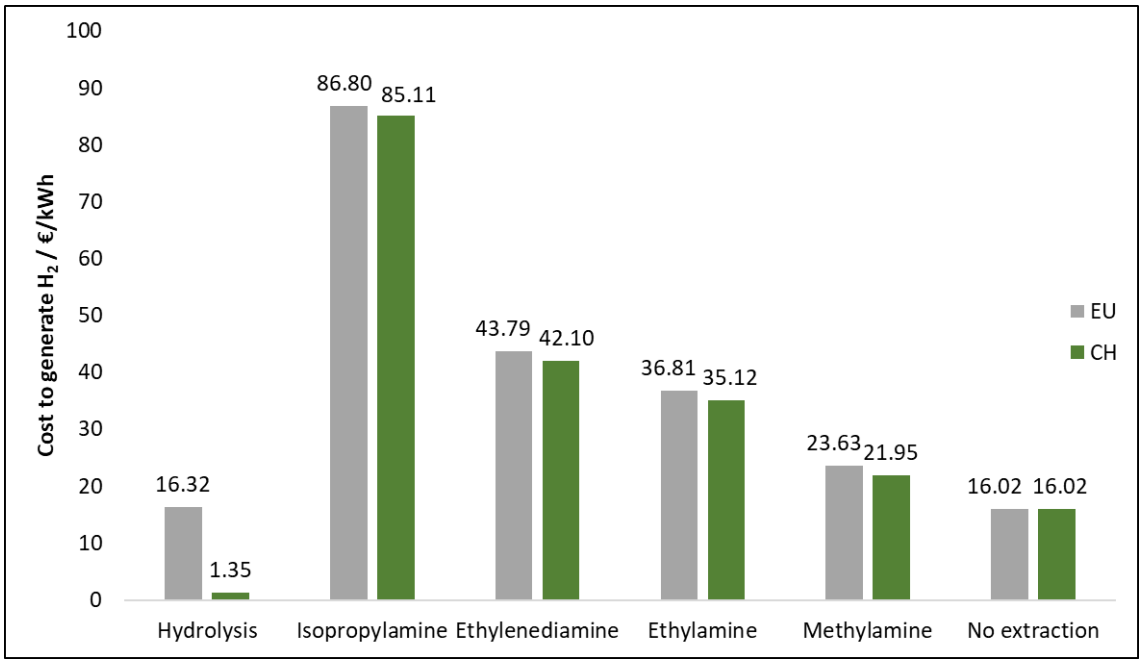


Figure 5.7. Cost to generate H_2 using M4 method with different extraction solvents and influence of the $NaBH_4$ commercial cost (lower: CH; higher: EU).

At last, it is important to check if sodium borohydride can be a cost-efficient method to generate green H_2 (obtained mostly from water PEM electrolysis, please recall Chapter 2) compared to current H_2 sources. Figure 5.8 presents the current green hydrogen range costs, considering that future expectations to be as low as 0.03 €/kWh [141]. The cost to generate H_2 from $NaBH_4$, considering the best methods presented in this study (Hydrolysis, T2, M4 and M5 without extraction and E1) are also represented.

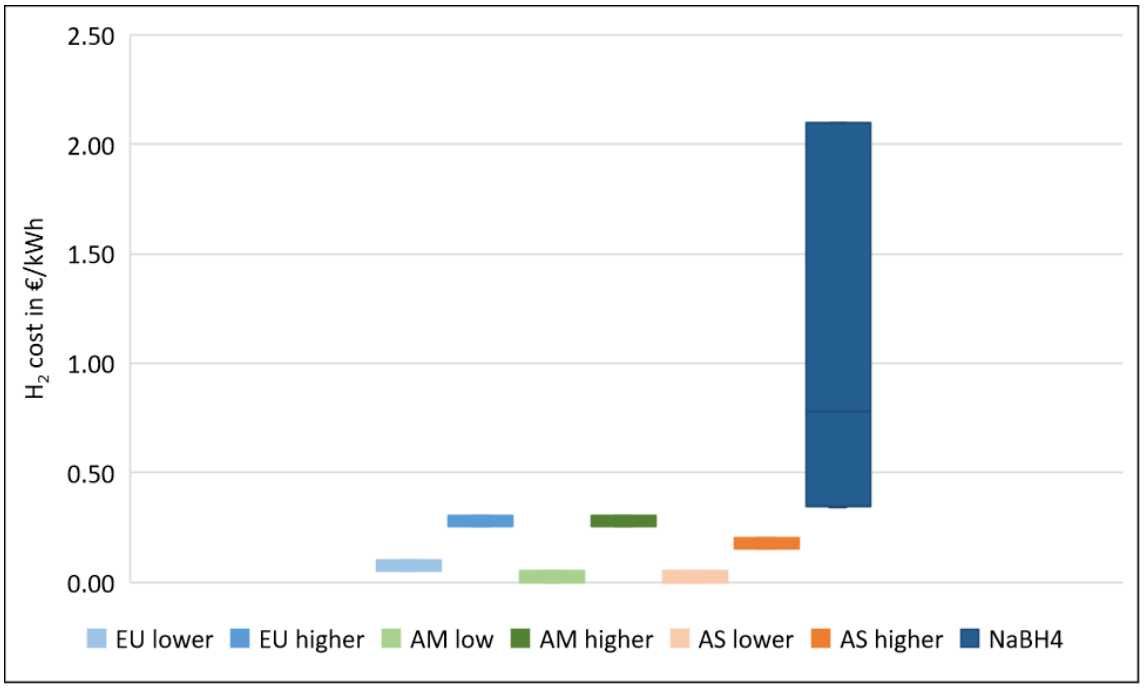


Figure 5.8. Green H_2 production cost gap and variation with location (Europe (EU), America (AM) and Asia (AS)) as well as H_2 production cost from the $NaBH_4$ hydrolysis [141].

From the simplified analysis performed in this chapter, we can observe that, although it has a wider range of costs, the lower-cost H_2 production from the hydrolysis of $NaBH_4$ can be competitive in the EU and AM market with the current H_2 technologies. However, the mechanochemical methods presented M4 and M5 are without extraction and energy and equipment costs were not calculated, as explained in the general considerations of this analysis, so it is expected that the difference between the $NaBH_4$ use for H_2 generation and the best green H_2 cost can be higher than the one here presented. Furthermore, it is essential to note the high commercial value of by-products such as MgO, which, if not recycled, can significantly impact the cost of the $NaBH_4$-H_2 cycle, by increasing the profit. Also, it does not consider the environmental impact of the current low-carbon and green technologies, where only hydrogen production by water electrolysis using renewable electric energy is considered green.

It is important here to consider, as a back-up solution, the possibility of valorize, without recycling, the by-product $NaB(OH)_4$, that according to the important findings in Chapter 3, can be obtained with a very high purity (around 100 %) [131]. In fact, as observed in Table 5.1, the commercial value of this borate is 502.50 €/5 mg, which is higher than the cost of commercial $NaBH_4$ (due to its low availability). Therefore, a more profound

analysis considering the equipment and energy costs, as well as the valorization of all by-products must be performed, to make this H_2 production (and storage) technology more viable.

5.3. Conclusions

A sensitive economic analysis of the hydrolysis of sodium borohydride and its regeneration to generate green H_2 was performed. The analysis demonstrated that the electrochemical processes are the most promising since no extraction of the borohydride – the higher-cost step of the thermo- and mechano-chemical processes – is required. The use of the more widely used and mature thermo- and mechanochemical processes, it is therefore essential to study cheaper solvents to extract $NaBH_4$, while also reducing the overall regeneration cost, which can be lower than the hydrolysis of commercial sodium borohydride. A comparison with other H_2 production technologies was also performed. It was demonstrated that the $NaBH_4$ hydrolysis for H_2 generation can be competitive in the EU and AM markets, but energy and equipment costs were not considered; nevertheless, it is a gap that can be further reduced by optimizing the system (for example, by recycling of by-products such as MgO back to Mg or MgH_2) and considering the high commercial value of by-products such as MgO. In fact, MgO has a higher commercial value than Mg, MgH_2 and isopropylamine (or any other amine solvent used in the mechano-chemical methods) combined, which will increase the balance (more profit) in favor of this technology. Additionally, we can consider the valorization of the $NaB(OH)_4$ hydrolysis by-product (with high commercial value and numerous applications) as a contingency solution that can make the process economically viable. To finish, it is always important to remind that the solution presented in this work, enabling the development of an off-grid safe system for H_2 production, has a market niche such as maritime applications and the comparison with other H_2 production/storage technologies is not straightforward.

6. Main conclusions and future work

The study of the composition of the sodium borohydride hydrolysis by-product(s) (sodium metaborate and its hydrated states) was performed. A set of experiments was performed to understand the rearrangement of $NaBO_2 \cdot 2H_2O$ into $NaB(OH)_4$ in the presence of additive CMC; however, this rearrangement was also observed in the presence of PAA and without the use of any additive. Also, the composition of the by-product(s) was not consistent throughout the experiments, which led to the indication that the by-product is affected by the presence of air while drying. With that in mind, an innovative post-treatment of the by-product extracted from the reactor was found. In the presence of vacuum drying and storage, pure or close to pure $NaB(OH)_4$ was formed which was a very important finding since this is a by-product with great interest for the recycling process. Several experiments were performed to replicate this result (hydrolysis conditions: SRc, x = 15/16 and a catalyst/$NaBH_4$ mass ratio of 0.4 g/g) and other hydrolysis conditions were considered to widen the range at which this innovative process can be applied (x = 6, 0.2 g/g). The same result was confirmed in all the assays. Therefore, this post-treatment process was subject of a provisional patent application approved [131]. To further investigate the importance of by-products handling, other by-product post-treatments were considered. When the by-product was dried in a low humidity environment, high concentrations of tincalconite were formed. However, some inconsistencies were found since the prolonged exposure to air has demonstrated reaction with the borate, forming non-borates species such as $Na_2CO_3.H_2O$ and decreasing the purity of the desired borate. On the other hand, the low humidity environment had a positive impact on the by-product dried open-to-air and no effect when dried under vacuum, given that it does not react with dried $NaB(OH)_4$, but with compounds with molecular water, increasing the purity of $NaB(OH)_4$.Moreover, low temperature drying tend to form pure $NaB(OH)_4 \cdot 2H_2O$, a less interesting borate for the $NaBH_4$ regeneration. As future work, it is essential to widen the post-treatment of the by-product to higher $NaBH_4$ concentrations (other values of excess of water) as well as NaOH concentrations, while also quantifying the effect of air in the by-product, in order to increase the purity of tincalconite in low humidity environments, as alternative to $NaB(OH)_4$, for example, by performing the drying under a controlled CO_2 environment.

Afterward, the regeneration of the sodium borohydride from its by-product was studied to close the $NaBH_4$-H_2 cycle. First, the mechano-chemical recycling of $NaB(OH)_4$ with MgH_2 was studied. Experiments were performed in a mixer mill with a grinding jar (specially designed to assure no H_2 leak). By-products dried with and without the innovative post-treatment process patented were ball milled. Although no $NaBH_4$ was detected in the XRD analysis of the experiments, $Mg(OH)_2$ – an intermediate of the reaction, reported by several authors in literature – was, indicating that the ball mill was likely to occur as expected. It was clear there is the need to use a ball miller with higher jar volume, to allow the optimization of the recycling conditions and promote the $NaBH_4$ formation, since the main parameters studied (mass of reactants, BPR and MgH_2 excess) were below the ones reported in literature (for example, the BPR reported is typically 30 or 50 and the one used in these experiments was below 5). Moreover, the study of other reducers such as Mg, Mg_2Si and LiH is essential to replace the MgH_2 which as low commercial availability and a very high price. The electrochemical regeneration of $NaBH_4$ was also studied. CV experiments of the $B(OH)_3$ reduction to BH_4^- were performed for the first time, as far the author is aware. A reduction peak in the borohydride potential range was observed, however it could not be replicated when a physical RE was implemented in the electrochemical cell mounted for the experiments. Moreover, N_2 bubbling was considered, however its influence on the cell could not be clearly identified as positive or negative, since both effects were noted. This was explained given that its use avoids air exposure but increases the interference between the electrodes and the electrolyte. Besides that, it was found that $B(OH)_3$ has a positive effect on the BDD WE by mitigating the HER reaction and widening its electrochemical window. As future work, it is essential to optimize the electrolyte conditions, the electrodes used, as well as the electrochemical cell built, to reduce the parasite and outside interferences, which impacts the BH_4^- formation.

Finally, an economic analysis of the hydrolysis of sodium borohydride and its regeneration to generate green H_2 was performed. The analysis demonstrated that the electrochemical $NaBH_4$ regeneration is the most promising process since no extraction of the borohydride – the higher-cost step of the thermo- and mechano-chemical processes – is required. A comparison with other green H_2 technologies was also performed. It was shown that the lower-cost $NaBH_4$ for H_2 generation can be competitive in the EU-AM

market, but energy and equipment cost were not considered for this analysis. However, the high commercial value of the recycling by-products such as MgO can have a very positive impact on the competitiveness of this source of H_2. As future work, it is essential to study better cost-effective solvents to extract $NaBH_4$, while also reducing the overall regeneration cost, including the by-products recycling or commercial valorization. Moreover, the energy balance and environmental impact of this H_2 technology must be also performed.

7. Follow-up work

As previously mentioned, it is noteworthy that the outputs from the present thesis, together with the other results obtained by the research group, resulted in a patent request which, consequently, required further experimental studies to improve the borate by-products post-treatment process and submit the patent. Over a year, the first draft was written and the provisional patent application was submitted in May 2021. Up to December 2022, when the final version was submitted (#118331) the patent was rewritten and optimized. The publication of the patent, allow to improve the use of $NaBH_4$ as an H_2 source in energy systems, increasing the TRL to a higher level. Moreover, it led to an invitation to participate in a program to accelerate business opportunities for potential products/services based on research projects developed at University of Porto (BIP Acceleration). In this context, the team joined together to create a start-up idea, named GENESIS – a projected committed to the development of an innovative off-grid safe system to simultaneously generate and store H_2 from $NaBH_4$, providing on-demand power to maritime transport applications, and off-grid solutions to help meeting the worldwide electrification (social impact). During a month, in the acceleration program, the GENESIS project was enhanced, and a business model was created. At the end, a final pitch was presented and awarded the 2nd place. As a result of this participation, the team was contacted by a business angel interested to invest in GENESIS and, therefore, a new horizon arised for the GENESIS creation. Thus, it is expected to begin the GENESIS activity in April 2023 and the development of the first scaled-up GENESIS product within a year. Therefore, the regeneration of sodium borohydride from the by-product formed in its hydrolysis and treated as described in the patent is even more essential, for which the financial investment in Genesis allows a leap to solve future needs, as well as the acquisition of equipment.

References

[1] International Energy Agency, “World Energy Outlook 2022,” 2022.

[2] International Energy Agency, “Covid-19 impact on electricity,” 2021. [Online]. Available: https://www.iea.org/reports/covid-19-impact-on-electricity. [Accessed: 12-Jan-2023].

[3] J. Delbeke, A. Runge-Metzger, Y. Slingenberg, and J. Werksman, “The Paris agreement,” *Towar. a Clim. Eur. Curbing Trend*, pp. 24–45, 2015, doi: 10.4324/9789276082569-2.

[4] The University of Tokyo, “UTokyo Climate Action,” 2022.

[5] International Trade Administration, “Energy - Carbon Neutrality Initiatives,” 2022. [Online]. Available: https://www.trade.gov/country-commercial-guides/south-korea-energy-carbon-neutrality-initiatives. [Accessed: 06-Jan-2023].

[6] European Parliament, “EU ban on the sale of new petrol and diesel cars from 2035 explained,” 2022. [Online]. Available: https://www.europarl.europa.eu/news/en/headlines/economy/20221019STO44572/eu-ban-on-sale-of-new-petrol-and-diesel-cars-from-2035-explained. [Accessed: 06-Jan-2023].

[7] Our World in Data, “Electricity mix.” [Online]. Available: https://ourworldindata.org/electricity-mix. [Accessed: 14-Sep-2022].

[8] S. Bobba, S. Carrara, J. Huisman, F. Mathieux, and C. Pavel, *Critical Raw Materials for Strategic Technologies and Sectors in the EU - a Foresight Study*. 2020.

[9] S. Bobba, S. Carrara, J. Huisman, F. Mathieux, and C. Pavel, *Critical Raw Materials for Strategic Technologies and Sectors in the EU - a Foresight Study*. 2020.

[10] Khan Academy, “Infographic: Chemical Abundances: The Universe,” *Analyzer*. p. 100.

[11] “Hydrogen.” [Online]. Available: http://www.engineeringtoolbox.com/hydrogen-d_1419.html. [Accessed: 13-Feb-2017].

[12] U.S. Department of Energy, “Hydrogen Storage.” [Online]. Available: https://energy.gov/eere/fuelcells/hydrogen-storage. [Accessed: 29-Jan-2020].

[13] Hydrogen Tools, “Comparative properties of hydrogen and other fuels,” 2022. [Online]. Available: https://h2tools.org/hyarc/hydrogen-data/comparative-properties-hydrogen-and-other-fuels. [Accessed: 09-Jan-2023].

[14] International Energy Agency, “Global Hydrogen Review 2022,” 2022.

[15] U.S. Department of Energy - Office of Energy Efficiency & Renewable Energy, “High-Pressure Hydrogen Tank Testing.” [Online]. Available: https://www.energy.gov/eere/fuelcells/high-pressure-hydrogen-tank-testing. [Accessed: 12-Sep-2022].

[16] International Energy Agency, “Sustainable Development Goal 7 - Access to electricity.” [Online]. Available: https://www.iea.org/sdg/electricity/. [Accessed: 18-Jul-2019].

[17] Our World in Data, “Electricity access,” 2020. [Online]. Available: https://ourworldindata.org/grapher/share-of-the-population-with-access-to-electricity. [Accessed: 11-Jan-2023].

[18] A. M. F. R. Pinto, M. J. F. Ferreira, V. R. Fernandes, and C. M. Rangel, “Durability and reutilization capabilities of a Ni-Ru catalyst for the hydrolysis of sodium borohydride in batch reactors,” *Catal. Today*, vol. 170, no. 1, pp. 40–49, 2011, doi: 10.1016/j.cattod.2011.03.051.

[19] M. J. F. Ferreira, V. R. Fernandes, L. Gales, C. M. Rangel, and A. M. F. R. Pinto, “Effects of the addition of an organic polymer on the hydrolysis of sodium tetrahydroborate in batch reactors,” *Int. J. Hydrogen Energy*, vol. 35, no. 20, pp. 11456–11469, 2010, doi: 10.1016/j.ijhydene.2010.07.079.

[20] M. J. F. Ferreira, F. Coelho, C. M. Rangel, and A. M. F. R. Pinto, “Batch sodium borohydride hydrolysis systems: Effect of sudden valve opening on hydrogen generation rate,” *Int. J. Hydrogen Energy*, vol. 37, no. 2, pp. 1947–1953, 2012, doi: 10.1016/j.ijhydene.2011.08.097.

[21] M. J. F. Ferreira, L. Gales, V. R. Fernandes, C. M. Rangel, and A. M. F. R. Pinto, “Alkali free hydrolysis of sodium borohydride for hydrogen generation under

pressure," *Int. J. Hydrogen Energy*, vol. 35, no. 18, pp. 9869–9878, 2010, doi: 10.1016/j.ijhydene.2010.02.121.

[22] M. J. F. Ferreira, C. M. Rangel, and A. M. F. R. Pinto, "Water handling challenge on hydrolysis of sodium borohydride in batch reactors," *Int. J. Hydrogen Energy*, vol. 37, no. 8, pp. 6985–6994, 2012, doi: 10.1016/j.ijhydene.2011.12.028.

[23] H. X. Nunes, M. J. F. Ferreira, C. M. Rangel, and A. M. F. R. Pinto, "Hydrogen generation and storage by aqueous sodium borohydride (NaBH4) hydrolysis for small portable fuel cells (H2-PEMFC)," *Int. J. Hydrogen Energy*, vol. 41, no. 34, pp. 15426–15432, 2016, doi: 10.1016/j.ijhydene.2016.06.173.

[24] S. Akbayrak and S. Özkar, "Ammonia borane as hydrogen storage materials," *Int. J. Hydrogen Energy*, vol. 43, no. 40, pp. 18592–18606, 2018, doi: 10.1016/j.ijhydene.2018.02.190.

[25] National Renewable Energy Laboratory, "Go / No-Go Recommendation for Sodium Borohydride for On-Board Vehicular Hydrogen Storage," 2007.

[26] Department of energy of the United States, "DOE Technical Targets for Hydrogen Storage Systems for Portable Power Equipment." [Online]. Available: https://www.energy.gov/eere/fuelcells/doe-technical-targets-hydrogen-storage-systems-portable-power-equipment. [Accessed: 29-Jan-2020].

[27] Department of Energy of the United States, "Technical System Targets: Onboard Hydrogen Storage," 2009.

[28] Department of Energy of the United States, "Targets for Onboard Hydrogen Storage Systems for Light-Duty Vehicles," 2009.

[29] U. B. Demirci, O. Akdim, J. Andrieux, J. Hannauer, R. Chamoun, and P. Miele, "Sodium borohydride hydrolysis as hydrogen generator: Issues, state of the art and applicability upstream froma fuel cell," *Fuel Cells*, vol. 10, no. 3, pp. 335–350, 2010, doi: 10.1002/fuce.200800171.

[30] H. N. Abdelhamid, "A review on hydrogen generation from the hydrolysis of sodium borohydride," *Int. J. Hydrogen Energy*, vol. 46, no. 1, pp. 726–765, 2021, doi: 10.1016/j.ijhydene.2020.09.186.

[31] B. H. Liu and Q. Li, "A highly active Co-B catalyst for hydrogen generation from

sodium borohydride hydrolysis," *Int. J. Hydrogen Energy*, vol. 33, no. 24, pp. 7385–7391, 2008, doi: 10.1016/j.ijhydene.2008.09.055.

[32] U. B. Demirci, O. Akdim, J. Hannauer, R. Chamoun, and P. Miele, "Cobalt, a reactive metal in releasing hydrogen from sodium borohydride by hydrolysis: A short review and a research perspective," *Sci. China Chem.*, vol. 53, no. 9, pp. 1870–1879, 2010, doi: 10.1007/s11426-010-4081-1.

[33] P. Krishnan, T.-H. Yang, W.-Y. Lee, and C.-S. Kim, "PtRu-LiCoO2—an efficient catalyst for hydrogen generation from sodium borohydride solutions," *J. Power Sources*, vol. 143, no. 1–2, pp. 17–23, 2005, doi: 10.1016/j.jpowsour.2004.12.007.

[34] C. Wu, H. Zhang, and B. Yi, "Hydrogen generation from catalytic hydrolysis of sodium borohydride for proton exchange membrane fuel cells," *Catal. Today*, vol. 93–95, pp. 477–483, 2004, doi: 10.1016/j.cattod.2004.06.095.

[35] S. Özkar and M. Zahmakiran, "Hydrogen generation from hydrolysis of sodium borohydride using Ru(0) nanoclusters as catalyst," *J. Alloys Compd.*, vol. 404–406, no. SPEC. ISS., pp. 728–731, 2005, doi: 10.1016/j.jallcom.2004.10.084.

[36] J. Zhang, F. Lin, L. Yang, and H. Dong, "Highly dispersed Ru/Co catalyst with enhanced activity for catalyzing NaBH4 hydrolysis in alkaline solutions," *Chinese Chem. Lett.*, vol. 31, no. 9, pp. 2512–2515, 2020, doi: 10.1016/j.cclet.2020.03.072.

[37] A. Balbay and C. Saka, "The effect of the concentration of hydrochloric acid and acetic acid aqueous solution for fast hydrogen production from methanol solution of NaBH4," *Int. J. Hydrogen Energy*, vol. 43, no. 31, pp. 14265–14272, Aug. 2018, doi: 10.1016/J.IJHYDENE.2018.05.131.

[38] E. K. H. H. I. Schlesinger, Erbert C. Brown, A. E. Finholt, James R. Gilbreath, Henry R. Hoekstra, "Sodium Borohydride , Its Hydrolysis and its Use as a Reducing Agent and in the Generation of Hydrogen," *J. Am. Chem. Soc.*, vol. 75, no. 3, pp. 215–219, 2007, doi: 10.1021/ja01097a057.

[39] S. Murugesan and V. (Ravi) Subramanian, "Effects of acid accelerators on hydrogen generation from solid sodium borohydride using small scale devices," *J. Power Sources*, vol. 187, no. 1, pp. 216–223, 2009, doi: 10.1016/j.jpowsour.2008.10.060.

[40] M. J. F. Ferreira, V. R. Fernandes, C. M. Rangel, L. Gales, and A. M. F. R. Pinto, "Successive loadings of reactant in the hydrogen generation by hydrolysis of sodium borohydride in batch reactors," *J. New Mater. Electrochem. Syst.*, vol. 12, no. 2–3, pp. 153–159, 2009, doi: 10216/69767.

[41] A. Ekinci, E. Cengiz, M. Kuncan, and Ö. Şahin, "Hydrolysis of sodium borohydride solutions both in the presence of Ni–B catalyst and in the case of microwave application," *Int. J. Hydrogen Energy*, Sep. 2020, doi: 10.1016/j.ijhydene.2020.08.264.

[42] S. C. Amendola *et al.*, "A Safe, portable, hydrogen gas generator using aqueous borohydride solution and Ru catalyst," *Int. J. Hydrogen Energy*, vol. 25, no. 10, pp. 969–975, 2000, doi: 10.1016/S0360-3199(00)00021-5.

[43] D. Hua, Y. Hanxi, A. Xinping, and C. Chuansin, "Hydrogen production from catalytic hydrolysis of sodium borohydride solution using nickel boride catalyst," *Int. J. Hydrogen Energy*, vol. 28, no. 10, pp. 1095–1100, 2003, doi: 10.1016/S0360-3199(02)00235-5.

[44] M. J. F. Ferreira, "Catalytic generation and storage of hydrogen from hydrolysis of sodium borohydride under pressure - Application in a hydrogen/oxygen fuel cell," Faculty of Engineering University of Porto, 2009.

[45] Mattuci, "Proton Exchange Fuel Cell Diagram," 2015. [Online]. Available: https://commons.wikimedia.org/wiki/File:Proton_Exchange_Fuel_Cell_Diagram.svg.

[46] U.S. Department of Energy - Office of Energy Efficiency & Renewable Energy, "Types of Fuel Cells." [Online]. Available: https://www.energy.gov/eere/fuelcells/types-fuel-cells. [Accessed: 12-Jul-2019].

[47] O. Akdim, U. B. Demirci, and P. Miele, "Acetic acid, a relatively green single-use catalyst for hydrogen generation from sodium borohydride," *Int. J. Hydrogen Energy*, vol. 34, no. 17, pp. 7231–7238, Sep. 2009, doi: 10.1016/J.IJHYDENE.2009.06.068.

[48] E. Y. Marrero-Alfonso, J. R. Gray, T. A. Davis, and M. A. Matthews, "Hydrolysis of sodium borohydride with steam," *Int. J. Hydrogen Energy*, vol. 32, no. 18, pp. 4717–4722, Dec. 2007, doi: 10.1016/J.IJHYDENE.2007.07.066.

[49] N. Stepanov, V. Uvarov, I. Popov, and Y. Sasson, "Study of by-product of NaBH4 hydrolysis and its behavior at a room temperature," *Int. J. Hydrogen Energy*, vol. 33, no. 24, pp. 7378–7384, 2008, doi: 10.1016/j.ijhydene.2008.09.052.

[50] P. P. Prosini and P. Gislon, "Water consumption during solid state sodium borohydride hydrolysis," *Int. J. Hydrogen Energy*, 2010, doi: 10.1016/j.ijhydene.2010.07.094.

[51] W. S. Abdul-Majeed, M. T. Arslan, and W. B. Zimmerman, "Application of acidic accelerator for production of pure hydrogen from NaBH4," *Int. J. Ind. Chem.*, vol. 5, no. 2, pp. 1–9, 2014, doi: 10.1007/s40090-014-0015-7.

[52] J. Andrieux *et al.*, "Revision of the NaBO2 – H2O phase diagram for optimized yield in the H2 generation through NaBH4 hydrolysis," *Int. J. Hydrogen Energy*, vol. 37, no. 7, pp. 5798–5810, 2012.

[53] National Library of Medicine, "Sodium metaborate." [Online]. Available: https://pubchem.ncbi.nlm.nih.gov/compound/Sodium-metaborate.

[54] D. Uysal, Ö. M. Dogan, and B. Z. Uysal, "Kinetics of Absorption of Carbon Dioxide into Sodium Metaborate Solution," *Int. J. Chem. Kinet.*, vol. 49, no. 6, pp. 377–386, 2017, doi: 10.1002/kin.21082.

[55] Geochemical Instrumentation and Analysis, "X-ray Powder Diffraction (XRD)." [Online]. Available: https://serc.carleton.edu/research_education/geochemsheets/techniques/XRD.html. [Accessed: 14-Jan-2019].

[56] "Bragg's Law - Chemistry LibreTexts." [Online]. Available: https://chem.libretexts.org/Bookshelves/Analytical_Chemistry/Supplemental_Modules_(Analytical_Chemistry)/Instrumental_Analysis/Diffraction_Scattering_Techniques/Bragg's_Law. [Accessed: 18-Jul-2019].

[57] TutorVista, "X-ray Study of Crystals." [Online]. Available: https://www.tutorvista.com/content/chemistry/chemistry-iv/solid-state/x-ray-crystals.php. [Accessed: 14-Jan-2019].

[58] XRPD, "What is XRPD - X-Ray Diffraction?" [Online]. Available: http://www.xrpd.eu/. [Accessed: 04-Jan-2019].

[59] Chemistry LibreTexts, “13.15: Some Vibrations Are Infrared Inactive.” [Online]. Available: https://chem.libretexts.org/Bookshelves/Organic_Chemistry/Map%3A_Organic_Chemistry_(Bruice)/13%3A_Mass_Spectrometry%2C_Infrared_Spectroscopy%2C_and_Ultraviolet%2F%2FVisible_Spectroscopy/13.15%3A_Some_Vibrations_Are_Infrared_Inactive. [Accessed: 23-Jan-2019].

[60] Chemistry LibreTexts, “Infrared: Theory.” [Online]. Available: https://chem.libretexts.org/Bookshelves/Physical_and_Theoretical_Chemistry_Textbook_Maps/Supplemental_Modules_(Physical_and_Theoretical_Chemistry)/Spectroscopy/Vibrational_Spectroscopy/Infrared_Spectroscopy/Infrared%3A_Theory. [Accessed: 04-Jan-2019].

[61] Amrita Vishwa Vidyapeetham Virtual Lab, “Michelson’s Interferometer-Wavelength of laser beamn.” [Online]. Available: http://vlab.amrita.edu/?sub=1&brch=189&sim=1106&cnt=1. [Accessed: 23-Jan-2019].

[62] Eva Martín Tapia, “Determinación cuantitativa de diisobutil ftalato en líquidos mediante ATR-FTIR: Estudio inicial,” Universidad de Burgos, 2018.

[63] Anonim, “Fourier Transformation of an IR Interferogram,” pp. 1–12, 2003.

[64] T. S. Michal S. Bradley, “FT-IR: How and Why?” [Online]. Available: http://players.brightcove.net/665001591001/default_default/index.html?videoId=5331226418001. [Accessed: 04-Jan-2019].

[65] Wikipedia, “File:FTIR-interferogram.svg.” [Online]. Available: https://en.wikipedia.org/wiki/File:FTIR-interferogram.svg. [Accessed: 04-Jan-2019].

[66] Tech-Faq, “What is FTIR Spectroscopy?” [Online]. Available: http://www.tech-faq.com/what-is-ftir-spectroscopy.html. [Accessed: 04-Jan-2019].

[67] C.-H. Liu and B.-H. Chen, “The Concept about the Regeneration of Spent Borohydrides and Used Catalysts from Green Electricity,” *Materials (Basel).*, vol. 8, no. 6, pp. 3456–3466, Jun. 2015, doi: 10.3390/ma8063456.

[68] U. B. Demirci, “Sodium borohydride for the near-future energy: A ‘rough

diamond' for Turkey," *Turkish J. Chem.*, vol. 42, no. 2, pp. 193–220, 2018, doi: 10.3906/kim-1712-6.

[69] Z. P. Li, N. Morigazaki, B. H. Liu, and S. Suda, "Preparation of sodium borohydride by the reaction of MgH2 with dehydrated borax through ball milling at room temperature," *J. Alloys Compd.*, vol. 349, no. 1–2, pp. 232–236, 2003, doi: 10.1016/S0925-8388(02)00872-1.

[70] M. T. Kelly and J. V Ortega, "Review of Chemical Processes for the Synthesis of Sodium Borohydride," *Millenn. cell Inc.*, no. August, p. DOE, 2004.

[71] H. X. Nunes, D. L. Silva, and C. M. Rangel, "Rehydrogenation of Sodium Borates to Close the NaBH4-H2 cycle - A review," pp. 1–28, 2021.

[72] U. B. Demirci, "The hydrogen cycle with the hydrolysis of sodium borohydride: A statistical approach for highlighting the scientific/technical issues to prioritize in the field," *Int. J. Hydrogen Energy*, vol. 40, no. 6, pp. 2673–2691, 2015, doi: 10.1016/j.ijhydene.2014.12.067.

[73] Y. Kojima and T. Haga, "Recycling process of sodium metaborate to sodium borohydride," *Int. J. Hydrogen Energy*, vol. 28, no. 9, pp. 989–993, 2003, doi: 10.1016/S0360-3199(02)00173-8.

[74] B. H. Liu, Z. P. Li, J. K. Zhu, N. Morigasaki, and S. Suda, "Sodium borohydride synthesis by reaction of Na2O contained sodium borate with Al and hydrogen," *Energy and Fuels*, vol. 21, no. 3, pp. 1707–1711, 2007, doi: 10.1021/ef0605448.

[75] U. B. Demirci, "Impact of H.I. Schlesinger's discoveries upon the course of modern chemistry on B−(N−)H hydrogen carriers," *Int. J. Hydrogen Energy*, vol. 42, no. 33, pp. 21048–21062, 2017, doi: 10.1016/j.ijhydene.2017.07.066.

[76] Y. Wu, M. T. Kelly, and J. V Ortega, "Review of Chemical Processes for the Synthesis of Sodium Borohydride," *Millenn. cell Inc.*, no. August, p. DOE, 2004.

[77] Ç. Çakanyildirim and M. Gürü, "Hydrogen cycle with sodium borohydride," *Int. J. Hydrogen Energy*, vol. 33, no. 17, pp. 4634–4639, 2008, doi: 10.1016/j.ijhydene.2008.05.084.

[78] B. H. Liu and Z. P. Li, "A review: Hydrogen generation from borohydride hydrolysis reaction," *J. Power Sources*, vol. 187, no. 2, pp. 527–534, 2009, doi:

10.1016/j.jpowsour.2008.11.032.

[79] S. S. Muir and X. Yao, "Progress in sodium borohydride as a hydrogen storage material: Development of hydrolysis catalysts and reaction systems," *Int. J. Hydrogen Energy*, vol. 36, no. 10, pp. 5983–5997, 2011, doi: 10.1016/j.ijhydene.2011.02.032.

[80] J. Mao and D. H. Gregory, "Recent Advances in the Use of Sodium Borohydride as a Solid State Hydrogen Store," pp. 430–453, 2015, doi: 10.3390/en8010430.

[81] U. B. Demirci, O. Akdim, and P. Miele, "Ten-year efforts and a no-go recommendation for sodium borohydride for on-board automotive hydrogen storage," *Int. J. Hydrogen Energy*, vol. 34, no. 6, pp. 2638–2645, 2009, doi: 10.1016/j.ijhydene.2009.01.038.

[82] L. Ouyang, H. Zhong, H.-W. Li, and M. Zhu, "A Recycling Hydrogen Supply System of NaBH4 Based on a Facile Regeneration Process: A Review," *Inorganics*, vol. 6, no. 1, p. 10, 2018, doi: 10.3390/inorganics6010010.

[83] G. Moussa, R. Moury, U. B. Demirci, T. Sener, and P. Miele, "Boron-based hydrides for chemical hydrogen storage Georges," *Int. J. Energy Res.*, vol. 37, pp. 825–842, 2013, doi: 10.1002/er.3027.

[84] K. Wang, Z. Pan, and X. Yu, "Metal B-N-H hydrogen-storage compound: Development and perspectives," *J. Alloys Compd.*, vol. 794, pp. 303–324, 2019, doi: 10.1016/j.jallcom.2019.04.240.

[85] C. R. Cloutier, "Electrochemical recycling of sodium borohydride for hydrogen storage: Physicochemical properties of sodium metaborate solutions," 2006.

[86] K. Eom, E. Cho, M. Kim, S. Oh, S. W. Nam, and H. Kwon, "Thermochemical production of sodium borohydride from sodium metaborate in a scaled-up reactor," *Int. J. Hydrogen Energy*, vol. 38, no. 6, pp. 2804–2809, 2013, doi: 10.1016/j.ijhydene.2012.12.053.

[87] B. H. Liu, Z. P. Li, and J. K. Zhu, "Sodium borohydride formation when Mg reacts with hydrous sodium borates under hydrogen," *J. Alloys Compd.*, vol. 476, no. 1–2, pp. 16–20, 2009, doi: 10.1016/j.jallcom.2008.09.057.

[88] B. H. Liu, Z. P. Li, and S. Suda, "Improving MgH2 formation kinetics and its effect

on NaBH4 synthesis," *J. Alloys Compd.*, 2009, doi: 10.1016/j.jallcom.2008.06.114.

[89] T. Ou, A. Giuliano, M. Panizza, A. Barbucci, and G. Cerisola, "Thermochemical recycling of hydrolyzed NaBH4. Part I: In-situ and ex-situ evaluations," *Int. J. Hydrogen Energy*, vol. 38, no. 35, pp. 15269–15274, 2013, doi: 10.1016/j.ijhydene.2013.09.058.

[90] T. Ou, M. Panizza, and A. Barbucci, "Thermochemical recycling of hydrolyzed NaBH4. Part II: Systematical study of parameters dependencies," *Int. J. Hydrogen Energy*, vol. 38, no. 36, pp. 15940–15945, 2013, doi: 10.1016/j.ijhydene.2013.09.061.

[91] A. Kantürk Figen and S. Pişkin, "Microwave assisted green chemistry approach of sodium metaborate dihydrate (NaBO2·2H2O) synthesis and use as raw material for sodium borohydride (NaBH4) thermochemical production," *Int. J. Hydrogen Energy*, vol. 38, no. 9, pp. 3702–3709, 2013, doi: 10.1016/j.ijhydene.2013.01.003.

[92] B. H. Liu, Z. P. Li, and S. Suda, "Influences of alkali in borates on recovery of sodium borohydride," *J. Alloys Compd.*, vol. 474, no. 1–2, pp. 6–9, 2009, doi: 10.1016/j.jallcom.2008.06.040.

[93] T. Kemmitt and G. J. Gainsford, "Regeneration of sodium borohydride from sodium metaborate, and isolation of intermediate compounds," *Int. J. Hydrogen Energy*, vol. 34, no. 14, pp. 5726–5731, 2009, doi: 10.1016/j.ijhydene.2009.05.108.

[94] İ. Kayacan, Ö. M. Doğan, and B. Z. Uysal, "Effect of magnesium on sodium borohydride synthesis from anhydrous borax," *Int. J. Hydrogen Energy*, vol. 36, no. 13, pp. 7410–7415, Jul. 2011, doi: 10.1016/J.IJHYDENE.2011.03.142.

[95] B. H. Liu, Z. P. Li, N. Morigasaki, and S. Suda, "Alkali oxide addition effects on borohydride formation during the reaction of Al, Si, and Ti with borate and hydrogen," *Energy and Fuels*, vol. 22, no. 3, pp. 1894–1896, 2008, doi: 10.1021/ef700787s.

[96] "Mixer Mill MM200." [Online]. Available: http://www.retsch.com/products/milling/ball-mills/mixer-mill-mm-200. [Accessed: 02-Mar-2017].

[97] W. Cao, "High energy ball milling process for nanomaterial synthesis," *Skyspring Nanomaterials, Inc.* [Online]. Available: https://www.understandingnano.com/nanomaterial-synthesis-ball-milling.html. [Accessed: 08-Jun-2020].

[98] T. T. Le *et al.*, "Efficient synthesis of alkali borohydrides from mechanochemical reduction of borates using magnesium-aluminum-basedwaste," *Metals (Basel).*, vol. 9, no. 10, 2019, doi: 10.3390/met9101061.

[99] L. Kong, X. Cui, H. Jin, J. Wu, H. Du, and T. Xiong, "Mechanochemical synthesis of sodium borohydride by recycling sodium metaborate," *Energy and Fuels*, vol. 23, no. 10, pp. 5049–5054, 2009, doi: 10.1021/ef900619y.

[100] C. L. Hsueh *et al.*, "Regeneration of spent-NaBH4 back to NaBH4 by using high-energy ball milling," *Int. J. Hydrogen Energy*, vol. 34, no. 4, pp. 1717–1725, 2009, doi: 10.1016/j.ijhydene.2008.12.036.

[101] C. Lang *et al.*, "NaBH4 regeneration from NaBO2 by high-energy ball milling and its plausible mechanism," *Int. J. Hydrogen Energy*, vol. 42, no. 18, pp. 13127–13135, 2017, doi: 10.1016/j.ijhydene.2017.04.014.

[102] H. Zhang, S. Zheng, F. Fang, G. Chen, G. Sang, and D. Sun, "Synthesis of NaBH4 based on a solid-state reaction under Ar atmosphere," *J. Alloys Compd.*, vol. 484, no. 1–2, pp. 352–355, 2009, doi: 10.1016/j.jallcom.2009.04.093.

[103] L. Ouyang, W. Chen, J. Liu, M. Felderhoff, H. Wang, and M. Zhu, "Enhancing the Regeneration Process of Consumed NaBH4 for Hydrogen Storage," *Adv. Energy Mater.*, vol. 7, no. 19, pp. 1–8, 2017, doi: 10.1002/aenm.201700299.

[104] W. Chen *et al.*, "Hydrolysis and regeneration of sodium borohydride (NaBH4) – A combination of hydrogen production and storage," *J. Power Sources*, vol. 359, pp. 400–407, 2017, doi: 10.1016/j.jpowsour.2017.05.075.

[105] H. Zhong *et al.*, "An one-step approach towards hydrogen production and storage through regeneration of NaBH4," *Energy Storage Mater.*, vol. 7, no. January, pp. 222–228, 2017, doi: 10.1016/j.ensm.2017.03.001.

[106] M. Huang *et al.*, "Efficient regeneration of sodium borohydride via ball milling dihydrate sodium metaborate with magnesium and magnesium silicide," *J. Alloys*

Compd., vol. 729, pp. 1079–1085, 2017, doi: 10.1016/j.jallcom.2017.09.262.

[107] C. Qin, L. Ouyang, H. Wang, J. Liu, H. Shao, and M. Zhu, "Regulation of high-efficient regeneration of sodium borohydride by magnesium-aluminum alloy," *Int. J. Hydrogen Energy*, May 2019, doi: 10.1016/J.IJHYDENE.2019.05.010.

[108] H. Zhong *et al.*, "Sodium borohydride regeneration via direct hydrogen transformation of sodium metaborate tetrahydrate," *J. Power Sources*, vol. 390, no. January, pp. 71–77, 2018, doi: 10.1016/j.jpowsour.2018.04.037.

[109] Ç. Çakanyildirim and M. Gürü, "The Production of NaBH4 from Its Elements by Mechano-chemical Reaction and Usage in Hydrogen Recycle," *Energy Sources, Part A Recover. Util. Environ. Eff.*, vol. 33, no. 20, pp. 1912–1920, 2011, doi: 10.1080/15567030903503175.

[110] İ. Ar, Ö. U. Güler, and M. Gürü, "Synthesis and characterization of sodium borohydride and a novel catalyst for its dehydrogenation," *Int. J. Hydrogen Energy*, vol. 43, no. 44, pp. 20214–20233, Nov. 2018, doi: 10.1016/J.IJHYDENE.2018.06.184.

[111] Ç. Çakanyildirim and M. Gürü, "The processing of NaBH 4 from Na2B4O7 by mechano-chemical synthesis and its catalytic dehydrogenation," *Energy Sources, Part A Recover. Util. Environ. Eff.*, vol. 34, no. 12, pp. 1104–1113, 2012, doi: 10.1080/15567031003753579.

[112] Y. Zhu *et al.*, "Closing the Loop for Hydrogen Storage: Facile Regeneration of NaBH4 from its Hydrolytic Product," *Angew. Chemie - Int. Ed.*, vol. 59, no. 22, pp. 8623–8629, 2020, doi: 10.1002/anie.201915988.

[113] W. Chen *et al.*, "Hydrolysis and regeneration of sodium borohydride (NaBH4) – A combination of hydrogen production and storage," *J. Power Sources*, vol. 359, pp. 400–407, 2017, doi: 10.1016/j.jpowsour.2017.05.075.

[114] L. Ouyang *et al.*, "Low-cost method for sodium borohydride regeneration and the energy efficiency of its hydrolysis and regeneration process," *J. Power Sources*, vol. 269, pp. 768–772, 2014, doi: 10.1016/j.jpowsour.2014.07.074.

[115] the revision website S-cool, "Electrochemical Cells - The Daniell Cell." [Online]. Available: https://www.s-cool.co.uk/a-level/chemistry/electrochemistry/revise-

it/electrochemical-cells. [Accessed: 18-Jan-2019].

[116] Chemistry LibreTexts, “19-2: Electrochemical Cells.” [Online]. Available: https://chem.libretexts.org/Courses/University_of_Arkansas_Little_Rock/Chem_1403%3A_General_Chemistry_2/Chapters/19%3A_Electron_Transfer_Reactions/19-2%3A_Electrochemical_Cells. [Accessed: 18-Jan-2019].

[117] Chemistry LibreTexts, “Electrolytic Cells.” [Online]. Available: https://chem.libretexts.org/Bookshelves/Analytical_Chemistry/Supplemental_Modules_(Analytical_Chemistry)/Electrochemistry/Electrolytic_Cells. [Accessed: 20-Jan-2019].

[118] W. A. P. Jefferson W. Tester, Elisabeth M. Drake, Michael J. Driscoll, Michael W. Golay, *Sustainable Energy: Choosing Among Options*. Cambridge, Massachusetts: Massachusetts Institute of Technology, 2005.

[119] X. Huang, Z. Zhang, and J. Jiang, “Fuel cell technology for distributed generation: An overview,” *IEEE Int. Symp. Ind. Electron.*, vol. 2, no. August 2006, pp. 1613–1618, 2006, doi: 10.1109/ISIE.2006.295713.

[120] Wikipedia, “Polymer electrolyte membrane electrolysis,” 2013. [Online]. Available: https://en.wikipedia.org/wiki/Polymer_electrolyte_membrane_electrolysis#Voltage_losses. [Accessed: 19-Jan-2023].

[121] Wikipedia, “Cyclic voltammety.” [Online]. Available: https://en.wikipedia.org/wiki/Cyclic_voltammetry. [Accessed: 04-Jan-2019].

[122] W. J. Basirun, S. T. Shah, M. Shalauddin, S. Akhter, N. S. Jamaludin, and A. Hayyan, “A Review of Electrochemical Reduction of Sodium Metaborate,” *Energies*, vol. 16, no. 1, 2023, doi: 10.3390/en16010015.

[123] R. A. Varin, M. Jang, T. Czujko, and Z. S. Wronski, “The effect of ball milling under hydrogen and argon on the desorption properties of MgH2 covered with a layer of Mg(OH)2,” *J. Alloys Compd.*, vol. 493, no. 1–2, pp. 29–32, 2010, doi: 10.1016/j.jallcom.2009.12.138.

[124] Q. Y. Zhu, C. G. Zhu, F. W. Wang, and Y. J. Wei, “Preparation of sodium borohydride by copper electrolysis,” *Asian J. Chem.*, vol. 25, no. 14, pp. 7749–

7752, 2013, doi: 10.14233/ajchem.2013.14593.

[125] Y. Shen, X. Yang, T. Sun, and J. Jia, "Innovative desulfurization process of coal water slurry under atmospheric condition via sodium metaborate electroreduction in the isolated slot," *Energy and Fuels*, vol. 25, no. 11, pp. 5007–5014, 2011, doi: 10.1021/ef201045m.

[126] Y. Shen, T. Sun, and J. Jia, "A novel desulphurization process of coal water slurry via sodium metaborate electroreduction in the alkaline system," *Fuel*, vol. 96, pp. 250–256, 2012, doi: 10.1016/j.fuel.2012.01.003.

[127] C. Shu, T. Sun, J. Jia, and Z. Lou, "A novel desulfurization process of gasoline via sodium metaborate electroreduction with pulse voltage using a boron-doped diamond thin film electrode," *Fuel*, vol. 113, pp. 187–195, Nov. 2013, doi: 10.1016/J.FUEL.2013.05.069.

[128] C. Shu, F. Lai, F. Zhu, and D. Luo, "Optimal extractive and reductive desulfurization process using sodium borohydride in situ generated via sodium metaborate electroreduction in ionic liquid," *Chem. Eng. Process. - Process Intensif.*, vol. 150, no. February, p. 107869, 2020, doi: 10.1016/j.cep.2020.107869.

[129] Polymer database, "Polyacrylamides." [Online]. Available: https://polymerdatabase.com/polymer classes/Polyacrylamide type.html. [Accessed: 24-Jan-2023].

[130] S. Earman, F. M. Phillips, and B. J. O. L. McPherson, "The role of 'excess' CO2 in the formation of trona deposits," *Appl. Geochemistry*, 2005, doi: 10.1016/j.apgeochem.2005.08.007.

[131] A. R. Pinto, D. Silva, H. Nunes, L. Marcon, and C. Archila, "Method to process borate by-products from sodium borohydride hydrolysis," 118331 T, 2022.

[132] M. Bilen, M. Gürü, and Ç. Çakanyıldırım, "Role of NaCl in NaBH4 production and its hydrolysis," *Energy Convers. Manag.*, vol. 72, pp. 134–140, Aug. 2013, doi: 10.1016/J.ENCONMAN.2012.08.031.

[133] G. Balakrishnan, R. Velavan, K. Mujasam Batoo, and E. H. Raslan, "Microstructure, optical and photocatalytic properties of MgO nanoparticles," *Results Phys.*, vol. 16, no. November 2019, p. 103013, 2020, doi:

10.1016/j.rinp.2020.103013.

[134] I. Kayacan, Ö. M. Doan, and B. Z. Uysal, "Effect of magnesium on sodium borohydride synthesis from anhydrous borax," *Int. J. Hydrogen Energy*, vol. 36, no. 13, pp. 7410–7415, 2011, doi: 10.1016/j.ijhydene.2011.03.142.

[135] S. G. Bratsch, "Standard Electrode Potentials and Temperature Coefficients in Water at 298.15 K," *J. Phys. Chem. Ref. Data*, vol. 18, no. 1, pp. 1–21, 1989, doi: 10.1063/1.555839.

[136] N. Hodnik *et al.*, "New insights into corrosion of ruthenium and ruthenium oxide nanoparticles in acidic media," *J. Phys. Chem. C*, vol. 119, no. 18, pp. 10140–10147, 2015, doi: 10.1021/acs.jpcc.5b01832.

[137] UCSB-CLAS, "Table of Acids with Ka and pKa Values*." [Online]. Available: http://clas.sa.ucsb.edu/staff/Resource Folder/Chem109ABC/Acid, Base Strength/Table of Acids w Kas and pKas.pdf. [Accessed: 18-Jan-2019].

[138] K. Eom, E. Cho, M. Kim, S. Oh, S. W. Nam, and H. Kwon, "Thermochemical production of sodium borohydride from sodium metaborate in a scaled-up reactor," *Int. J. Hydrogen Energy*, vol. 38, no. 6, pp. 2804–2809, 2013, doi: 10.1016/j.ijhydene.2012.12.053.

[139] L. Z. Ouyang *et al.*, "Low-cost method for sodium borohydride regeneration and the energy efficiency of its hydrolysis and regeneration process," *J. Power Sources*, vol. 269, pp. 768–772, 2014, doi: 10.1016/j.jpowsour.2014.07.074.

[140] Hydrogen Tools, "Lower and higher heating values of fuels," 2022. [Online]. Available: https://h2tools.org/hyarc/calculator-tools/lower-and-higher-heating-values-fuels. [Accessed: 10-Jan-2023].

[141] E. Penrod, "Green hydrogen prices have nearly tripled as energy costs climb: S&P," 2022. [Online]. Available: https://www.utilitydive.com/news/green-hydrogen-prices-global-report/627776/. [Accessed: 04-Jan-2023].

Appendix A – Patent no. 118331 T

DESCRIPTION

METHOD TO PROCESS BORATE BY-PRODUCTS FROM SODIUM BOROHYDRIDE HYDROLYSIS

TECHNICAL FIELD

[0001] The present disclosure relates to a method to process a by-product of sodium borohydride hydrolysis leading to the regeneration of $NaBH_4$ with economic potential, allowing its further re-hydrogenation.

BACKGROUND

[0002] The hydrolysis of sodium borohydride for on-demand hydrogen generation has been studied as a clean alternative method to generate energy for portable and stationary devices, and additionally has a high potential as an off-grid solution. The process has relatively high hydrogen capacity (10.8 wt.%), releasing hydrogen with high purity at relatively low operational temperatures, producing environmentally benign by-products in a controllable reaction. One of its main disadvantages is the difficulty in obtaining a stable reaction by-product and further regenerating it back to sodium borohydride and closing the $NaBH_4$-H_2 cycle. Nevertheless, there has been little focus on its regeneration and even less on identification of the by-product effectively formed during the H_2 generation. This by-product can be formed in numerous hydration states, but since the main rehydrogenation methods studied only consider commercial borates, this has not been yet considered in the literature (Zhu *et al. Angew. Chem. Int. Ed.*, 2020, 59, 8623–8629).

[0003] Indeed, the regeneration of sodium borohydride from its by-product is essential to close the $NaBH_4$-H_2 cycle and allow the viability of this method to generate H_2 as an energy carrier. However, the by-product formed on the $NaBH_4$ hydrolysis is not easily known and its stability is difficult to control. As listed in Table 1, the borate $NaBO_2$ is rehydrogenated with greater efficiency by thermo- and electrochemical processes. Mechanochemical processes are cleaner, and therefore these processes have been preferentially used to regenerate $NaBH_4$. As reported in the literature (Table 1) the

mechanochemical processes are more efficient when the re-hydrogenated borate is $NaB(OH)_4$. Moreover, the by-product of the hydrolysis reaction of NaBH4 is usually obtained in this form, thus not being necessary to apply dehydration methods before its rehydrogenation into $NaBH_4$. Furthermore, the composition of this by-product is quite unstable when extracted in an uncontrolled manner and may contain various compounds.

Table A.1 – Literature review on the efficiency of borate re-hydrogenation.

Method	Author	Borate	Hydration	Chemical Structure	Efficiency %	DOI reference
Mechano	Kong	$NaBO_2$	-	$NaBO_2$	71.0	10.1021/ef900619y
	Çakanyildirim	$Na_2B_4O_7$	-	$Na_2B_4O_7$	38.0	10.1080/15567031003753579
	Chen	$NaBO_2$	2	$NaB(OH)_4$	89.8	10.1016/j.jpowsour.2017.05.075
	Chen	$NaBO_2$	4	$NaB(OH)_4 \bullet 2H_2O$	88.3	10.1016/j.jpowsour.2017.05.075
	Chen	$NaBO_2$	2 and 4	$NaB(OH)_4$ and $NaB(OH)_4 \bullet 2H_2O$	82.0	10.1016/j.jpowsour.2017.05.075
Thermo	Kojima	$NaBO_2$	-	$NaBO_2$	98.0	10.1016/S0360-3199(02)00173-8
	Figen	$NaBO_2$	-	$NaBO_2$	91.0	10.1016/j.ijhydene.2013.01.003
Electro	Shu	$NaBO_2$	-	$NaBO_2$	97.0	10.1016/j.fuel.2013.05.069

[0004] Document CN105271119 discloses preparation method for sodium borohydride, wherein $Na_2B_4O_7$ and NaOH are dissolved in water, a reaction is carried out at a temperature of 60 °C-80 °C, and $NaBO_2$ is prepared; then a methanol solution and $NaBO_2$ are reacted at a temperature of 50 °C -90 °C, and $NaB(OCH_3)_4$ is prepared; the obtained $NaB(OCH_3)_4$ is prepared into a THF and triethyl silicane solution, which is subjected to a synthetic reaction in an inert gas or vacuum environment, and the target product $NaBH_4$ is prepared. However, the disclosed method does not use a by-product of sodium borohydride hydrolysis, thus not closing the H_2 production circle.

[0005] Document JPH02208218 discloses a method to obtain high-purity sodium borohydride by reacting a specific trialkyl borate with sodium aluminum hydride. However, the disclosed method does not use a by-product of sodium borohydride hydrolysis, thus not closing the H_2 production circle.

[0006] These facts are disclosed in order to illustrate the technical problem addressed by the present disclosure.

GENERAL DESCRIPTION

[0007] The present disclosure relates to a method to process a by-product compound, resulting from sodium borohydride hydrolysis, as soon as the hydrolysis reaction has been completed, to obtain the desired borate in the optimal structural form, which allows its regeneration to $NaBH_4$ in optimal cost-benefit conditions. After hydrolysis, the by-product can be extracted, separated from the catalyst by sedimentation and dried in a desiccator under vacuum for 6 to 8 days. Surprisingly, pure $NaB(OH)_4$ is obtained and ready to be rehydrogenated.

[0008] The disclosed method may result in a laboratory/industrial procedure, essential for the cost-effective regeneration of sodium borohydride. It can also be implemented in a $NaBH_4$-H_2 device for on-demand applications and off-grid hydrogen generation alternative solutions. It optimizes a green and safe H_2 generation process, further developing an essential step for its on-demand application: the by-product of reaction handling after the H_2 generation.

[0009] In an embodiment, the method presented has the ability to optimize the whole system by presenting an innovative process to handle the by-product formed upon sodium borohydride hydrolysis, leading to the obtention of a pure borate, i.e., borate with a purity of at least 90%. The processing of the borate by-product using the disclosed method reduces the time and cost required for its rehydrogenation and application in any possible $NaBH_4$-H_2 system.

[0010] The present disclosure relates to a method to obtain sodium borohydride from a liquid mixture comprising borate, the method comprising the following steps: separating the borate compound from the mixture by sedimentation; collecting the supernatant comprising the borate compound drying the borate compound, preferably in a desiccator under vacuum, to obtain a pure borate compound; and rehydrogenating the pure borate compound into sodium borohydride.

[0011] An aspect of the present disclosure relates to a method to obtain hydrogen comprising a step of obtaining sodium borohydride as described in the present disclosure.

[0012] In an embodiment, the method further comprises the following steps: adding a catalyst into a reactor; injecting a mixture of sodium borohydride and aqueous sodium hydroxide into the reactor; hydrolysing the sodium borohydride into hydrogen with formation of a liquid mixture comprising borate.

[0013] In an embodiment, the concentration of sodium hydroxide ranges from 0.5 to 70 % (m/m), preferably from 0.7 to 10 % (m/m), more preferably from 1 to 7% (m/m).

[0014] In an embodiment, the hydrogen generation and storage are obtained by injecting a $NaBH_4$ with NaOH aqueous solution in a stainless-steel batch reactor, using a metal catalyst. After hydrolysis, the application of the disclosed method assures the maximum conservation of the byproduct stability in the form of $NaB(OH)_4$, which is the best viable compound to be integrated in the rehydrogenation process (borate with higher cost-benefit).

[0015] In an embodiment, the hydrogen generation and storage are obtained by injecting a solution of 5-15 wt.% $NaBH_4$ with a 1-10 wt. % NaOH aqueous solution. Preferably, by injecting a solution of 10 wt.% $NaBH_4$ with a 7 wt. % NaOH aqueous solution.

[0016] In an embodiment, the $NaBH_4$ and NaOH aqueous solution are injected in a cylindrical reactor, preferably a cylindrical reactor with interior conical bottom.

[0017] In an embodiment, the hydrogen generation and storage are obtained by injecting a 10 wt. % $NaBH_4$ with 7 wt. % NaOH aqueous solution in a stainless-steel batch cylindrical reactor with interior conical bottom, using a Ni-Ru catalyst.

[0018] In an embodiment, the disclosed process comprises the extraction of a borate by-product in a liquid form, for example by using a pipette or other suction means, separation of the catalyst by sedimentation and drying under vacuum for 6 to 8 days. Pure or close to pure $NaB(OH)_4$ is obtained and prepared to be rehydrogenated. The obtained borate has great advantages for the rehydrogenation process, due to a lower energy demand by not requiring water evaporation, while also generating and storing pure H_2.

[0019] Surprisingly, the method described in the present disclosure results in a higher process efficiency, lower need of fresh $NaBH_4$, lower hydrogen cost and reduced economic and energetic costs.

[0020] The present disclosure also relates to a method for processing a liquid by-product of sodium borohydride hydrolysis to obtain a borate compound, the method comprising

the following steps: separating the liquid by-product by sedimentation, to obtain a borate-rich supernatant; drying the borate-rich supernatant under vacuum to obtain a solid composition comprising a borate compound, wherein the borate compound is sodium boron hydroxide ($NaB(OH)_4$).

[0021] In an embodiment, the crystal form of the borate compound has an XRD pattern essentially the same as shown in Fig. 6B having a melting point ranging from 53 °C to 58 °C.

[0022] In an embodiment, the solid composition comprises at least 90 % (w/w) of the borate compound. In a further embodiment, the solid composition comprises at least 95 % (w/w) of the borate compound.

[0023] In an embodiment, the borate-rich supernatant is dried under vacuum for 6 to 8 days.

[0024] In an embodiment, the method further comprises a step of rehydrogenating the borate compound into sodium borohydride.

[0025] In an embodiment, the rehydrogenation step is a thermochemical process, a mechanochemical process or an electrochemical process, preferably electrochemical.

[0026] In an embodiment, the sedimentation occurs by natural sedimentation, or by centrifugation. In a preferred embodiment, the sedimentation occurs for up to 12 hours, or the centrifugation occurs for up to 5 minutes.

[0027] An aspect of the present disclosure comprises a crystalline sodium boron hydroxide obtainable by the method described in any of the previous claims wherein the crystalline hydroxide form has an XRD pattern essentially the same as shown in Fig. 6B having a melting point ranging from 53 °C to 58 °C.

[0028] In an embodiment, the crystalline sodium boron hydroxide comprises the absence of peaks at diffraction angles (2θ) of 21.4-21.6, 32.2-32-4 and 37.8-37.9 (Fig. 6B).

[0029] An aspect of the present disclosure comprises a composition obtainable by the disclosed method comprising at least 90% (w/w) of sodium boron hydroxide. In an embodiment, the composition obtainable by the disclosed method comprises at least 90% (w/w) of sodium boron hydroxide and up to 10% (w/w) of thermonatrite.

[0030] The present disclosure also relates to the use of the disclosed composition or crystalline sodium boron hydroxide as a source of borate in the production of sodium borohydride and/or hydrogen.

[0031] An aspect of the present disclosure comprises a method for obtaining hydrogen comprising a step of processing a liquid by-product of sodium borohydride hydrolysis as disclosed.

[0032] In an embodiment, the method for obtaining hydrogen further comprises the following steps: adding a catalyst into a reactor; injecting a mixture of sodium borohydride and aqueous sodium hydroxide into the reactor; hydrolysing the sodium borohydride into hydrogen with formation of a liquid by-product.

[0033] In an embodiment the catalyst is a metallic catalyst. In a preferred embodiment, the metallic catalyst is a bimetallic catalyst, preferably Ni-Ru.

[0034] In an embodiment the concentration of sodium borohydride ranges from 5 to 20 % (w/w), preferably from 10 to 15% (w/w).

[0035] In an embodiment, the concentration of sodium hydroxide ranges from 0.5 to 70 % (w/w), preferably from 0.7 to 10 % (w/w), more preferably from 1 to 7% (m/m).

[0036] In an embodiment the mass ratio between sodium borohydride, sodium hydroxide and catalyst ranges from 10.0: 7.0: 4.0 to 10.0: 7.0: 6.3.

[0037] In an embodiment the hydrolysis step occurs at a temperature ranging from 18 to 27 °C.

[0038] In an embodiment, the hydrolysis step starts at a pressure ranging from 60 to 102 kPa, preferably 101.325 kPa.

BRIEF DESCRIPTION OF THE DRAWINGS

[0039] The following figures provide preferred embodiments for illustrating the disclosure and should not be seen as limiting the scope of invention.

Figure A.1: Schematic representation of an embodiment of a hydrogen synthesis method comprising the disclosed method to recover the borate by-product (1).

Figure A.2: Embodiment of the separation of the by-product by sedimentation of the catalyst.

Figure A.3: Embodiment of the by-product appearance after drying.

Figure A.4: Embodiment of results of by-product comparison (in mass %) between air exposure or vacuum drying.

Figure A.5: Embodiment of the hydrolysis' by-product composition (in mass %) under vacuum drying, for four different samples (numbered as 1,2,3 and 4).

Figure A.6: Embodiment of X-ray powder diffraction spectra for $NaB(OH)_4$ obtained by common drying process ("common drying") or by the method described in the present disclosure ("present disclosure").

DETAILED DESCRIPTION

[0046] The present disclosure relates to a method for processing a liquid by-product of sodium borohydride hydrolysis to obtain a borate compound, the method comprising the following steps: separating the liquid by-product by sedimentation, to obtain a borate-rich supernatant; drying the borate-rich supernatant under vacuum to obtain a solid composition comprising a borate compound, wherein the borate compound is sodium boron hydroxide.

[0047] The present disclosure relates to a method to obtain sodium borohydride from a liquid mixture comprising borate, the method comprising the following steps: separating the borate compound from the mixture by sedimentation; drying the borate compound to obtain a pure borate compound; and rehydrogenating the pure borate compound into sodium borohydride. An aspect of the present disclosure relates to a method to obtain hydrogen comprising the step of obtaining sodium borohydride from a liquid mixture comprising borate disclosed.

[0048] In an embodiment, $NaBH_4$ was used to produce hydrogen, in particular molecular hydrogen, via hydrolysis at room pressure and temperature.

[0049] For the scope and interpretation of the present disclosure, "room pressure" is defined as normal air pressure ranging from 60 – 102 kPa, preferably 101.325 kPa; and "room temperature" is defined as a temperature ranging from 15 to 27°C, preferably 18 to 25 °C.

[0050] In an embodiment, a catalyst was used to obtain hydrogen from sodium borohydride, preferably a metallic catalyst, more preferably a bimetallic catalyst such Ni-Ru.

[0051] In an embodiment, 10 % (m/m) of $NaBH_4$ was injected together with 7 % (m/m) NaOH aqueous solution in a stainless-steel batch reactor, using 0.40-0.63 mass of catalyst per mass (mg) of sodium borohydride. After hydrolysis, the application of the disclosed method assures the maximum conservation of the byproduct stability in the form of $NaB(OH)_4$, which is the best viable compound to be integrated in the rehydrogenation process (borate with higher cost-benefit).

[0052] In an embodiment, the disclosed process comprises the extraction of a borate by-product in a liquid form following the production of H_2, separation of the catalyst used in H_2 production by natural sedimentation or forced sedimentation through centrifuge for up to 5 minutes, and drying the resulting supernatant under vacuum, preferably in an enclosed desiccator or similar equipment (for example a glove box) for 6 to 8 days. Pure or close to pure $NaB(OH)_4$ is obtained after drying, which is ready to be rehydrogenated. This is the best borate to rehydrogenate (lower energy demand by not requiring water evaporation) while also generating and storing pure H_2.

[0053] In an embodiment, the Ni-Ru catalyst can be reused. After sedimentation, the formed pellet can be collected and transferred to a glass beaker, washed, preferably at least three times, at room temperature and dried at 80°C for 1 hour to be reused.

[0054] In an embodiment, the liquid by-product of reaction (supernatant resulting from sedimentation) is transferred to a container with a size adapted to the volume in consideration. For example, the container can be a glass petri dish. The container is then placed in an enclosed environment, e.g., a desiccator, under vacuum using a vacuum pump. For an average of 6 to 8 days the desiccator must remain closed during drying to avoid unnecessary contact with air. The by-product is dried when no liquid and only crystals are visible in the petri dish. As comparative example, the liquid by-product of reaction was also dried by air exposure at room temperature without any pressure control (no vacuum).

[0055] In an embodiment, X-ray powder diffraction (XRD) was used for phase identification of the obtained crystals. Briefly, this method allows the identification and quantification of the compounds present in a crystalline sample. Each compound reflects

the x-rays that cross the sample in a different angle and intensity and, with the use of XRD databases, this compound can be identified. In an embodiment, the XRD patterns were recorded at room temperature using monochromatic Cu K-α radiation (λ = 1.5406 Å). The range of the XRD patterns were 4 º < 2θ < 70 º.

[0056] Figure 4 shows an embodiment of results of by-product comparison (in mass %) between air exposure or vacuum drying, showing that the vacuum drying results in an higher mass percentage of $NaB(OH)_4$ (99.3%) than Na_2CO_3 (0.7%)), as compared to the results obtained with air drying (68.6% of $NaB(OH)_4$ and 31.4% of Na_2CO_3). Figure 5 shows an embodiment of the hydrolysis' by-product composition (in mass %) under vacuum drying, for four different samples (numbered as 1,2,3 and 4).

[0057] In an embodiment, the XRD analysis revealed that the crystalline sodium boron hydroxide obtained from the disclosed method comprises the absence of peaks at diffraction angles (2θ) of 21.4-21.6, 32.2-32-4 and 37.8-37.9 (Fig. 6B), which can be observed for the crystalline material obtained with common drying (Fig. 6A).

[0058] In an embodiment, after the vacuum drying, as described in the present disclosure, it is obtained a solid composition comprising at least 90 % (w/w) of the borate compound, preferably $NaB(OH)_4$. This composition has great advantages for the process of rehydrogenation of sodium borohydride, and therefore its use on the production of hydrogen via sodium hydroxide hydrolysis, since it is a non-hydrated compound, thus not requiring dehydration upon rehydrogenation. Also, the obtained composition comprises at least 90 % (w/w) of the borate compound, thus increasing the effectiveness of the rehydrogenation method by not giving rise to other unwanted compounds.

[0059] In an embodiment, crystals formed can be milled with a pestle and mortar to store the solid composition comprising the borate compound in powder. This step can be performed open to air, however minimal contact to air is preferred. When in no use, the solid composition comprising the borate compound can be stored in the same container, under vacuum.

[0060] In the state of the art, the regeneration of sodium borohydride may occur by different methods, such as thermochemical, mechano-chemical, or electrochemical processes. Thermochemical processes are based on reactions that involve high pressure and/or temperature; the mechano-chemical processes are similar to the thermochemical ones, but the source of energy used in this type of process relies on mechanical forces;

the electrochemical processes use electric energy to produce sodium borohydride by reducing or oxidizing other borates.

[0061] After regeneration, the obtained sodium borohydride can be used on the production of hydrogen, via sodium borohydride hydrolysis, thus closing the $NaBH_4$-H_2 cycle.

[0062] The term "comprising" whenever used in this document is intended to indicate the presence of stated features, integers, steps, components, but not to preclude the presence or addition of one or more other features, integers, steps, components or groups thereof.

[0063] The disclosure should not be seen in any way restricted to the embodiments described and a person with ordinary skill in the art will foresee many possibilities to modifications thereof. The above described embodiments are combinable.

[0064] The following claims further set out particular embodiments of the disclosure.

CLAIMS

1. A method for processing a liquid by-product of sodium borohydride hydrolysis to obtain a borate compound, the method comprising the following steps:
   separating the liquid by-product by sedimentation, to obtain a borate-rich supernatant;
   drying the borate-rich supernatant under vacuum to obtain a solid composition comprising a borate compound;
   wherein the borate compound is sodium boron hydroxide.

2. The method according to the previous claim wherein the crystal form of the borate compound has an XRD pattern essentially the same as shown in Fig. 6B having a melting point ranging from 53 °C to 58 °C.

3. The method according to any of the previous claims wherein the solid composition comprises at least 90 % (w/w) of the borate compound.

4. The method according to any of the previous claims wherein the solid composition comprises at least 95 % (w/w) of the borate compound.

5. The method according to any of the previous claims wherein the borate-rich supernatant is dried under vacuum for 6 to 8 days.

6. The method according to any of the previous claims further comprising a step of rehydrogenating the borate compound into sodium borohydride.

7. The method according to the previous claim wherein the rehydrogenation step is a thermochemical process, a mechanochemical process or an electrochemical process, preferably electrochemical.

8. The method according to any of the previous claims wherein the sedimentation occurs by natural sedimentation, or by centrifugation.

9. The method according to the previous claim wherein the sedimentation occurs for up to 12 hours, or the centrifugation occurs for up to 5 minutes.

10. A crystalline sodium boron hydroxide obtainable by the method described in any of the previous claims wherein the crystalline hydroxide form has an XRD pattern essentially the same as shown in Fig. 6B having a melting point ranging from 53 °C to 58 °C.

11. The crystalline sodium boron hydroxide according to the previous claim comprising the absence of peaks at diffraction angles (2θ) of 21.4-21.6, 32.2-32.4 and 37.8-37.9.

12. Composition obtainable by the method described in any of the previous claims 1-9 comprising at least 90% (w/w) of sodium boron hydroxide, and thermonatrite.

13. Use of a composition as described in the previous claim or a crystalline sodium boron hydroxide as described in any of previous claims 10-11 as a source of borate in the production of sodium borohydride and/or hydrogen.

14. A method for obtaining hydrogen comprising a step of processing a liquid by-product of sodium borohydride hydrolysis as described in claim 1.

15. The method according to the previous claim further comprising the following steps:
    adding a catalyst into a reactor;
    injecting a mixture of sodium borohydride and aqueous sodium hydroxide into the reactor;
    hydrolysing the sodium borohydride into hydrogen with formation of a liquid by-product.

16. The method according to any of the previous claims wherein the catalyst is a metallic catalyst.

17. The method according to the previous claim wherein the metallic catalyst is a bimetallic catalyst, preferably Ni-Ru.

18. The method according to any of the previous claims 14-17 wherein the concentration of sodium borohydride ranges from 5 to 20 % (w/w), preferably from 10 to 15% (w/w).

19. The method according to any of the previous claims 14-18 wherein the concentration of sodium hydroxide ranges from 0.5 to 70 % (w/w), preferably from 1 to 7 % (w/w).

20. The method according to any of the previous claims 14-19 wherein the mass ratio between sodium borohydride, sodium hydroxide and catalyst ranges from 10.0: 7.0: 4.0 to 10.0: 7.0: 6.3.

21. The method according to any of the previous claims 14-20 wherein the hydrolysis step occurs at a temperature ranging from 18 to 27 °C.

22. The method according to any of the previous claims 14-21 wherein the hydrolysis step starts at a pressure ranging from 60 to 102 kPa, preferably 101.325 kPa.

ABSTRACT

METHOD TO PROCESS BORATE BY-PRODUCTS FROM SODIUM BOROHYDRIDE HYDROLYSIS

The present disclosure relates to a method for processing a liquid by-product of sodium borohydride hydrolysis to obtain a borate compound, the method comprising the following steps: separating the liquid by-product by sedimentation, to obtain a borate-rich supernatant; drying the borate-rich supernatant under vacuum to obtain a solid composition comprising a borate compound. An aspect of the present disclosure relates composition obtainable by the disclosed method comprising at least 90% (w/w) of sodium boron hydroxide and its use as a source of borate in the production of sodium borohydride and/or hydrogen.

DRAWINGS

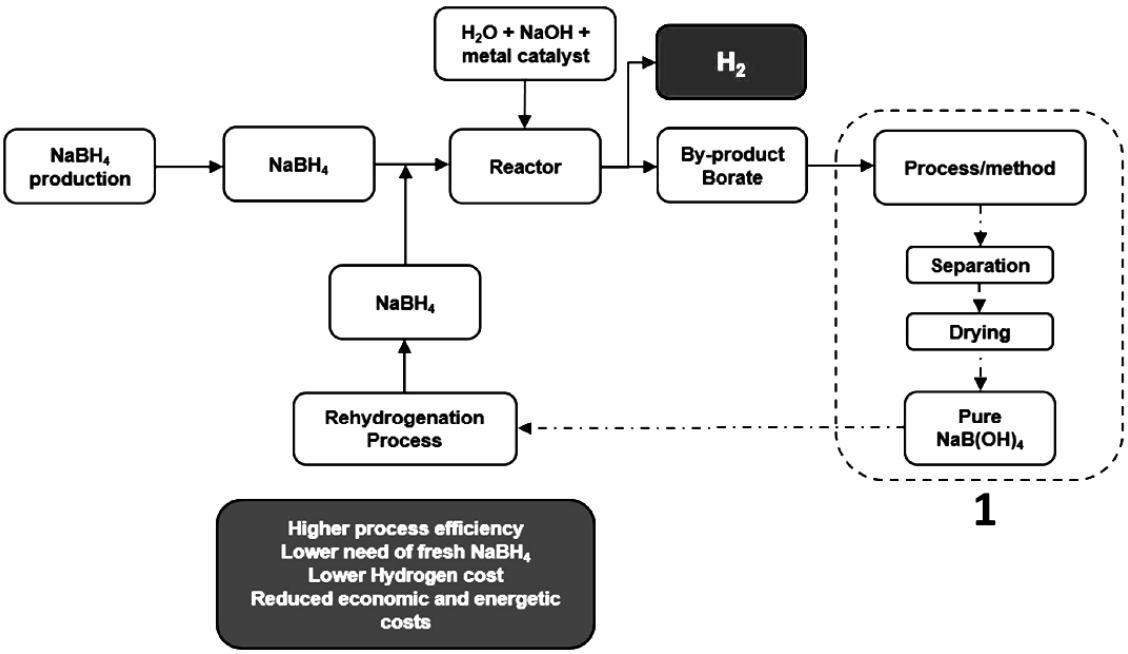


Fig. A.1

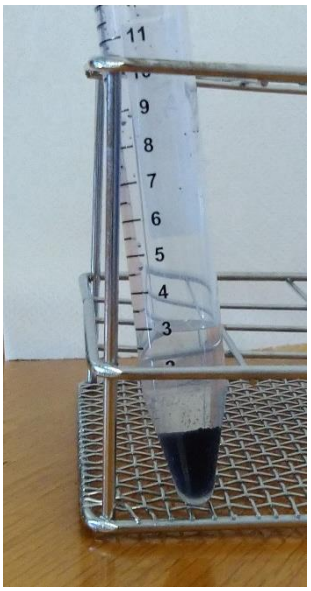


Fig. A.2

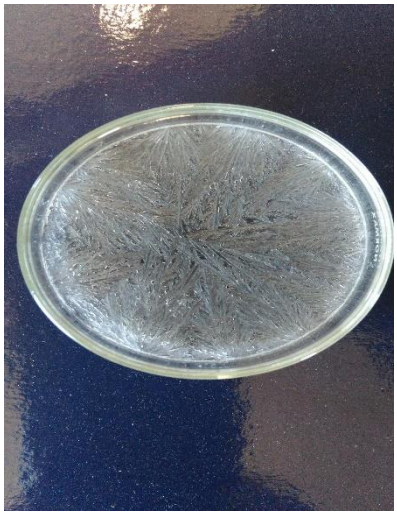


Fig. A.3

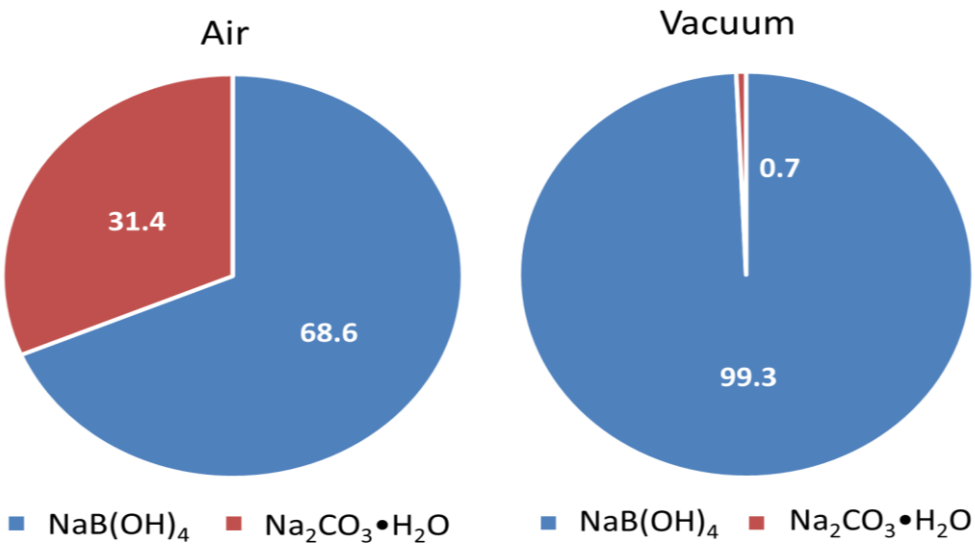

Air
31.4
68.6
NaB(OH)4
Na2CO3•H2O
Vacuum
0.7
99.3
NaB(OH)4
Na2CO3•H2O

Fig. A.4

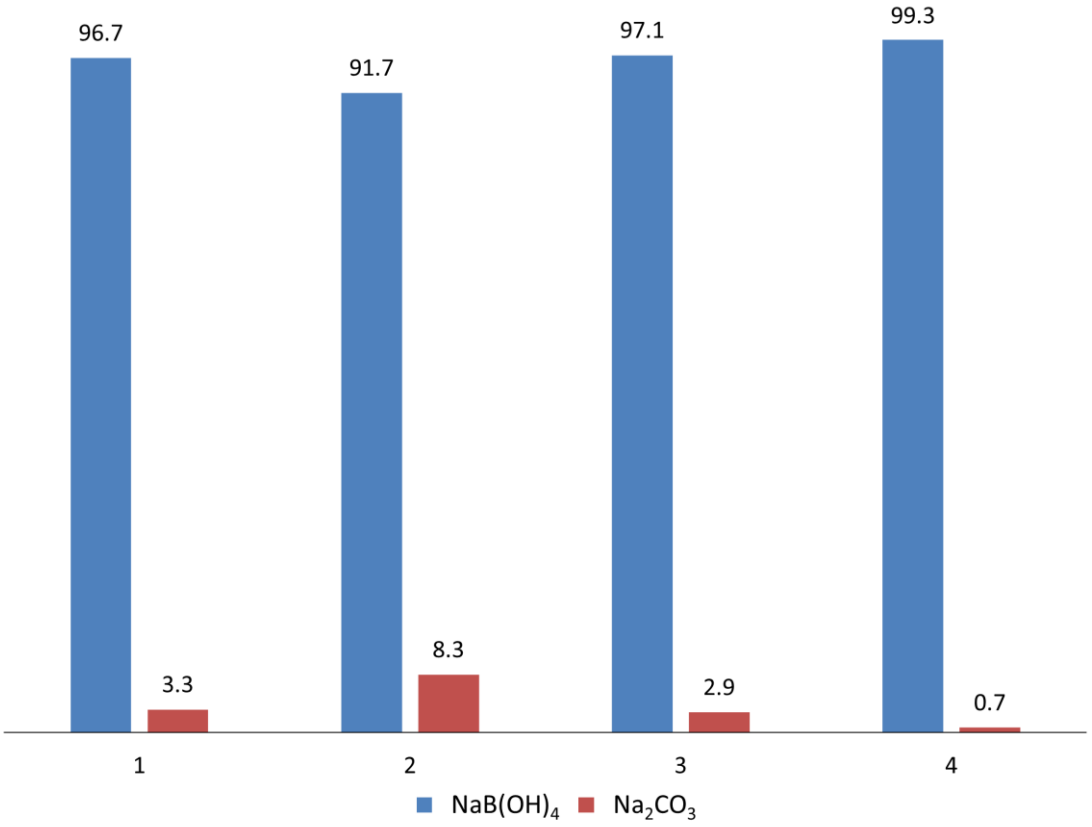


Fig. A.5

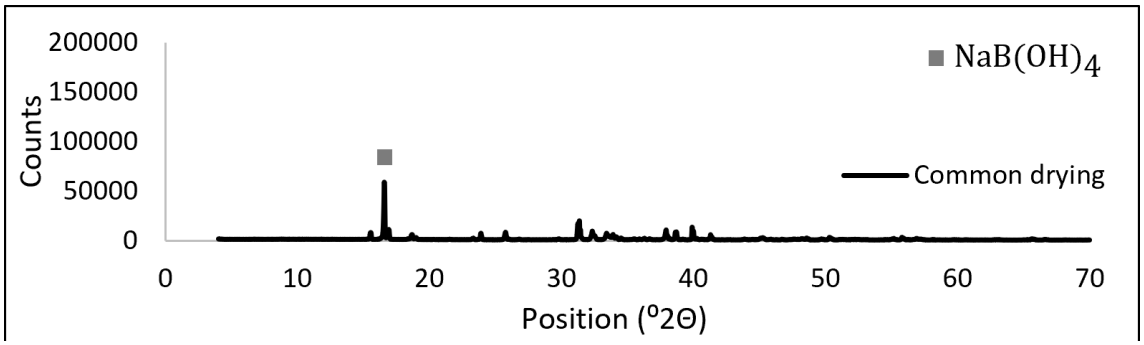


Fig. A.6A

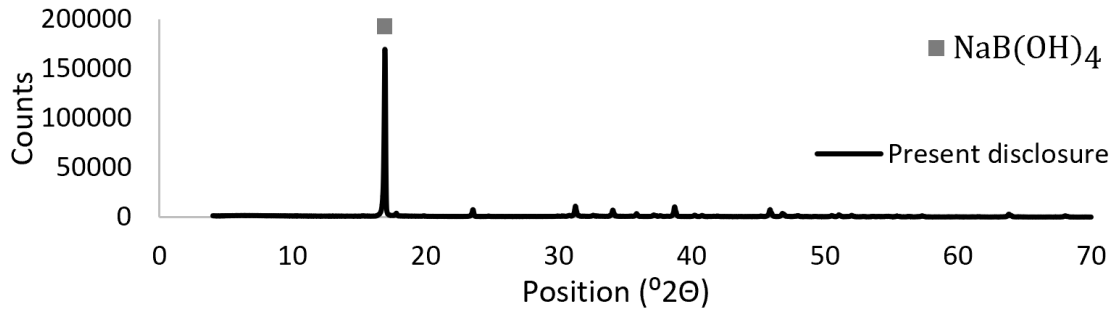

200000
150000
100000
50000
0
Counts
0
10
20
30
40
50
60
70
Position (°2Θ)
NaB(OH)4
Present disclosure

Fig. A.6B